

Appendix 5:
Currents in Minas Basin
(Oceans Ltd. 2009)

Current in Minas Basin
May 1, 2008 – March 29, 2009

Submitted To:
Minas Basin Pulp and Power
P.O. Box 401
53 Prince Street
Hansport, NS, B0P 1P0

by


202, Purdy's Wharf Tower 2
1969 Upper Water Street
B3J 3R7
Telephone: 902 492 9220
Facsimile: 902 492 4545

May 2009

Table of Contents

1.0	Introduction.....	1
1.1	Minas Basin Tides.....	1
1.2	Data Information.....	2
2.0	Vessel-mounted ADCP Data	5
3.0	Moored ADCP Data.....	15
3.1	Current Speed and Direction.....	16
3.1.1	Mean and Maximum Current Speed	16
3.1.2	Current Speed during Spring/Neap Tides	17
3.2	Rose Plots.....	20
3.3	Semidiurnal Tides	24
3.4	Power Spectral Density	28
3.5	Time Series of Surface Currents and Tidal Heights	29
3.6	Time Series of Current Speed and Direction	33
4.0	Bottom Current Data.....	35
4.1	Current Speed during Spring/Neap Tides	35
4.2	Rose Plot	36
4.3	Harmonic Analysis.....	37
5.0	Water Level Data	38
5.1	Time Series of Water Level Data from Meter 819 at Site 1	38
5.2	Time Series of Water Level Data from Meter 819 at Site 3	41
6.0	Bottom Temperature Data.....	44
6.1	Time Series of Bottom Temperature from ADCP, at Site 1	44
6.2	Time Series of Bottom Temperature from the ADCP at Site 3	47
6.3	Time Series of Bottom Temperature from the ADCP at Site 4	49
6.4	Time Series of Bottom Temperature from the ADCP at Site 5	52
Appendix 1	Time Series Plots, ADCP at Site 1	54
Appendix 2	Time Series Plots, ADCP at Site 2	65
Appendix 3	Time Series Plots, ADCP at Site 3	68
Appendix 4	Time Series Plots at Site 4	79
Appendix 5	Time Series Plots, ADCP at Site 5	90
Appendix 6	Time Series Plots, for the InterOceanS4 Current Meter at Site 5	103
Appendix 7	Time Series of the Pressure, Temperature, and Salinity Data from the InterOcean S4 Current Meter at Site 5	107
Appendix 8	Time Series of Bottom Temperature from the Water Level Recorder at Site 1	114
Appendix 9	Time Series of Bottom Temperature from the Water Level Recorder at Site 3	118

List of Tables

Table 1. List of Instruments in Minas Basin 2008 - 2009	4
Table 2: Mean and Maximum Current from Each Site.....	16
Table 3. M ₂ Tidal Constituents	25
Table 4. S ₂ Tidal Constituents	26

List of Figures

Figure 1. Map of Minas Basin	1
Figure 2. Mooring Location at Minas Passage	2
Figure 3. Mooring Positions in Minas Passage.....	3
Figure 4. Locations of Profiling Current Data on May 1, 2008.....	6
Figure 5. Stick plots of the profiling data on May 1, 2008	7
Figure 6. Transect Plots of profiling data on May 1, 2008	9
Figure 7. Locations of Profiling Current Data on July 10, 2008	10
Figure 8. Stick Plots of Profiling Data on July 10, 2008	11
Figure 9. Transect Plots of Profiling Data on July 10, 2008.....	13
Figure 10. Mooring Diagram, Minas Basin	15
Figure 11. Current Speed during Spring Tides	18
Figure 12. Current Speed during Neap Tides	20
Figure 13. Rose Plots for Site 1	21
Figure 14. Rose Plots for Site 3	22
Figure 15. Rose Plots for Site 4	23
Figure 16. Rose Plots for Site 5	24
Figure 17. M ₂ Tidal Ellipses at each site	27
Figure 18. Power Spectral Density from ADCP data at each site	29
Figure 19. Surface Current and Tidal Height at Site 1	30
Figure 20. Surface Current and Tidal Height at Site 3	31
Figure 21. Surface Current and Tidal Height at Site 4	32
Figure 22. Surface Current and Tidal Height at Site 5	33
Figure 23 Current at Spring Tide on March 10, 2009.....	35
Figure 24 Currents at Neap Tide on March 21, 2009	36
Figure 25 Rose Plot near the Bottom at Site 5.....	36
Figure 26 M2 Tidal Ellipse near Bottom	37
Figure 27. Water Level Data at Site 1.....	39
Figure 28. Water Level Data at Site 3.....	42
Figure 29. Water Temperature 1.5 metres above Bottom at Site 1.....	44
Figure 30. Water Temperature 1.5 Metres above Bottom at Site 3	47
Figure 31. Water Temperature 1.5 Metres above Bottom at Site 4	49
Figure 32. Water Temperature 1.5 Meters above Bottom at Site 5	52

1.0 Introduction

1.1 Minas Basin Tides

Minas Basin is a semi-enclosed basin located on the southern branch of the upper Bay of Fundy. It is comprised of four distinct regions: Minas Channel at the mouth; central Minas Basin, which is connected to Minas Channel by Minas Passage; a southward bulge called the Southern Bight; and Cobequid Bay, forming the innermost extremity (see Figure 1). The waters of Minas Basin exchange with the main part of the Bay of Fundy through Minas Channel which flows between Cape Split and Cape Sharp, creating extremely strong tidal currents. Tides in Minas Basin are greatly amplified and have a range of the order of 12 metres. The primary cause of the immense tides is resonance in the Bay of Fundy because its dimensions support the oscillation of a standing wave. The system has a natural period of oscillation of approximately 13 hours which is close to the 12.4 hours period of the dominant semi-diurnal (lunar) tide of the Atlantic Ocean.

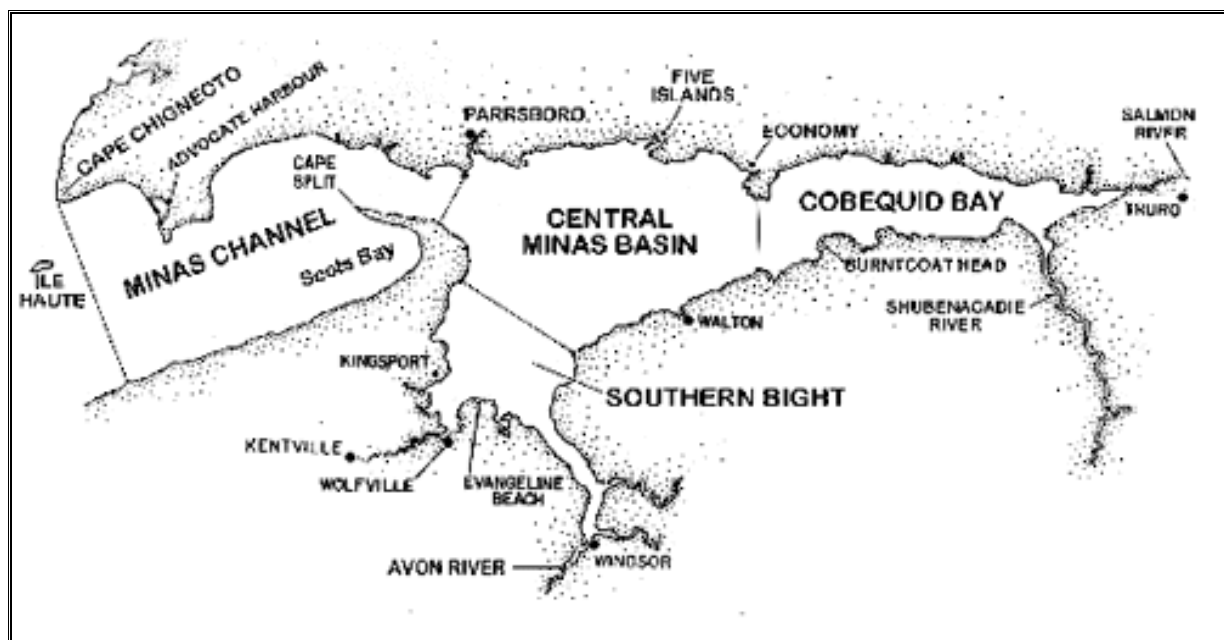


Figure 1. Map of Minas Basin

(from BoFEP Fundy Issues #19)

Strong tidal power as a clean renewable source of energy is attracting attention worldwide. The interest in development of this new energy is being driven by the concern with long-term energy supply and environmental consequences of the release of greenhouse gases from consumption of fossil fuels. The Bay of Fundy with its resonance tides and strong tidal currents makes this area unique for the generation of tidal power.

1.2 Data Information

The initial task taken on by Oceans Ltd in 2008 was to identify the most appropriate sites with respect to current flow for the placement of turbines in Minas Channel and Minas Passage. Currents were measured in Minas Passage since May, 2008 using ADCPs, in both downward-looking and moored upward-looking modes. A moored Aanderaa Water Level Recorder was used to measure tidal heights. Figure 2 and Figure 3 give the area of the moorings and the positions for each site, respectively. Table 1 provides details on the instruments in Minas Passage.

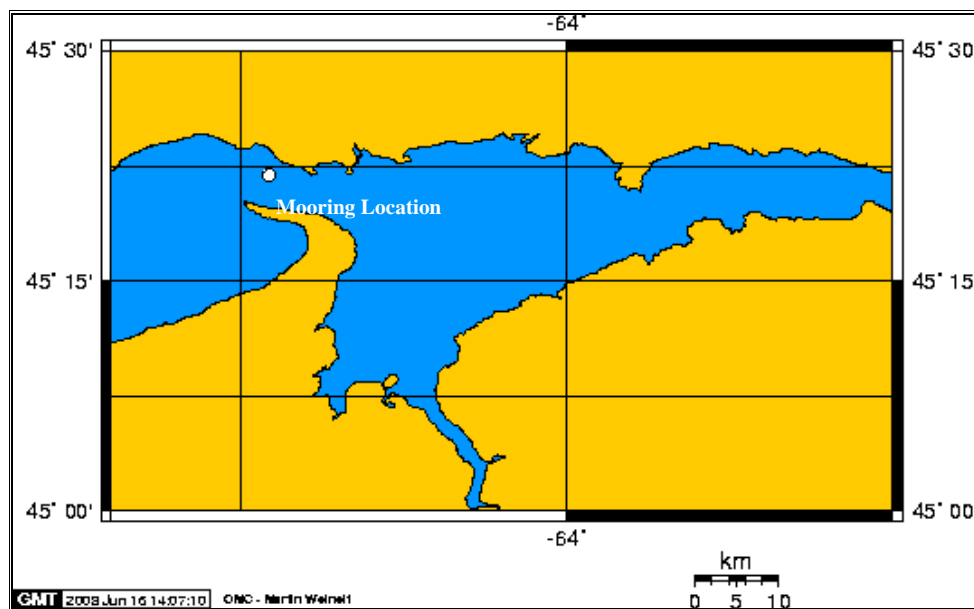


Figure 2. Mooring Location at Minas Passage

The ADCPs used in Minas Passage were 300 kHz Workhorse broadband systems. The ADCPs were moored on the bottom and collected data from the near bottom to near surface with a sampling interval of 10 minutes (ensemble average) and a depth interval of 4 m. At site 5, an InterOcean S4 meter was fixed to the mooring and measured the bottom currents at a height of 0.5 m above the sea floor. The vessel-mounted ADCPs were placed on the vessel Tide Force and collected data through the water column at different locations with a sampling interval of 10 minutes and a bin size of 4 m on May 1, 2008, and 1 m on July 10, 2008. Water Level Recorders were placed on the ADCP bottom stand at sites 1 and 3 and measured the water level and bottom water temperature with a sampling interval of 20 minutes. In this report water depth refers to the distance from the surface at mid-tide.

The following section of this report presents stick plots and transect plots that represent the current spatial distributions at different depths from the vessel-mounted ADCP data. In section 3, time series data from moored ADCPs are analyzed by means of statistical analysis, rose plots, tidal analysis, and power spectral density plots. The time series plots are presented in Appendices 1 to 5. The time series of water level and bottom temperature data during each sampling period are presented in Sections 4 and 5, respectively. The time series of bottom temperatures from the water level recorders and the InterOceans S4 current meter are presented in Appendices 7 to 9.

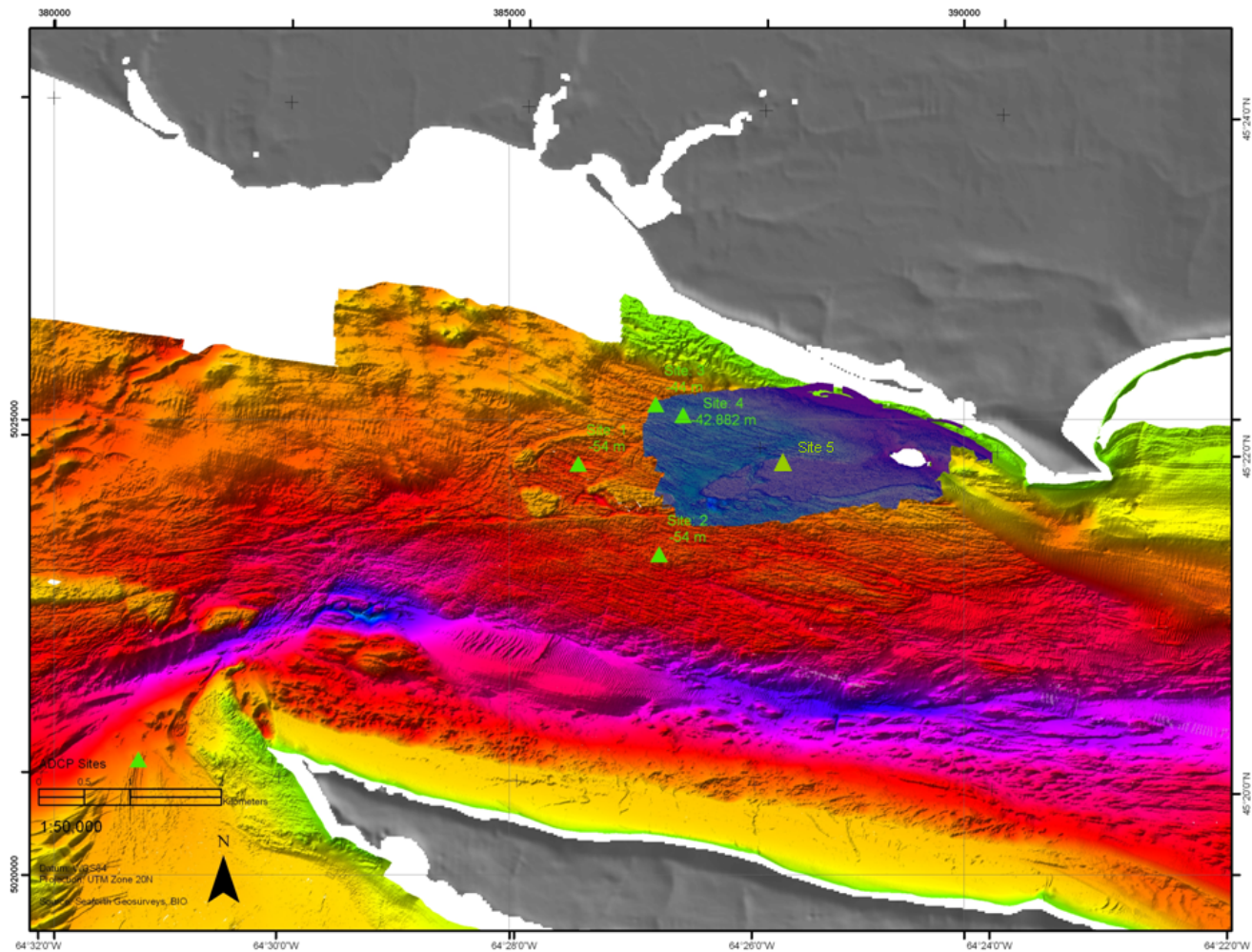


Figure 3. Mooring Positions in Minas Passage

Table 1. List of Instruments in Minas Basin 2008 - 2009

Instruments	Date	Location	Site No.	Meter Depth at mid-tide	Sampling Interval	Bin Size
Vessel-Mounted ADCPs	May 1, 2008	-	-	Surface	10 minutes	4 m
	July 10, 2008	-	-	Surface	10 minutes	1 m
Moored ADCPs	May 2 - June 4, 2008	45° 21' 53''N 64° 27' 32''W	Site 1	58 m	10 minutes	4 m
	May 4 – May 5, 2008	45° 21' 22''N 64° 27' 50''W	Site 2	57 m	10 minutes	4 m
	June 5 – July 9, 2008	45° 22' 15''N 64° 26' 53''W	Site 3	52 m	10 minutes	4 m
	August 21 – September 23, 2008	45° 22' 11''N 64° 26' 38''W	Site 4	51 m	10 minutes	4 m
	February 14 – March 28, 2009	45° 21' 56''N 64° 25' 32''W	Site 5	46 m	10 minutes	4 m
InterOcean S4	February 12 – March 28, 2009	45° 21' 56''N 64° 25' 32''W	Site 5	48 m	10 minutes	-
Water Level recorder 819	May 2 - June 4, 2008	45° 21' 53''N 64° 27' 32''W	Site 1	58 m	20 minutes	-
	June 5 – July 9, 2008	45° 22' 15''N 64° 26' 53''W	Site 3	52 m	20 minutes	-

2.0 Vessel-mounted ADCP Data

Prior to the deployment an ADCP was mounted to the survey vessel, the TideForce 1 (owned and operated by Mark Taylor) on May 1, 2008, during falling tide. This unit was used to carry out a series of bottom track profiles in the locations shown in Figure 4. Precise navigation was provided by Seaforth Engineering. The 3 hours 20 minutes profiling data are of good quality with no gaps or erroneous values.

The following analysis in Figure 5 shows the stick plots of the current at depths of 7 m, 19 m, 31 m and 43 m, respectively. The numbers in the plots are the station numbers. Current directions had no significant change with depth during the sampling time. Current speed had a magnitude of 2.5 m/s at the surface, approximately 2 to 2.5 m/s at mid depths and decreased to 1.5 m/s over the bottom. The current directions were toward the northwest from surface to bottom with an average speed of 2 m/s.

Transect plots in Figure 6 show three vertical sections of speed versus depth, and direction versus depth along the ship's track. The position coordinates are labeled at the starting (left) and ending positions (right) of the plots. The 1st (station 5 to 11) and 3rd (station 15 to 21) tracks are parallel and the 2nd track is along the diagonal. The currents were profiled during falling tide and tend to have lower values than rising tide. All the graphical representations are based on automatically generated long term averaged (LTA) files.

Profiling was also carried out at low water on July 10, 2008 at the locations shown in Figure 7. At mid-depth, the current speed was approximately 1.5 m/s (Figure 8). Vertical sections of speed and direction both across and along the Channel are shown in Figure 9.

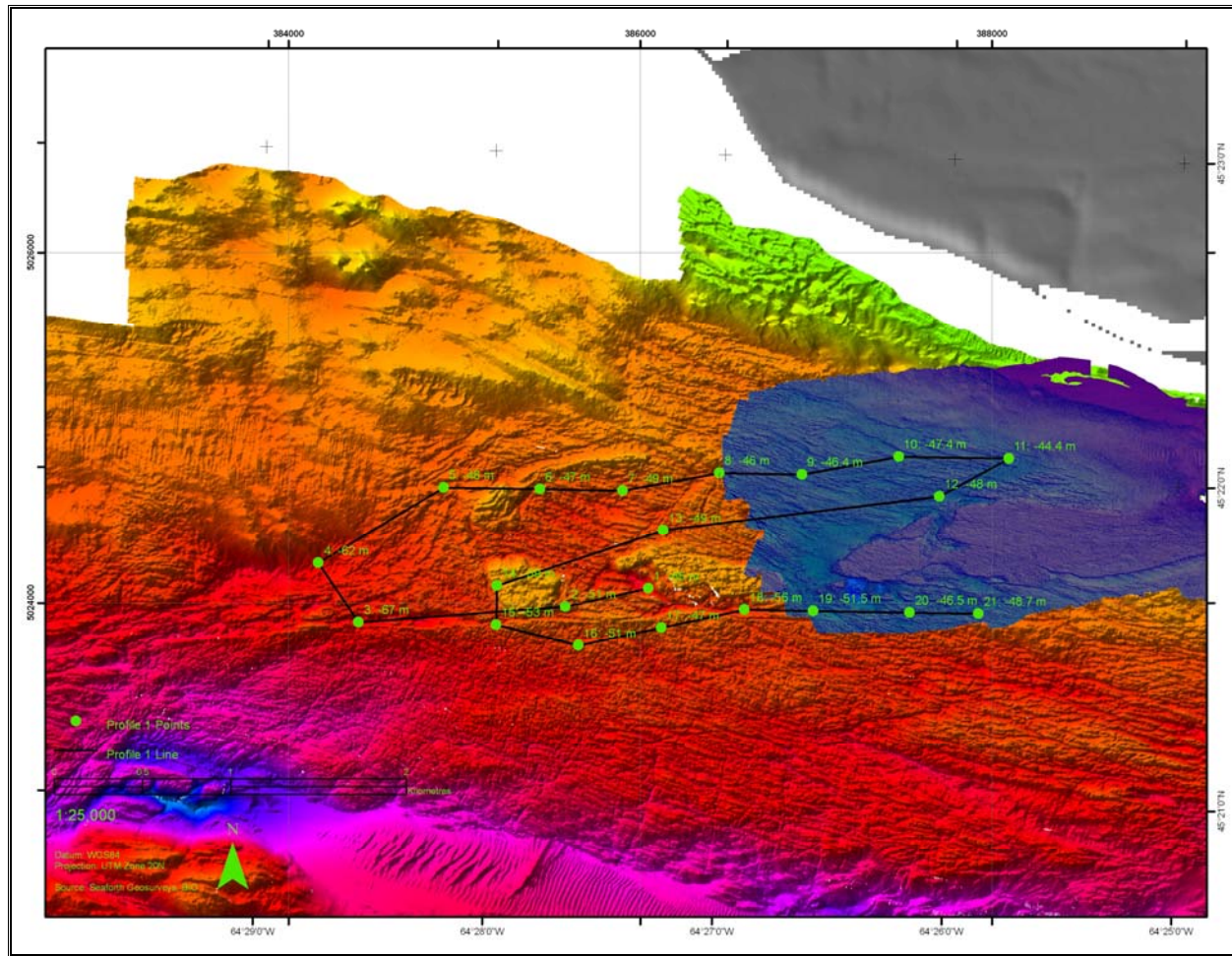


Figure 4. Locations of Profiling Current Data on May 1, 2008

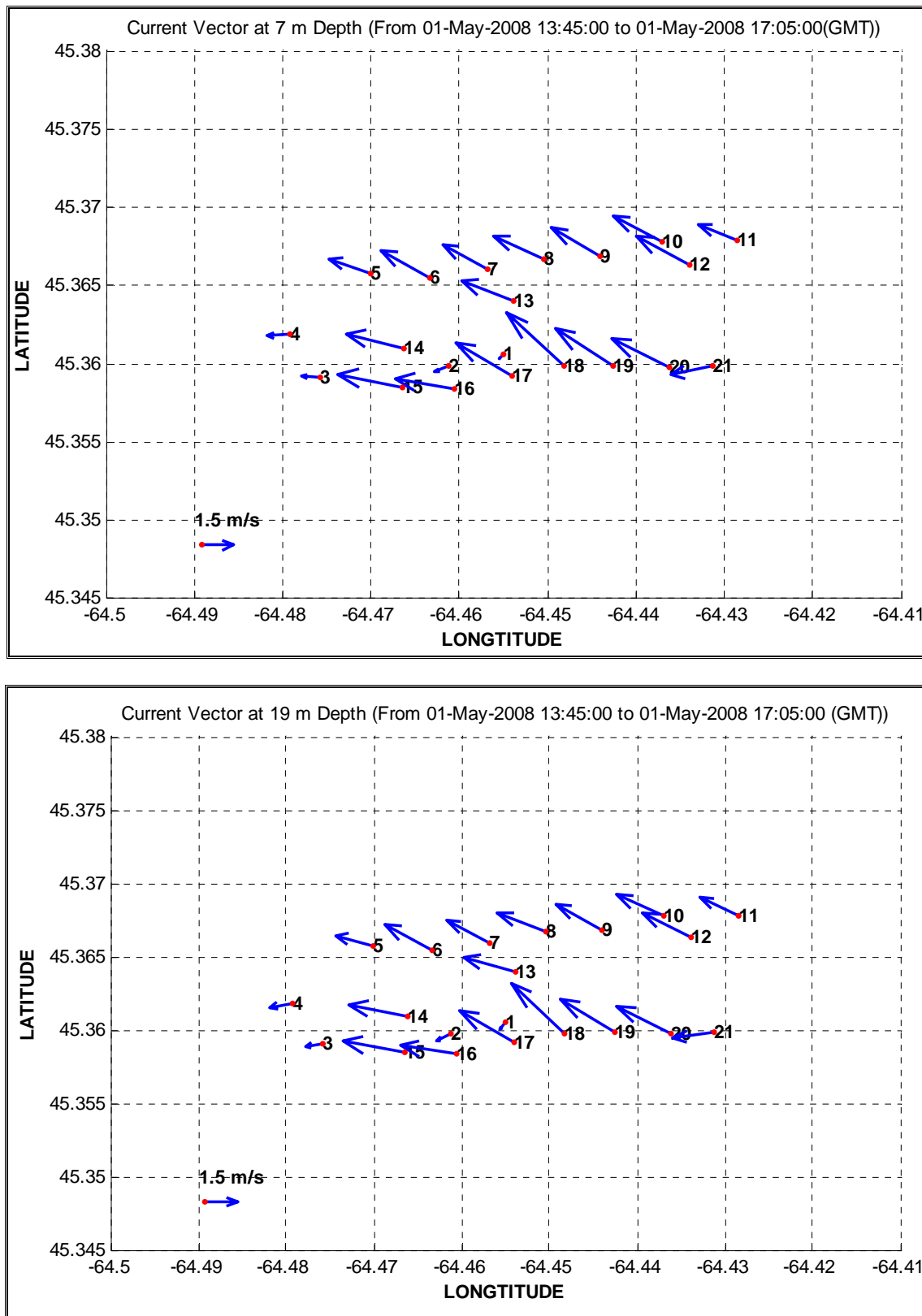


Figure 5. Stick plots of the profiling data on May 1, 2008

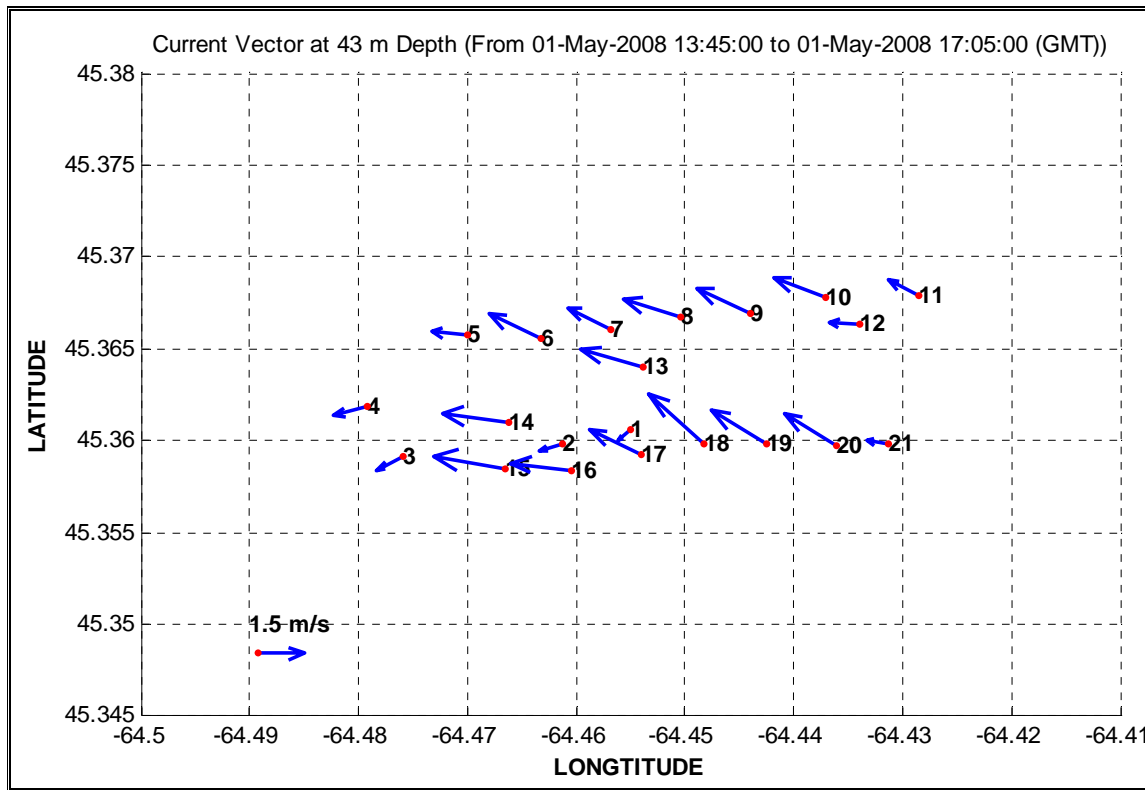
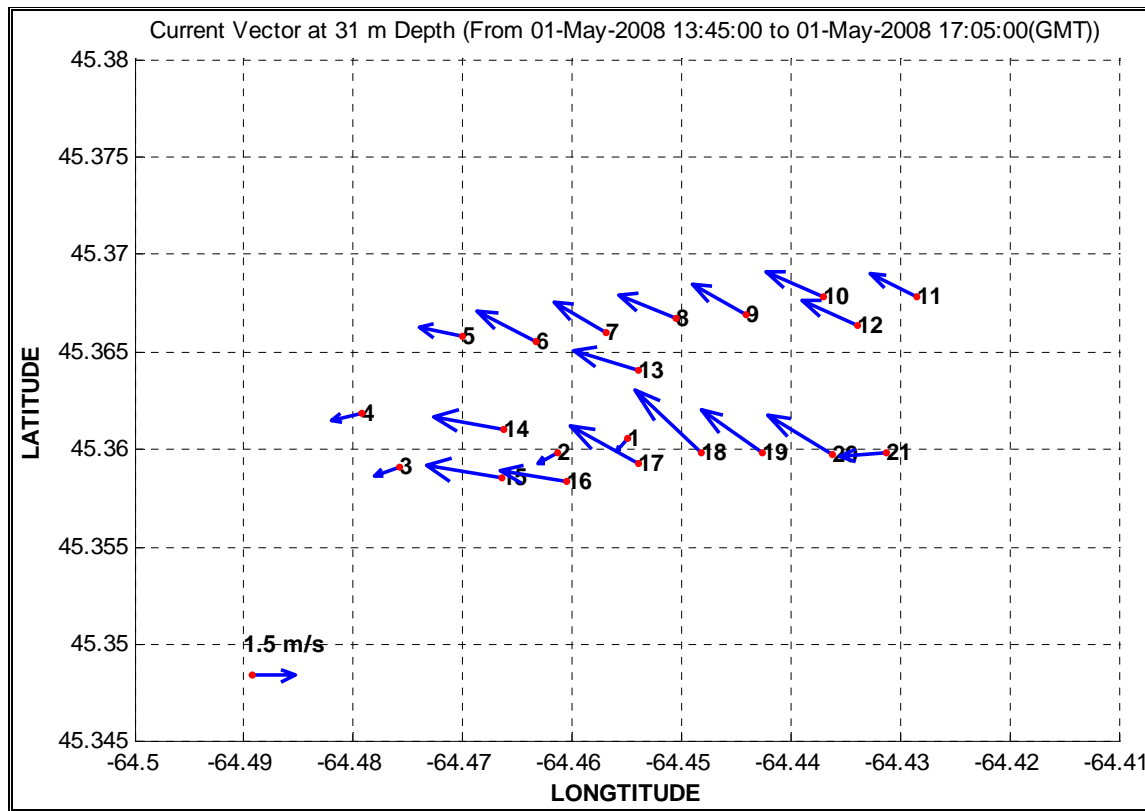
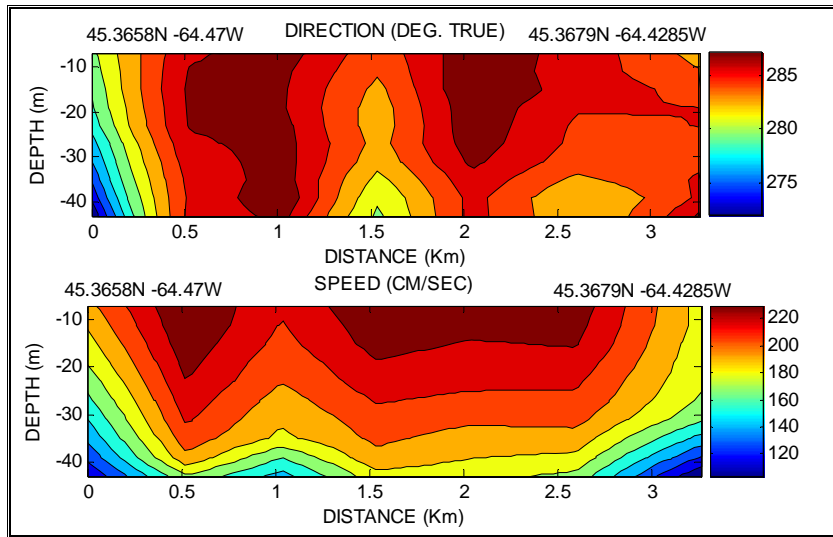
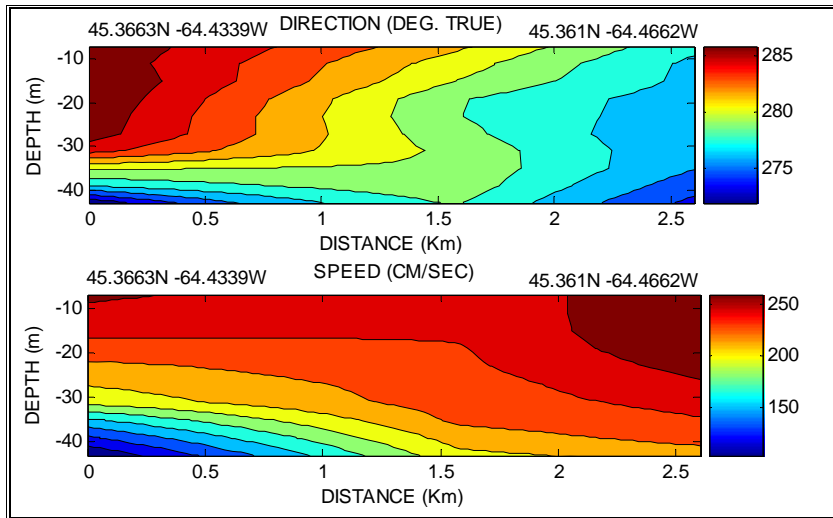


Figure 5. (cont'd) Stick plots of profiling data on May 1, 2008

From Station 5 to Station 11



From Station 12 to Station 14



From Station 15 to Station 21

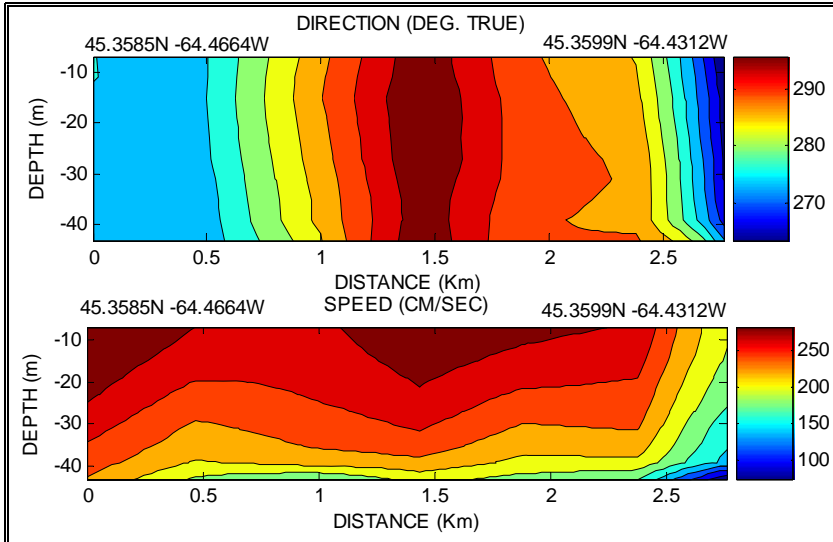


Figure 6. Transect Plots of profiling data on May 1, 2008

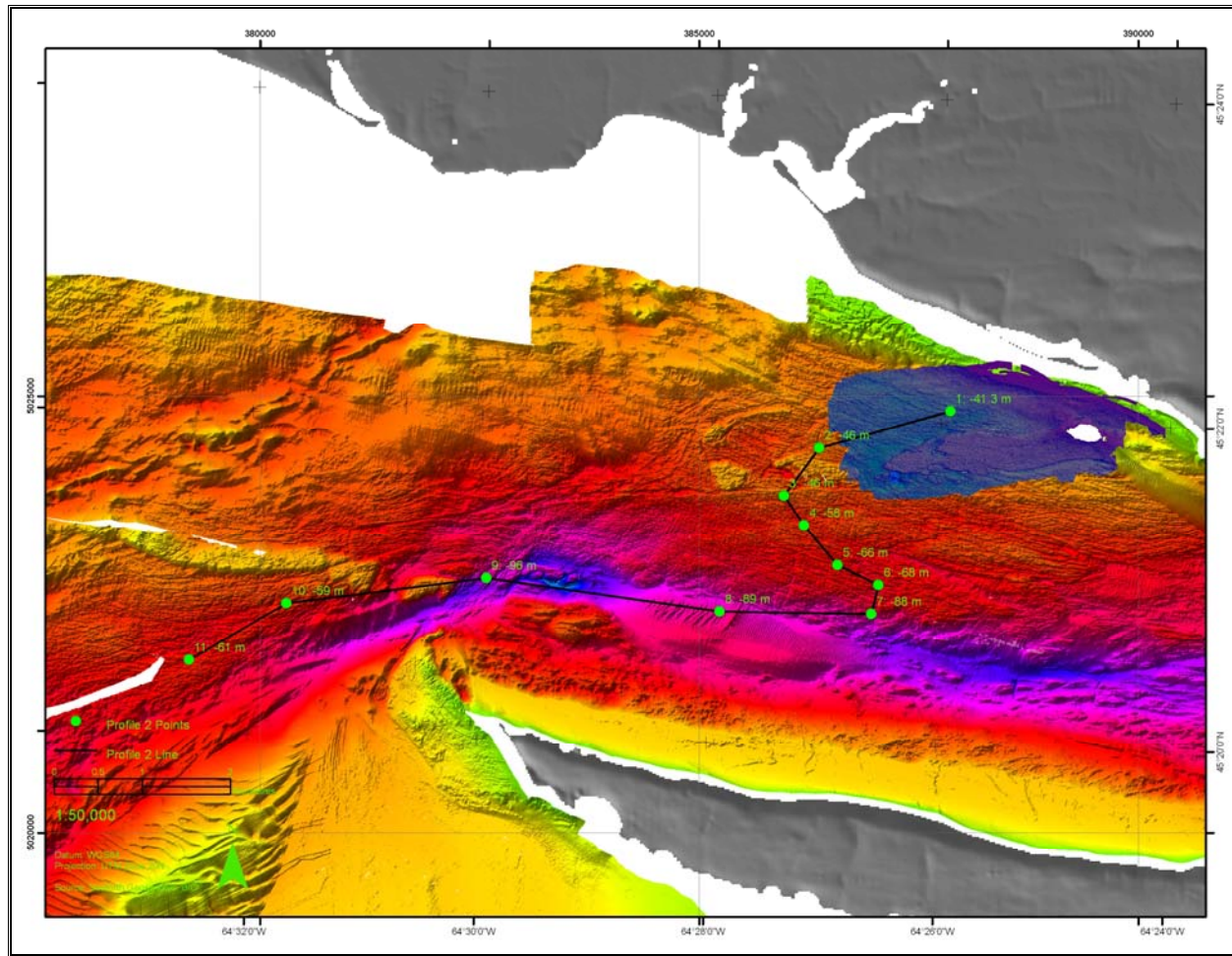


Figure 7. Locations of Profiling Current Data on July 10, 2008

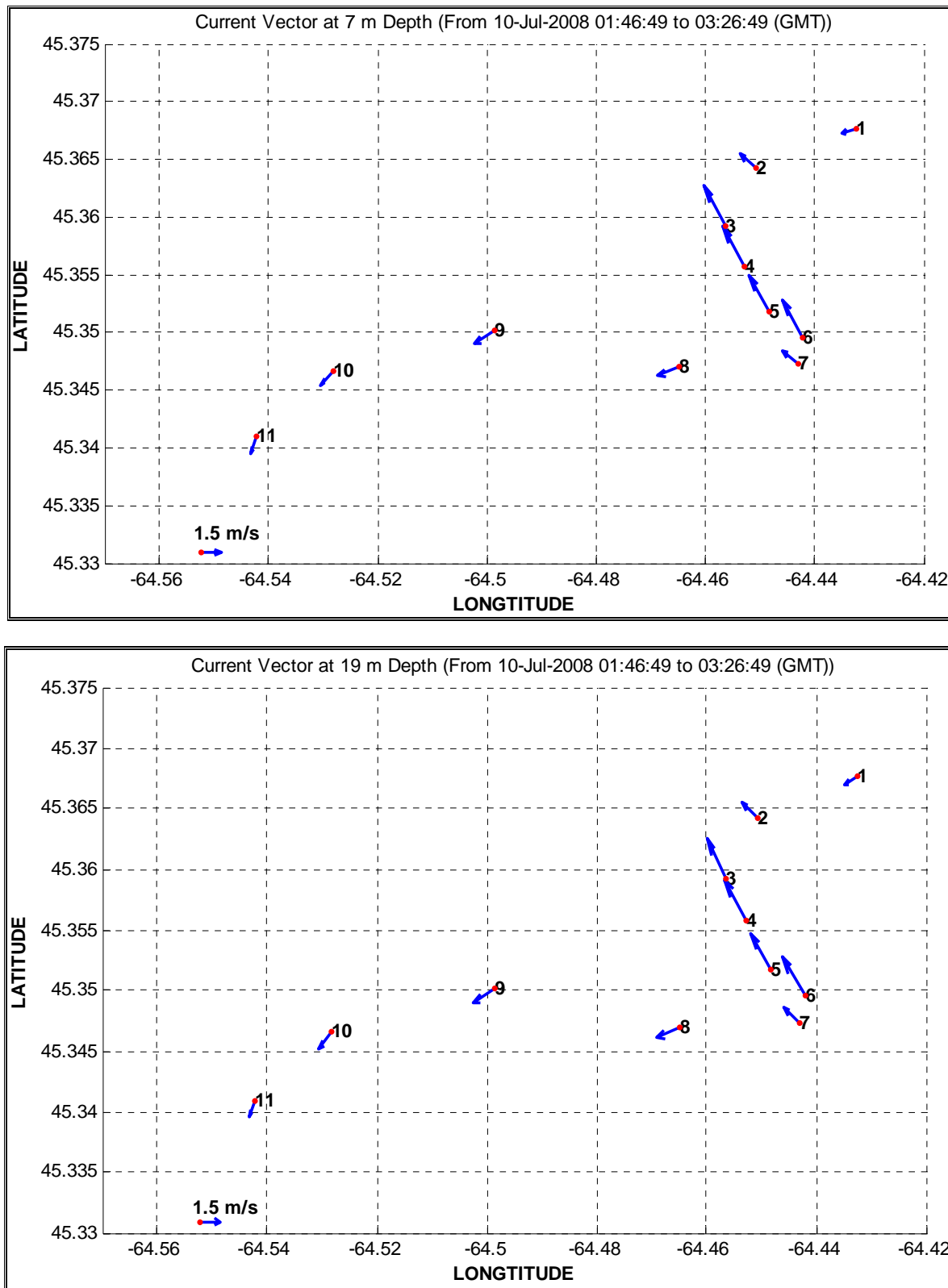


Figure 8. Stick Plots of Profiling Data on July 10, 2008

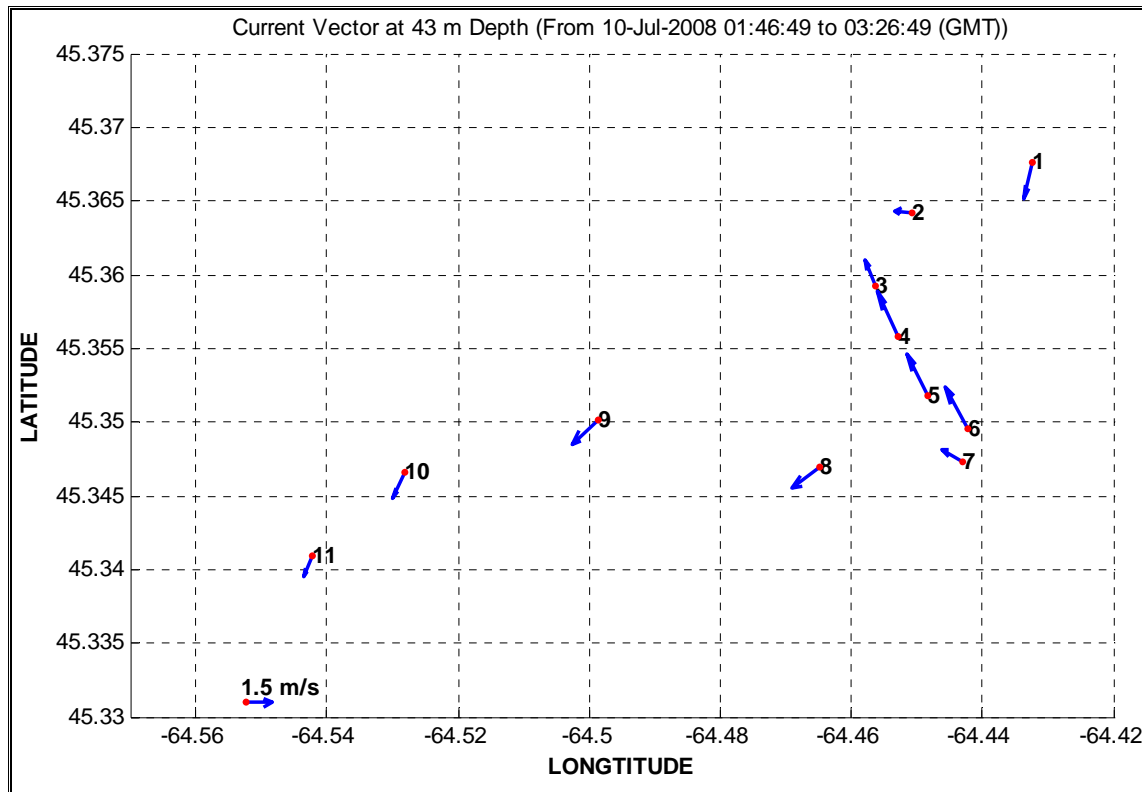
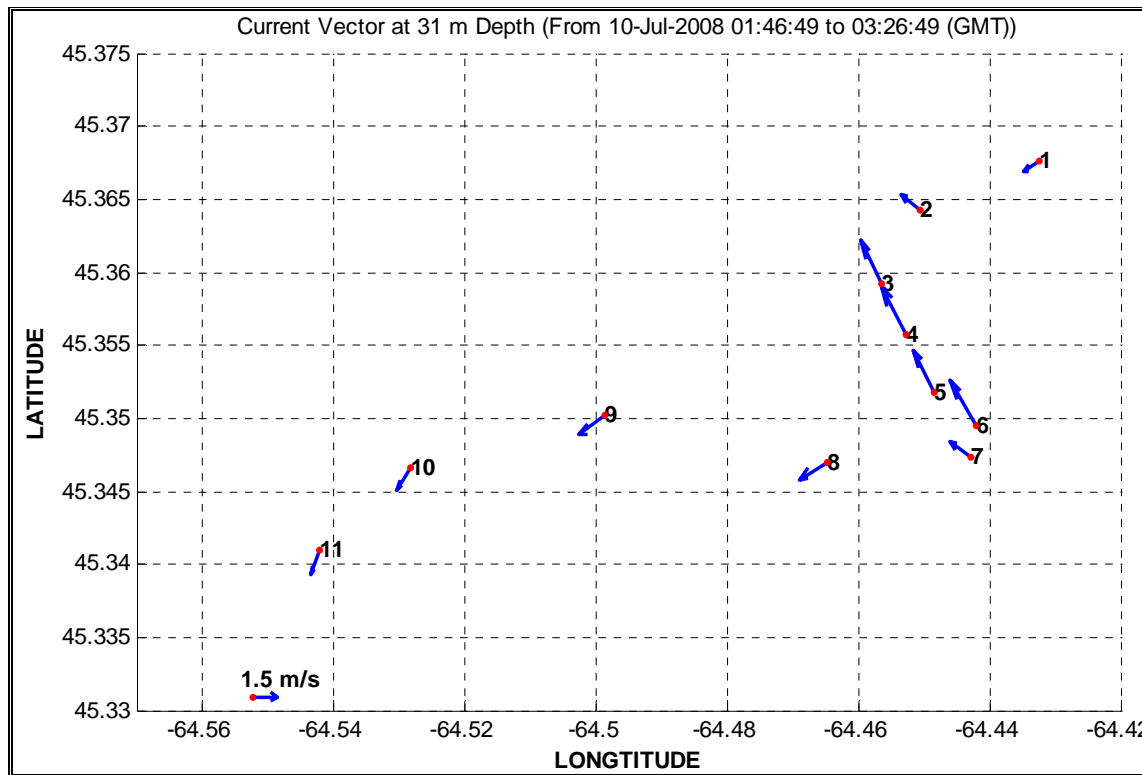


Figure 8. (cont'd): Stick plots of profiling data on July 10, 2008

From Station 1 to Station 6

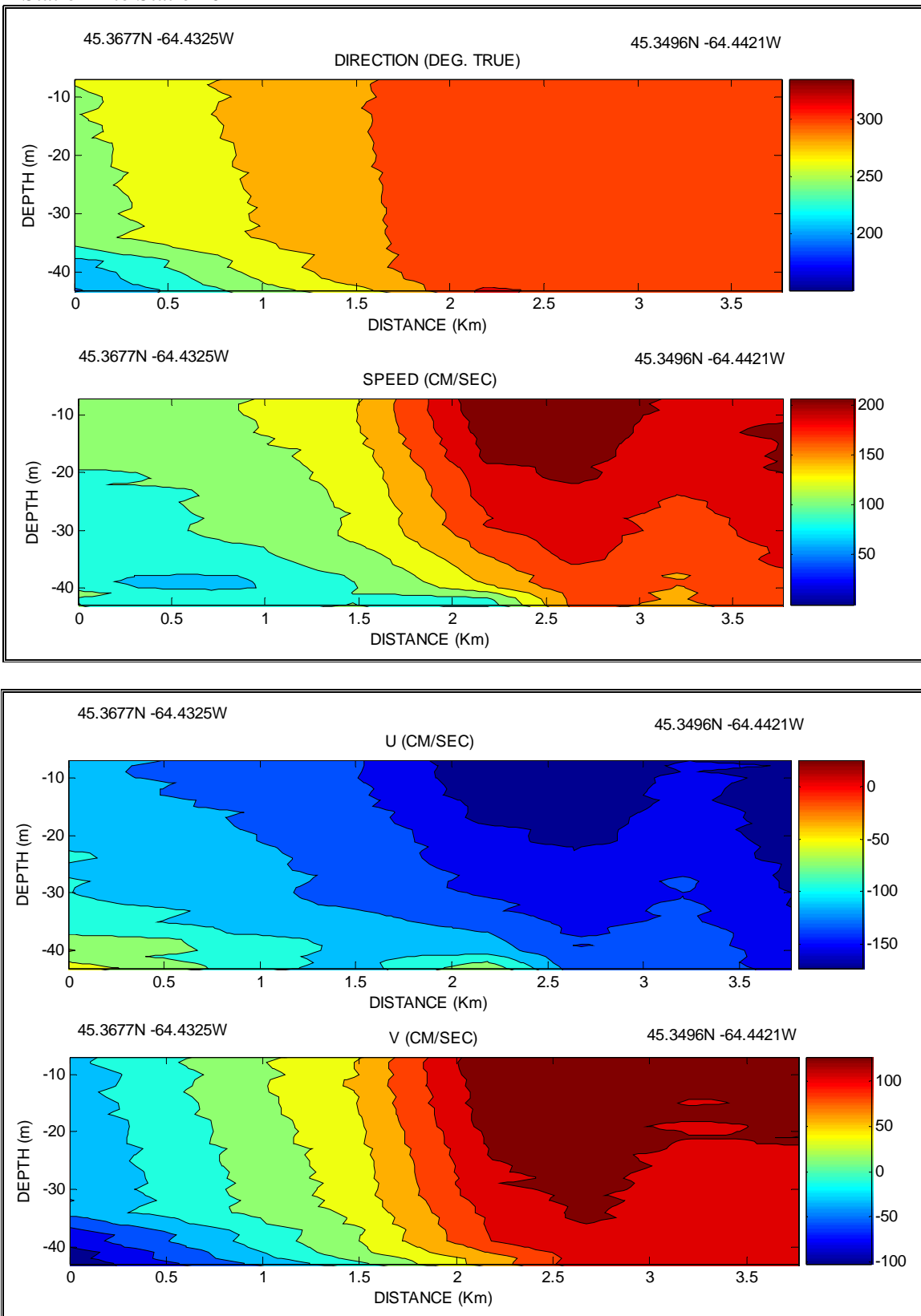


Figure 9. Transect Plots of Profiling Data on July 10, 2008

From Station 7 to Station 10

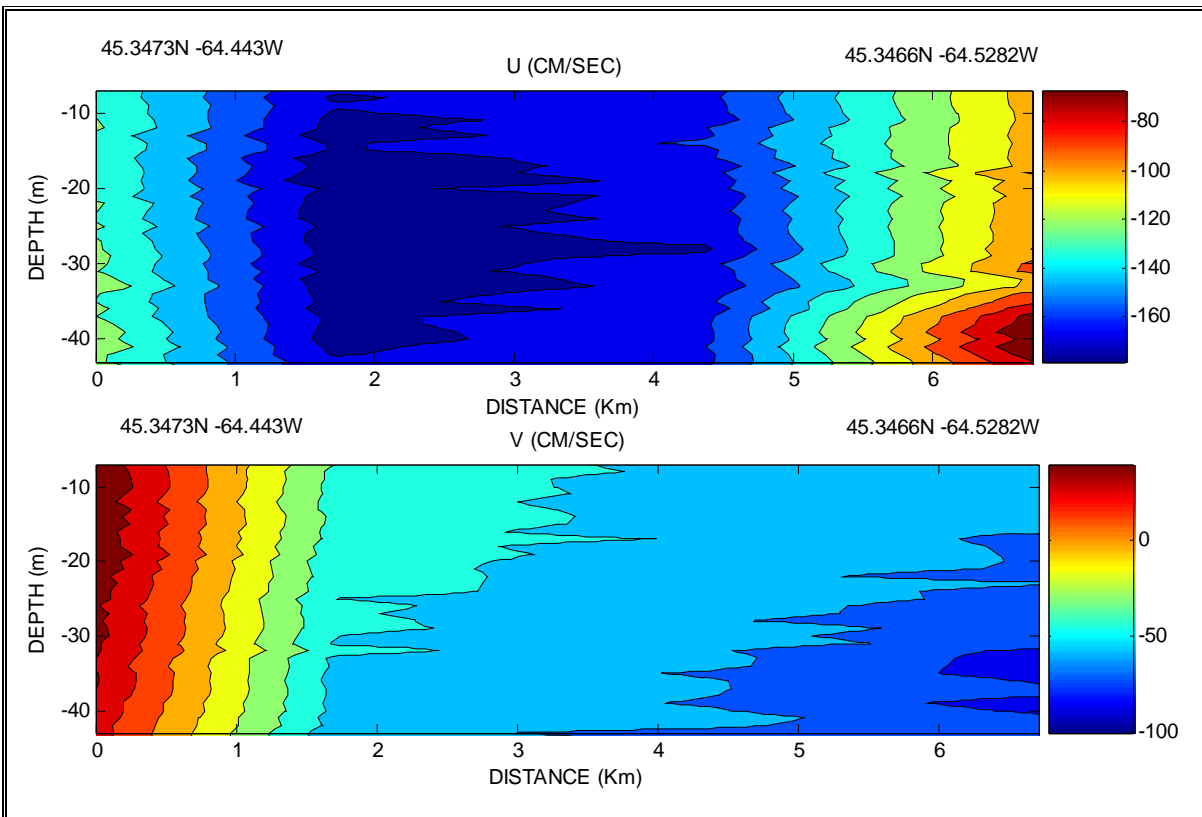
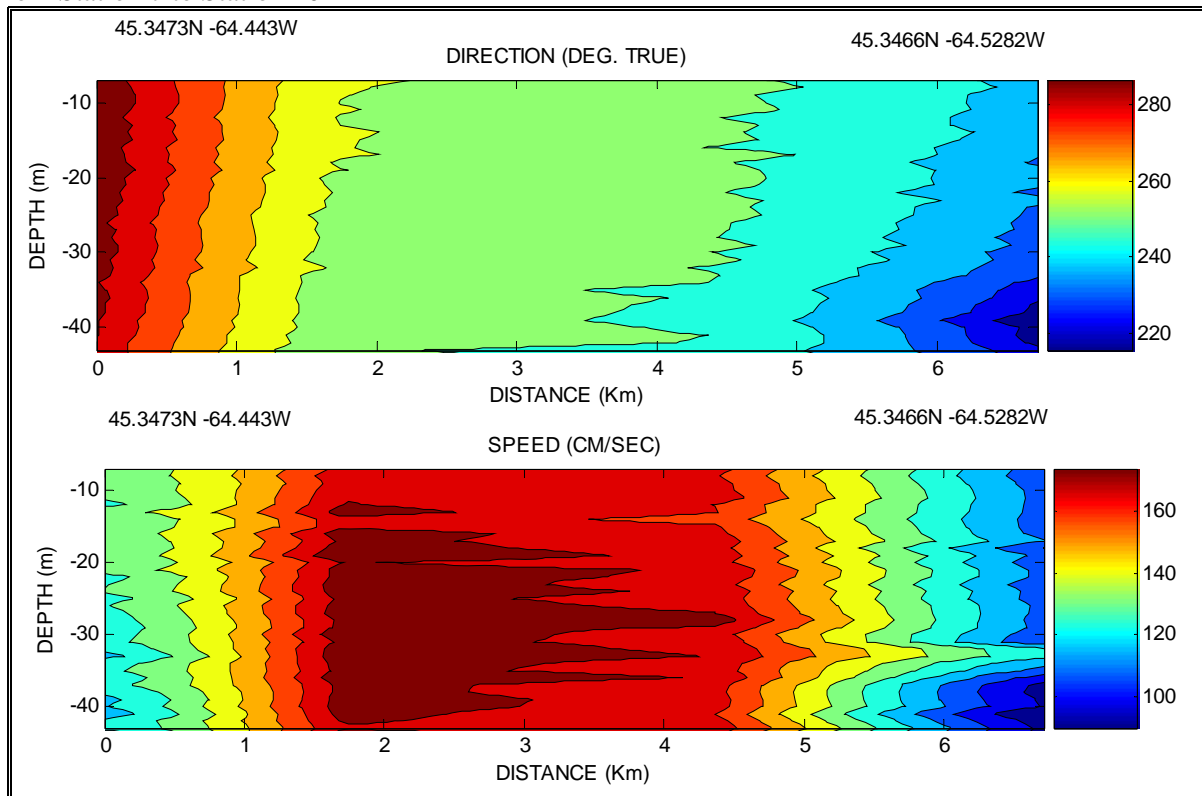


Figure 9. (cont'd) Transect Plots of Profiling Data on July 10, 2008

3.0 Moored ADCP Data

ADCPs measure time series of water current velocities through the water column. Currents in Minas Passage were measured by a bottom-mounted RDI 300 kHz ADCP at 4 different sites for a month period. There is only 1 day of data for Site 2. Figure 10 gives the mooring diagram of the instruments.

- Site 1: May 2 – June 4, 2008
- Site 2: May 4 – May 5, 2008
- Site 3: June 4 - July 9, 2008
- Site 4: August 20 – September 23, 2008
- Site 5: February 14 – March 28, 2009

In this section, the analyses of the ADCP data for sites 1, 3, 4, and 5 were presented by rose plots, harmonic analysis of tidal currents, power spectral density plots, time series plots, and statistical summaries. Data from site 2 were only presented in time series plots due to the short period that the data covered. Figure 10 gives the mooring diagram of the instruments.

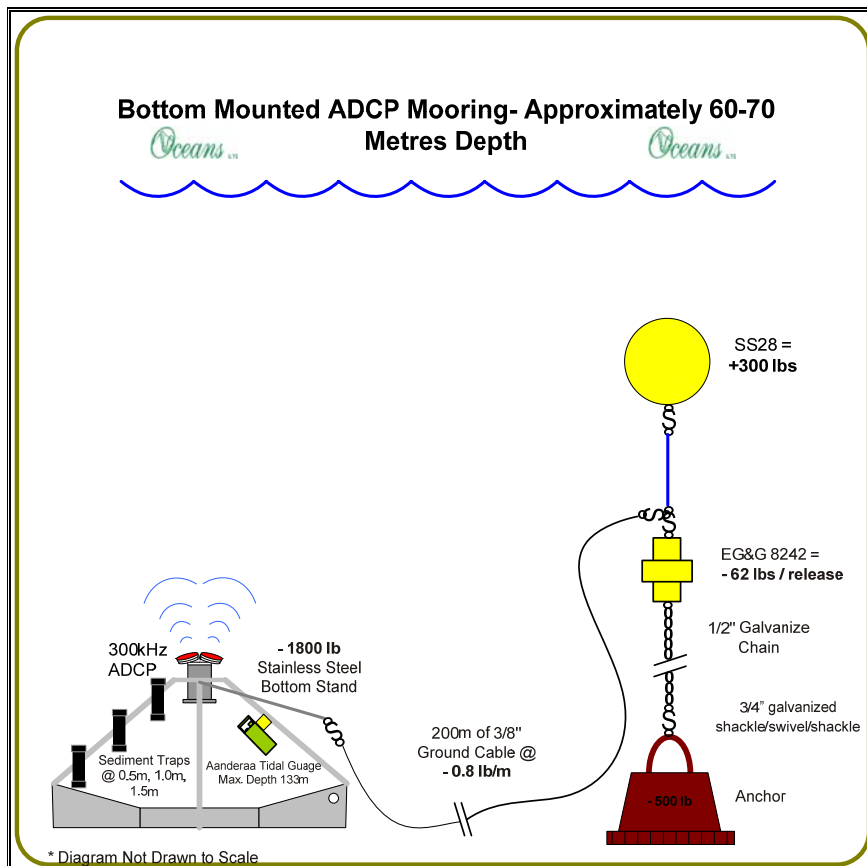


Figure 10. Mooring Diagram, Minas Basin

3.1 Current Speed and Direction

3.1.1 Mean and Maximum Current Speed

The mean speed, mean velocity and maximum current speeds with the corresponding directions at specific water depths at each site are presented in Table 2. Currents were extremely high reaching speeds between 4.5 and 5.2 m/s at the surface during spring tides. The currents had similar speeds at each site. The strongest currents were measured at site 1 located near the center of the Channel. Its near-surface speeds were approximately 0.6 m/s higher than the current speeds at the other three sites. Current speeds decreased gradually with depth. Usually, the difference in maximum speeds was approximately 1.3 m/s between surface and bottom at each site. The currents were still extremely high near the bottom with maximum speeds between 3 and 4 m/s. Currents were mainly aligned in the along-channel direction throughout the water column. The slight difference in current directions between the five sites was probably due to the bottom bathymetry.

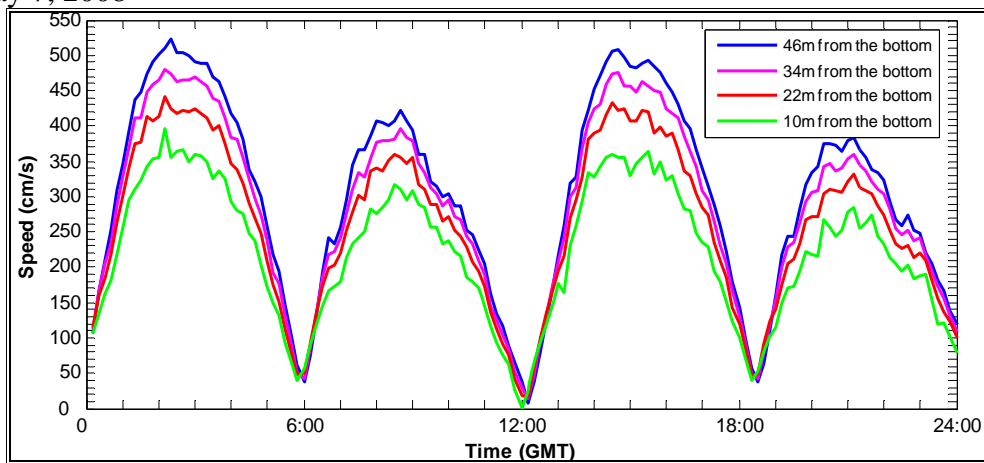
Table 2: Mean and Maximum Current from Each Site

Site No.	Depth (m)	No. of observations	Mean Speed (cm/s)	Mean Velocity (cm/s)	Dir (°T)	Max speed (cm/s)	Dir (°T)
Site 1	12	4845	249.8	42.4	SE	522.1	108
	24	4845	234.8	41.4	SE	483.9	111
	32	4845	221.6	40.2	SE	451.9	111
	36	4845	214.2	39.1	SSE	441.8	111
	48	4845	183.1	35.0	SSE	396.8	112
Site 3	14	5029	203.6	63.7	SEE	458.0	116
	22	5029	194.9	60.5	SEE	523.7	240
	30	5029	183.5	56.0	SEE	423.6	120
	38	5029	168.5	49.2	SEE	385.2	115
	46	5029	142.5	38.0	SEE	324.4	115
Site 4	14	4863	204.3	63.9	SEE	441.3	113
	22	4863	195.9	60.9	SEE	429.8	112
	30	4863	184.5	56.0	SEE	410.0	117
	38	4863	169.1	49.0	SEE	374.2	112
	46	4863	139.2	34.8	SEE	302.4	111
Site 5	12	6887	210.8	35.0	SE	464.3	107
	24	6887	188.4	32.6	SE	406.0	107
	32	6887	165.6	29.8	SE	360.4	104
	40	6887	129.8	25.2	SE	287.4	117

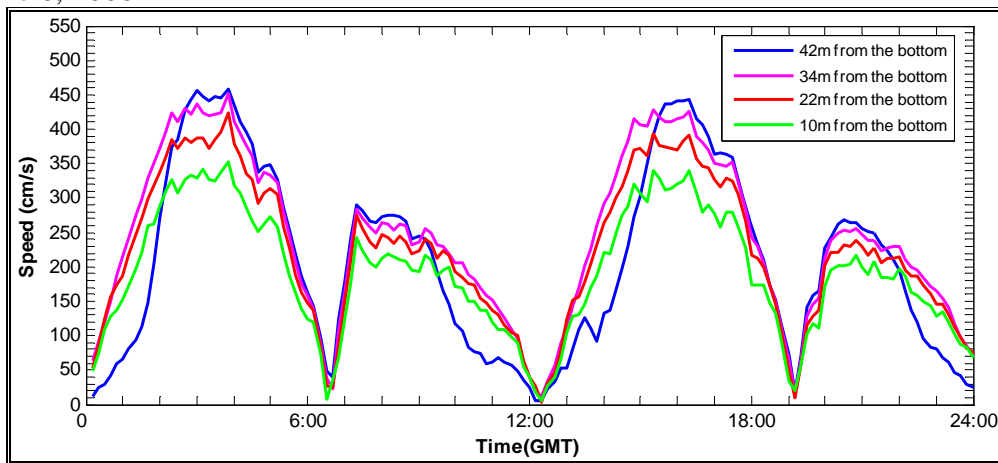
3.1.2 Current Speed during Spring/Neap Tides

The current in Minas Basin is dominated by the lunar tide with a period of 12.4 hours. Current speeds at four different depths during spring/neap tides at each site are presented in Figures 11 and 12. Current speeds showed some variation with depth for each site. On May 7, 2008, low current was at low tide (11:40) and high tide (5:20 and 17:50). The lowest currents always occur at low and high tide over a very short duration. During neap tides, the magnitudes of speeds decreased by 1 m/s as compared with spring tidal currents. The plots show that the flood (rising tide) and ebb (falling tide) periods in Minas Passage were not equal in duration: flood period was 0.5 hour shorter than ebb at site 1, and 1 hour shorter at sites 3, 4 and 5. As a result of tidal asymmetry, the flood currents in Minas Basin are normally stronger than ebb currents: peak flood current is approximately 1 m/s stronger than the peak ebb current. This tidal asymmetry may have effects on sediment transport.

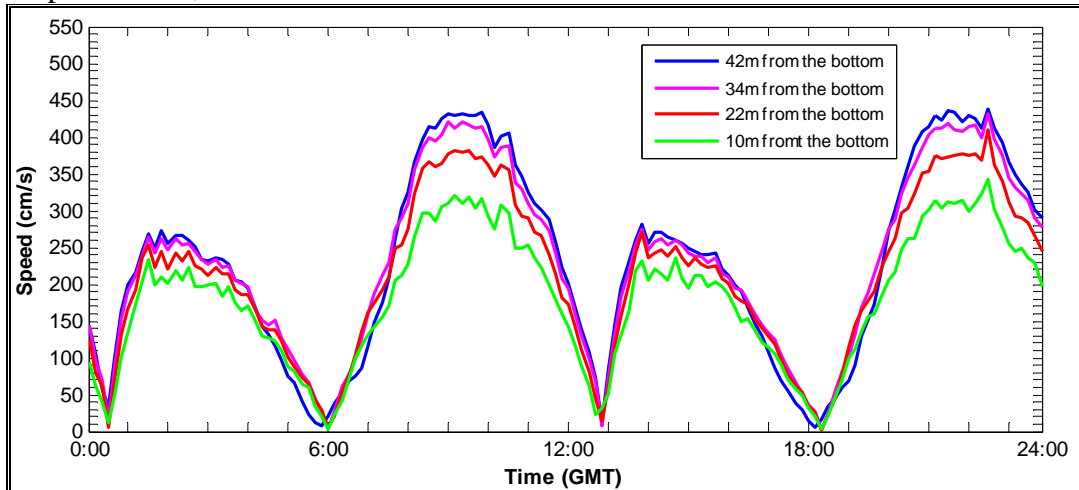
Site 1: May 7, 2008



Site 3: June 6, 2008



Site 4: September 18, 2008



Site 5: March 10, 2009

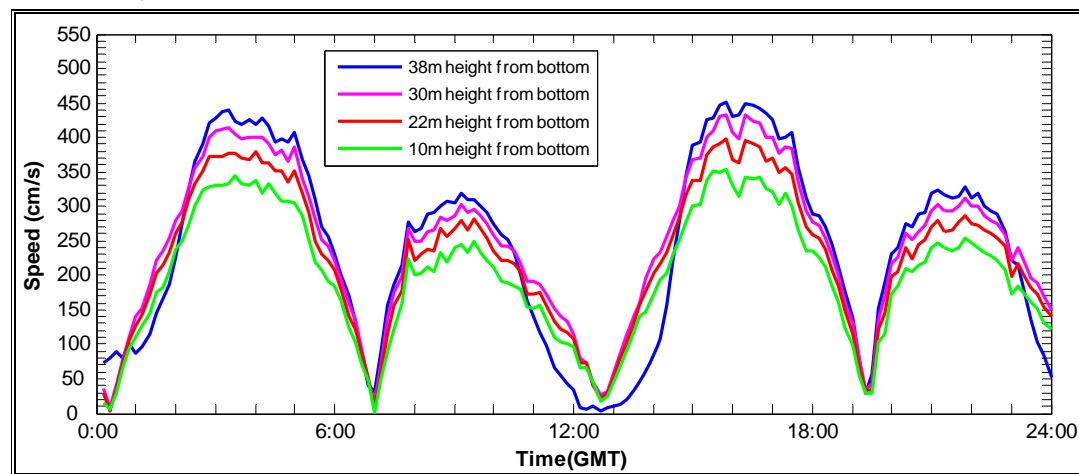
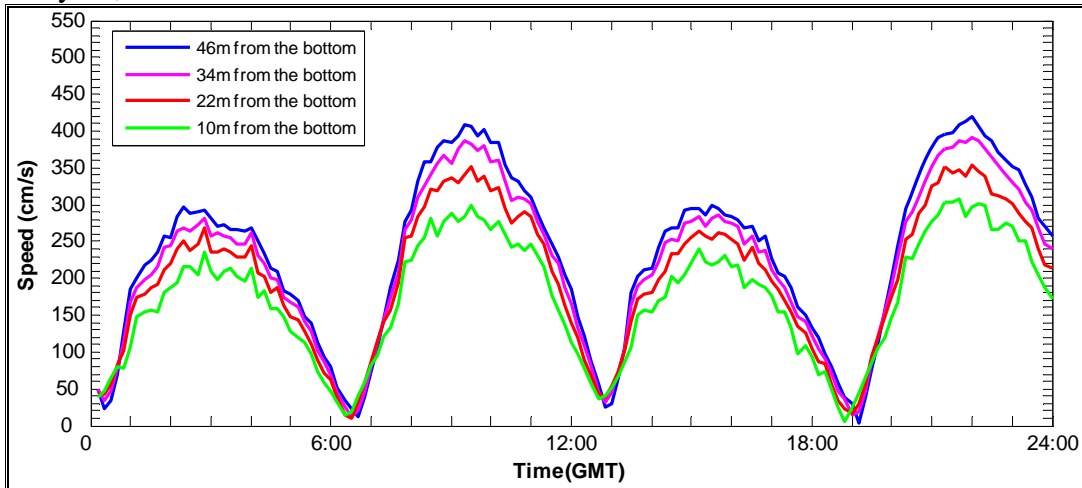
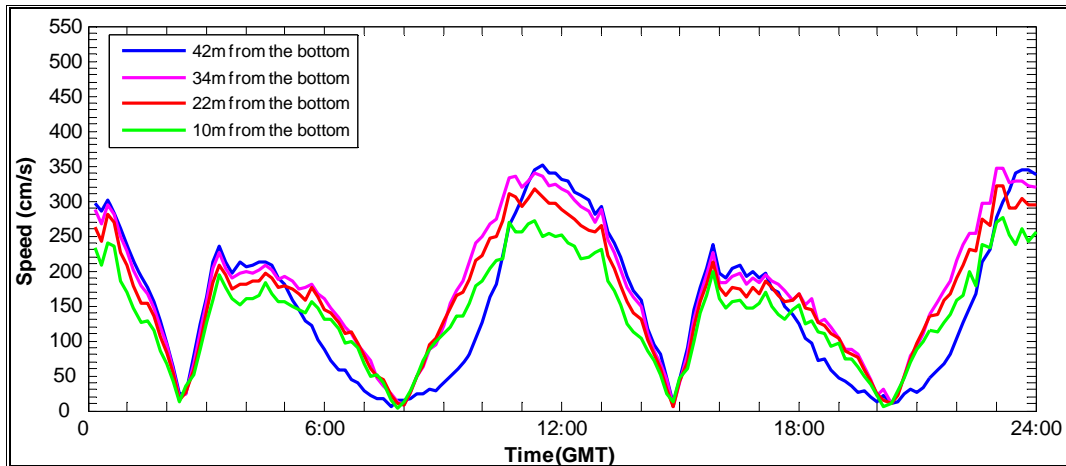


Figure 11. Current Speed during Spring Tides

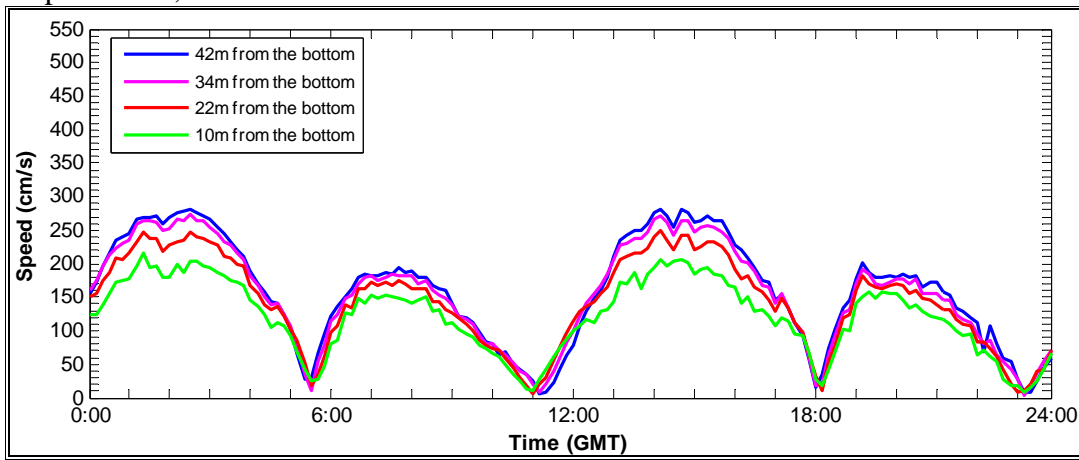
Site 1: May 14, 2008



Site 3: June 15, 2008



Site 4: September 9, 2008



Site 5: March 21, 2009

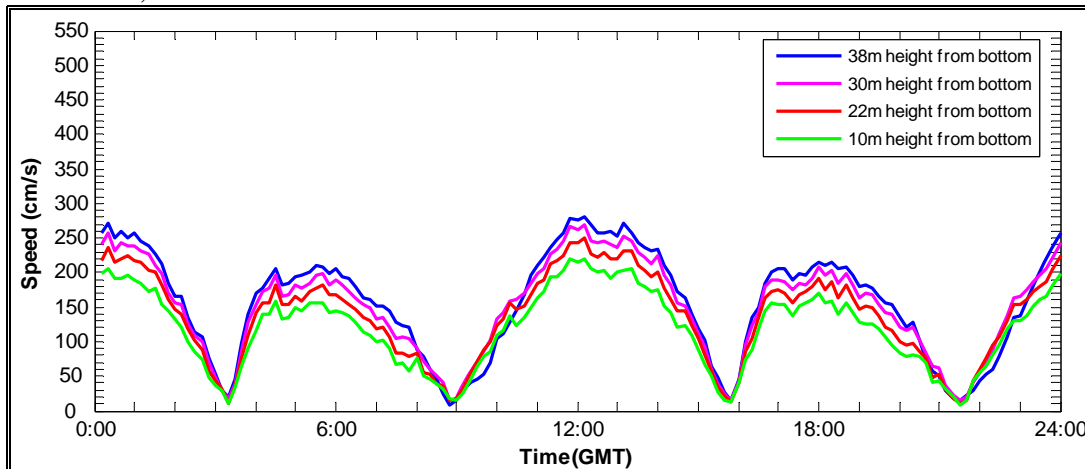


Figure 12. Current Speed during Neap Tides

3.2 Rose Plots

Rose plots show the current direction and percentage frequency of speed in specific intervals. For example, at a depth of 12 m at site 1 the speed is greater than 4 m/s for 12% of the measurement period and these speeds occur during rising tide. The rose plots in Figures 13 to 16 give details of the described pattern of flood and ebb circulation. Asymmetry was noted between flood and ebb current directions. At sites 1 and 3, during falling tide there was a slight counter-clockwise shift in current direction from the main axis of Minas Passage, and this shift was more obvious below 36 m depth, indicating that it probably resulted from geometric and inertial effects due to bottom topography. There was no asymmetry in current direction at sites 4 and 5 since falling tide was in an opposite direction to rising tide.

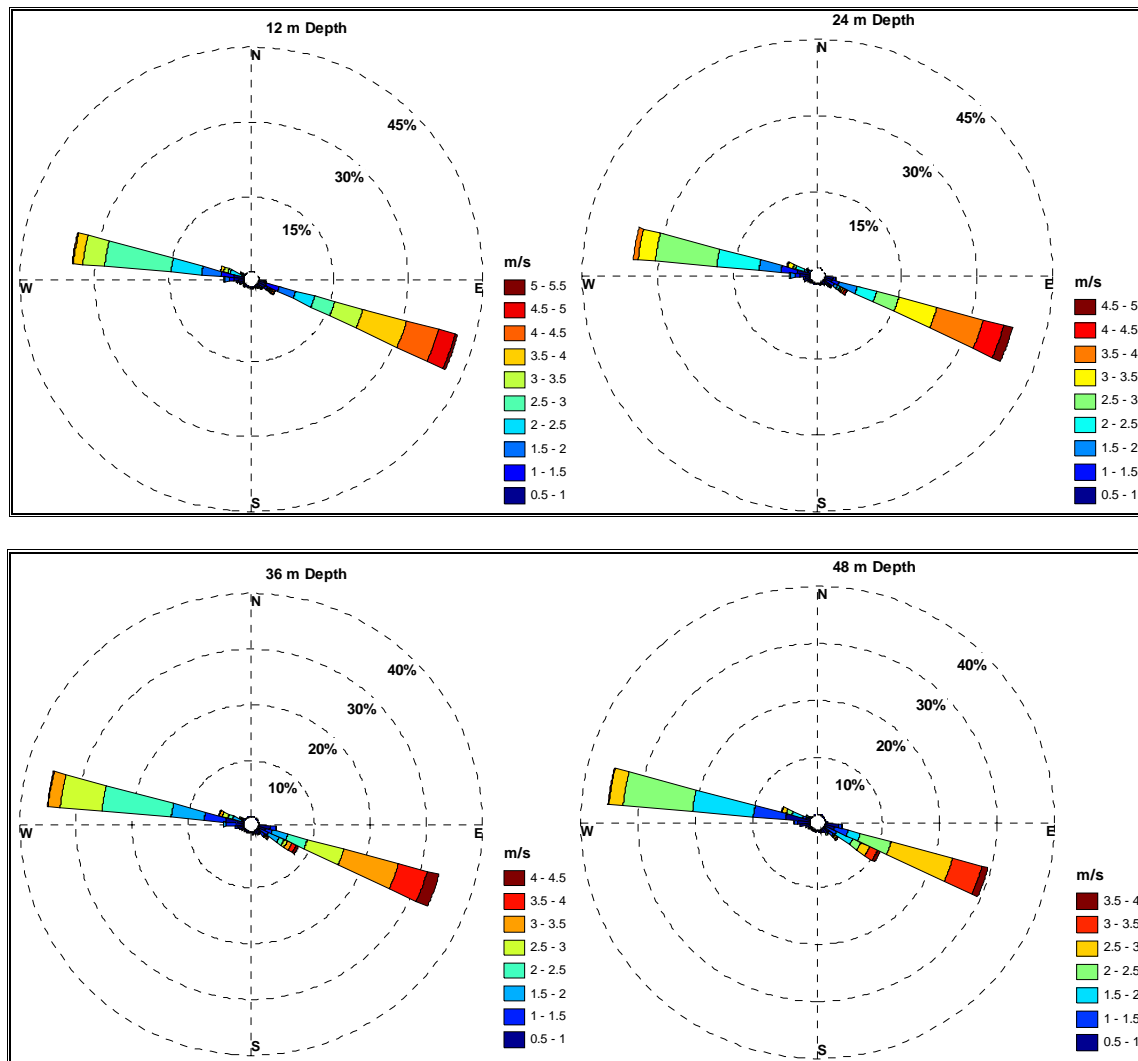


Figure 13. Rose Plots for Site 1

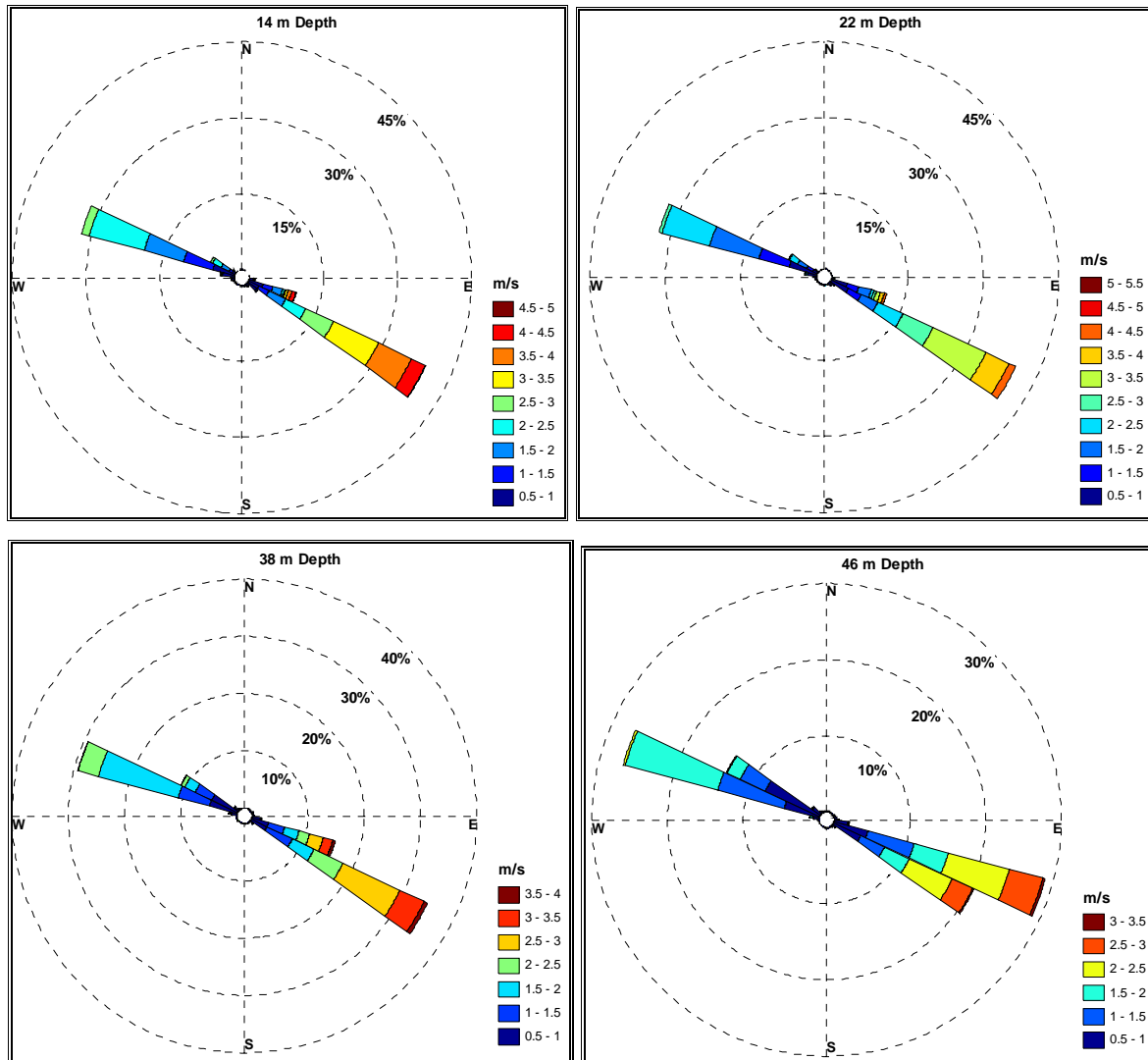


Figure 14. Rose Plots for Site 3

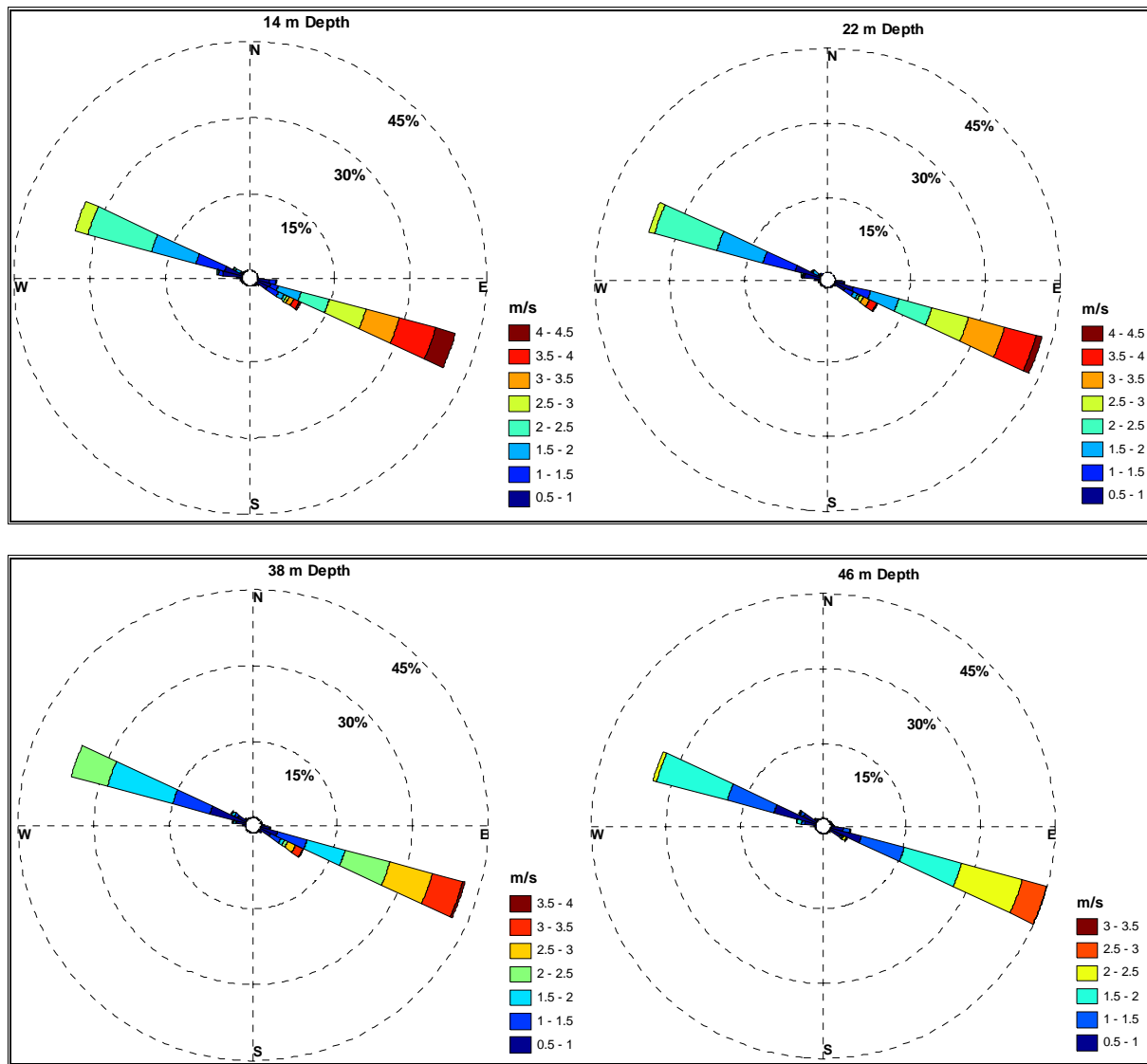


Figure 15. Rose Plots for Site 4

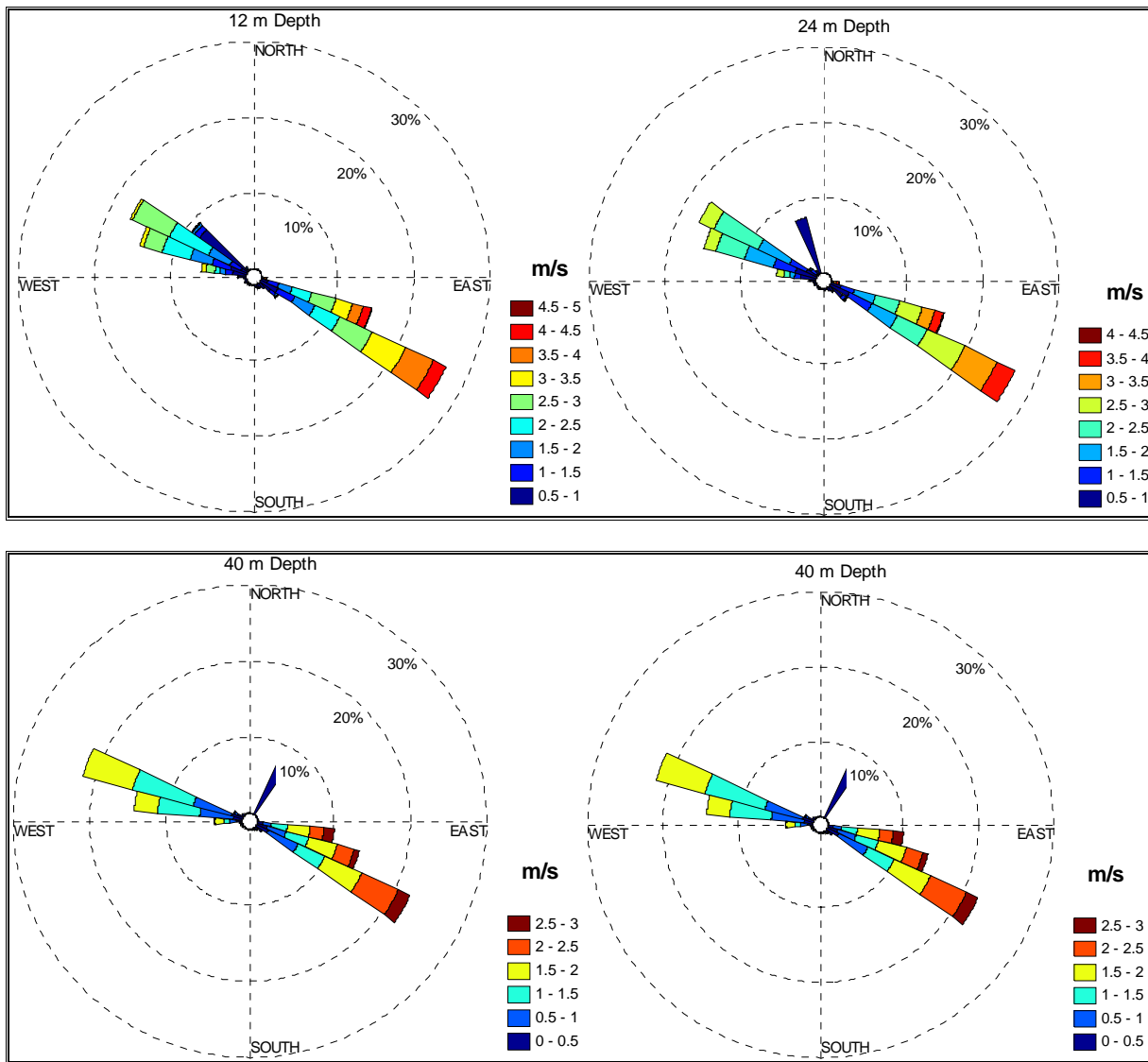


Figure 16. Rose Plots for Site 5

3.3 Semidiurnal Tides

A harmonic tidal analysis was performed to calculate the values of the major constituents in Minas Basin. M_2 is the semidiurnal lunar constituent which has a frequency of two cycles per lunar day. The lunar day is 50 minutes longer than the solar day because the moon advances about 12.5° in its orbit each day with respect to the sun's position. S_2 , the semidiurnal solar constituent has a frequency of two cycles per solar day. In Minas Passage, the current due to M_2 and S_2 are in the same direction. During spring tides the semidiurnal tidal current are $M_2 + S_2$ and during neap tides the semidiurnal tidal current is the difference between M_2 and S_2 . As M_2 was several times larger in amplitude than S_2 in Minas Basin, M_2 was the dominant tidal

constituent. The values for the M_2 constituent at different depths are presented in Table 3 and the values for S_2 are presented in Table 4. At sites 1 and 3, M_2 was 8 and 10 times larger than S_2 , respectively. At sites 4 and 5, M_2 was 5 times larger than S_2 . The relative variation in magnitude between M_2 and S_2 was probably due to the different sampling times during the year.

The magnitude of M_2 decreased with depth from a value of approximately 3.5 m/s near the surface to 2 m/s near bottom. The small amplitudes of the minor axes indicate a weak cross-channel flow. The rotation angle of the tidal ellipses gives an estimate of the orientation of the tidal constituent at the given frequency, with respect to a pre-established coordinate system. A positive value for the length of the semi-minor axis indicates that the current rotates counter-clockwise around the tidal ellipse, while a negative value indicates a clockwise rotation. In Minas Basin, the direction of the tide changed so quickly that it was not possible to resolve the direction of the tidal rotation, whether it was clockwise or counter-clockwise. For instance, M_2 tides had negative minor axes indicating clockwise rotation for site 1, 3 and 4, and positive minor axes at site 5 indicating counter-clockwise rotation.

M_2 ellipses for different depths at each site are presented in Figure 17 which shows the direction and speed of the major semidiurnal constituents during a tidal cycle. The inclinations of tidal ellipses represent the degrees the major axes make with respect to east. The results show that tidal currents were aligned along the axis of the Passage with the exception of site 5 where the tidal currents were rotated clockwise by an angle of approximately 20 degrees, probably due to the bottom topography.

Table 3. M_2 Tidal Constituents

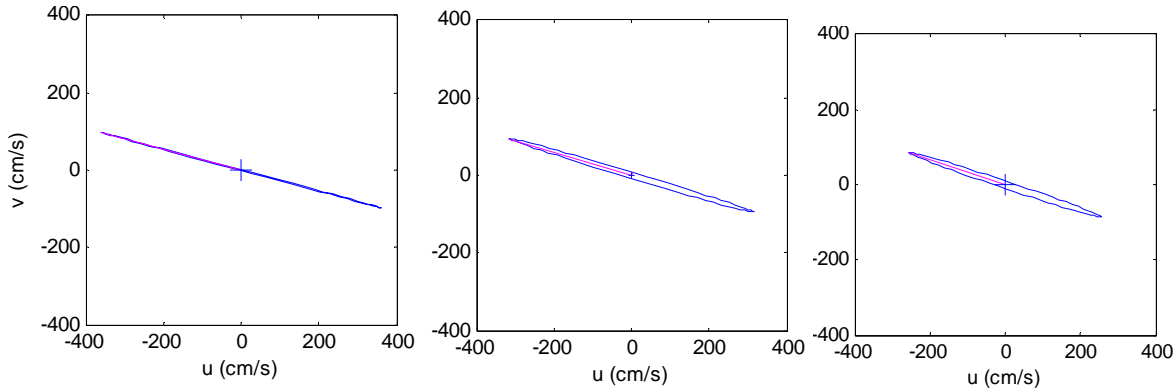
Site Number	Depth (m)	Major Axis (cm/s)	Minor Axis (cm/s)	Inclination (°)	Phase (°)
Site 1	12	373.85	-0.8286	164.93	219.19
	20	357.68	-3.7664	164.25	218.77
	32	329.95	-7.8485	163.33	217.82
	40	306.14	-9.4544	162.46	217.32
	48	271.71	-9.6922	161.42	216.91
Site 3	14	301.11	-2.7494	154.66	211.33
	22	287.57	-2.4893	154.65	211.34
	30	270.89	-2.3513	154.73	211.37
	38	248.39	-1.9836	155.02	211.27

	46	211.11	-1.5281	155.79	211.02
Site 4	14	307.08	-3.5380	158.99	298.16
	22	294.02	-2.4568	158.69	298.12
	30	276.62	-1.9272	158.45	298.02
	38	253.47	-2.1138	158.58	297.90
	46	208.52	-2.1191	160.33	297.28
Site 5	12	285.475	2.407	154.34	358.38
	24	255.225	2.693	154.36	358.19
	32	224.333	2.487	155.45	358.06
	40	175.515	0.404	161.08	357.96

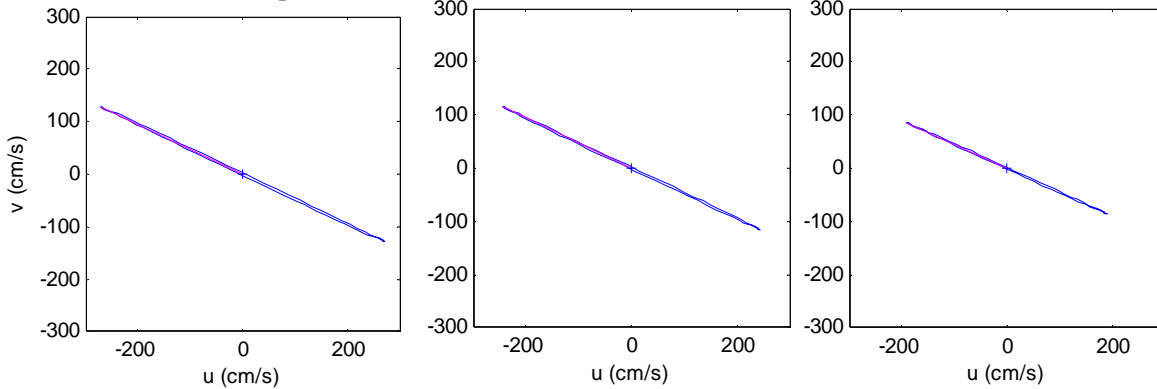
Table 4. S₂ Tidal Constituents

Site Number	Depth (m)	Major Axis (cm/s)	Minor Axis (cm/s)	Inclination (°)	Phase (°)
Site 1	12	47.127	3.8990	162.80	257.64
	20	45.643	4.3195	163.20	259.57
	32	41.255	3.1828	161.79	256.41
	40	38.654	2.8604	161.29	256.48
	48	34.402	2.7543	160.52	256.52
Site 3	14	29.518	-0.6586	156.06	270.86
	22	28.015	-0.8003	155.43	271.37
	30	26.379	-1.0309	154.85	271.73
	38	24.472	-0.6975	154.90	271.17
	46	20.471	-0.8695	155.67	270.39
Site 4	14	58.464	-0.7290	158.83	25.06
	22	55.946	-1.0270	158.65	25.71
	30	52.339	-1.4160	158.37	25.57
	38	47.827	-1.7000	158.32	25.72
	46	39.210	-1.8190	160.05	25.39
Site 5	12	49.628	1.819	162.18	103.64
	24	44.812	1.668	162.28	104.81
	32	38.951	1.495	163.71	105.08
	40	29.956	1.194	169.48	105.26

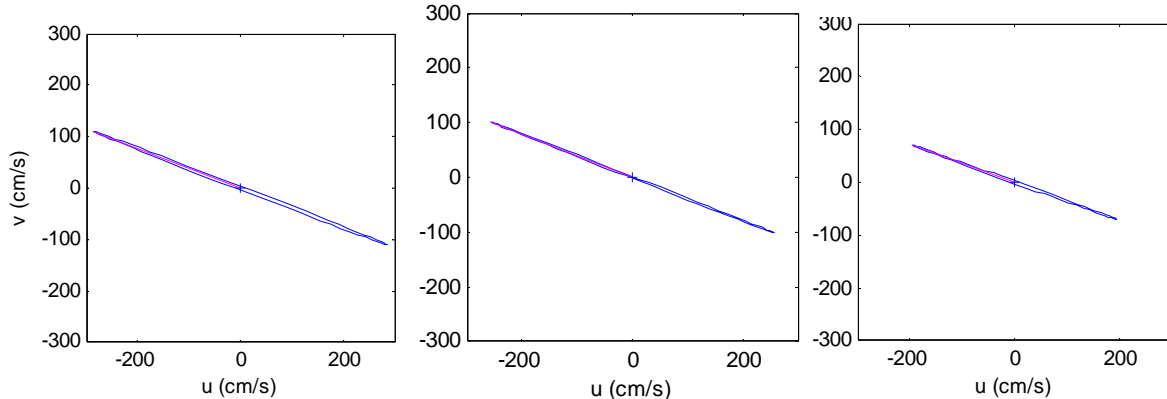
Site 1, 12m, 32m, 48m Depth



Site 3, 14m, 30m, 46m Depth



Site 4, 14m, 30m, 46m Depth



Site 5, 12m, 32m, 40m Depth

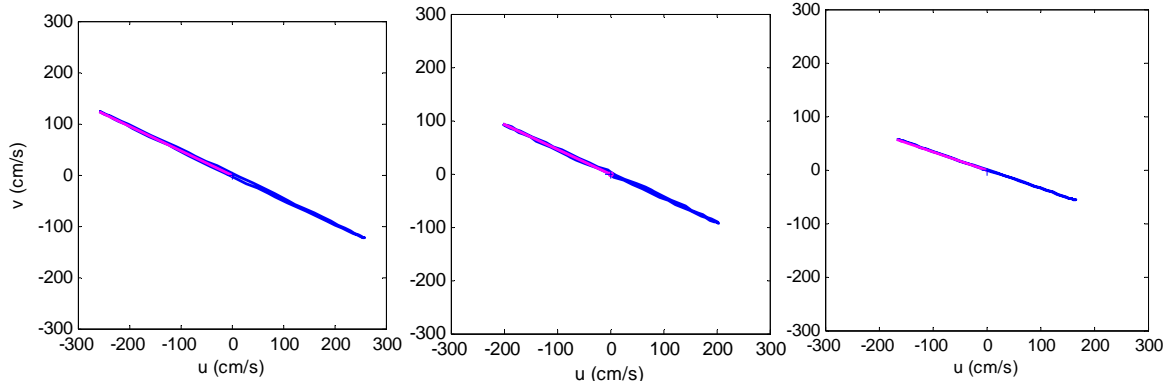
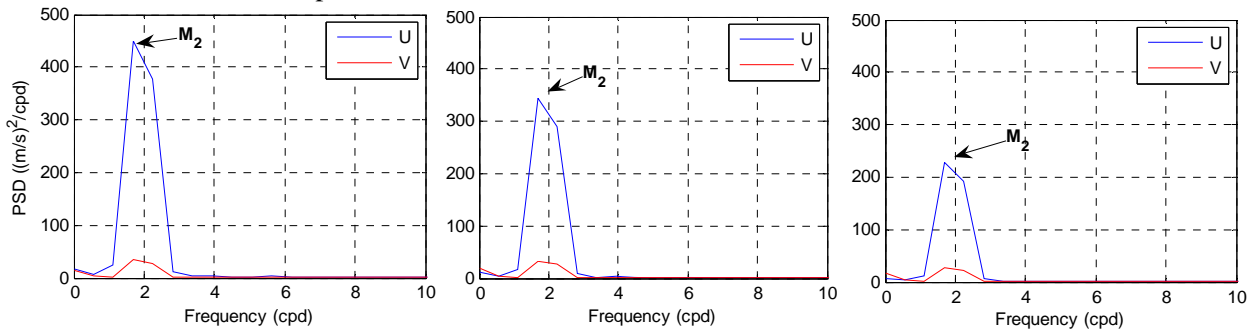


Figure 17. M₂ Tidal Ellipses at each site

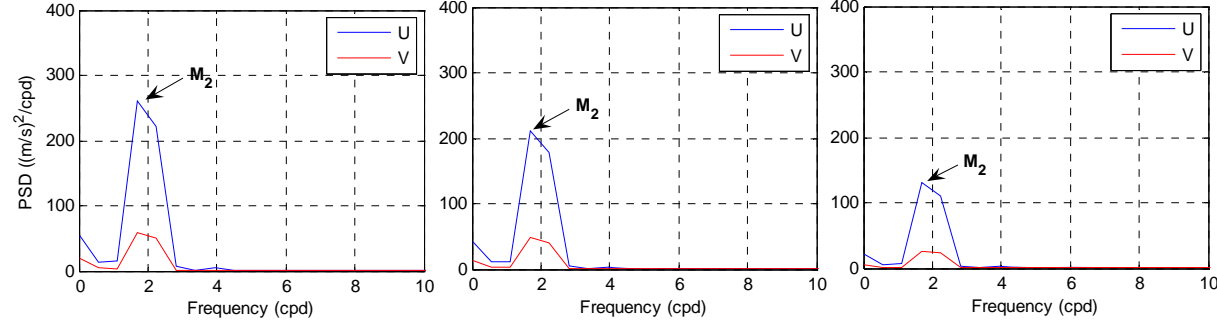
3.4 Power Spectral Density

Time series of current data from each site was decomposed into the East-West component U, and North-South component V. The Power Spectral Density (PSD) technique was performed on each of them separately. The following plots in Figure 18 show the results of the spectral calculations for both the U and V components. The results indicate that the semidiurnal tides with a frequency of 2 cycles per day dominated the energy spectrum at each depth for each site. Based on the tidal analysis in the previous section, the tidal constituent was the M_2 tide. The dominant velocity was the along channel.

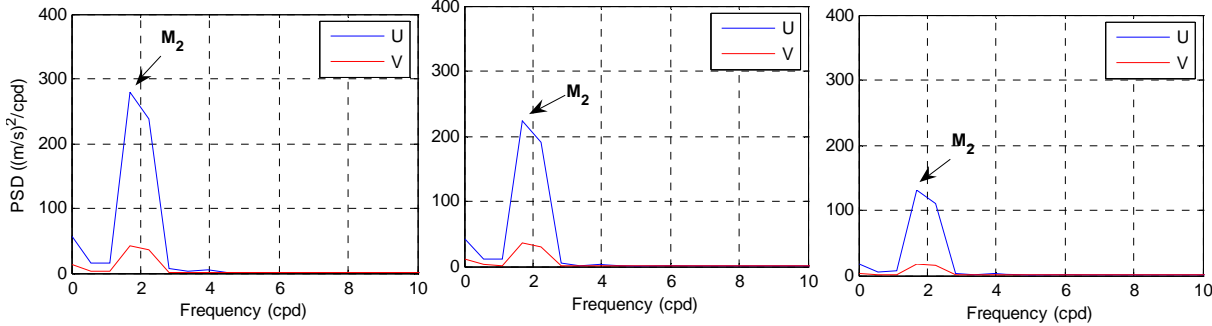
Site 1, 12m, 32m, 48m Depth



Site 3, 14m, 30m, 46m Depth



Site 4, 14m, 30m, 46m Depth



Site 5, 12m, 32m, 40m Depth

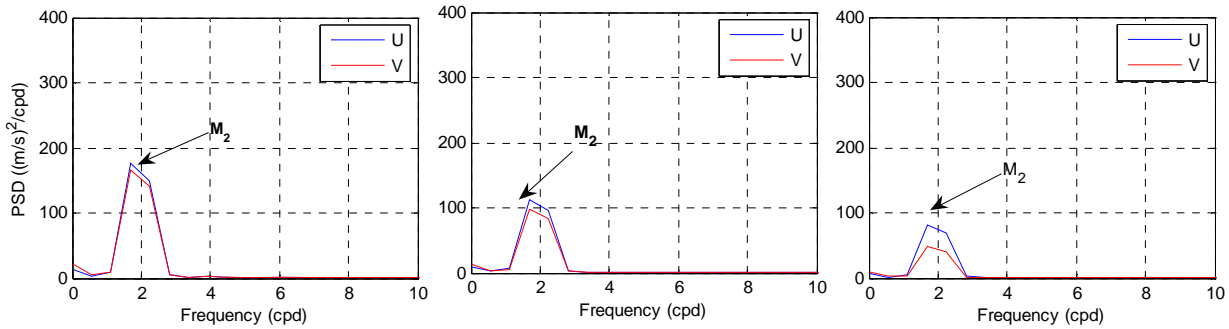


Figure 18. Power Spectral Density from ADCP data at each site

3.5 Time Series of Surface Currents and Tidal Heights

The time series plots of the current speeds and the corresponding tidal heights (Figures 19 to 22) at each site demonstrate the importance of the dominant semi-diurnal currents which have a frequency of two cycles per day. The tidal heights at sites 1 and 3 were measured by Aanderra water level recorders while the tidal heights at sites 4 and 5 were plotted from the pressure sensor on the ADCPs. The data for each site were chosen during spring tides at Minas Passage when the strong currents were due to $M_2 + S_2$. Since S_2 was much smaller than M_2 , the currents were still high during neap tides when the magnitudes of tidal currents were $M_2 - S_2$.

Site 1: May 5 - May 11, 2008

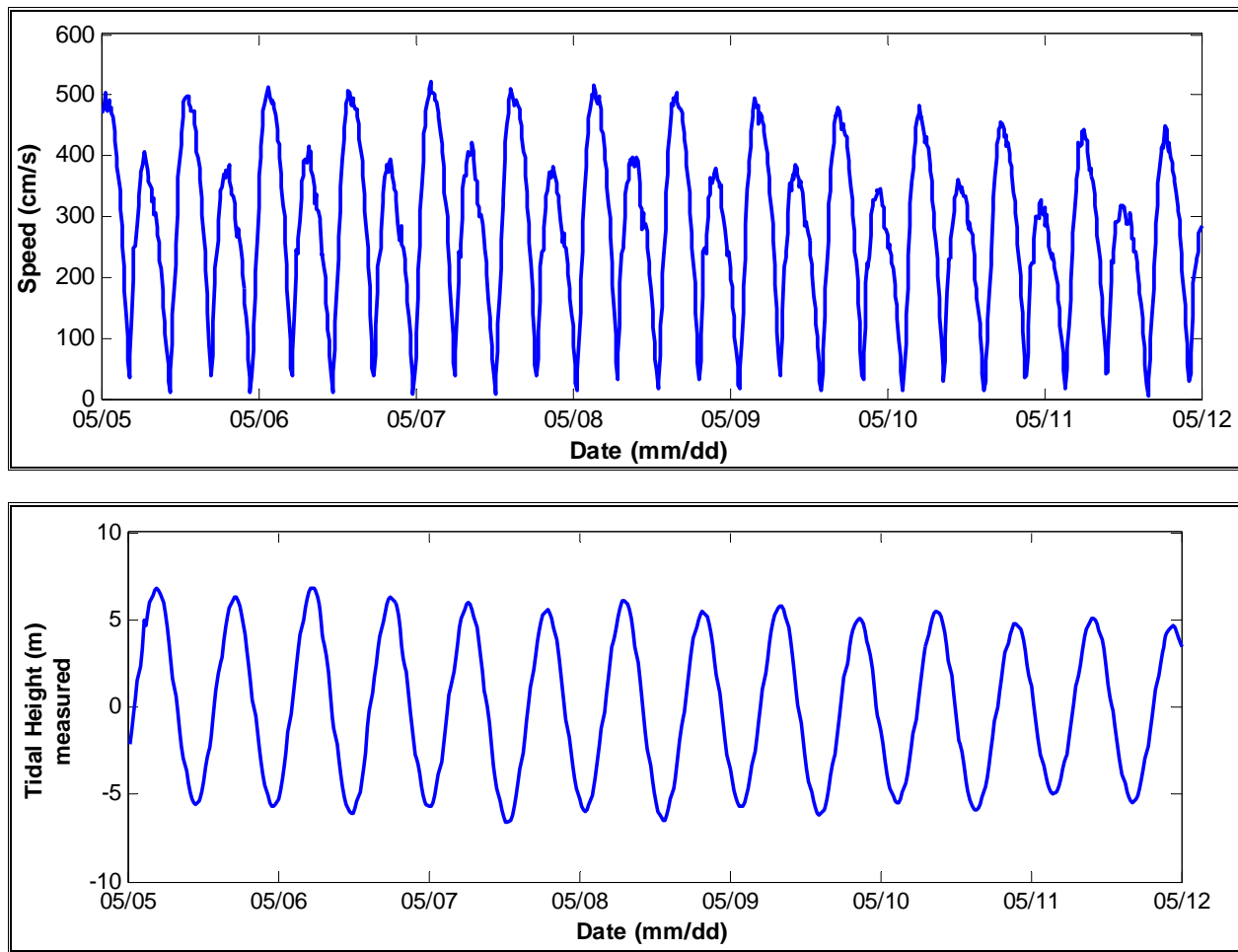


Figure 19. Surface Current and Tidal Height at Site 1

Site 3: June 6 - June 12, 2008

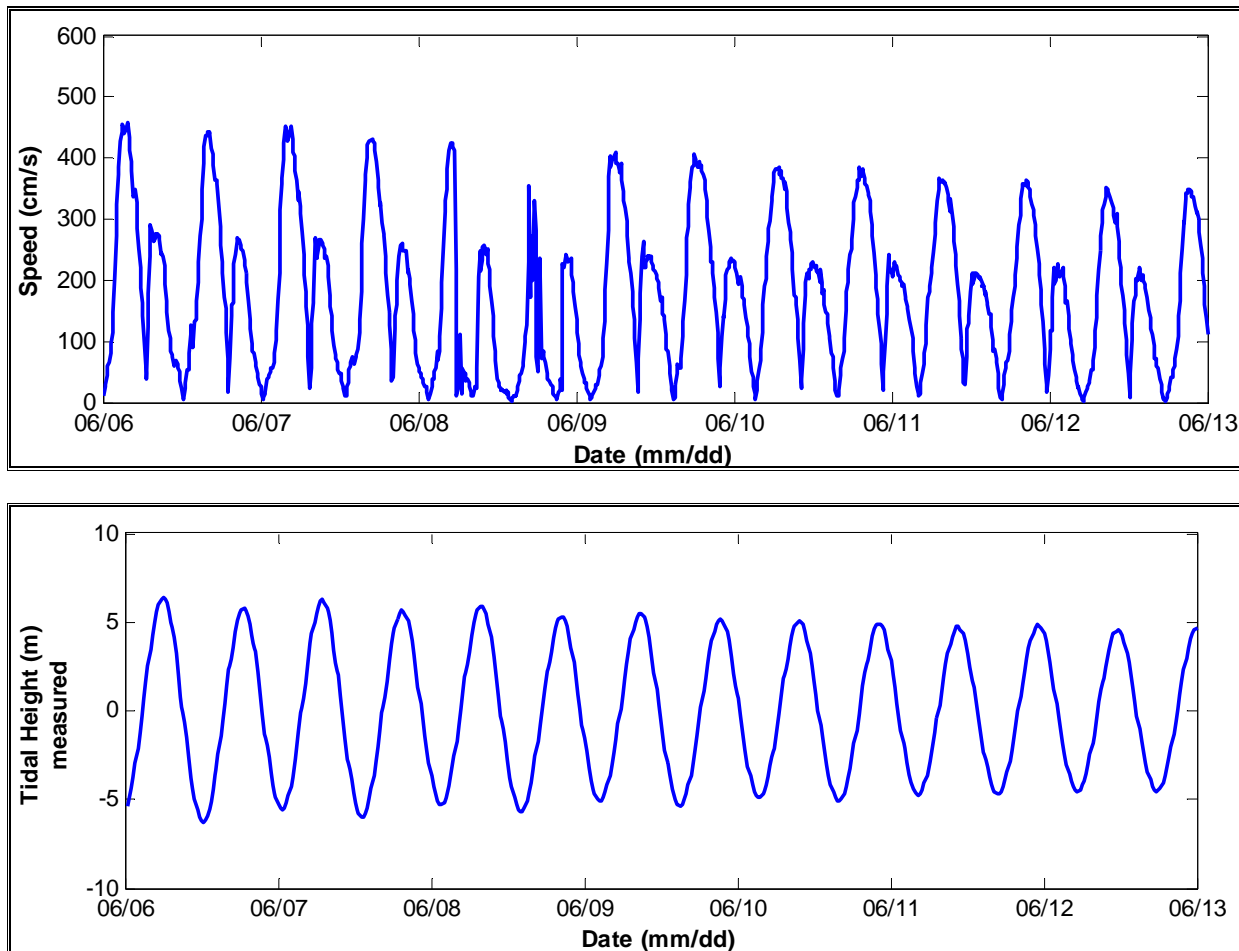


Figure 20. Surface Current and Tidal Height at Site 3

Site 4: September 16 - September 22, 2008

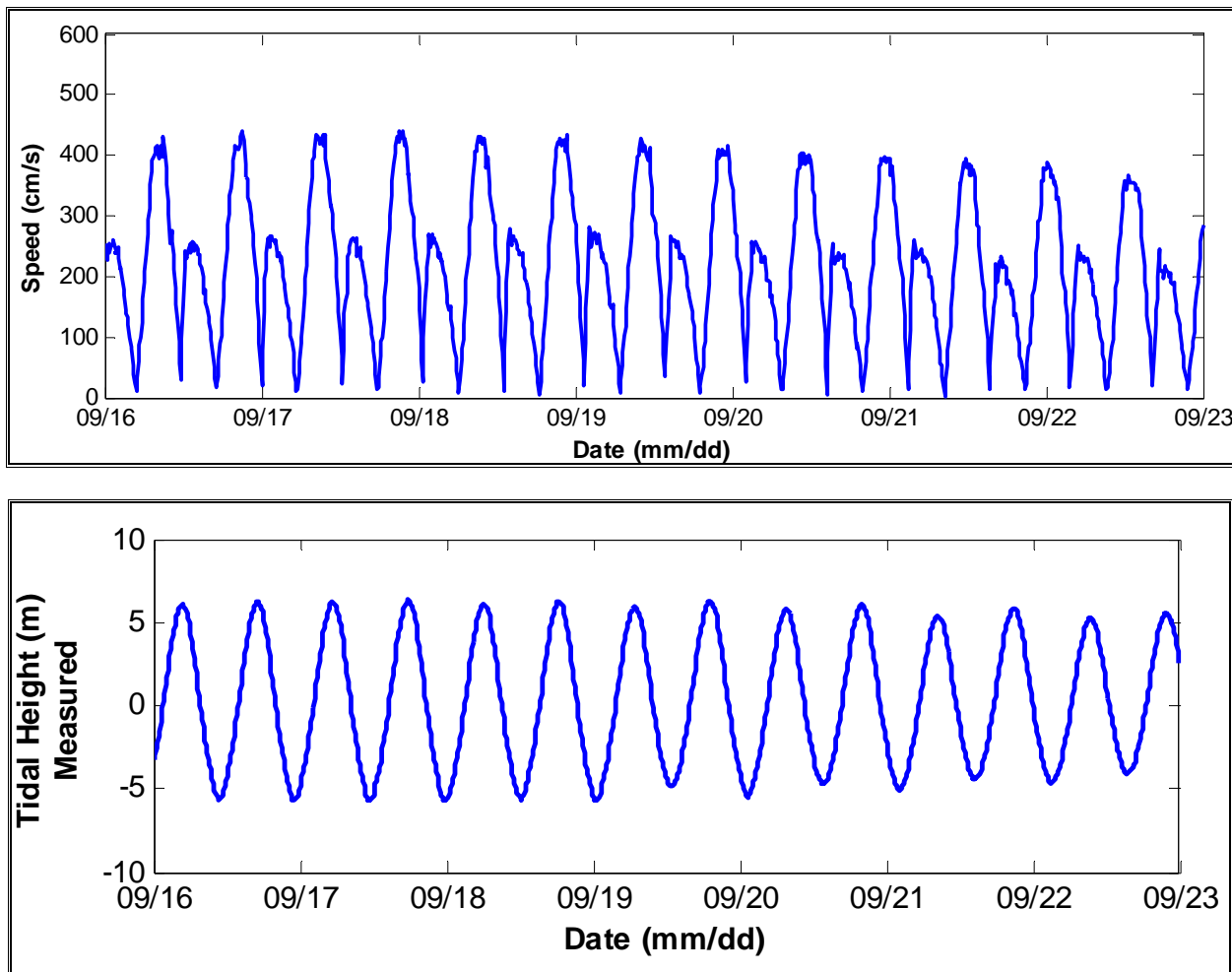


Figure 21. Surface Current and Tidal Height at Site 4

Site 5: March 7 – March 14, 2009

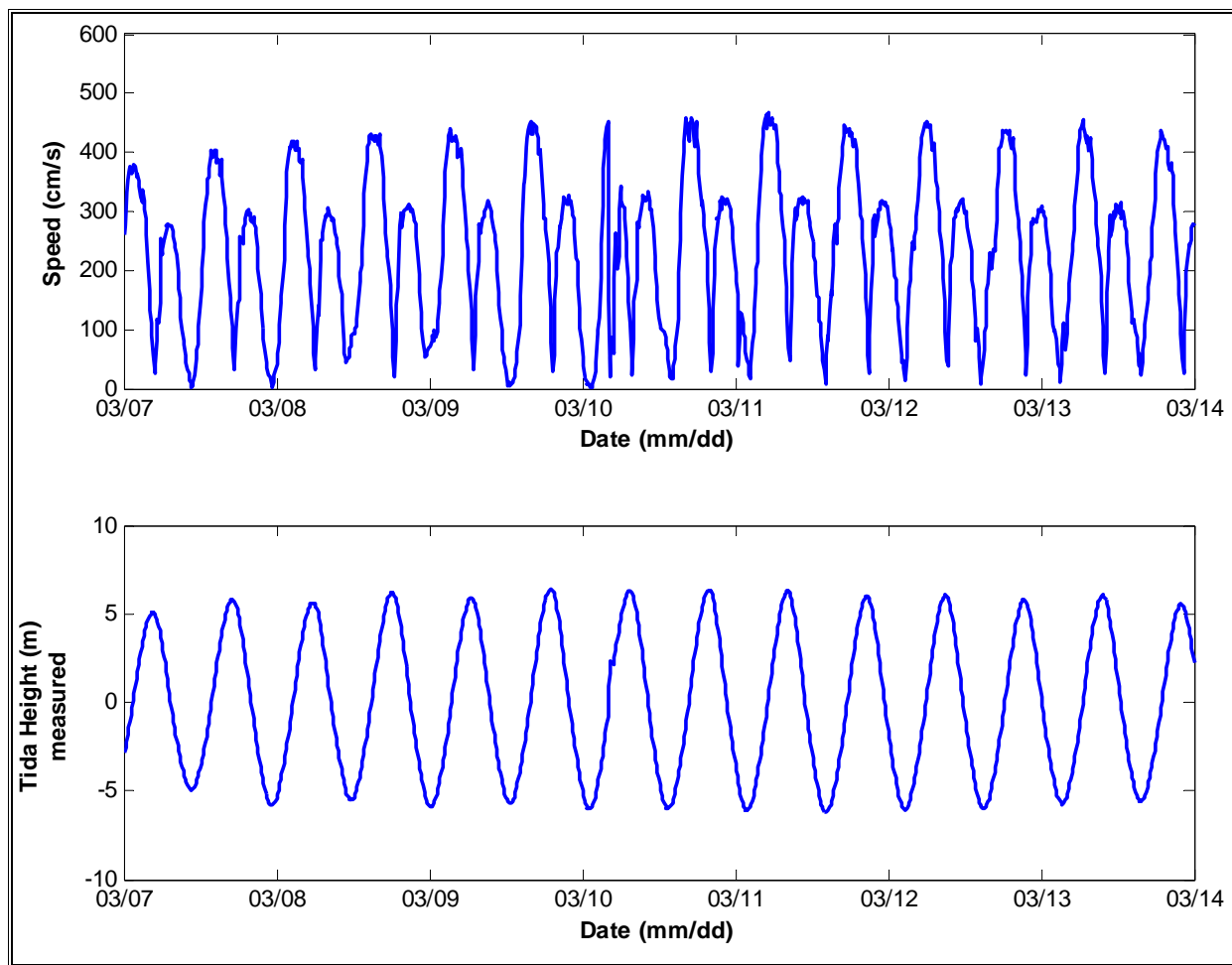


Figure 22. Surface Current and Tidal Height at Site 5

3.6 Time Series of Current Speed and Direction

The time series plots from the ADCPs are presented in Appendices 1 to 5. The time series plots demonstrate that the currents in Minas Passage followed a consistent and predictable pattern. It also verifies the previous observations and analysis. The tides were semidiurnal having two high tides and two low tides per day. The current tended to flow in two directions, out of Minas Basin during ebb tide and into the Basin during flood tide. The maximum current on each tidal cycle occurred during flood tide because flood tide was of shorter duration than ebb tide. The maximum speed during ebb tide had a value of approximately 1 m/s less than the maximum speed during the previous flood tide. The time series plots show that the time interval for the currents to reverse direction was very short.

Some anomalous phenomena have been observed by the ADCPs at site 5 during spring tides on February 13 and 14, March 11, and March 29 and at site 3 on June 8, 2009 (spring tides). The currents change direction and tend to have lower speeds than normal. The source of the phenomena has not been identified. It may be due to some oscillation or simply turbulence from the interaction of the high currents with physical boundaries. The phenomena was observed to occur during in-coming tides.

4.0 Bottom Current Data

An InteOcean S4 vector averaging current meter was attached to the bottom stand at a height of 0.5 m above the seabed at Site 5 during the sampling period of February 12 to March 29, 2009. The time series of the current data is presented in Appendix 6 and the time series for the pressure, temperature and salinity data is presented in Appendix 7. .

In the boundary layer, near bottom, the mean current speed was 77.4 cm/s as compared to 210.8 cm/s at a depth of 12 m from mean sea level from the ADCP. The maximum current speed was 211.3 cm/s.

4.1 Current Speed during Spring/Neap Tides

The currents during spring and neap tides are shown in Figures 23 and 24, respectively. During spring tide the maximum current is approximately 150 m/s and during neap tide the maximum current is approximately 100 cm/s. The time series data shows that there is a significant amount of turbulence near the bottom, as well as through the entire water column. The same anomalous phenomena is present in the InterOcean S4 data near the bottom during spring tides as present in the ADCP data.

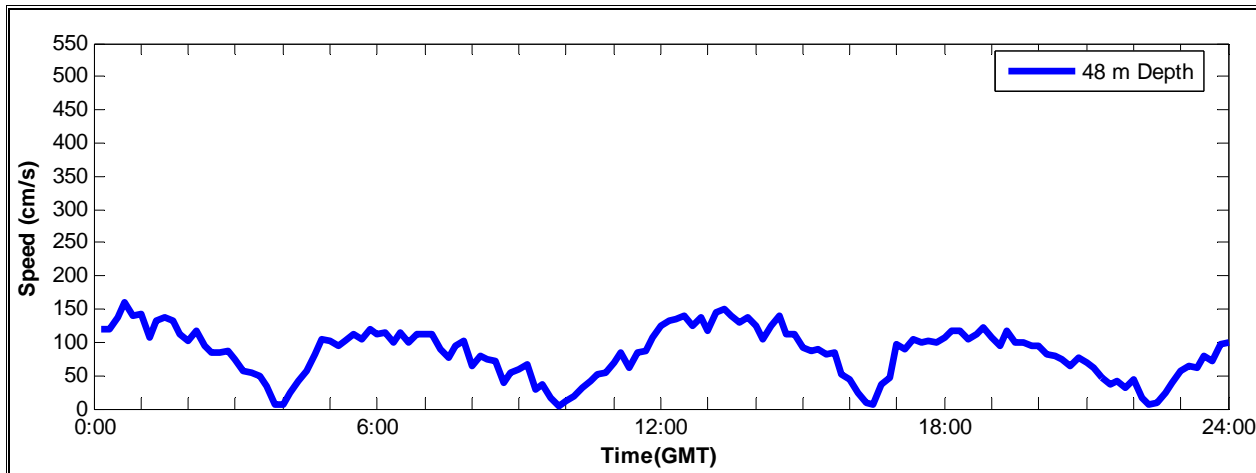


Figure 23 Current at Spring Tide on March 10, 2009

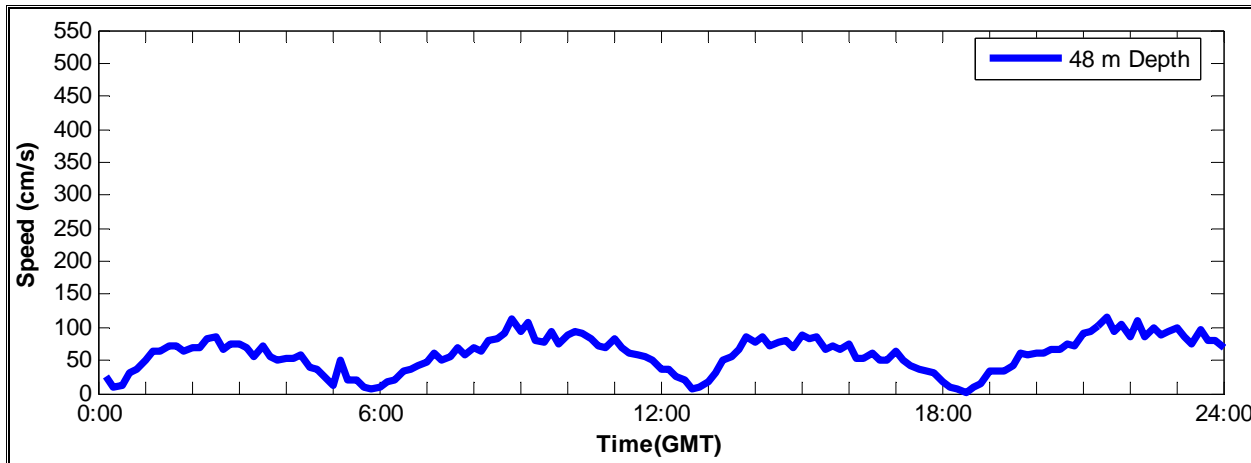


Figure 24 Currents at Neap Tide on March 21, 2009

4.2 Rose Plot

The rose plot in Figure 25 shows that the currents near bottom are higher during flood tide than during ebb, consistent with the observations at higher levels in the water column at site 5 and at the other locations. During ebb tide, there is a slight counterclockwise shift in the current direction as compared with flood tide.

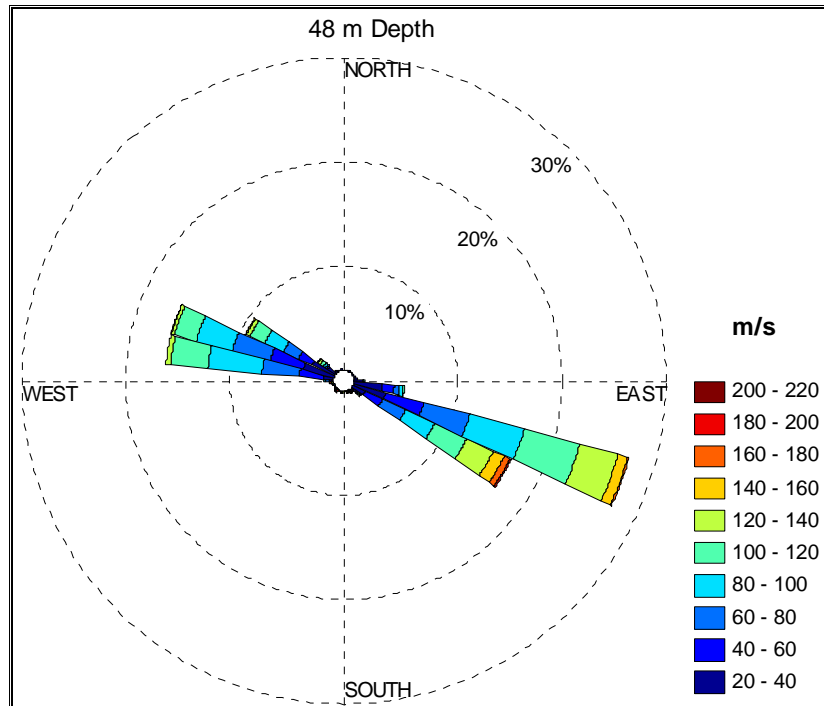


Figure 25 Rose Plot near the Bottom at Site 5

4.3 Harmonic Analysis

A harmonic analysis on the data produced values of 112.9 cm/s for M_2 and 22.8 cm/s for S_2 . M_2 was approximately 5 times greater than S_2 . During spring tides the semidiurnal tidal current is $M_2 + S_2$, or approximately 136 cm/s, and during neap tide the semidiurnal tidal current is $M_2 - S_2$, or approximately 90 cm/s. The tidal ellipse for M_2 is shown in Figure 26.

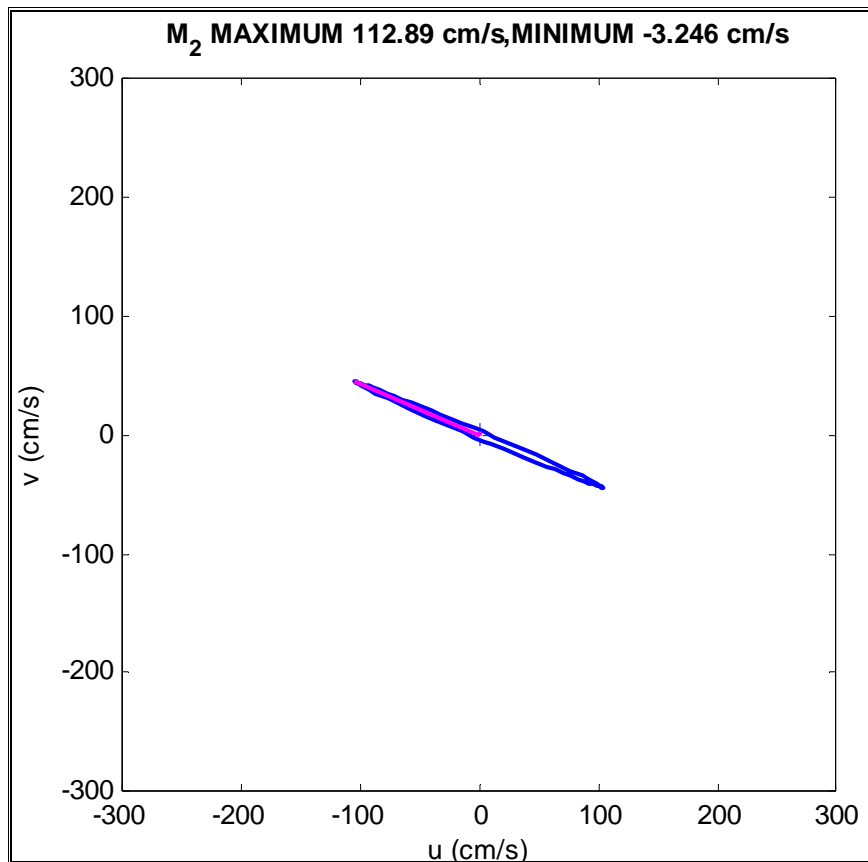


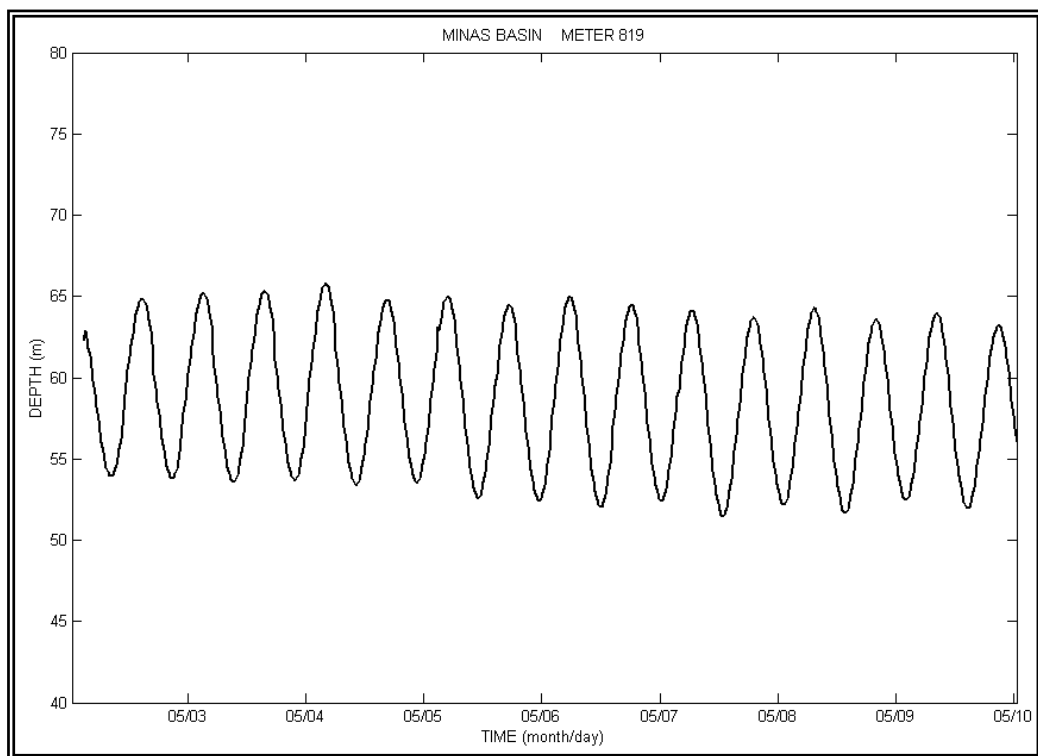
Figure 26 M2 Tidal Ellipse near Bottom

5.0 Water Level Data

The water level recorders were moored at sites 1 and 3 to measure surface height during the whole sampling period. The time series plots clearly show the semi-diurnal tidal pattern. The water depth was 58 m at site 1, and 52 m at site 3 above the tidal gauge at mid-tide. The water level recorder was installed in a bottom stand at a height of 1 m above the sea floor. The water level difference was approximately 12 m between high tide and low tide at both sites.

5.1 Time Series of Water Level Data from Meter 819 at Site 1

The following time series plots were for the period of May 2 to June 4, 2008 at Site 1.



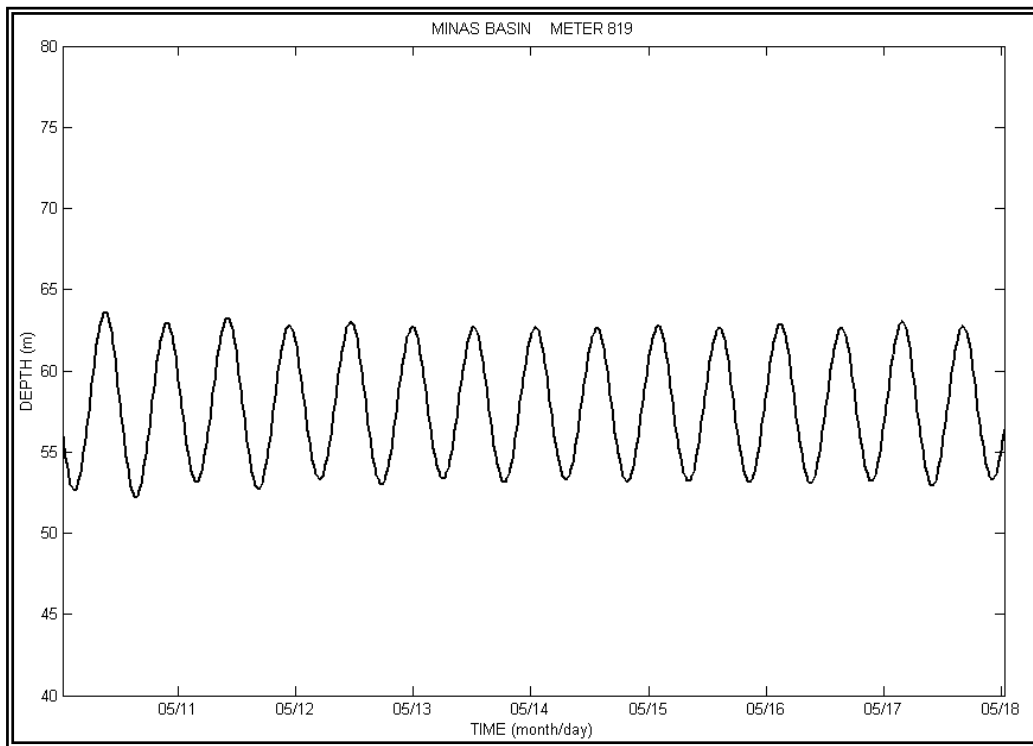
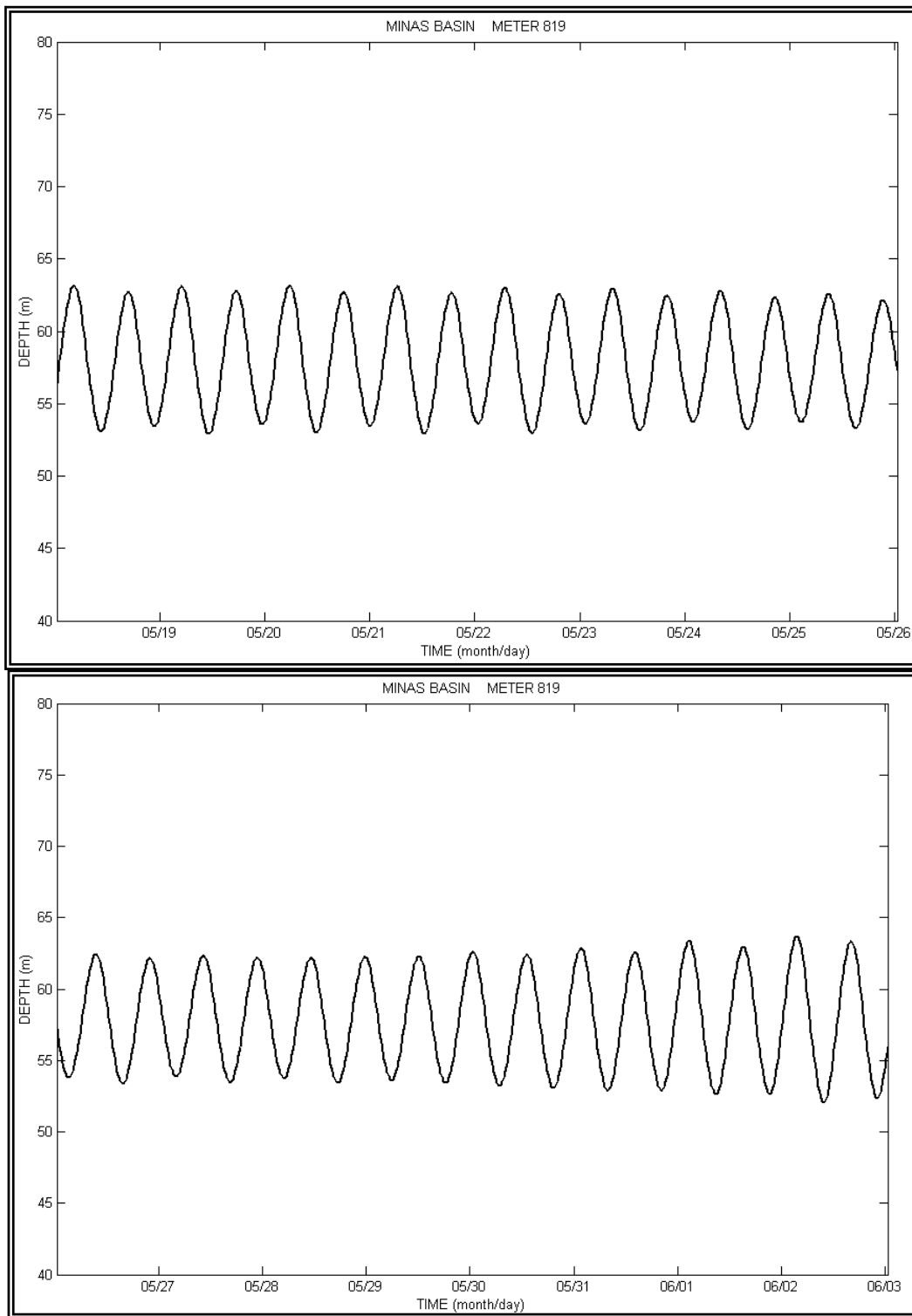
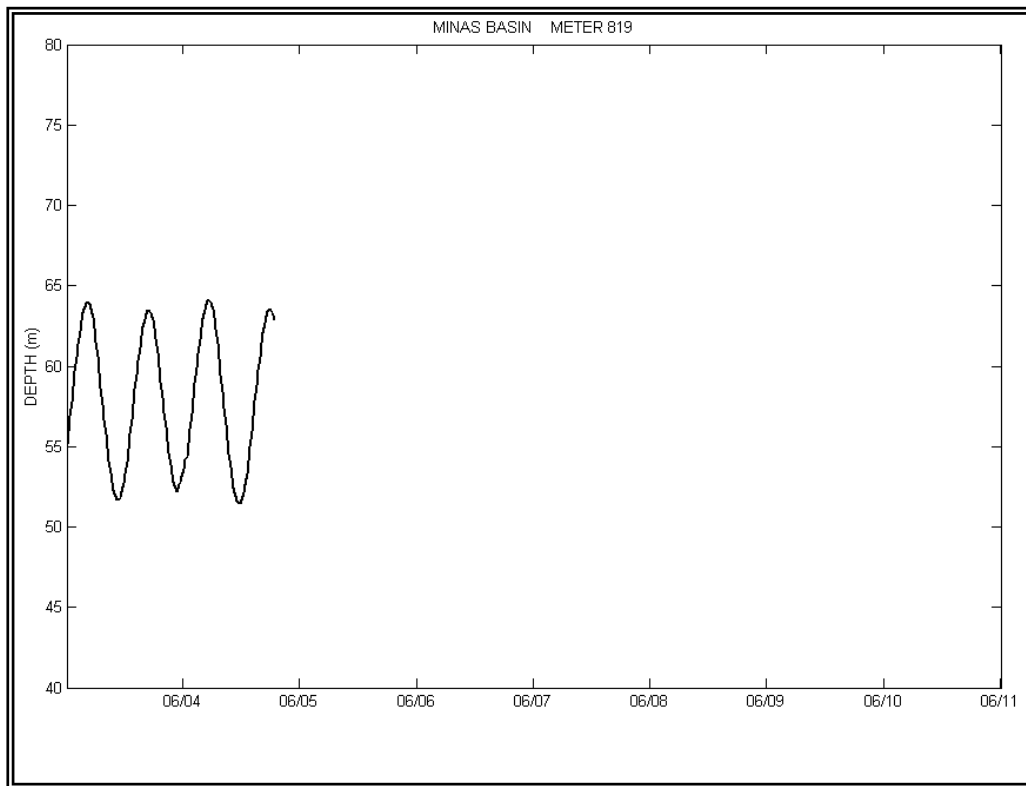


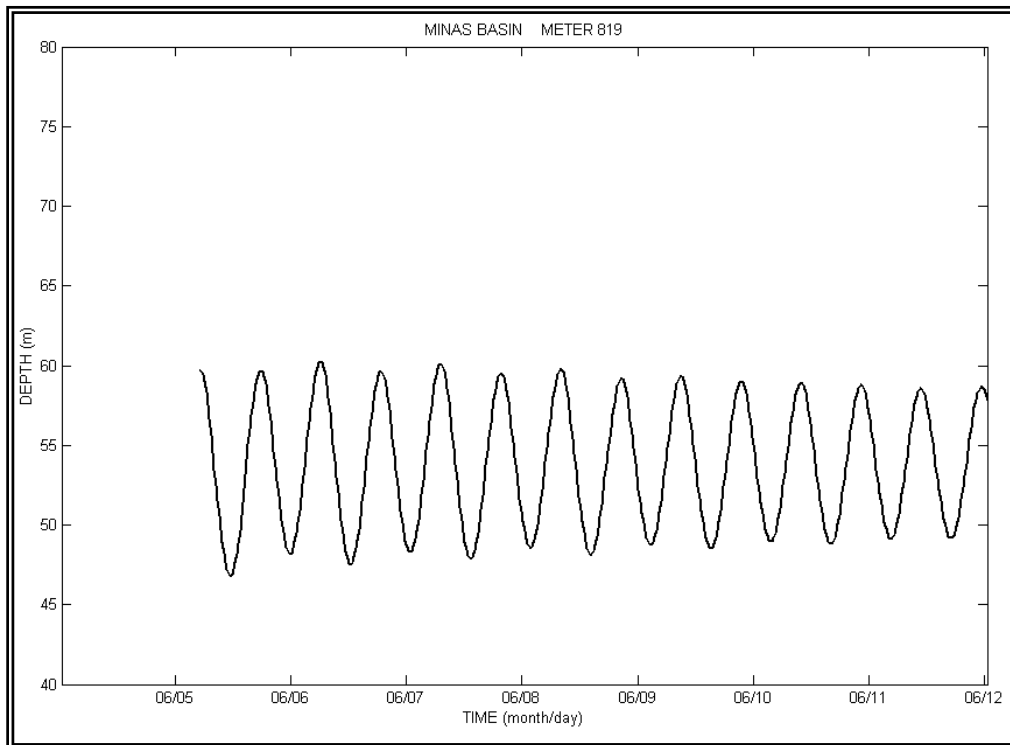
Figure 27. Water Level Data at Site 1

**Figure 27 (cont)**



5.2 Time Series of Water Level Data from Meter 819 at Site 3

The following time series plots were for the period of June 5 to July 9, 2008 at Site 3.



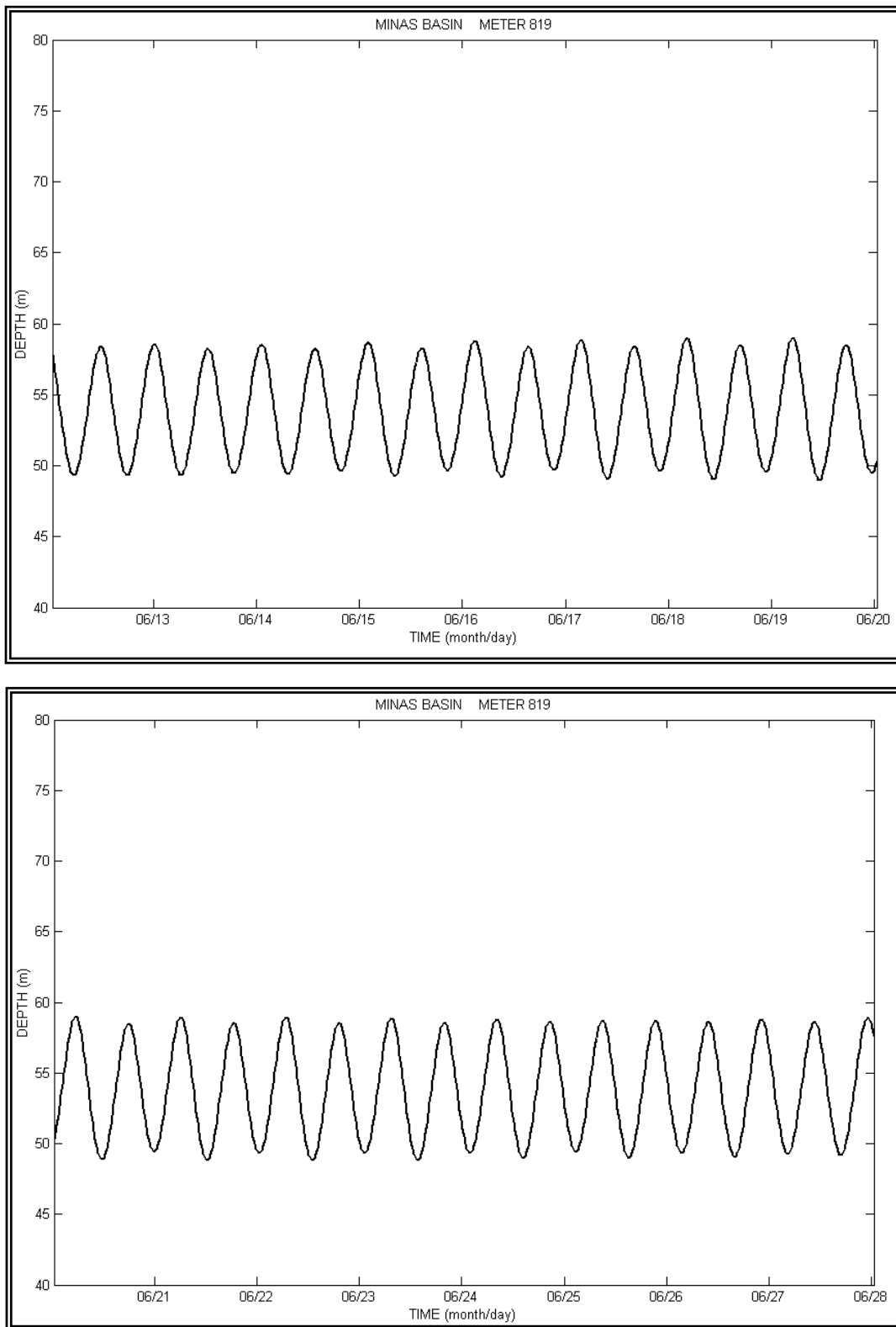
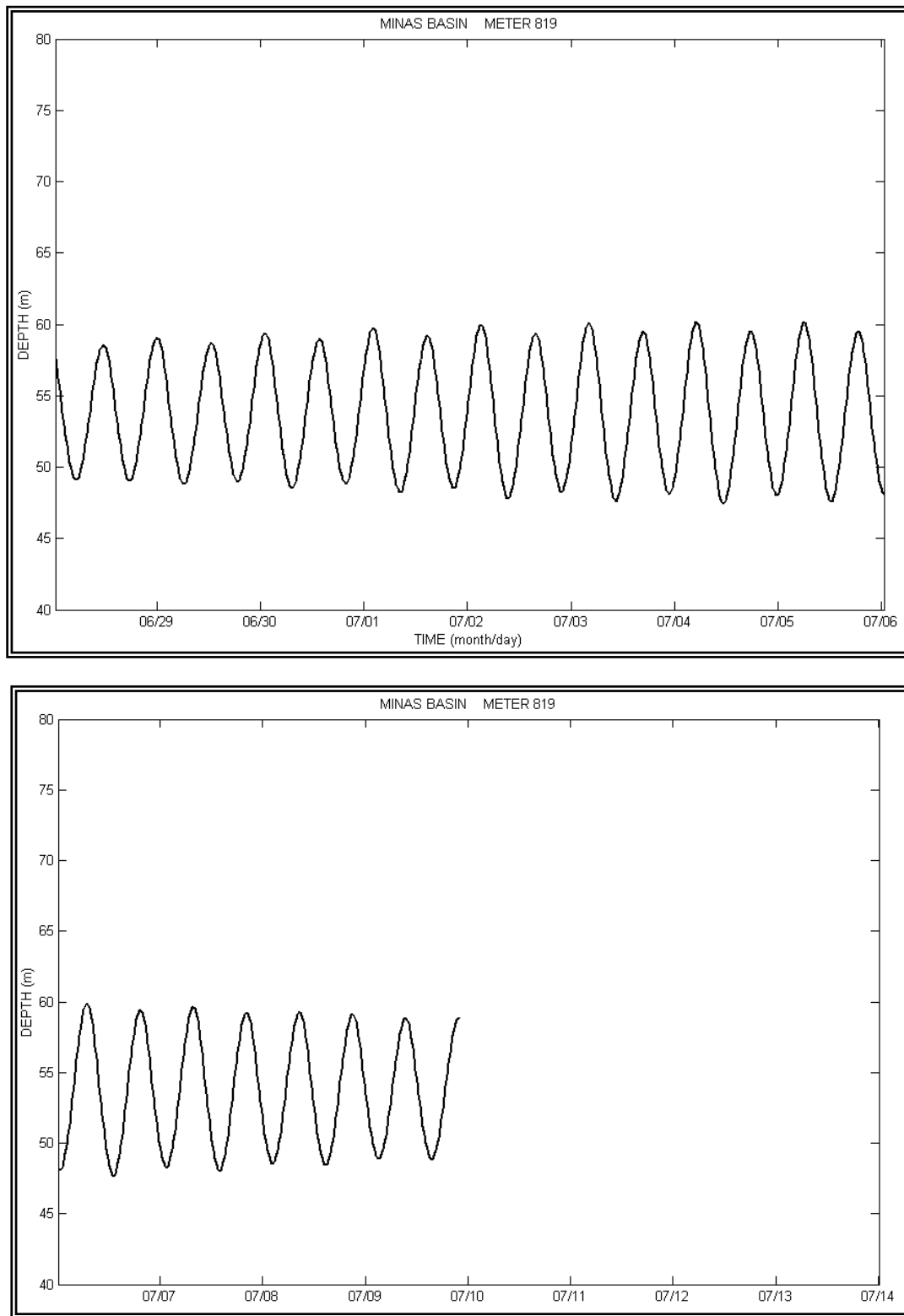


Figure 28. Water Level Data at Site 3

**Figure 28 (cont'd)**

6.0 Bottom Temperature Data

Time series of temperature data near the sea floor were collected at each site by the moored ADCPs and Water Level Recorders. The time series plots of temperature data from the ADCPs are presented in Figures 29 to 32 and the time series plots of temperature data from the Water Level Recorders are presented in Appendices 8 and 9. During spring and summer the mean bottom temperature increased gradually from approximately 4°C at the beginning of May, 2008 to 8°C in June and to 12°C in July, 2008. It reached its maximum of approximately 15°C in mid-August and remained stable to the end of the sampling period. During winter the bottom temperature increased from -1°C in mid-February, 2009 to 1°C at the end of March, 2009. The bottom temperature displayed a semi-diurnal pattern in the time series data corresponding to the pattern of the semi-diurnal tides. On each day, the water temperature decreased when the colder water of the Bay of Fundy was transported into the basin during flood tide, and then increased during ebb tide.

6.1 Time Series of Bottom Temperature from ADCP, at Site 1

The following time series plots were from the data collected by a temperature sensor on the ADCP for the period of May 2 to June 4, 2008, at Site 1.

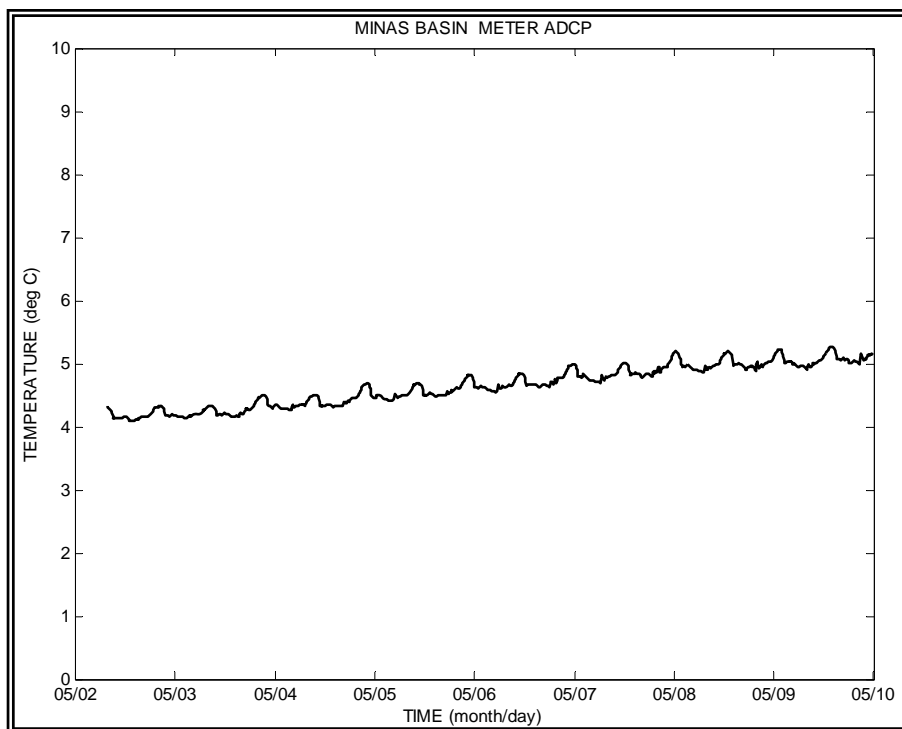


Figure 29. Water Temperature 1.5 metres above Bottom at Site 1

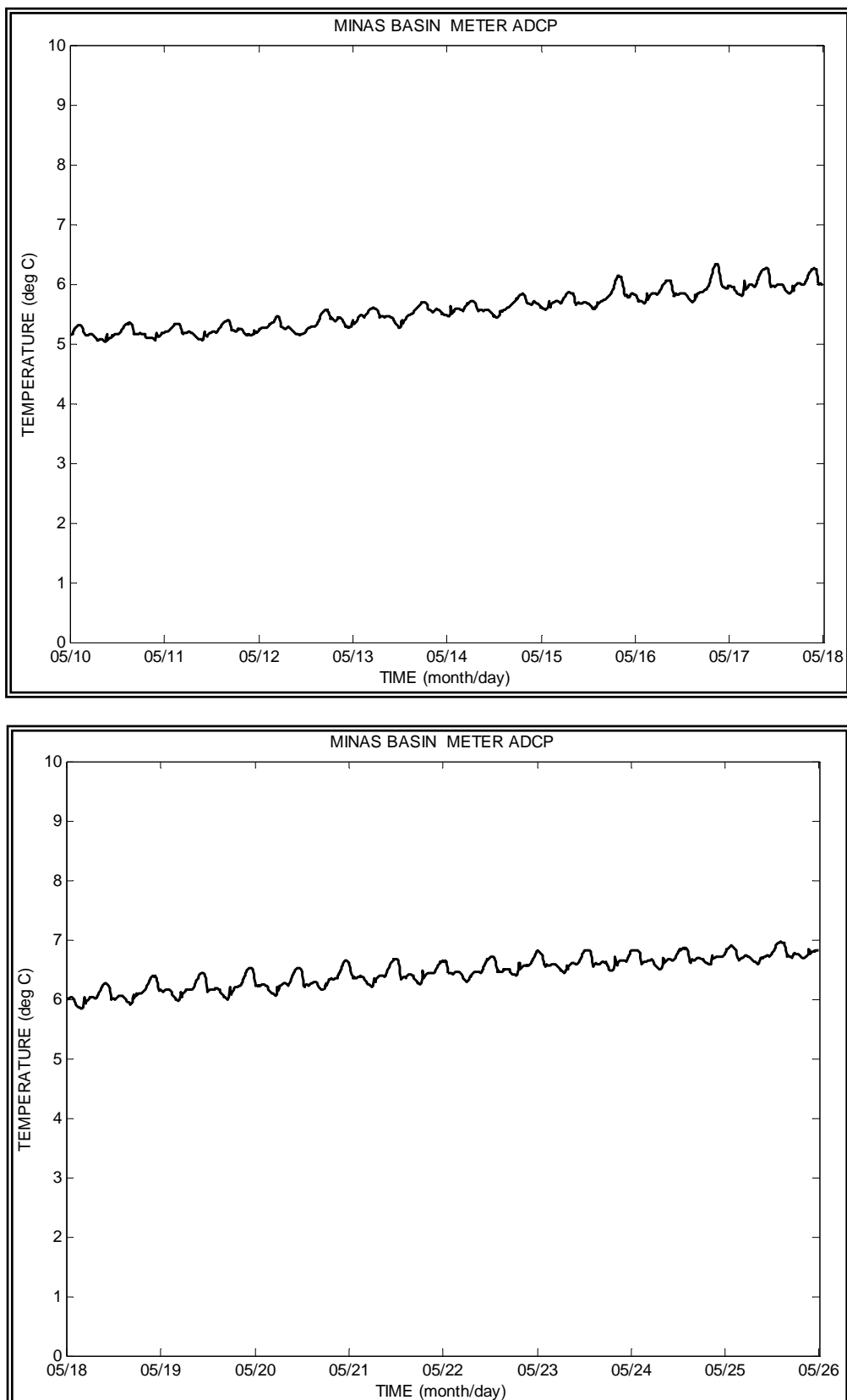
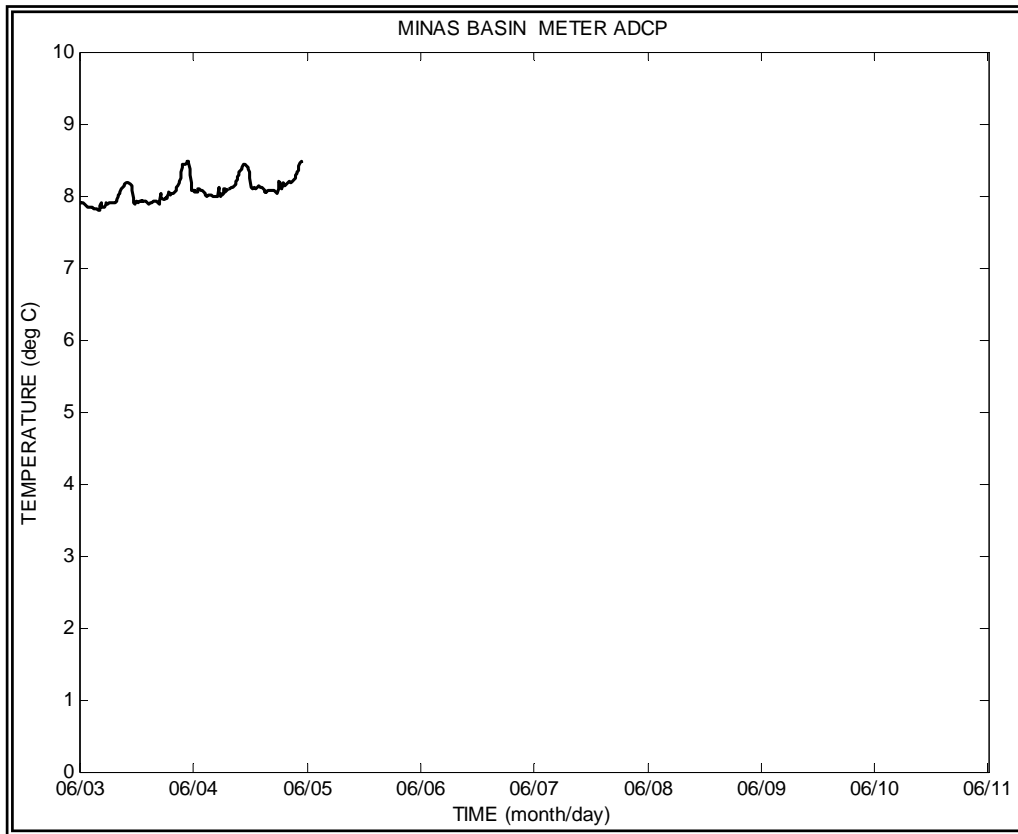
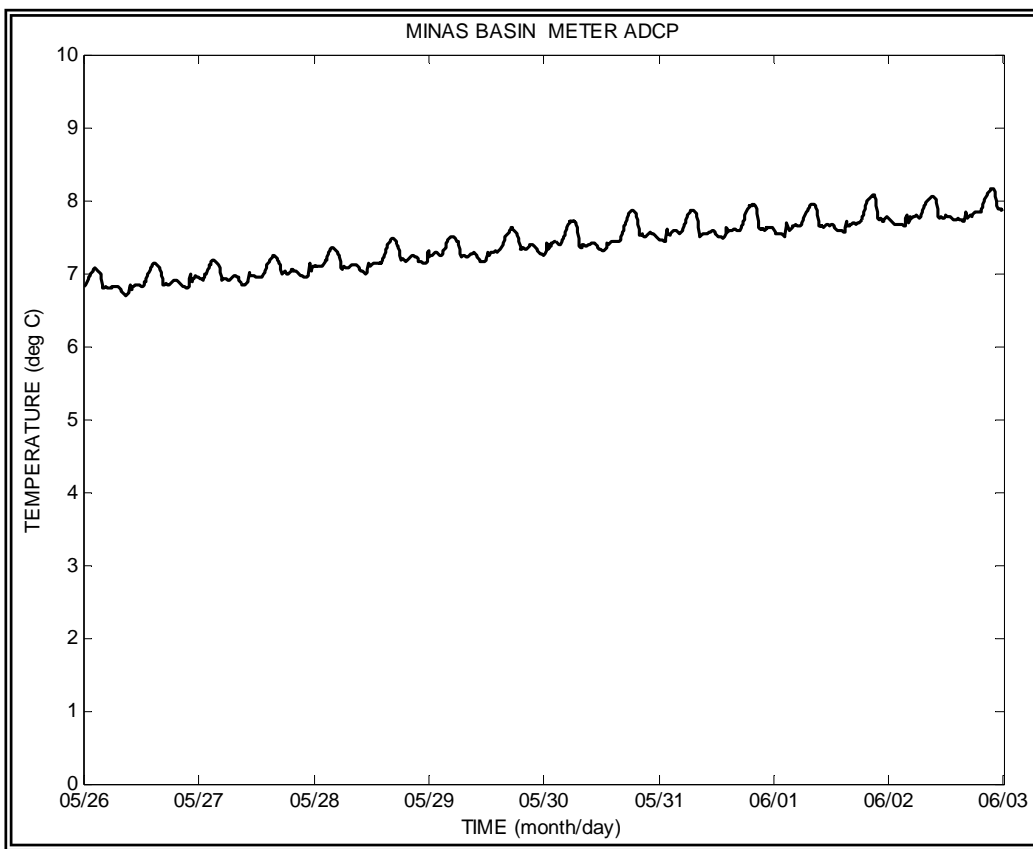


Figure 29 (cont'd)



6.2 Time Series of Bottom Temperature from the ADCP at Site 3

The following time series plots were from data collected by a temperature sensor on the ADCP from the period of June 5 to July 9, 2008 at Site 3.

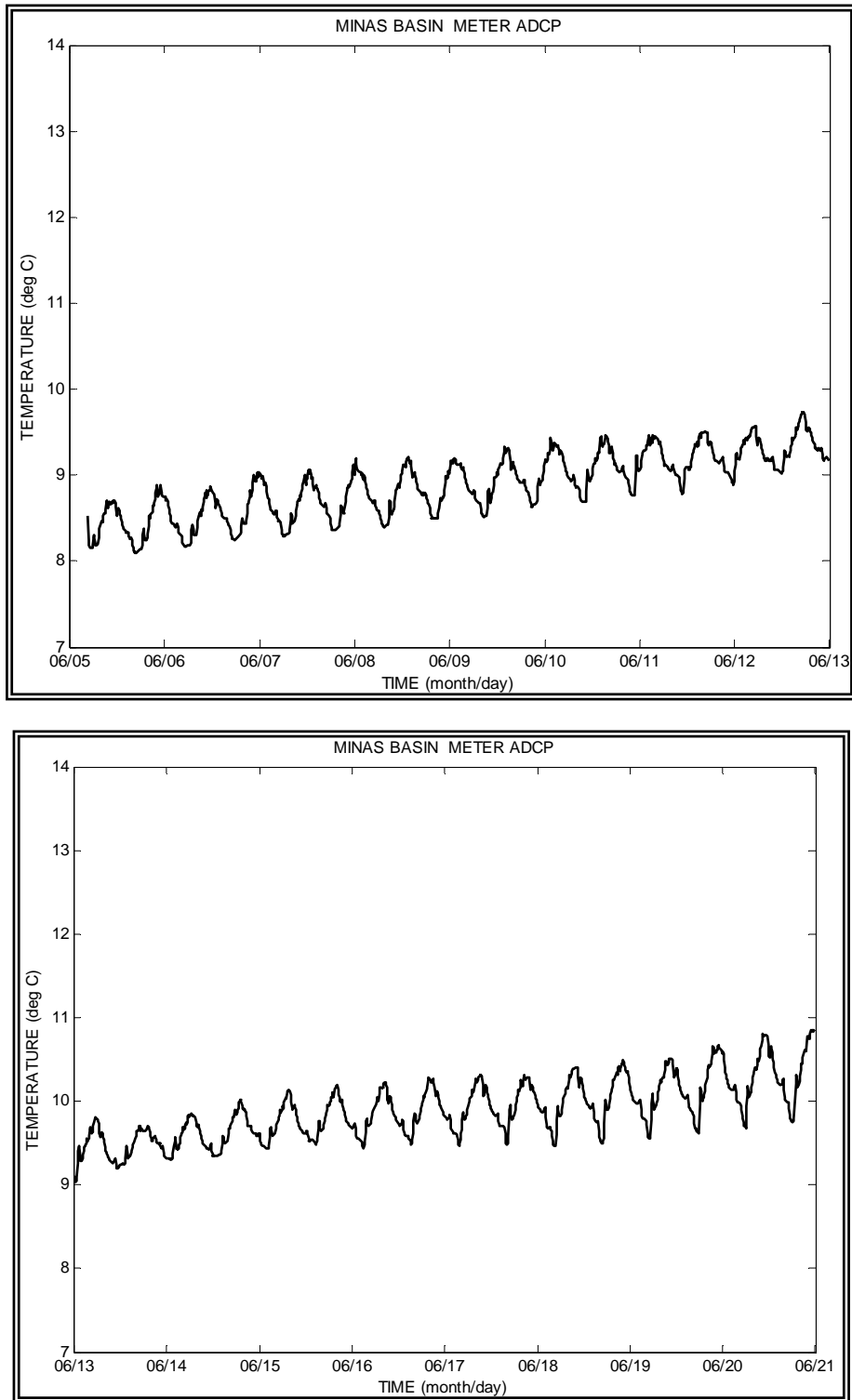


Figure 30. Water Temperature 1.5 Metres above Bottom at Site 3

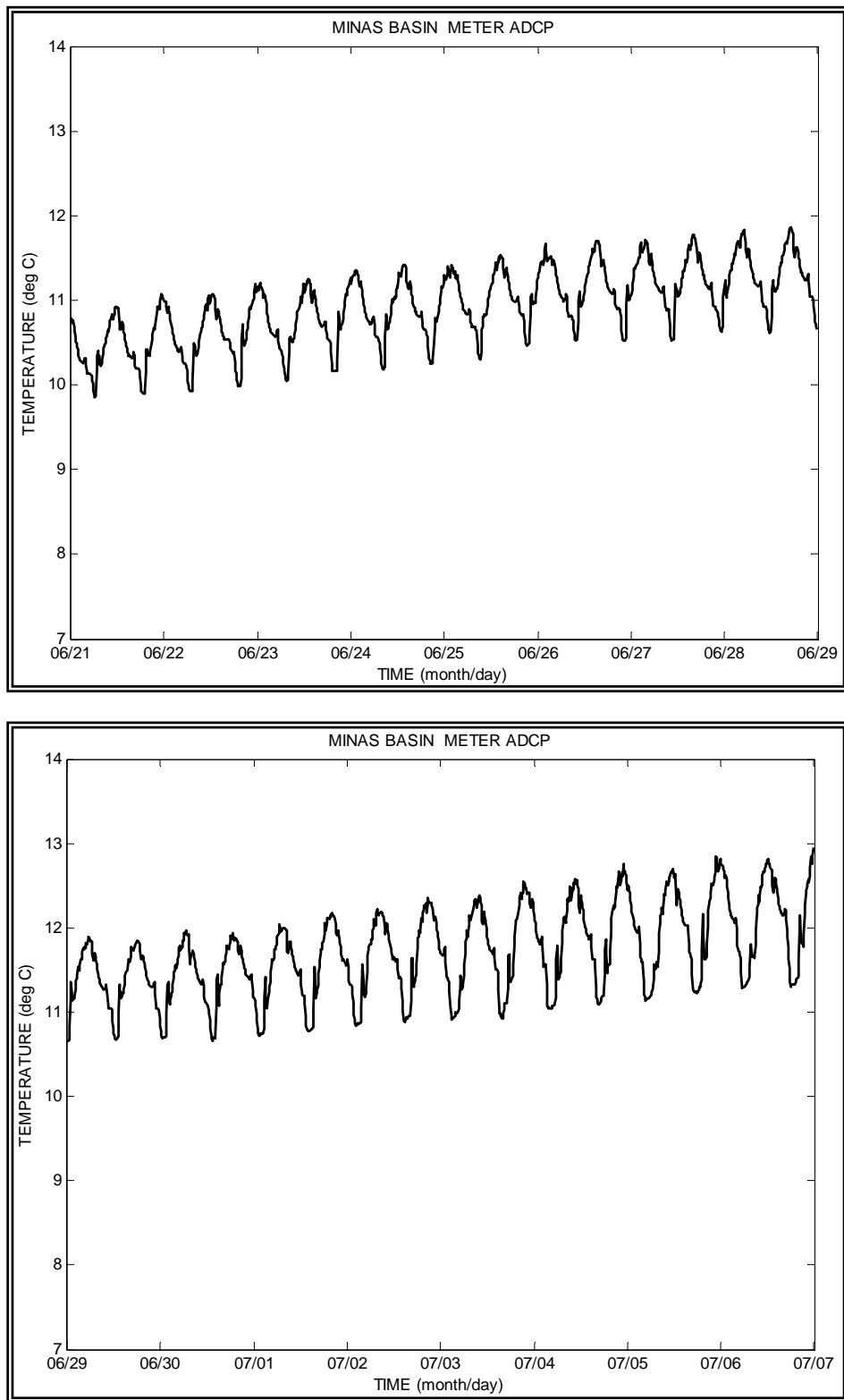


Figure 30 (cont'd)

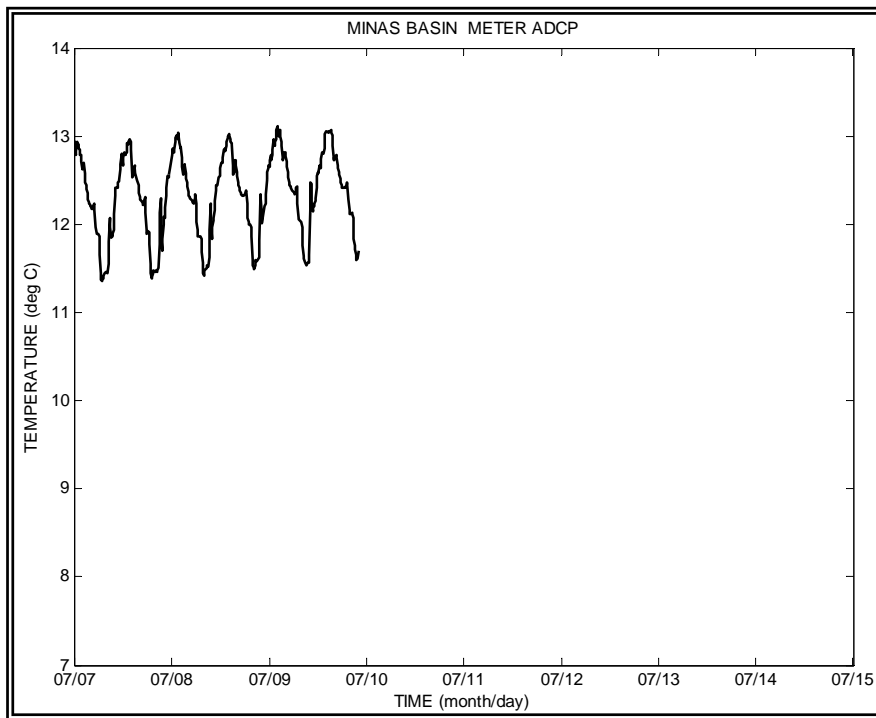


Figure 30 (cont'd)

6.3 Time Series of Bottom Temperature from the ADCP at Site 4

The following time series plots were from data collected by a temperature sensor on the ADCP for the period of August 8 to September 23, 2008, at Site 4.

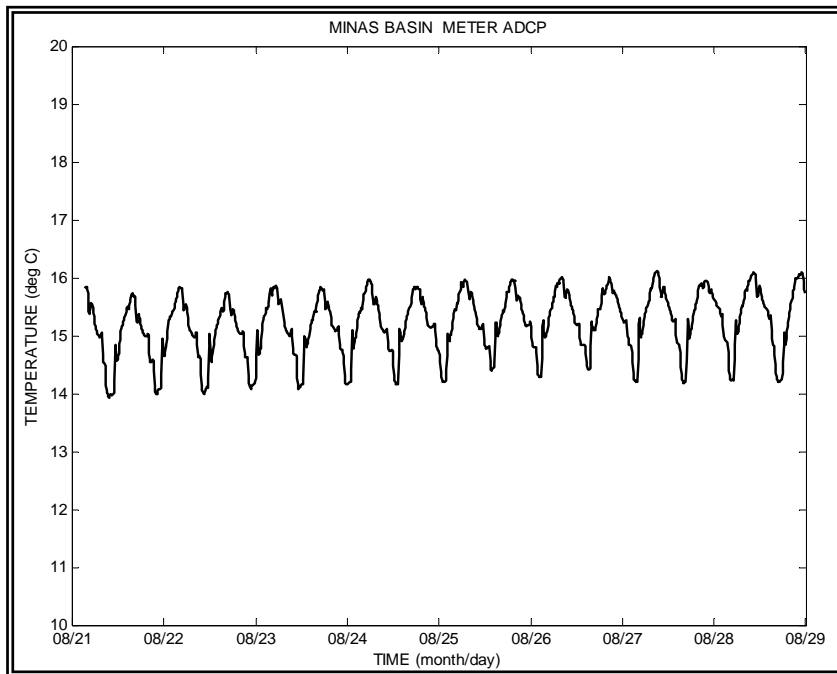


Figure 31. Water Temperature 1.5 Metres above Bottom at Site 4

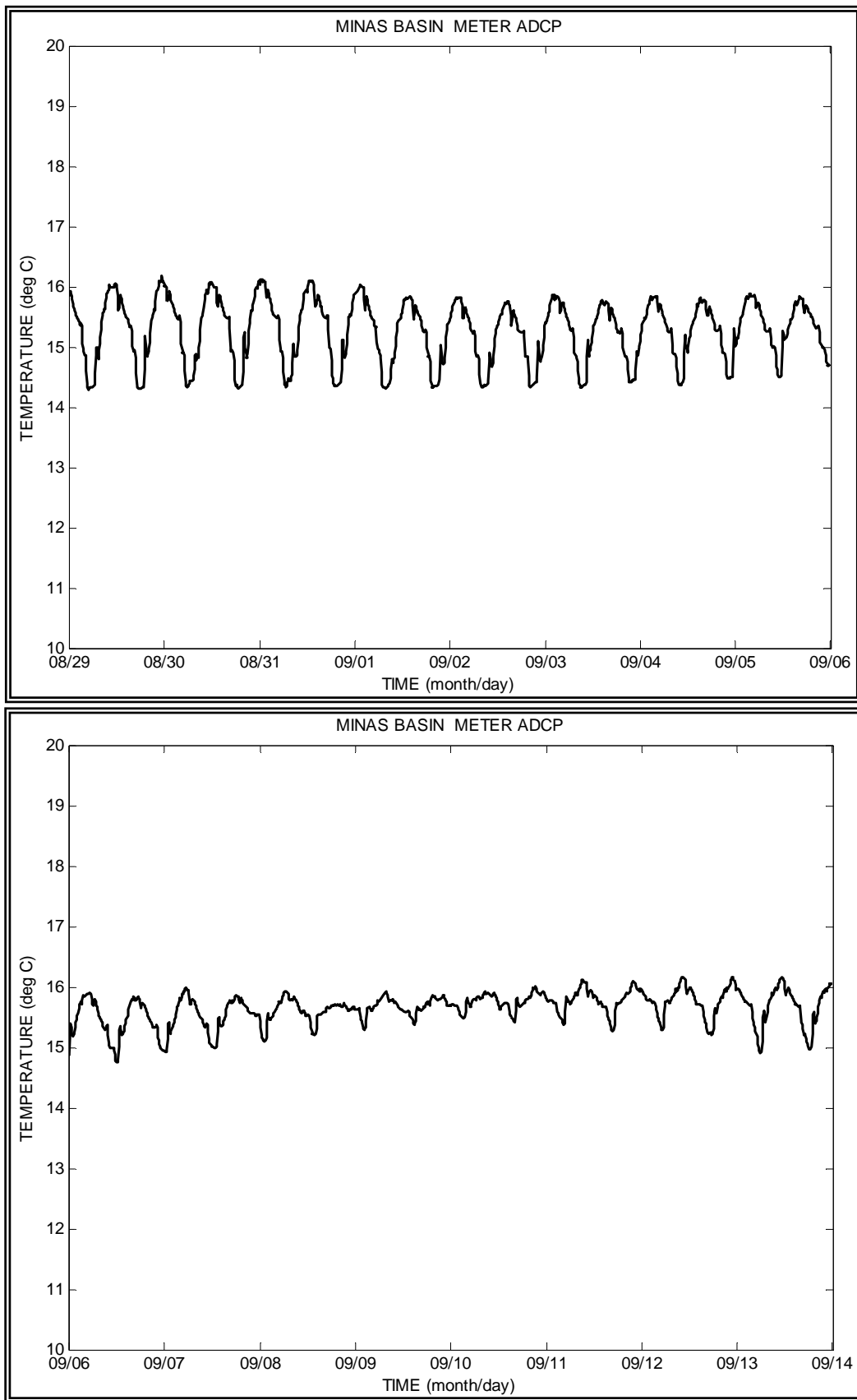
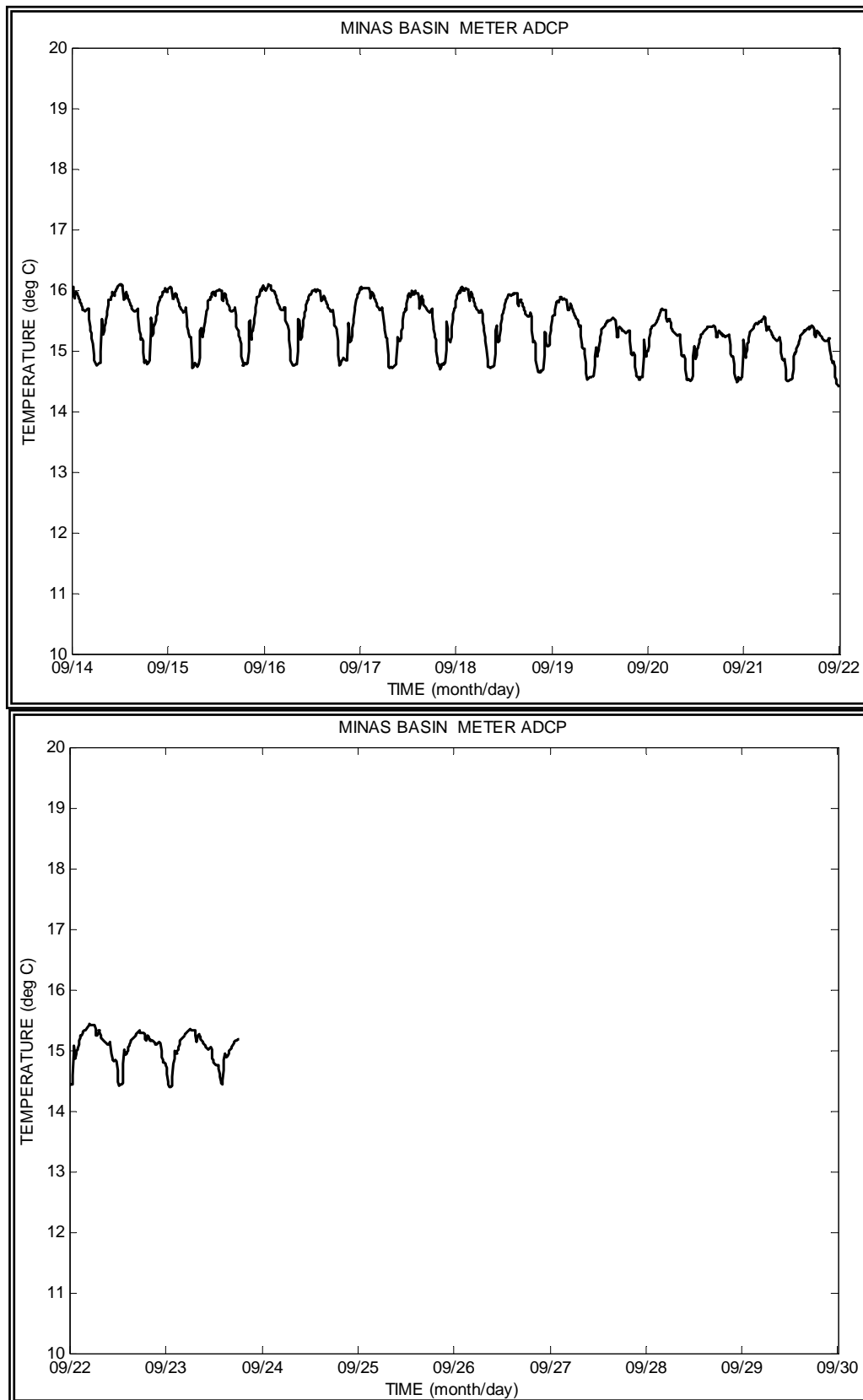


Figure 31 (cont'd)

**Figure 31 (cont'd)**

6.4 Time Series of Bottom Temperature from the ADCP at Site 5

The following time series plots were from data collected by a temperature sensor on the ADCP for the period of February 14 to March 28, 2009, at Site 5.

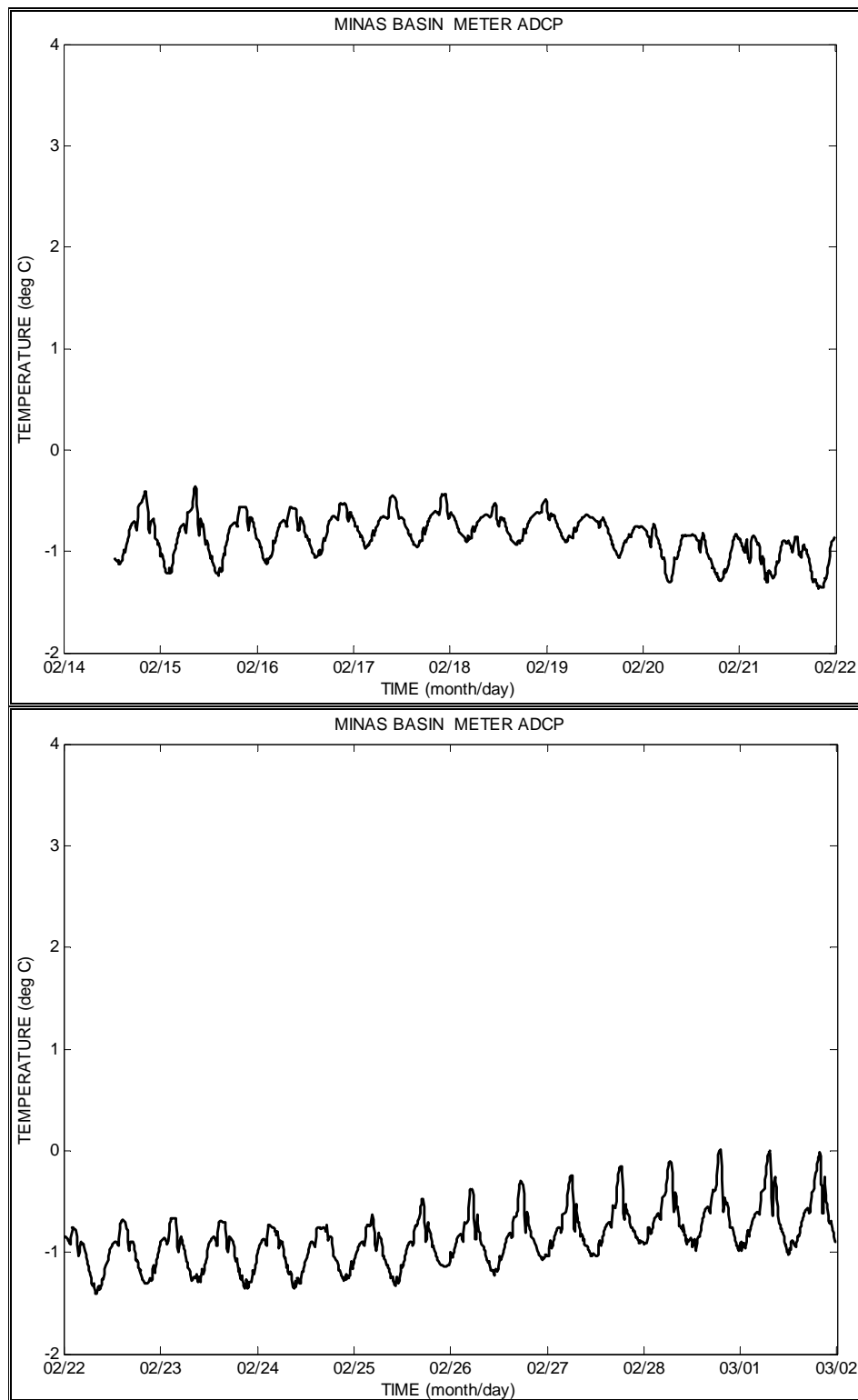


Figure 32. Water Temperature 1.5 Meters above Bottom at Site 5

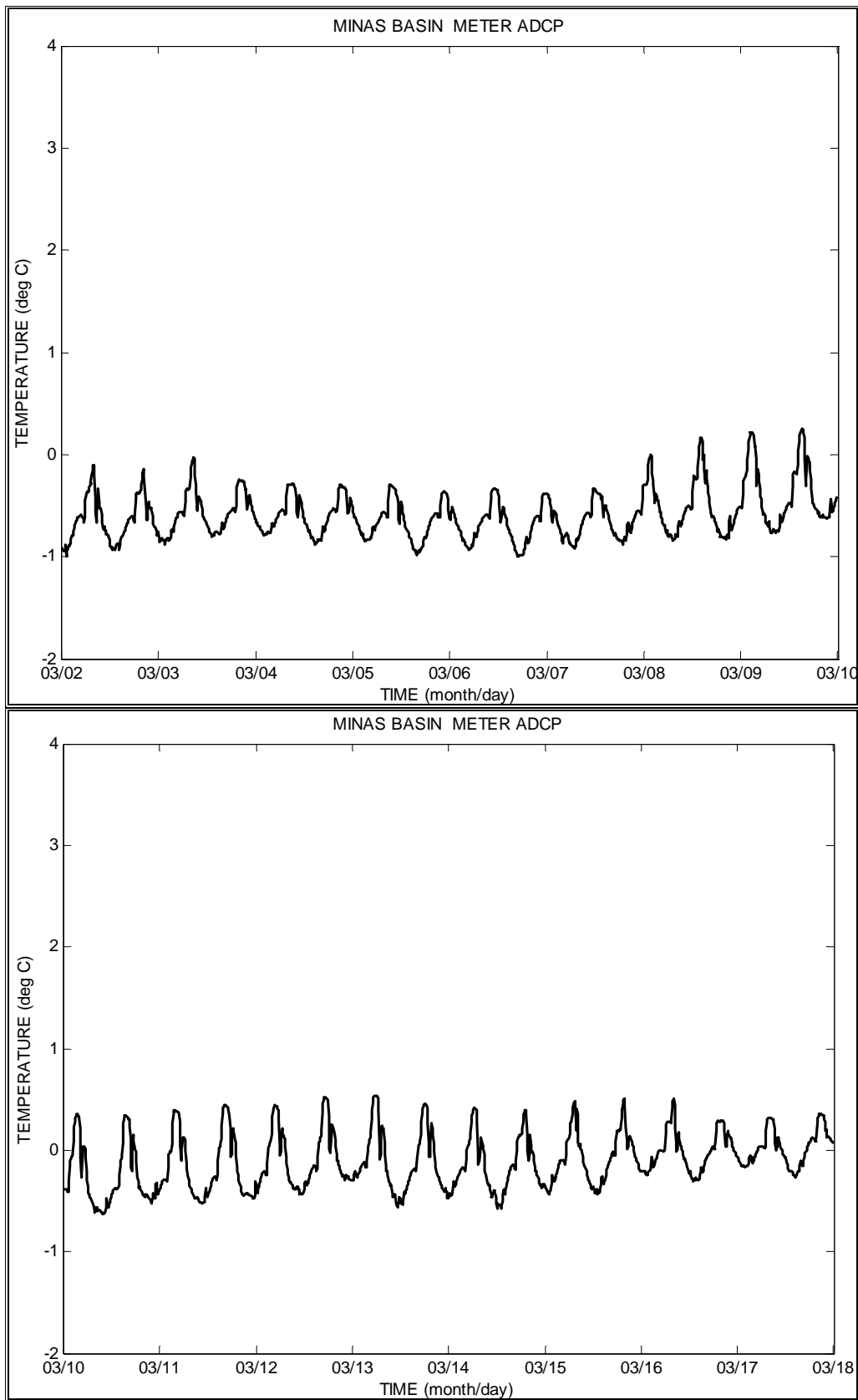


Figure 32 (cont'd)

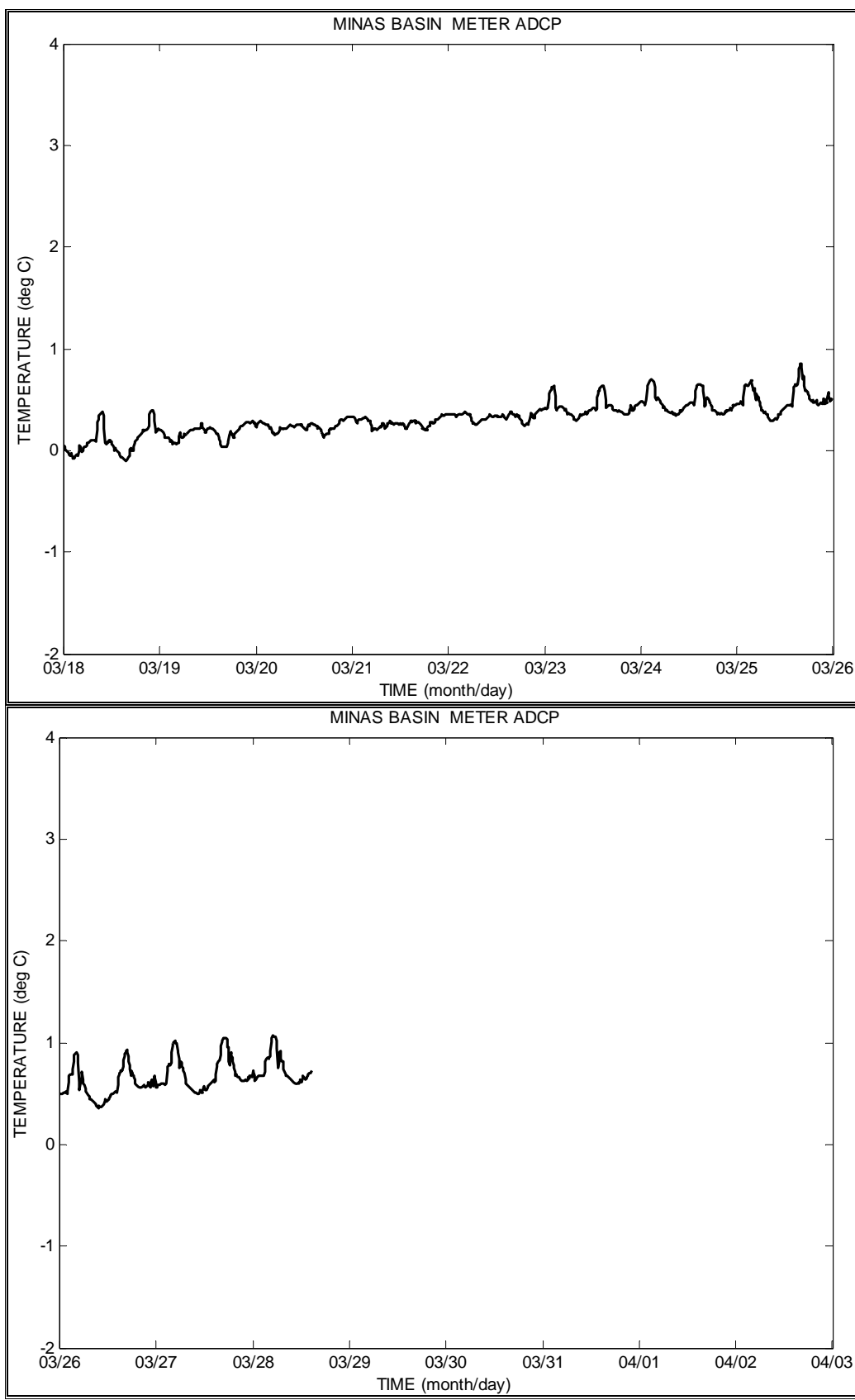
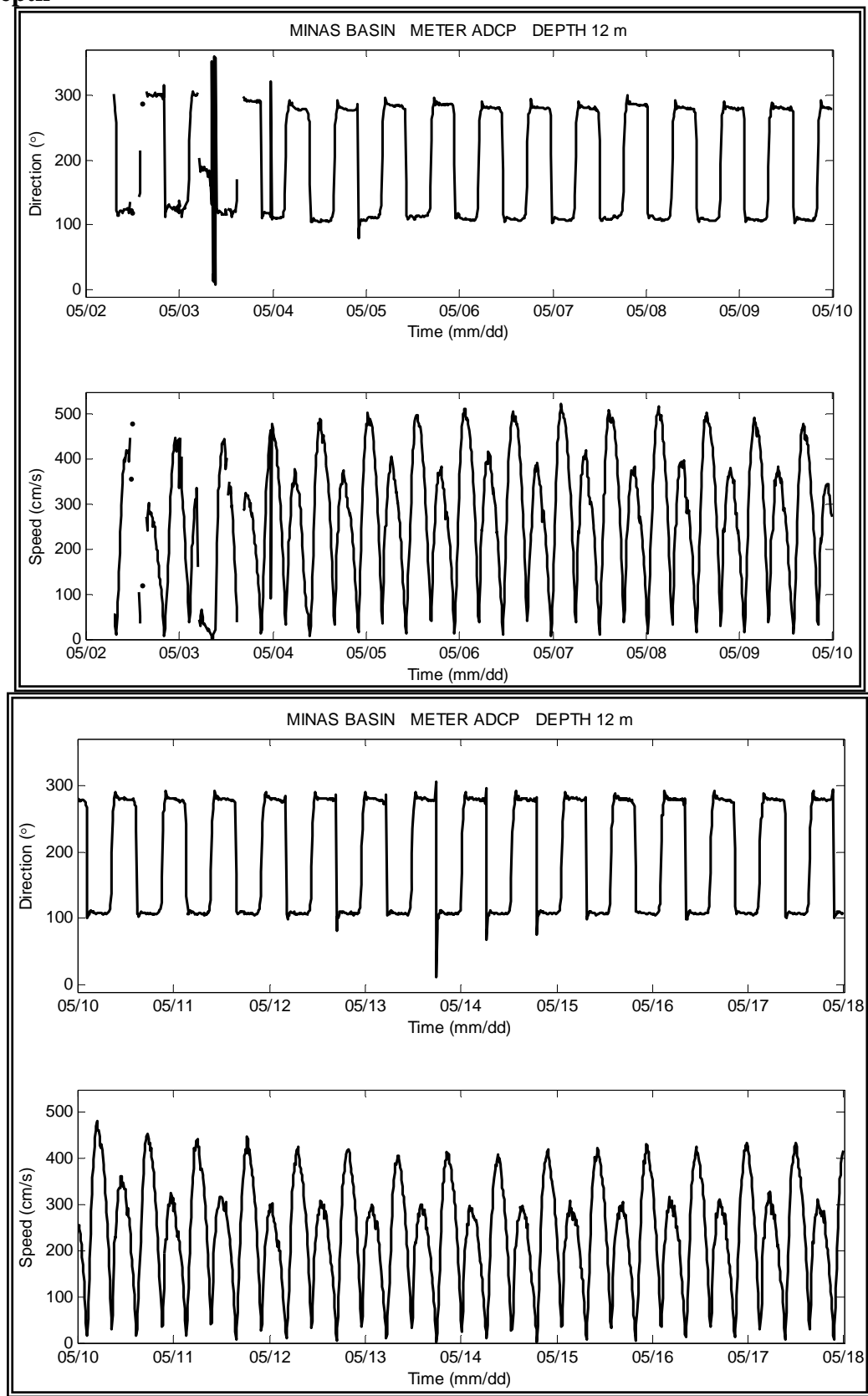
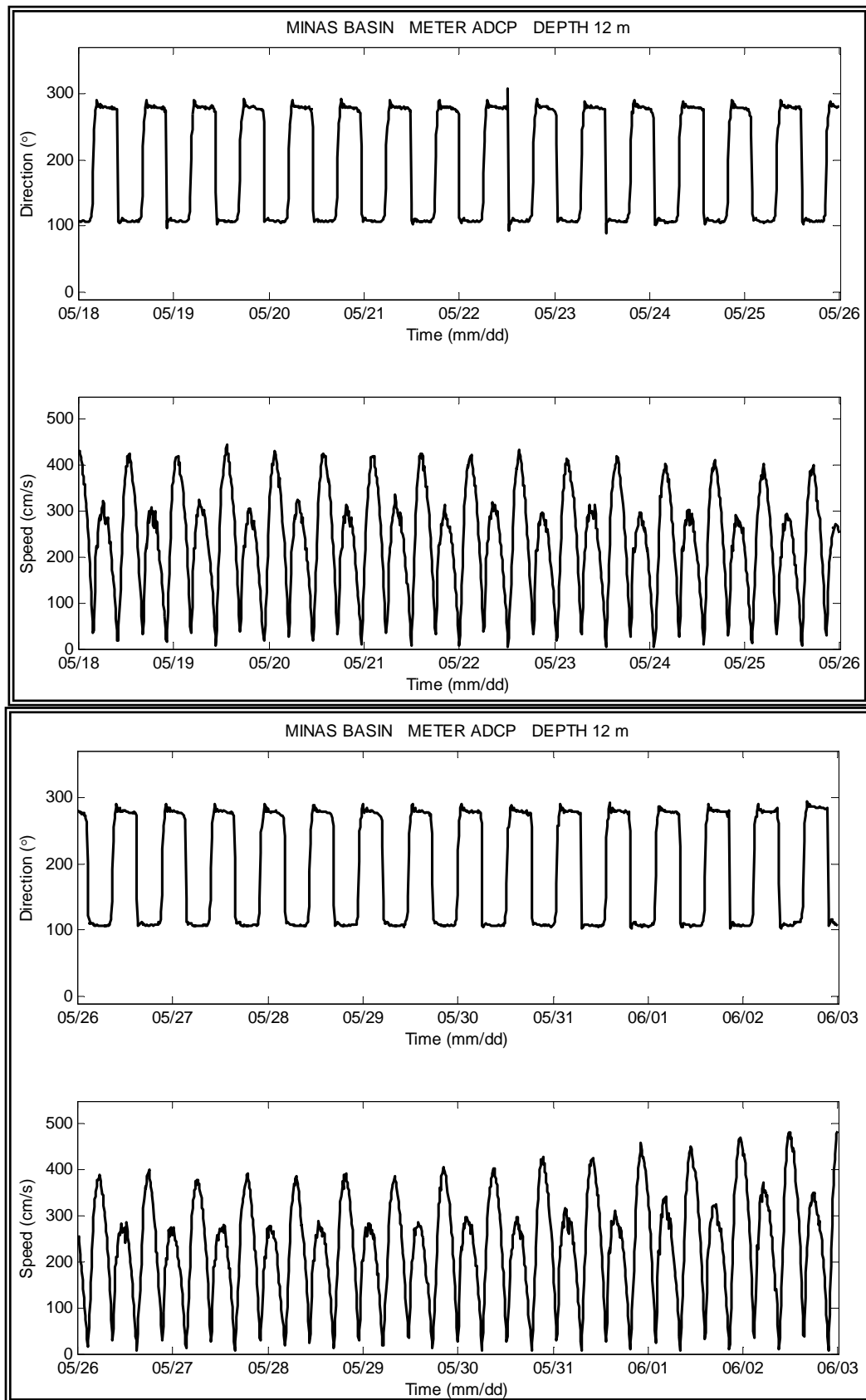


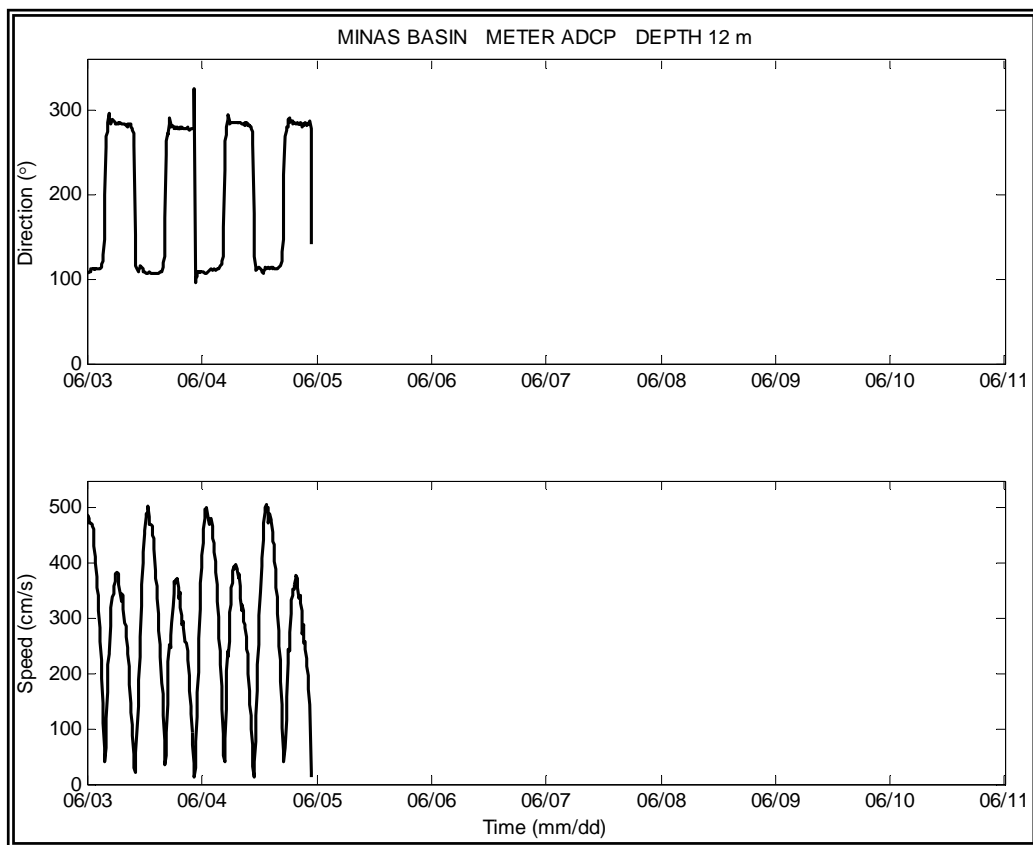
Figure 32 (cont'd)

Appendix 1

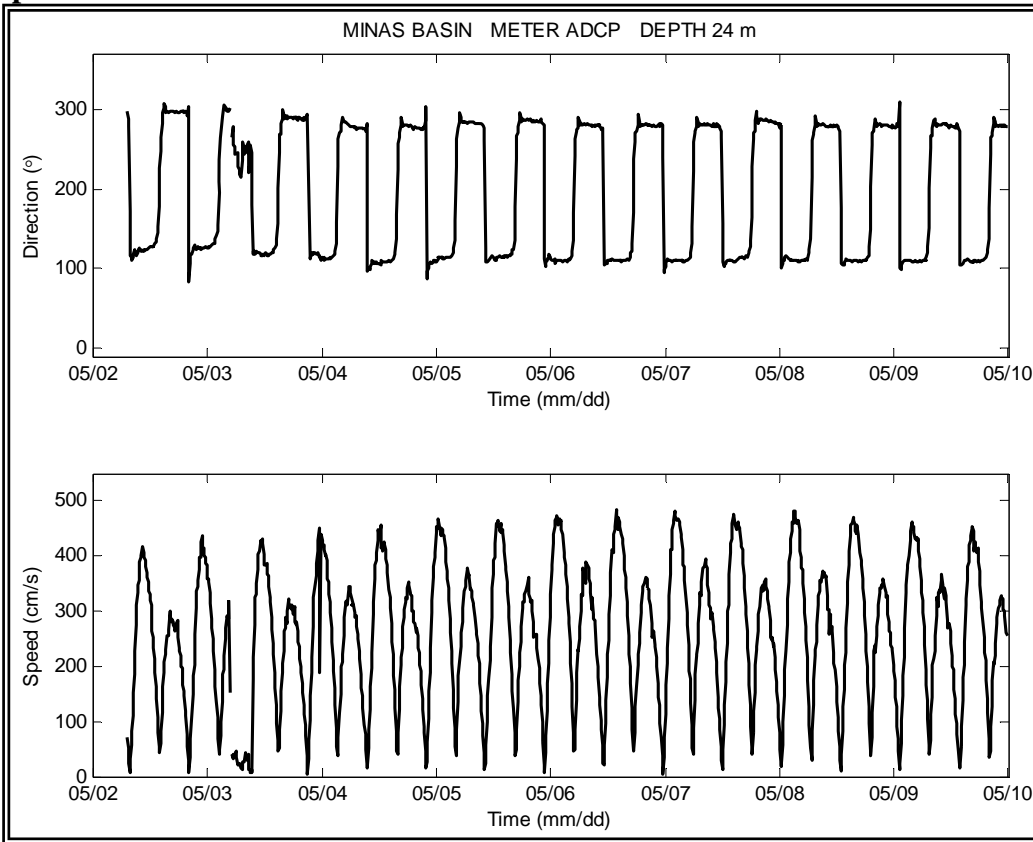
Time Series Plots, ADCP at Site 1

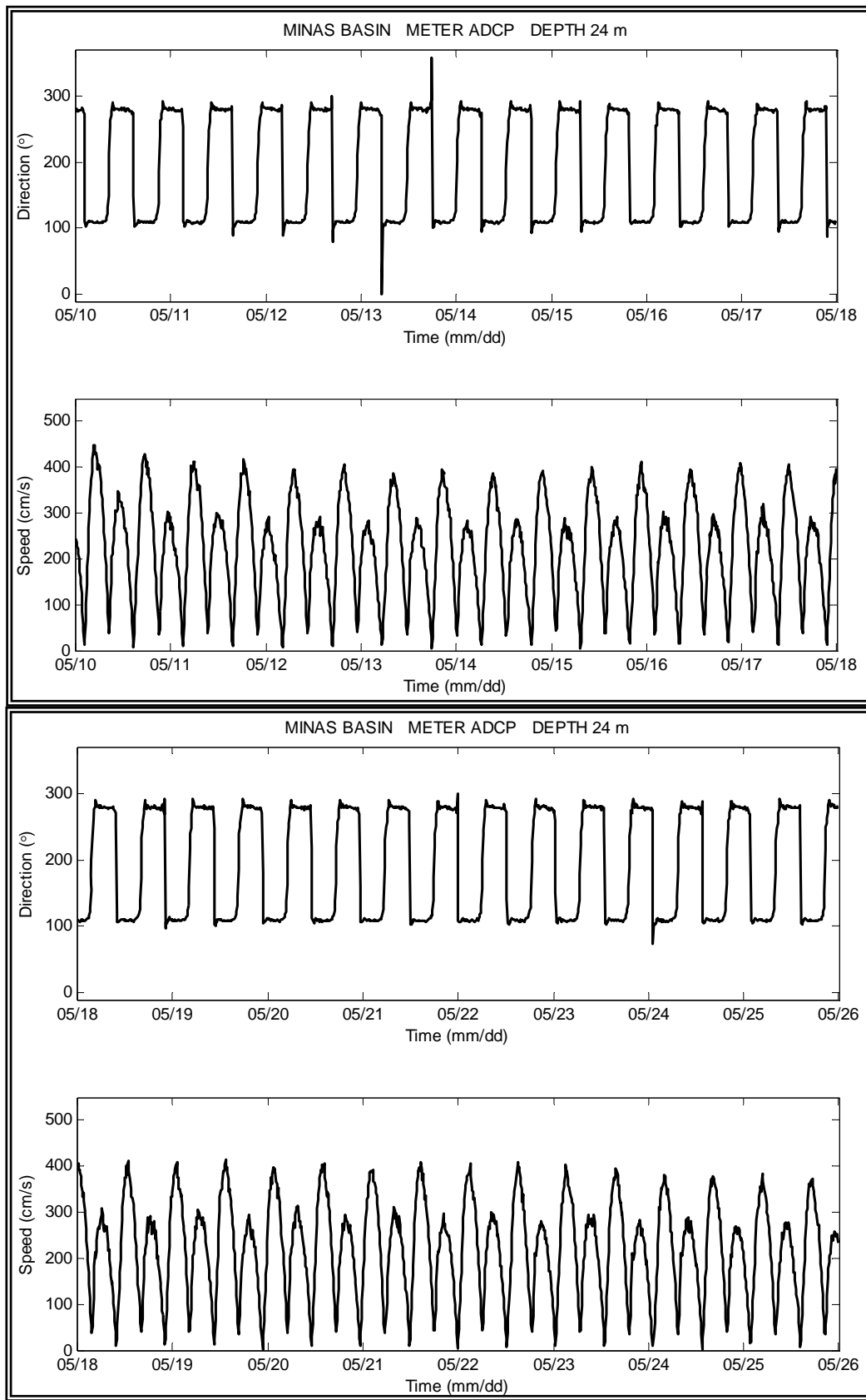
12 m Depth


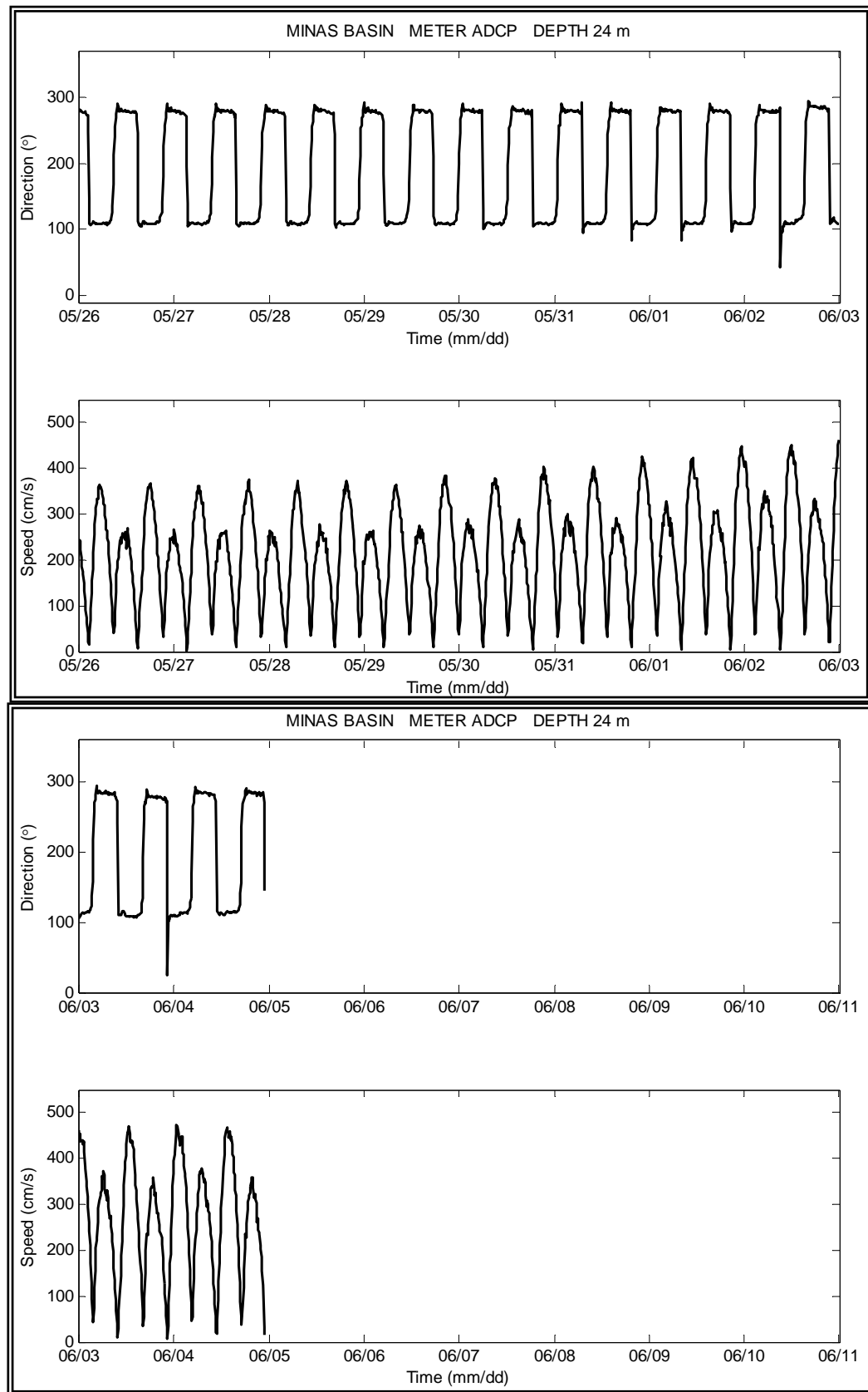


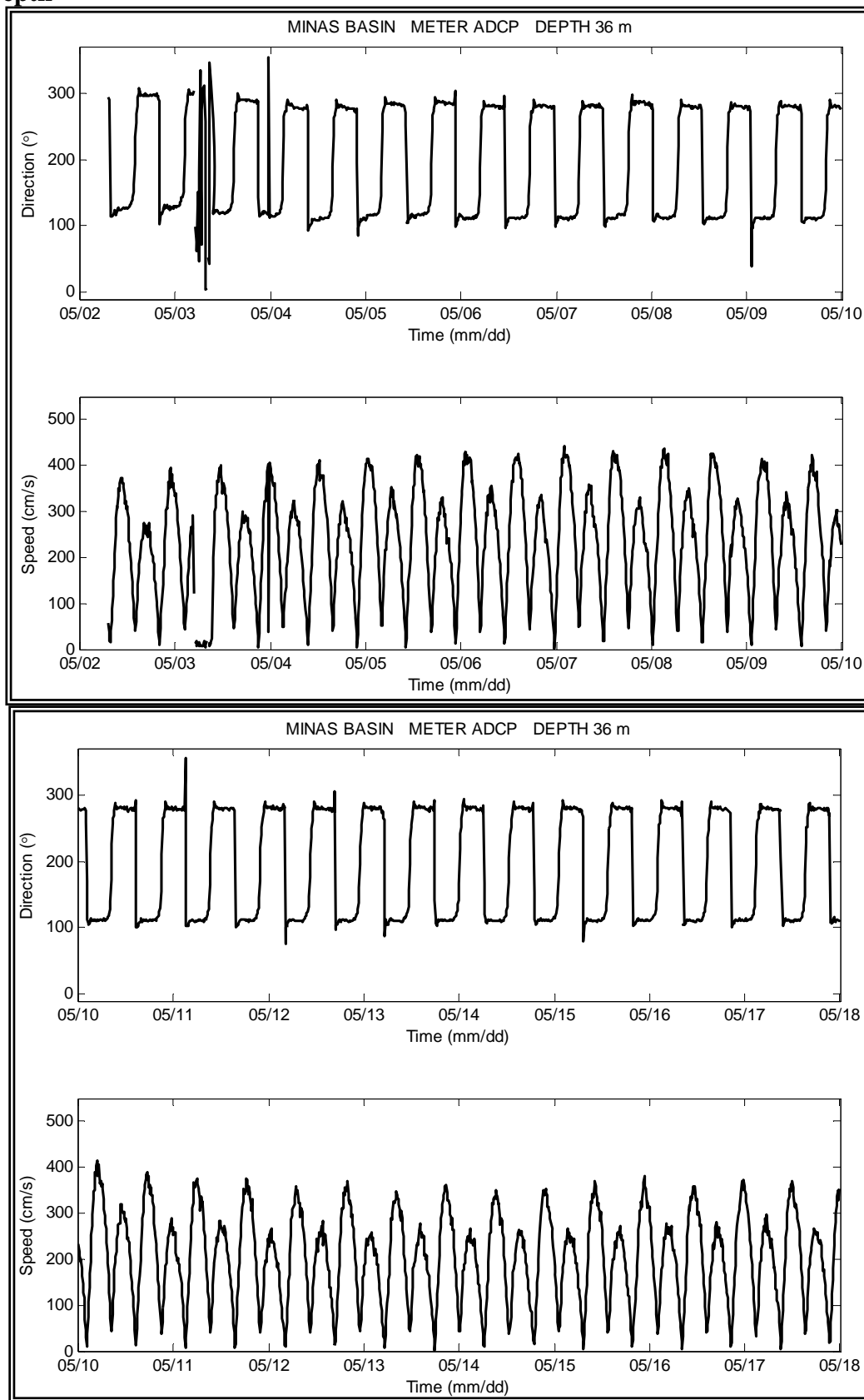


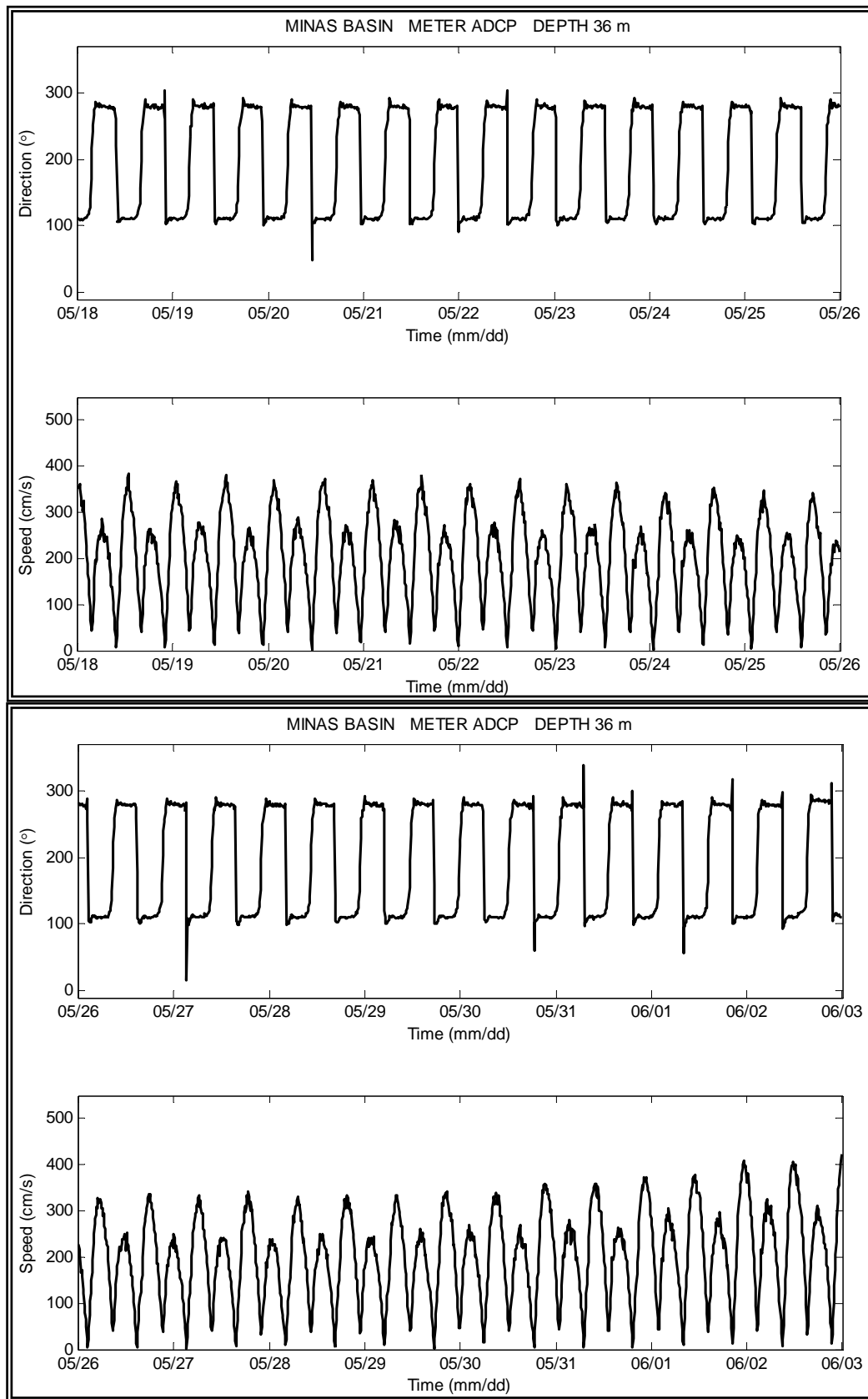
24 m Depth

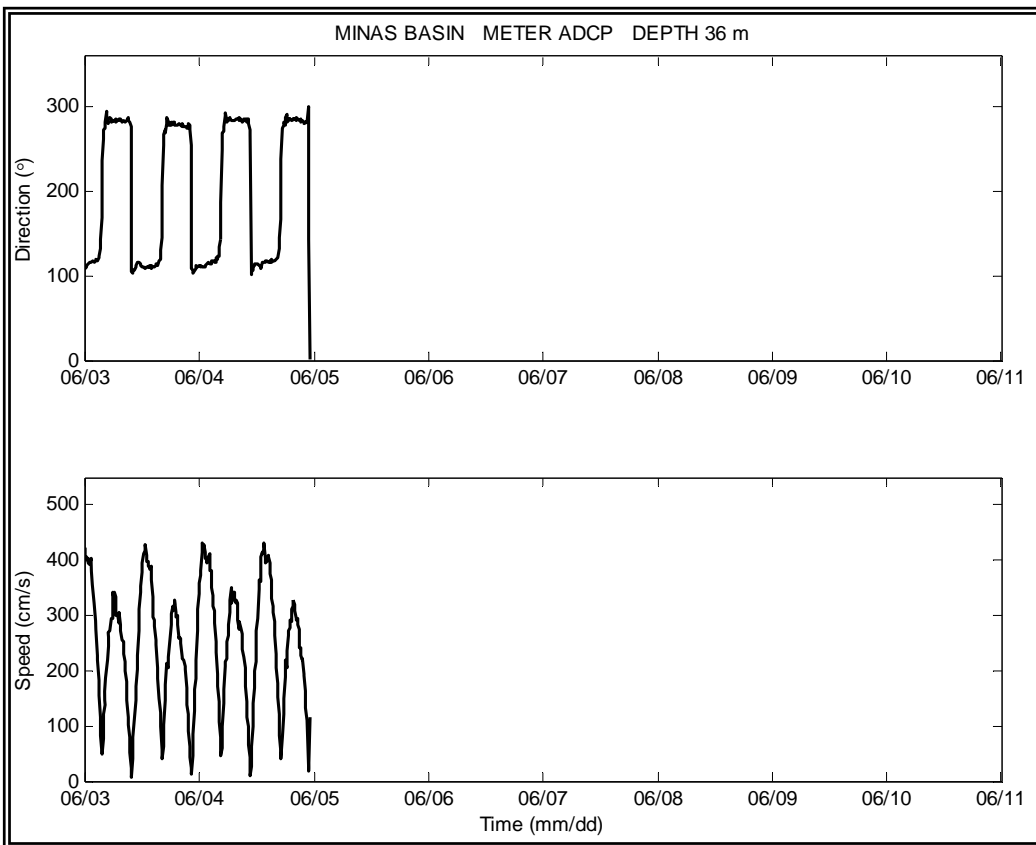




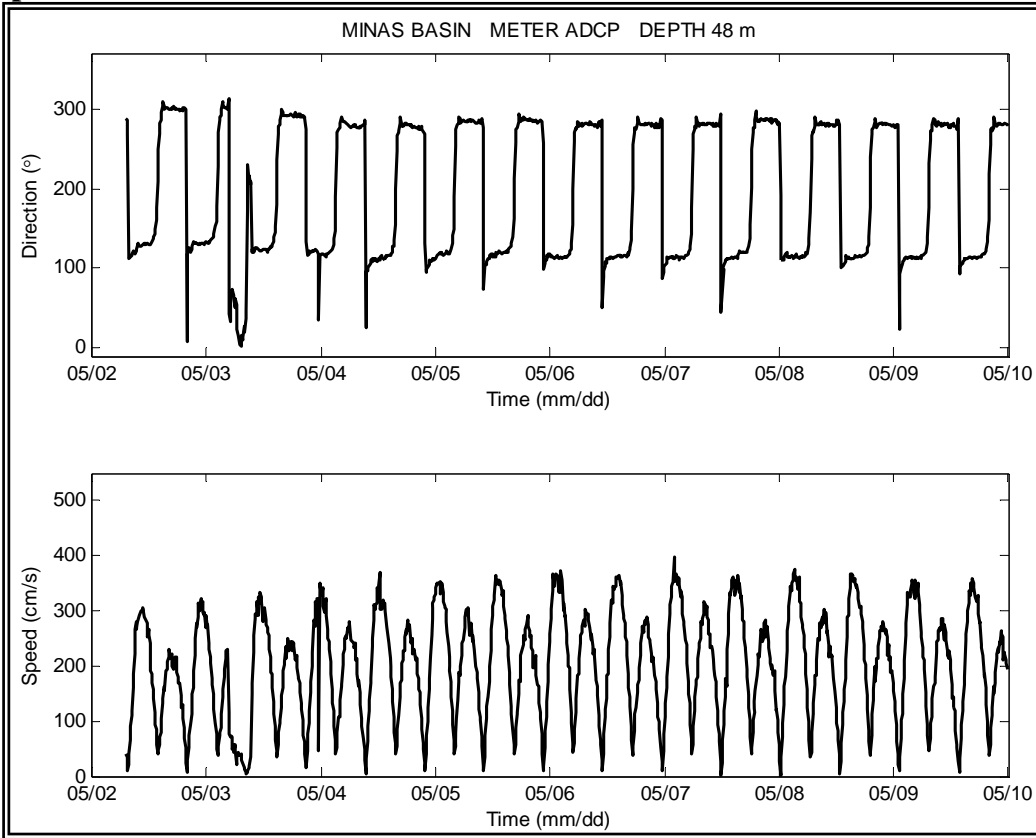


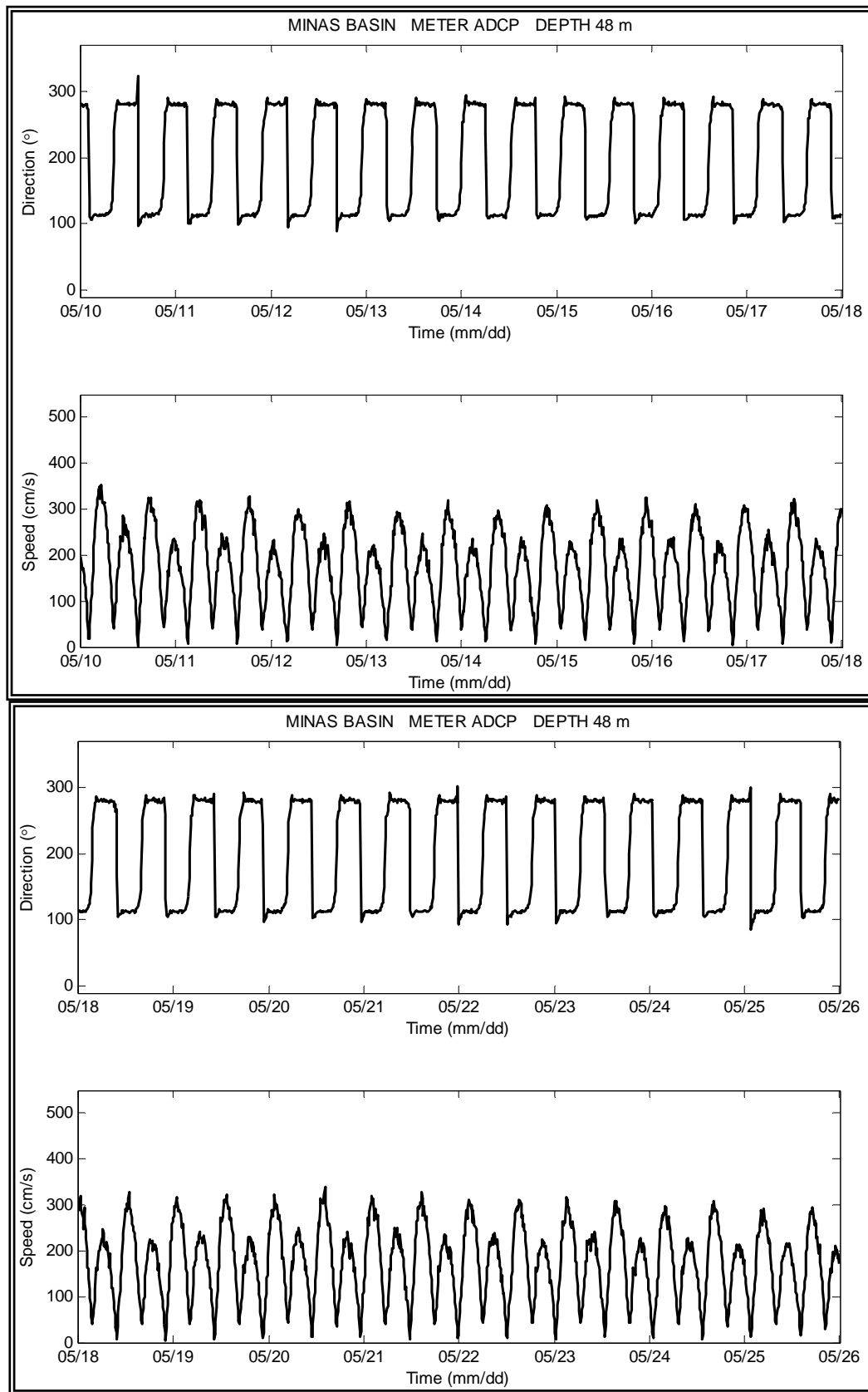
36 m Depth


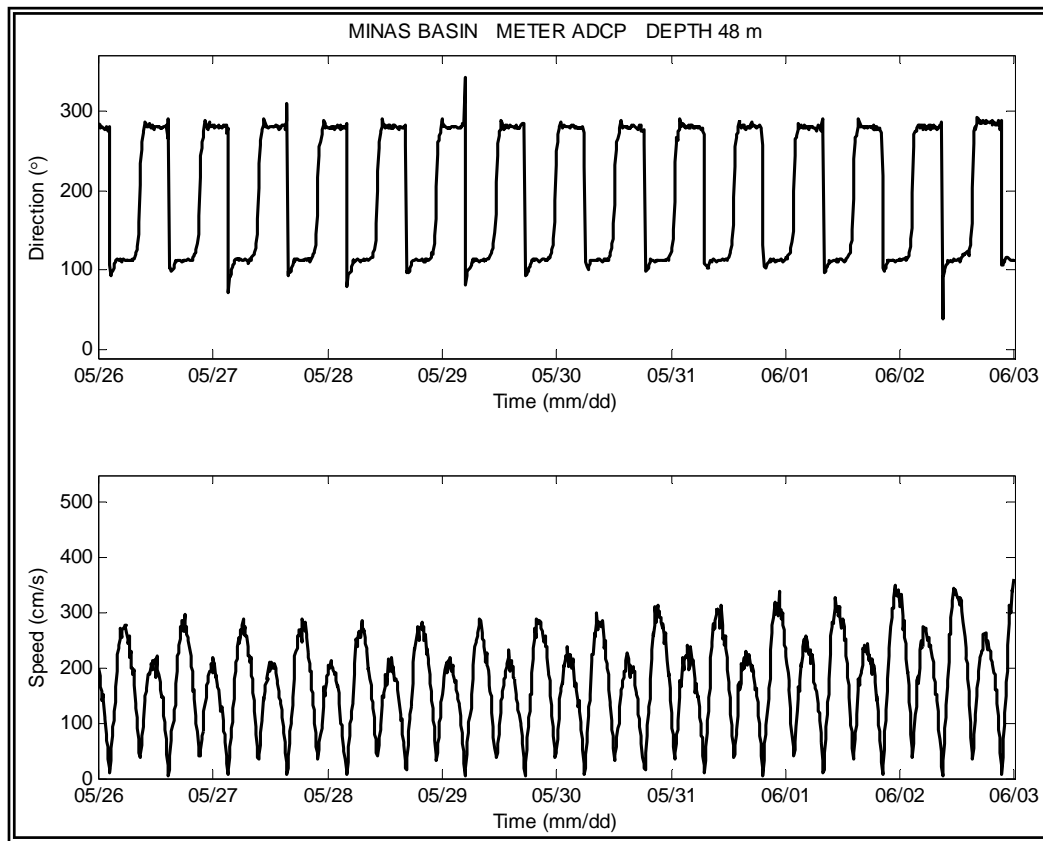




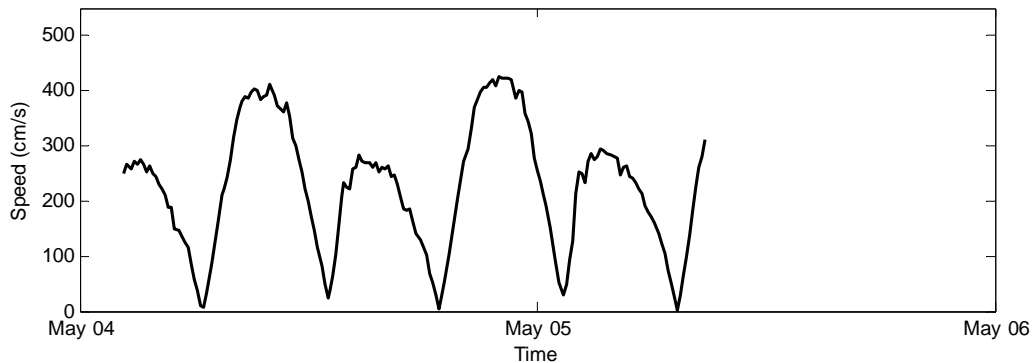
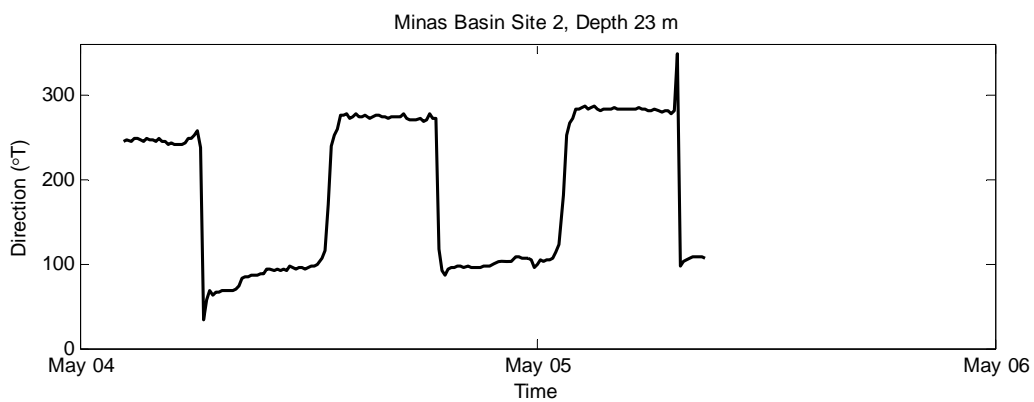
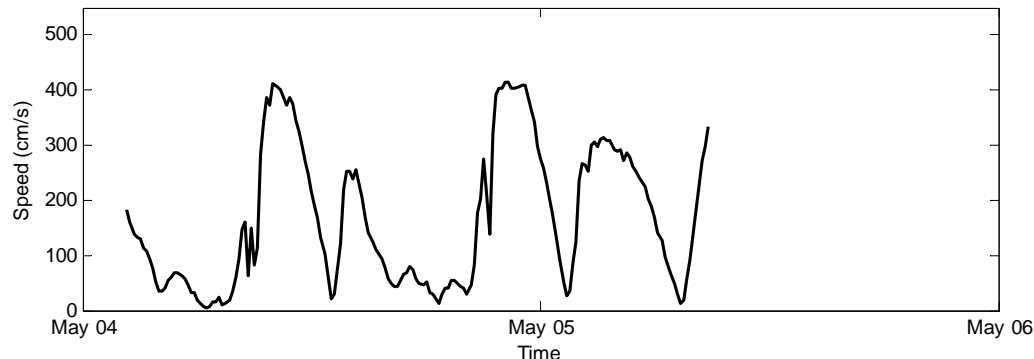
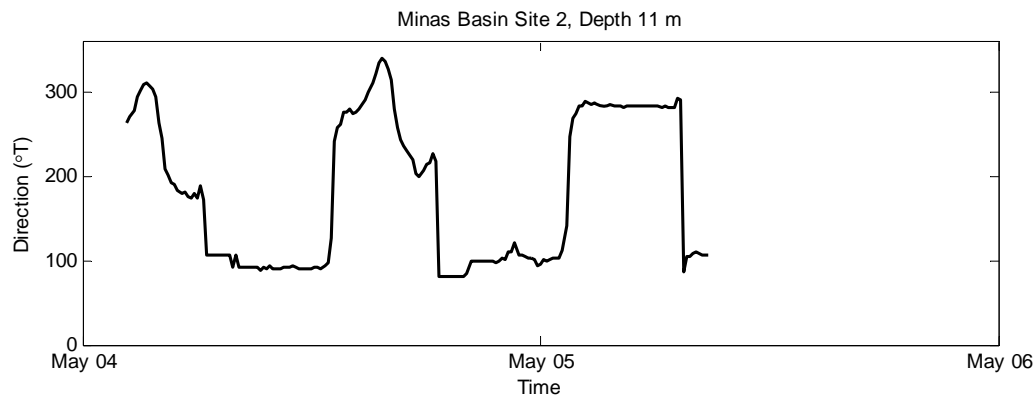
48 m Depth



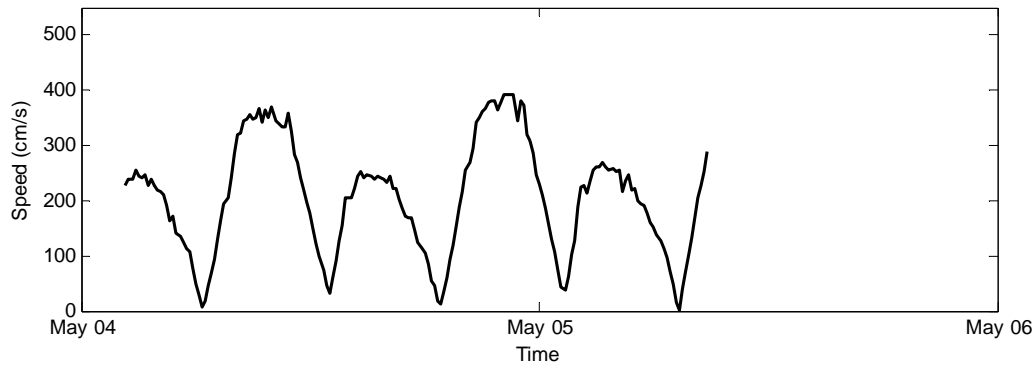
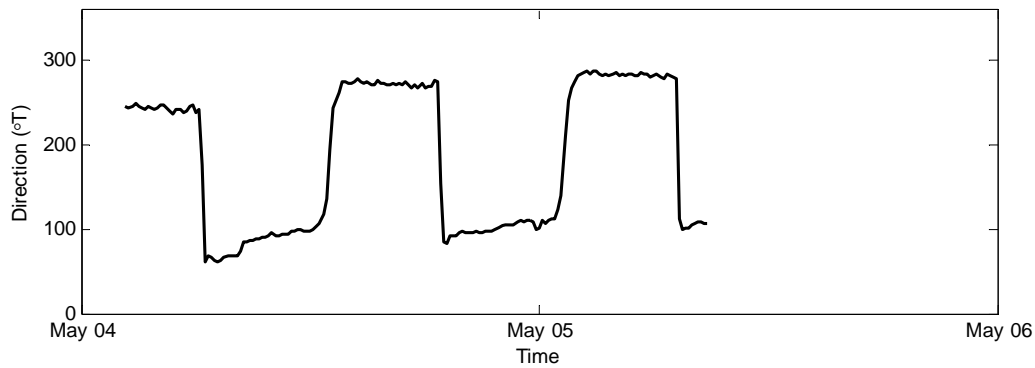




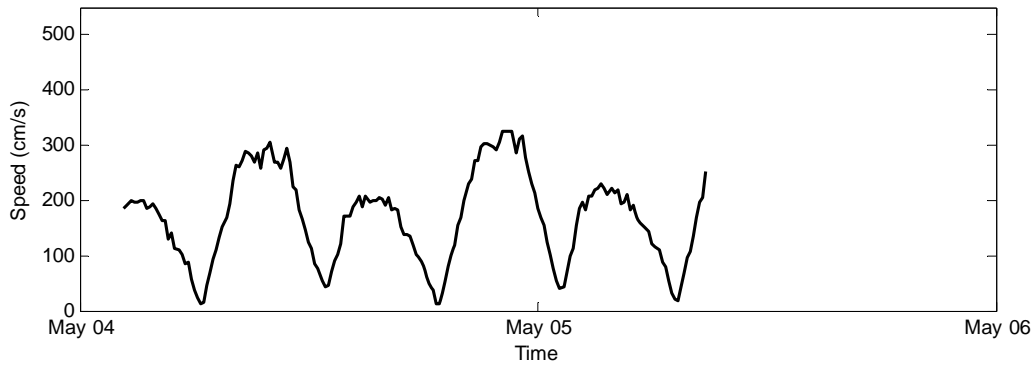
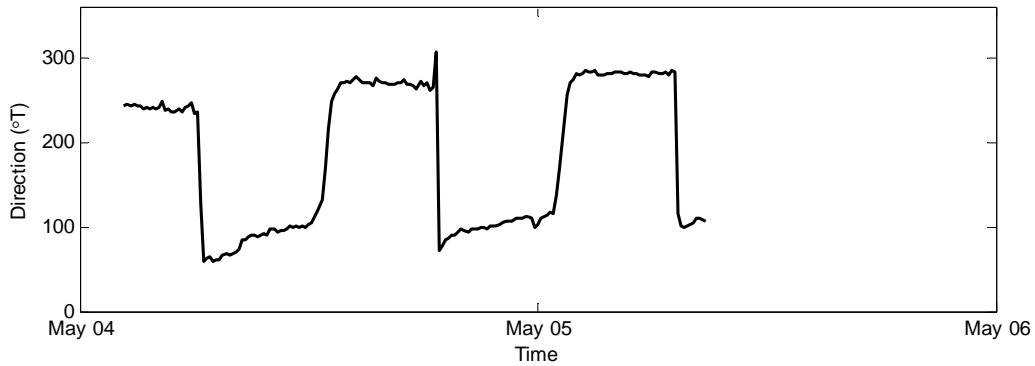
Appendix 2
Time Series Plots, ADCP at Site 2



Minas Basin Site 2, Depth 35 m

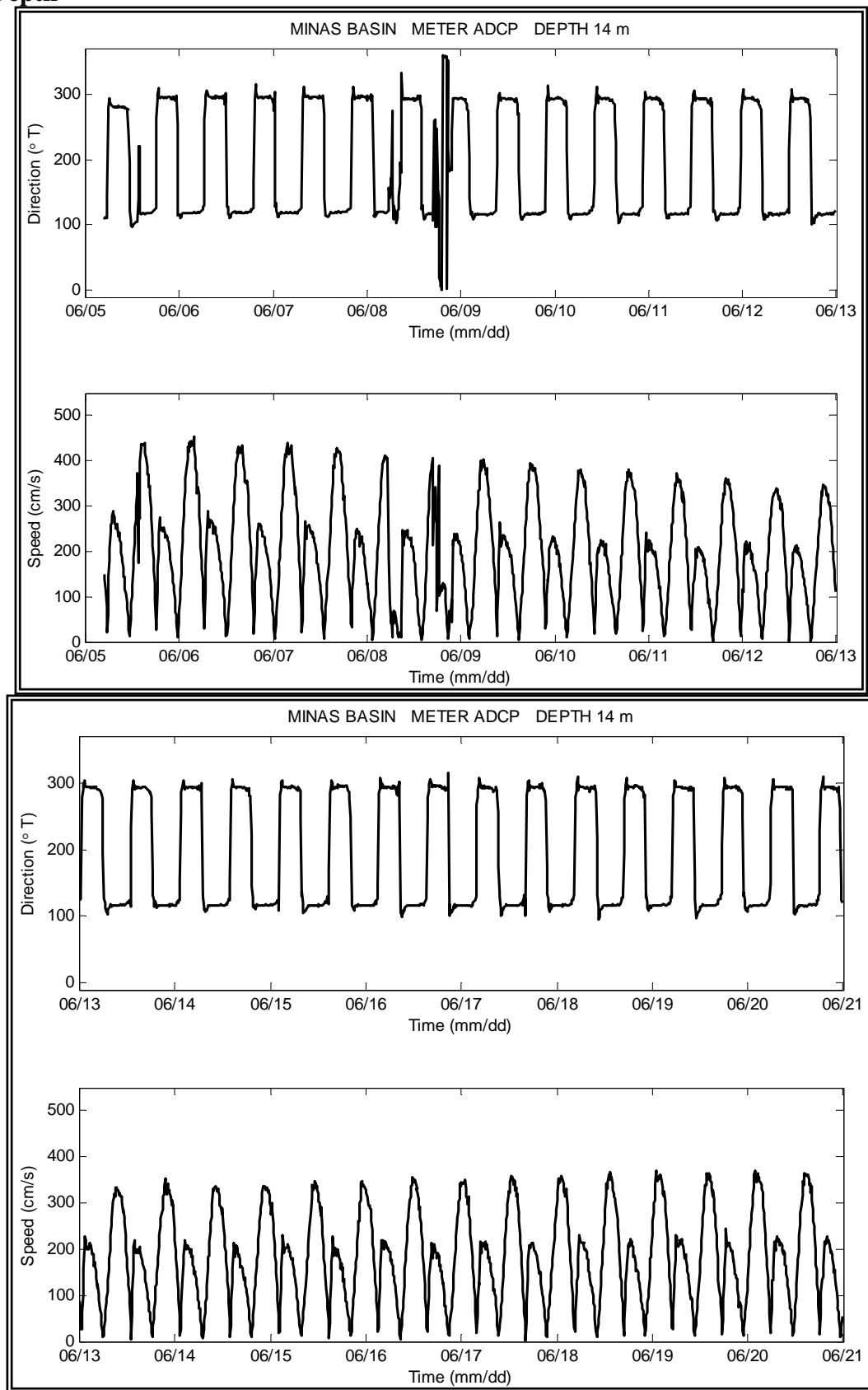


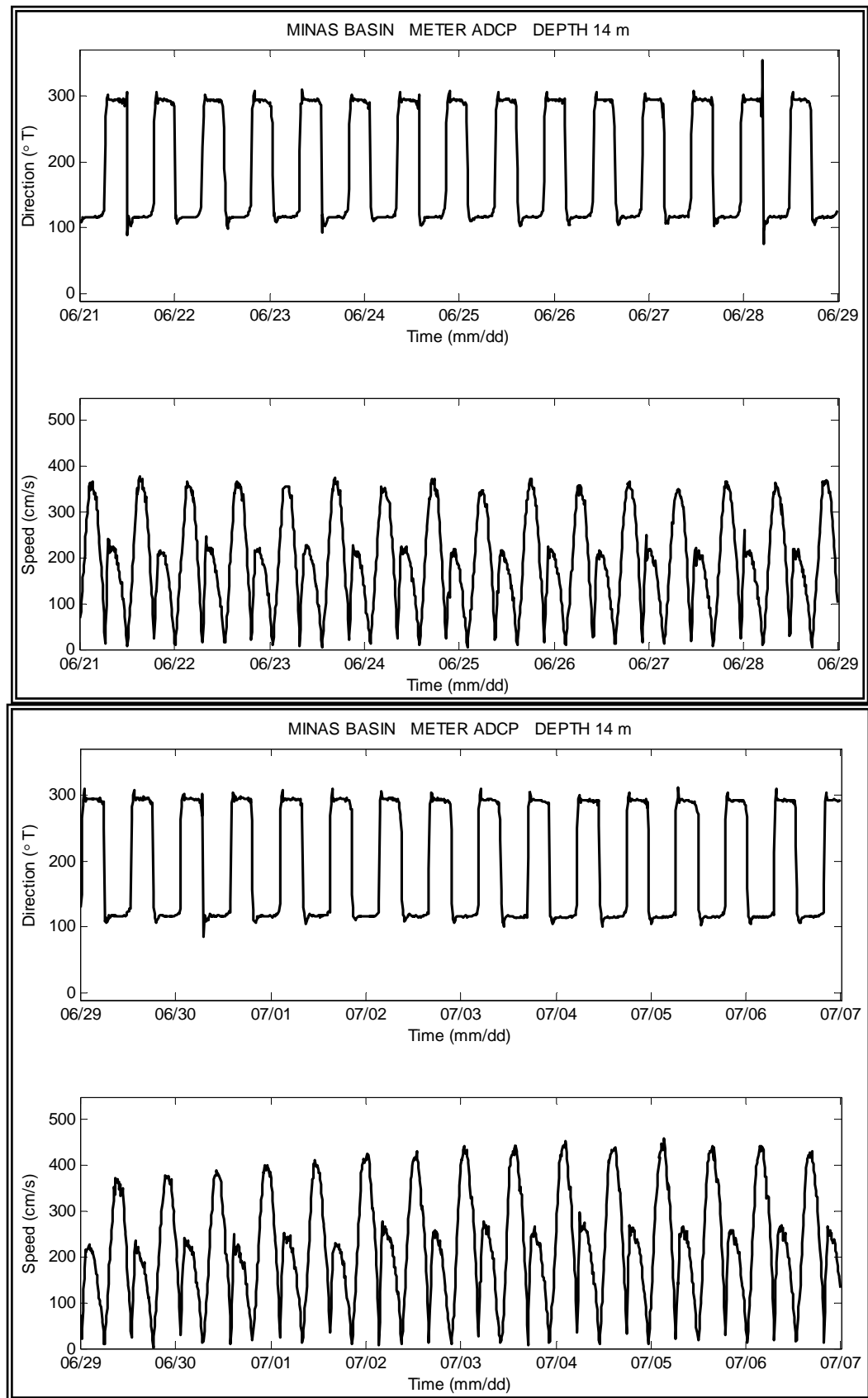
Minas Basin Site 2, Depth 47 m

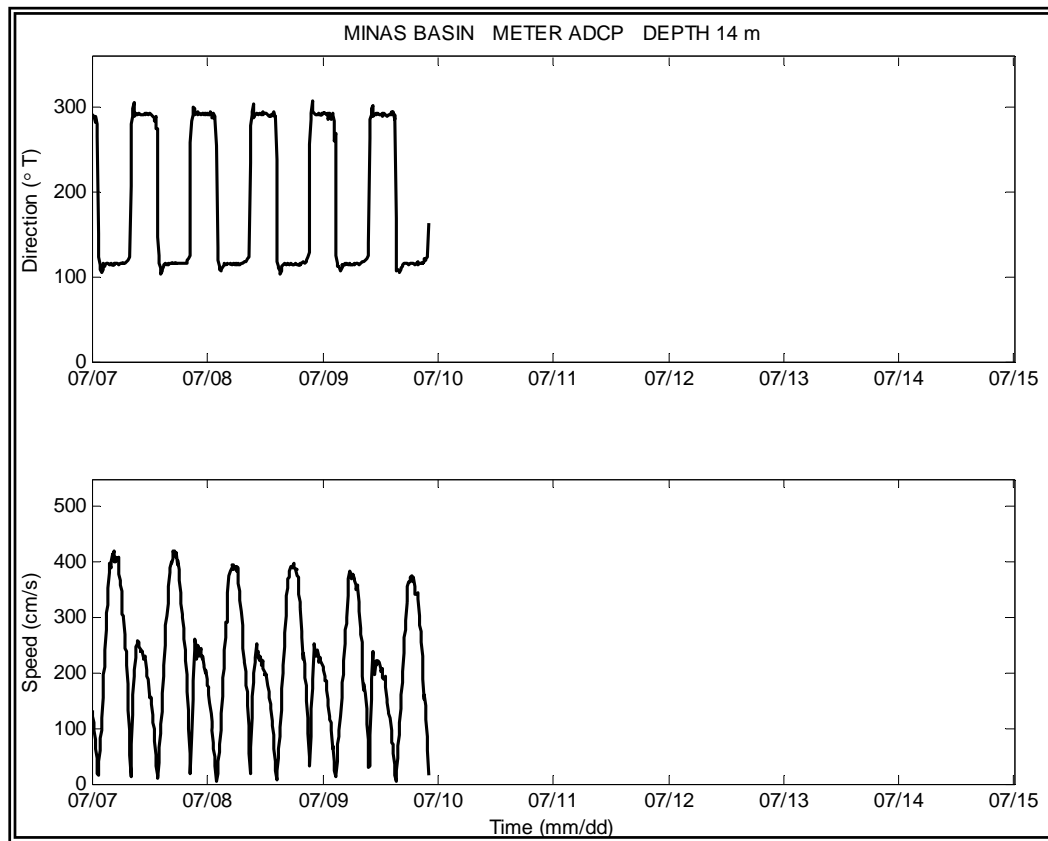


Appendix 3

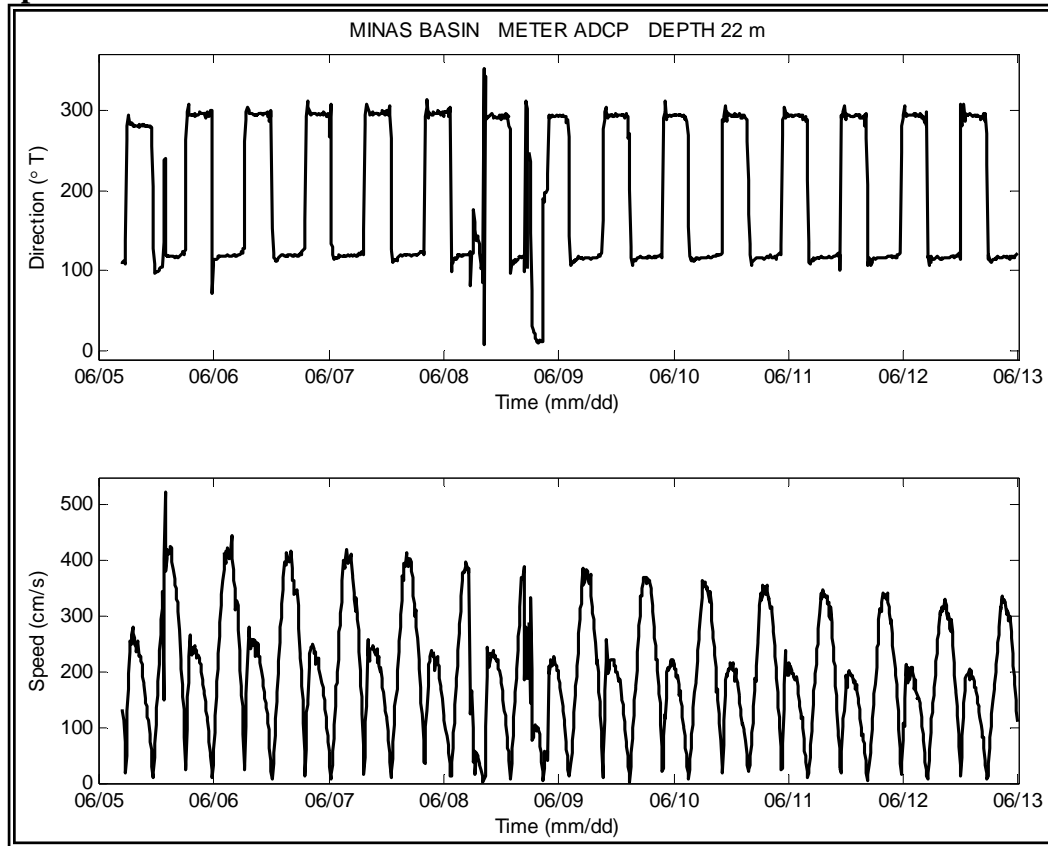
Time Series Plots, ADCP at Site 3

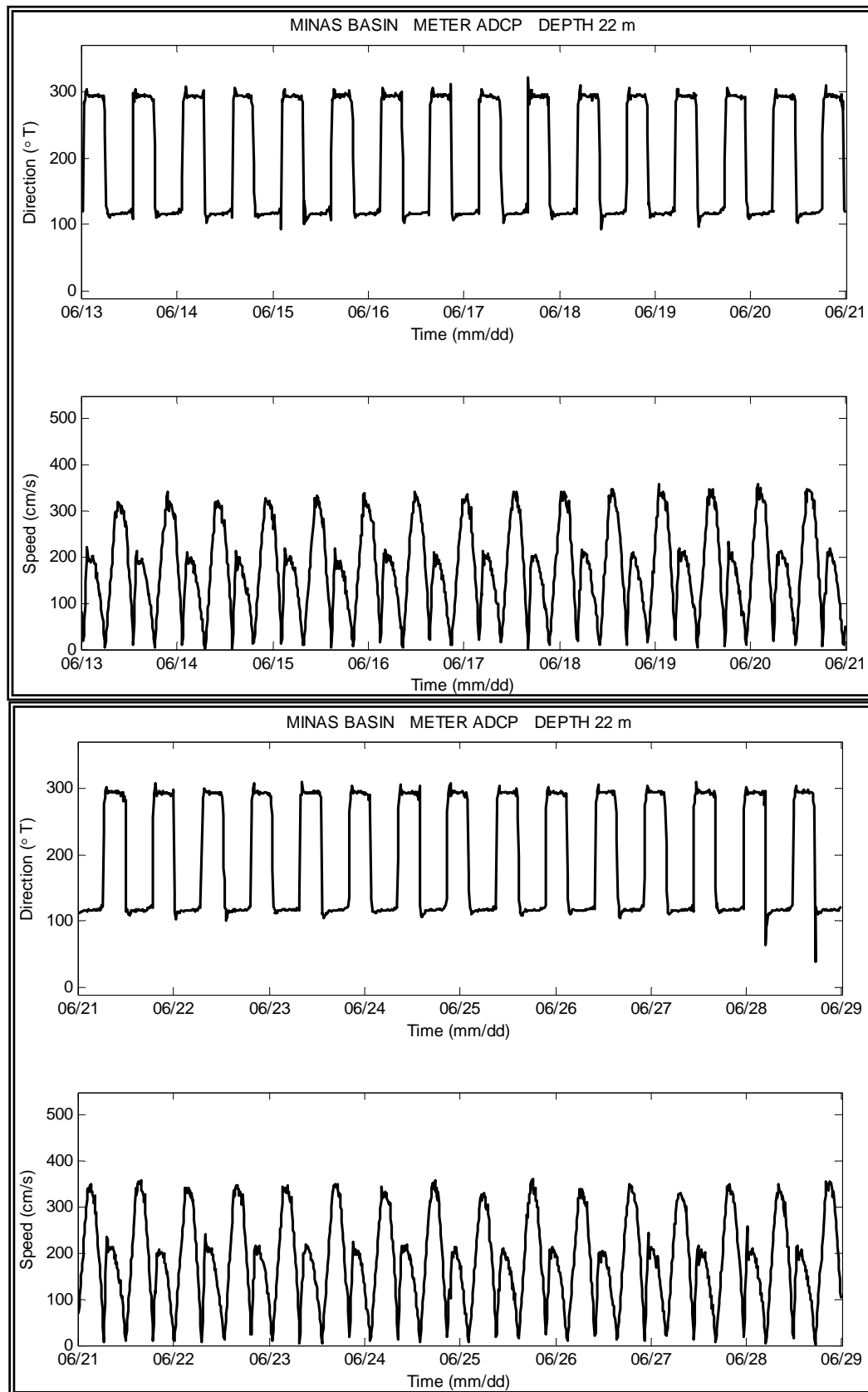
14 m Depth


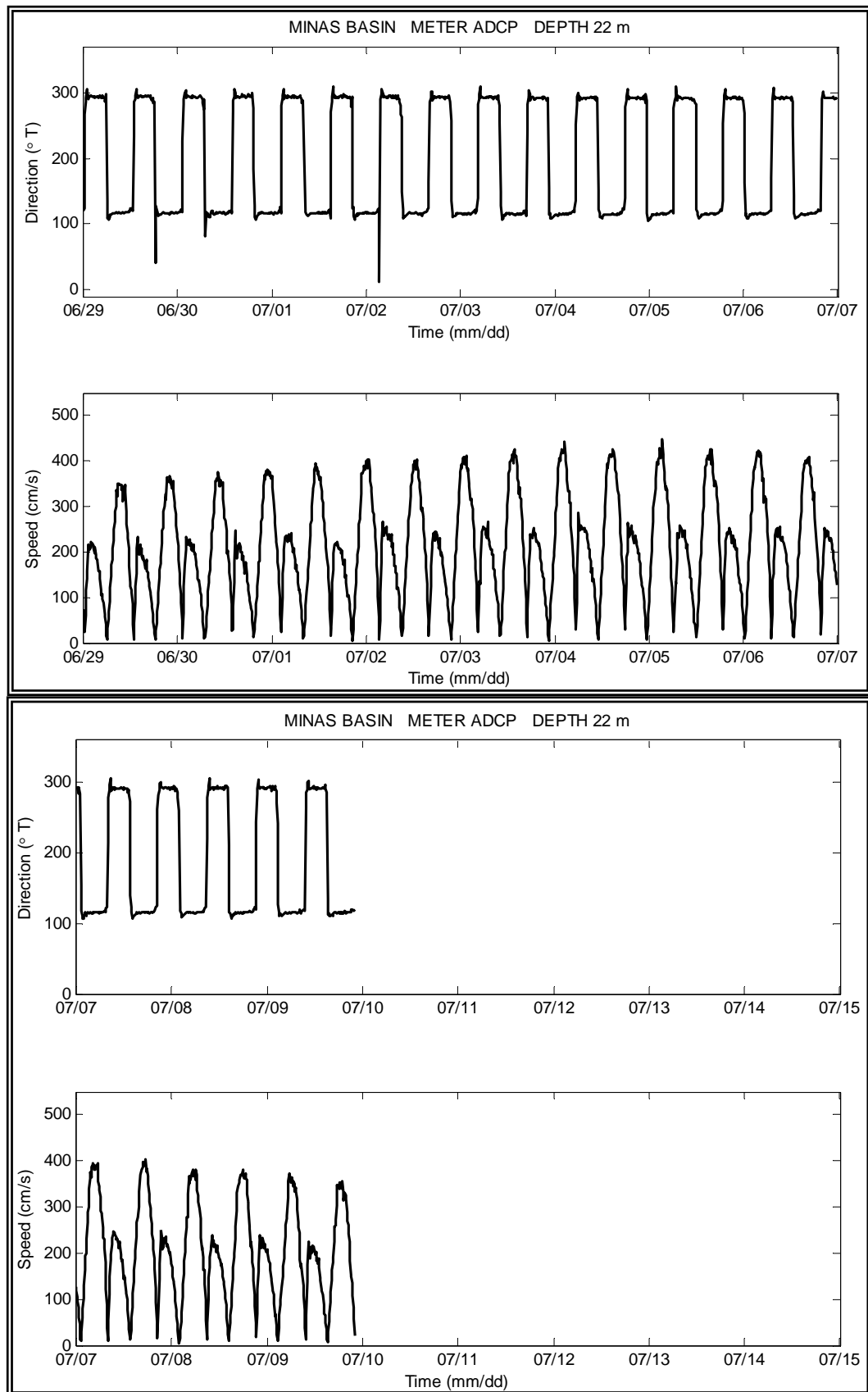




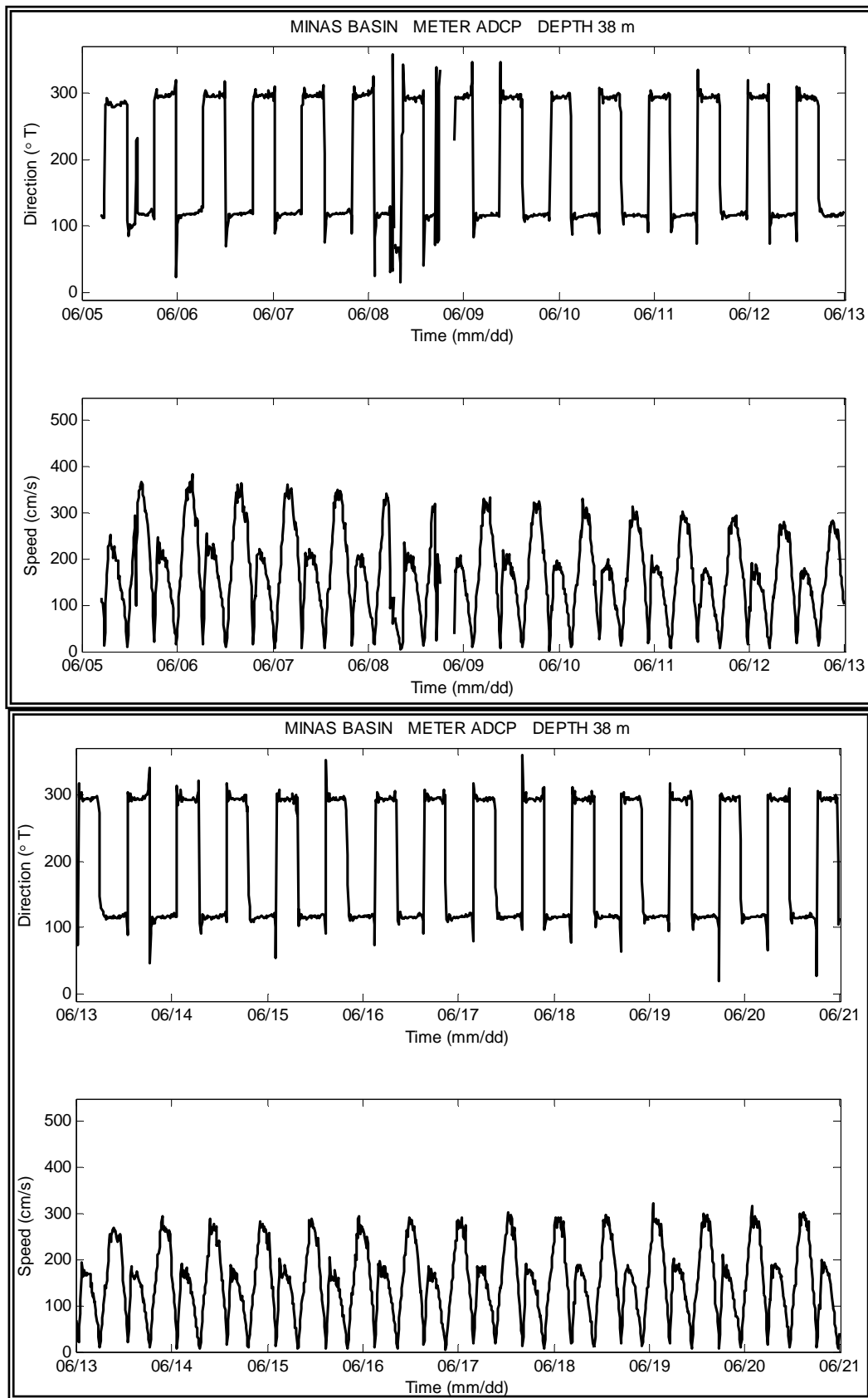
22 m Depth

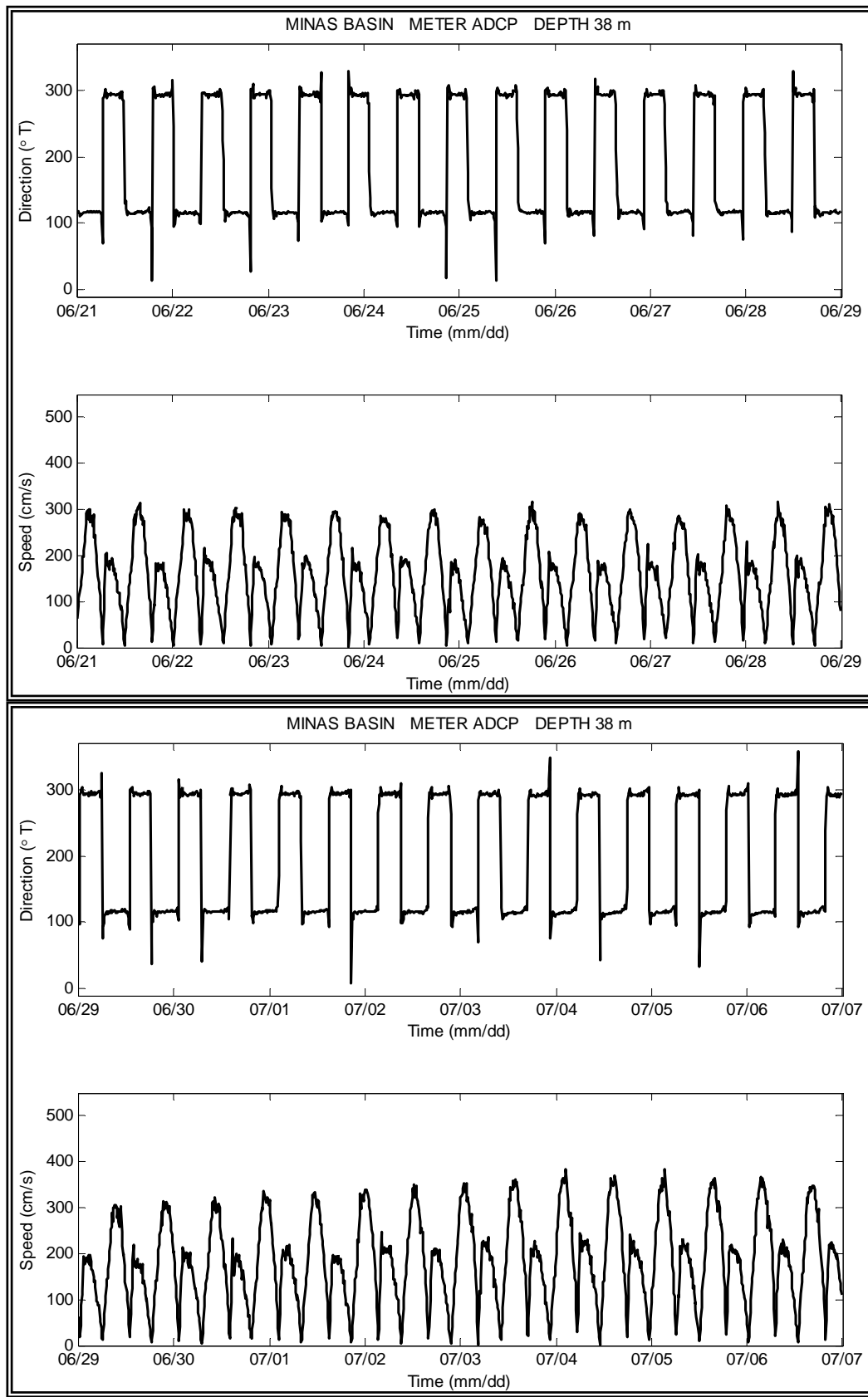


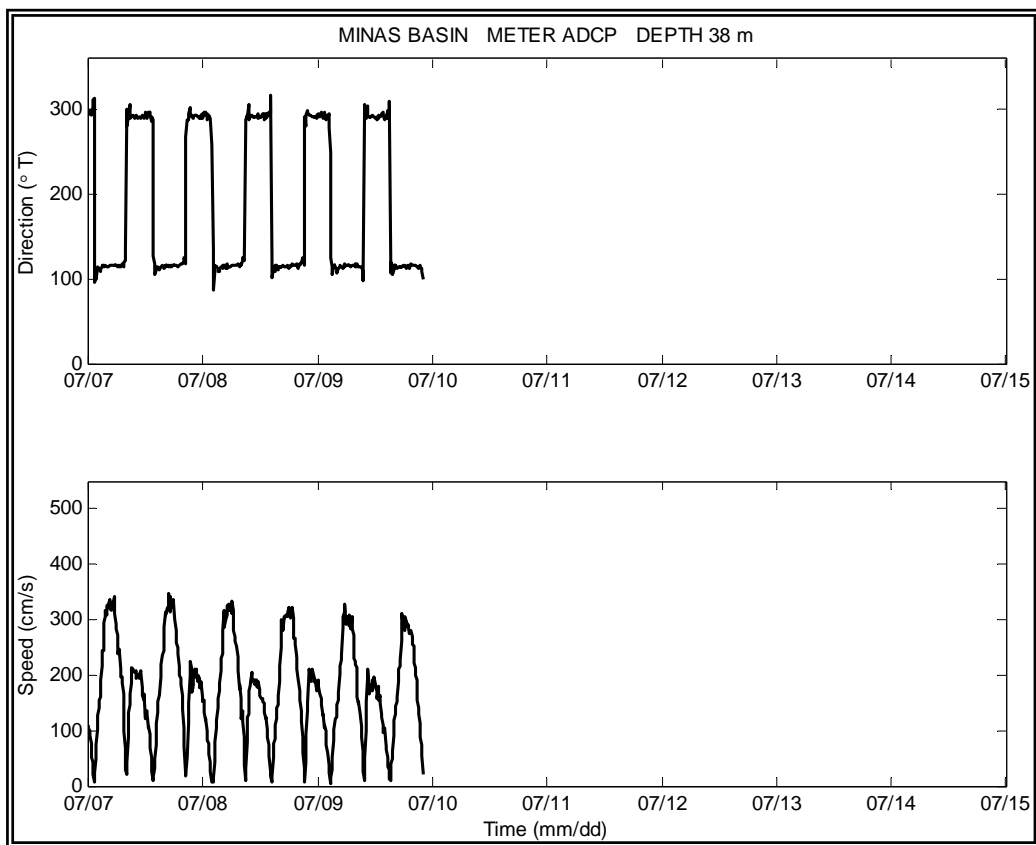




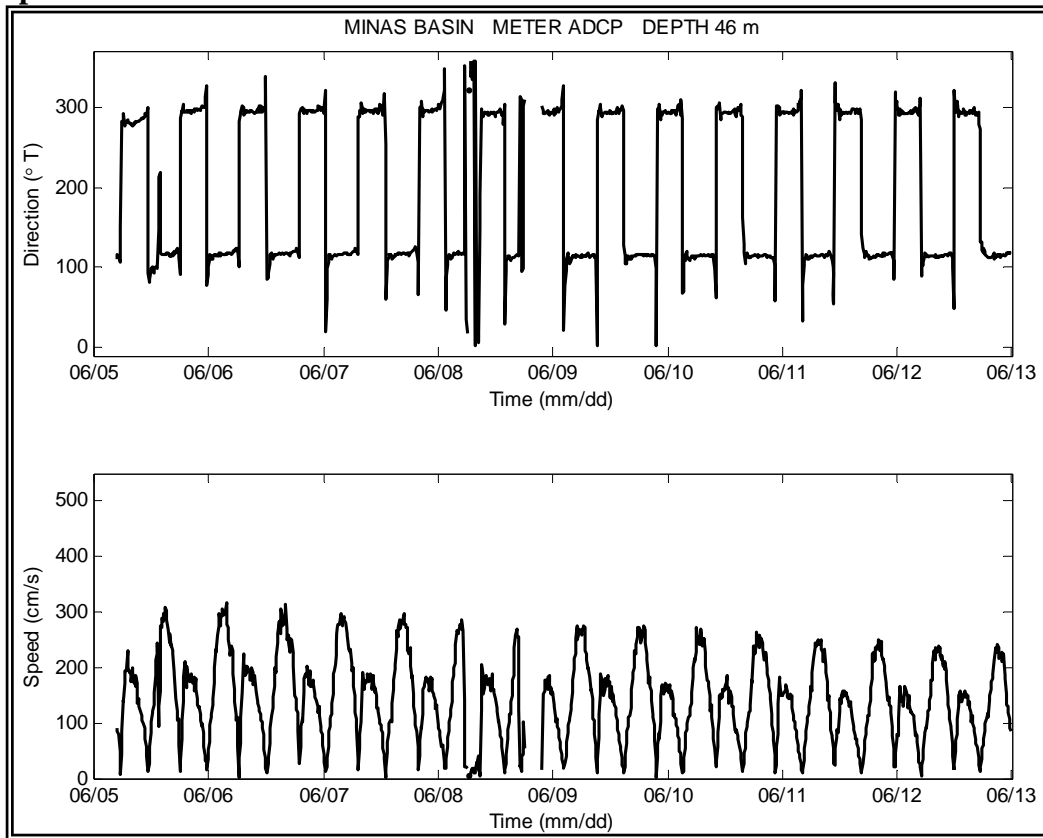
38 m Depth

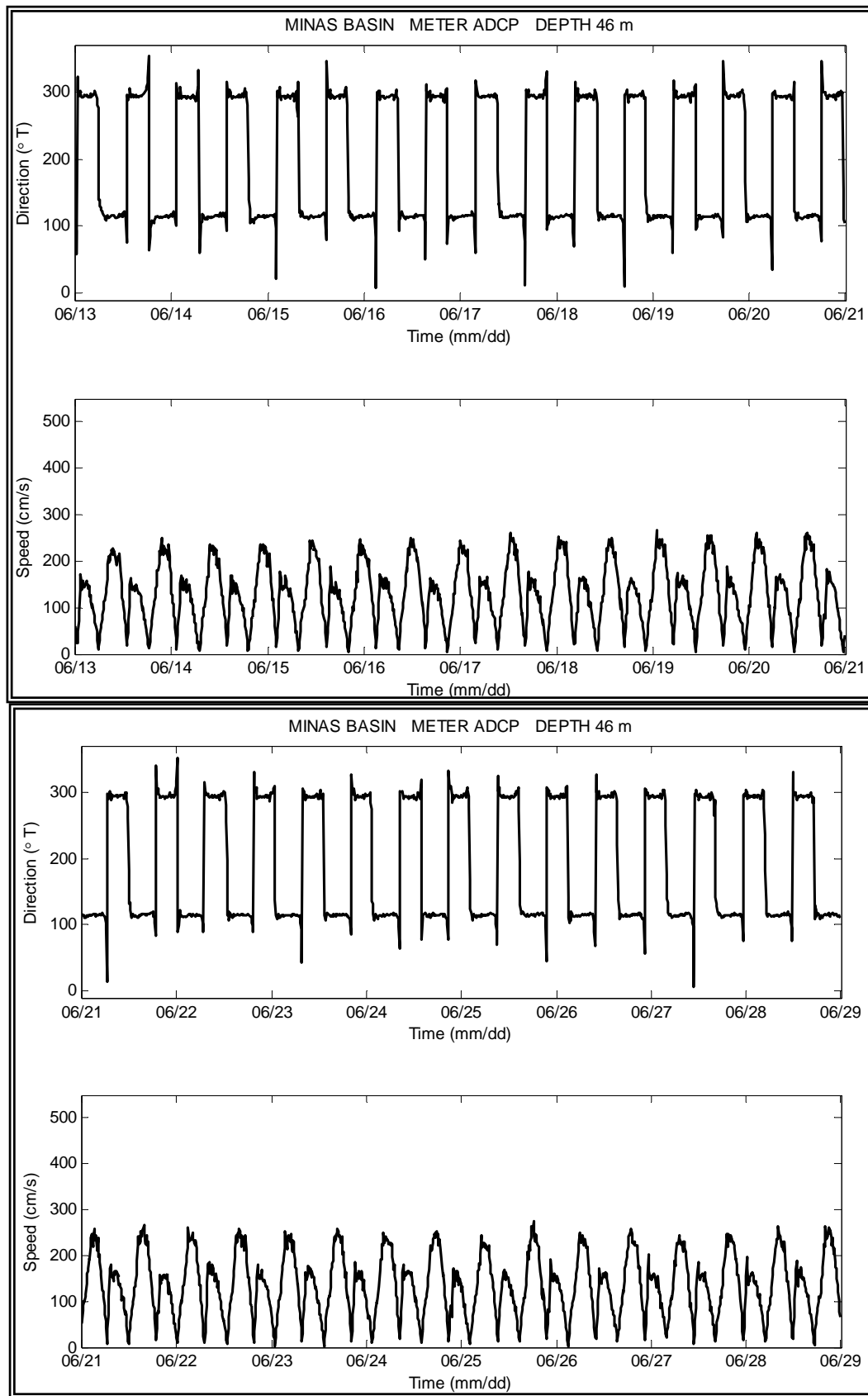


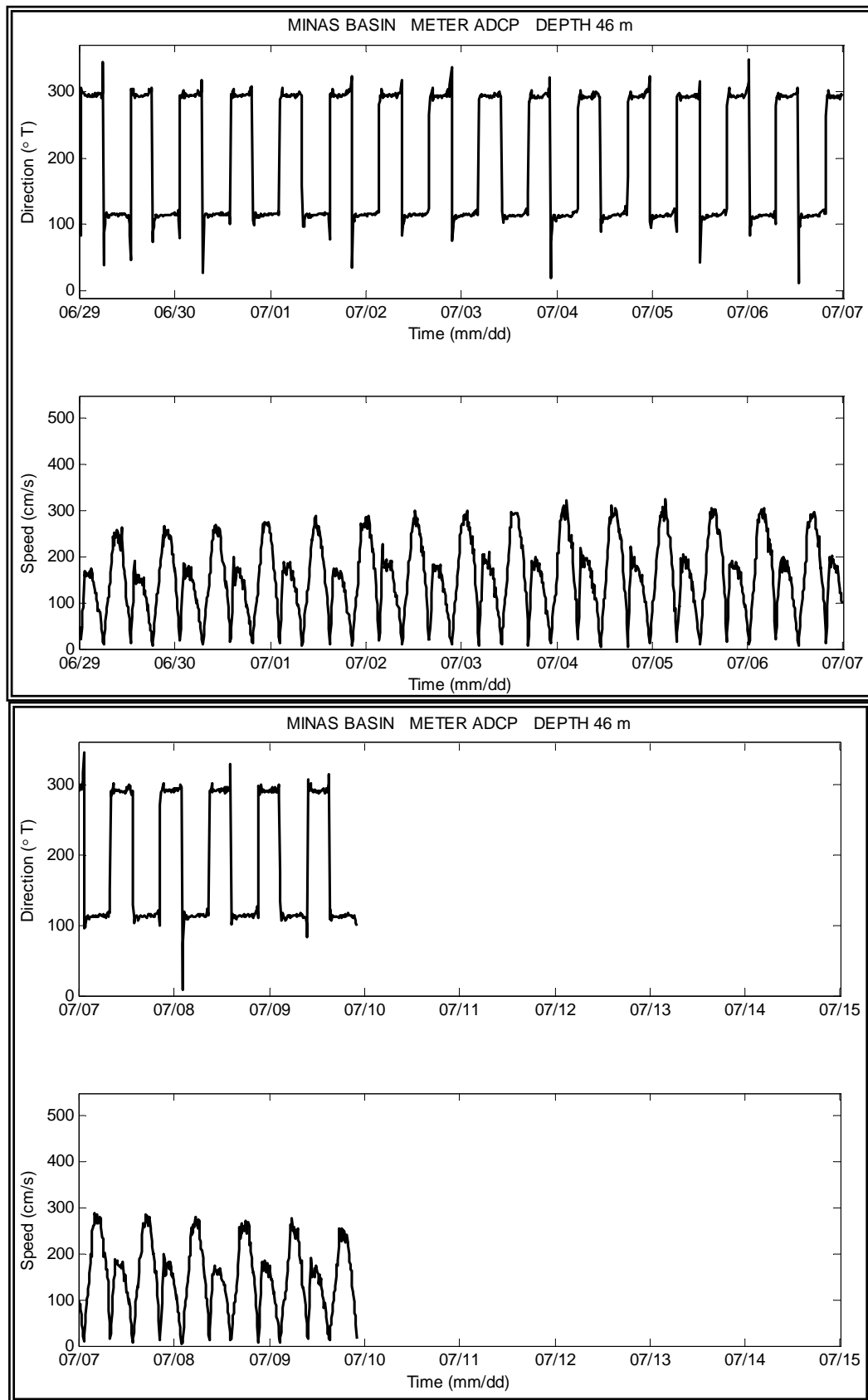




46 m Depth



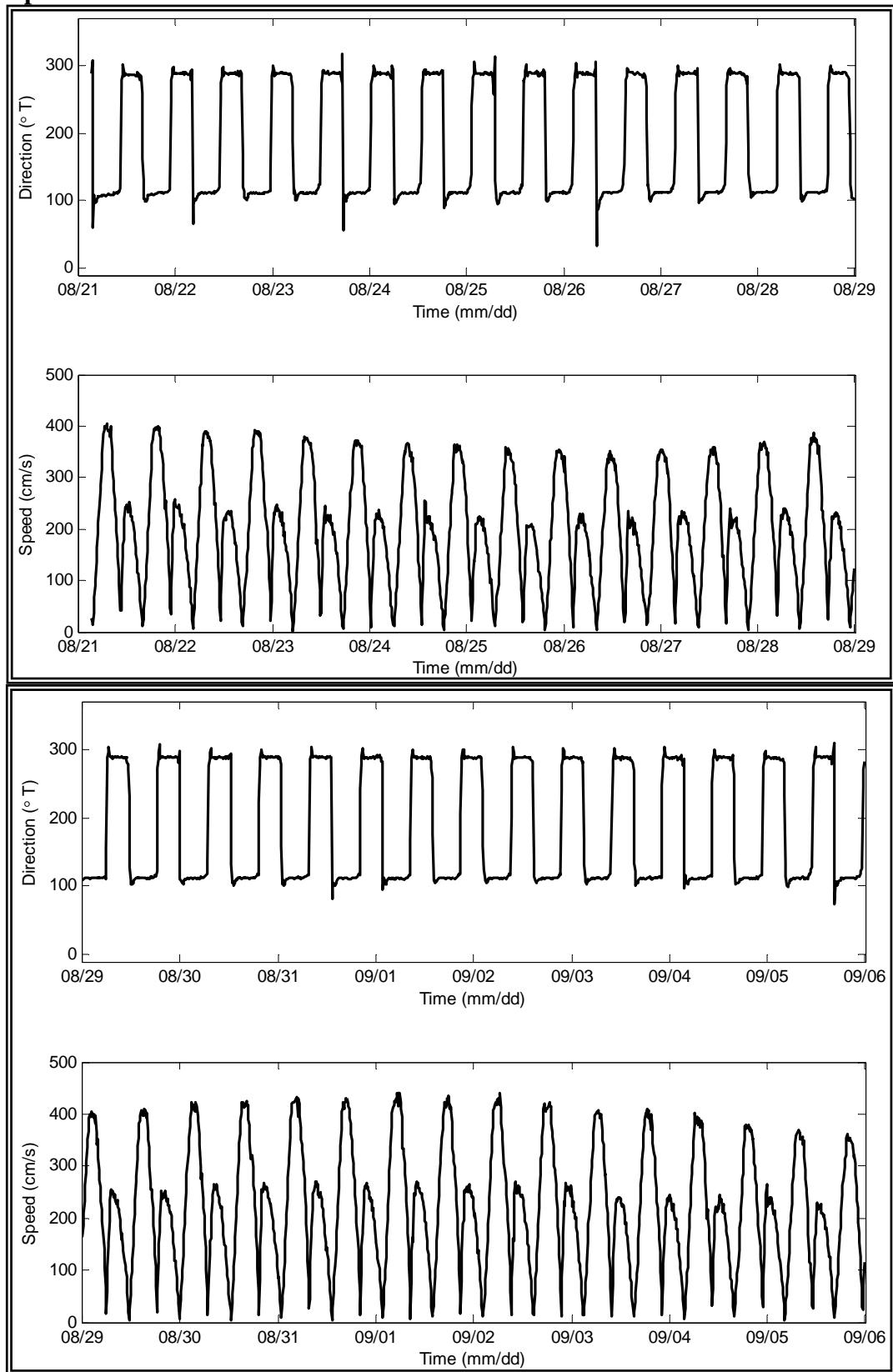


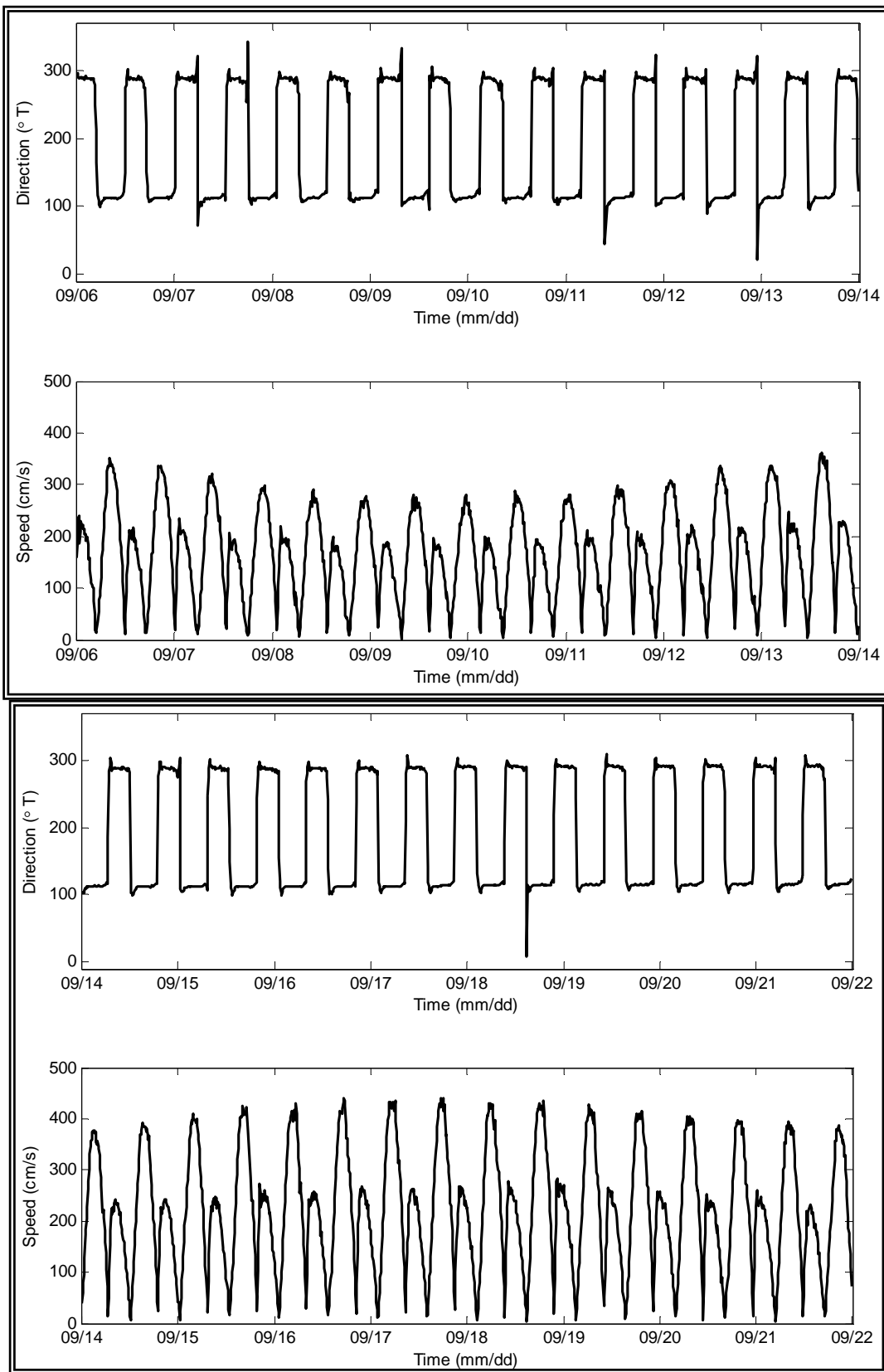


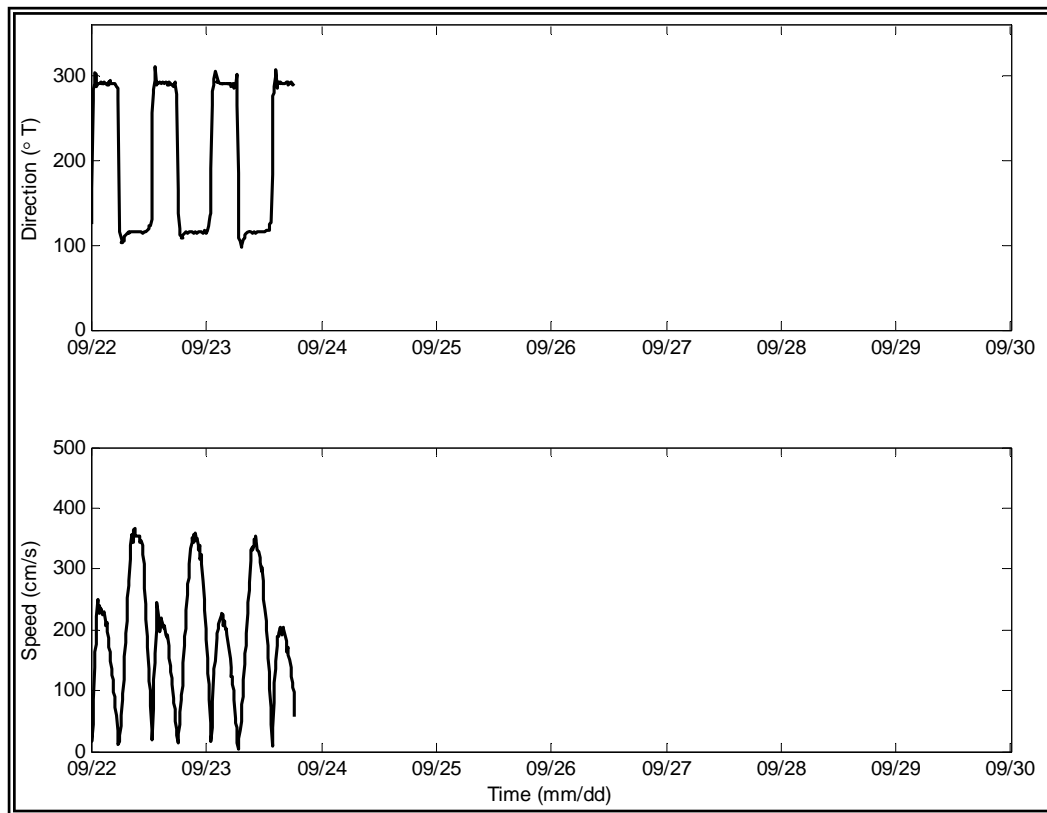
Appendix 4

Time Series Plots at Site 4

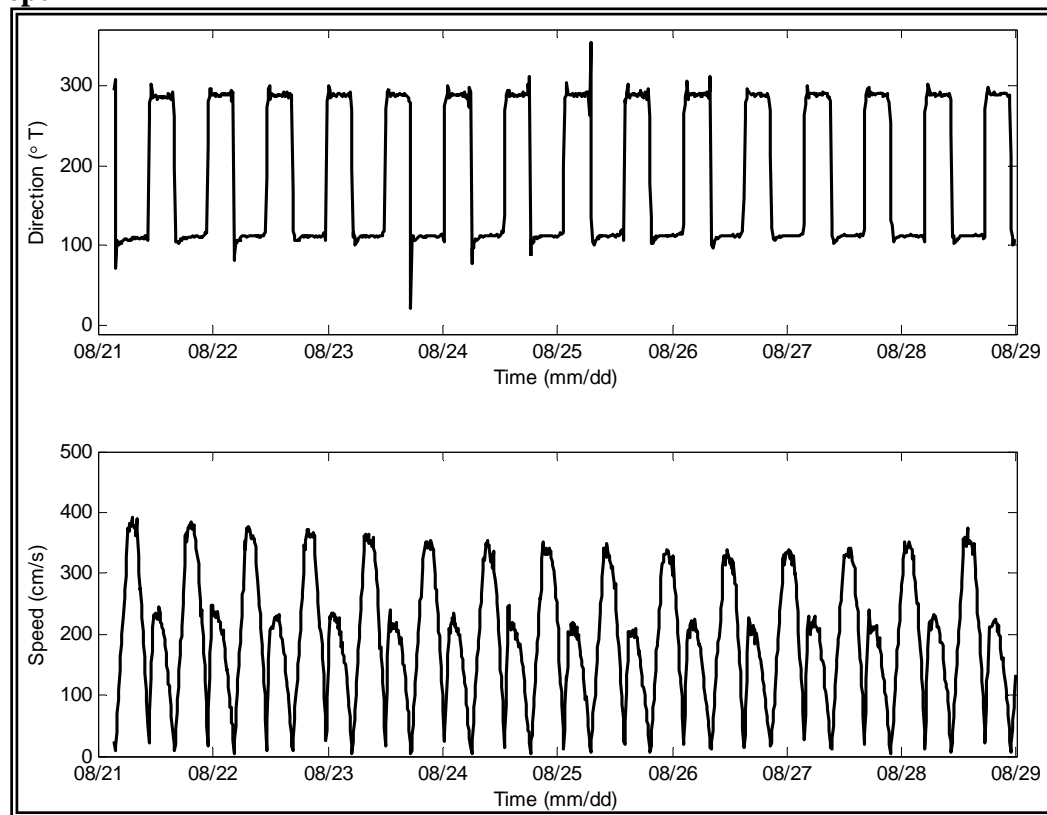
14 m Depth

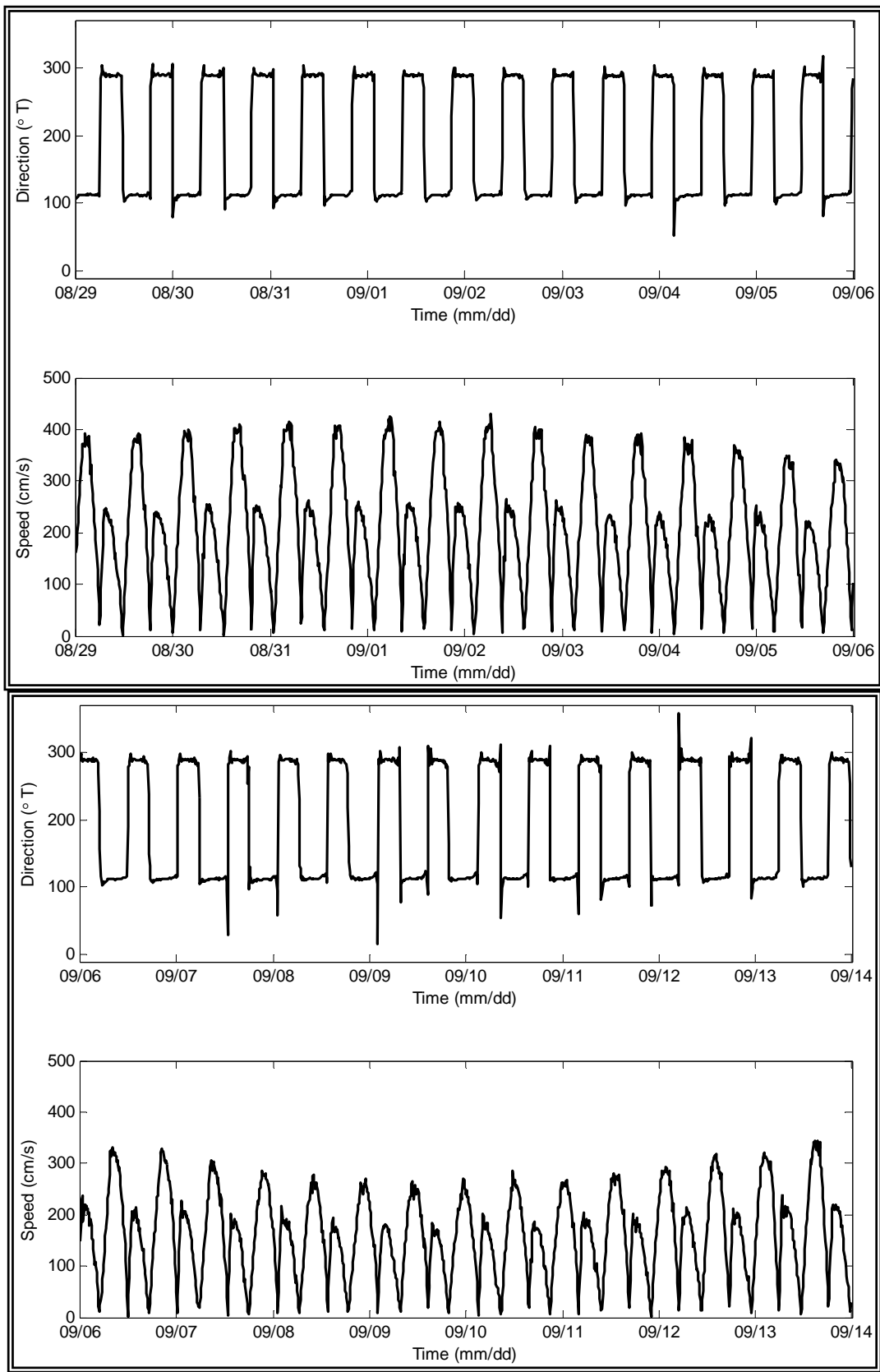


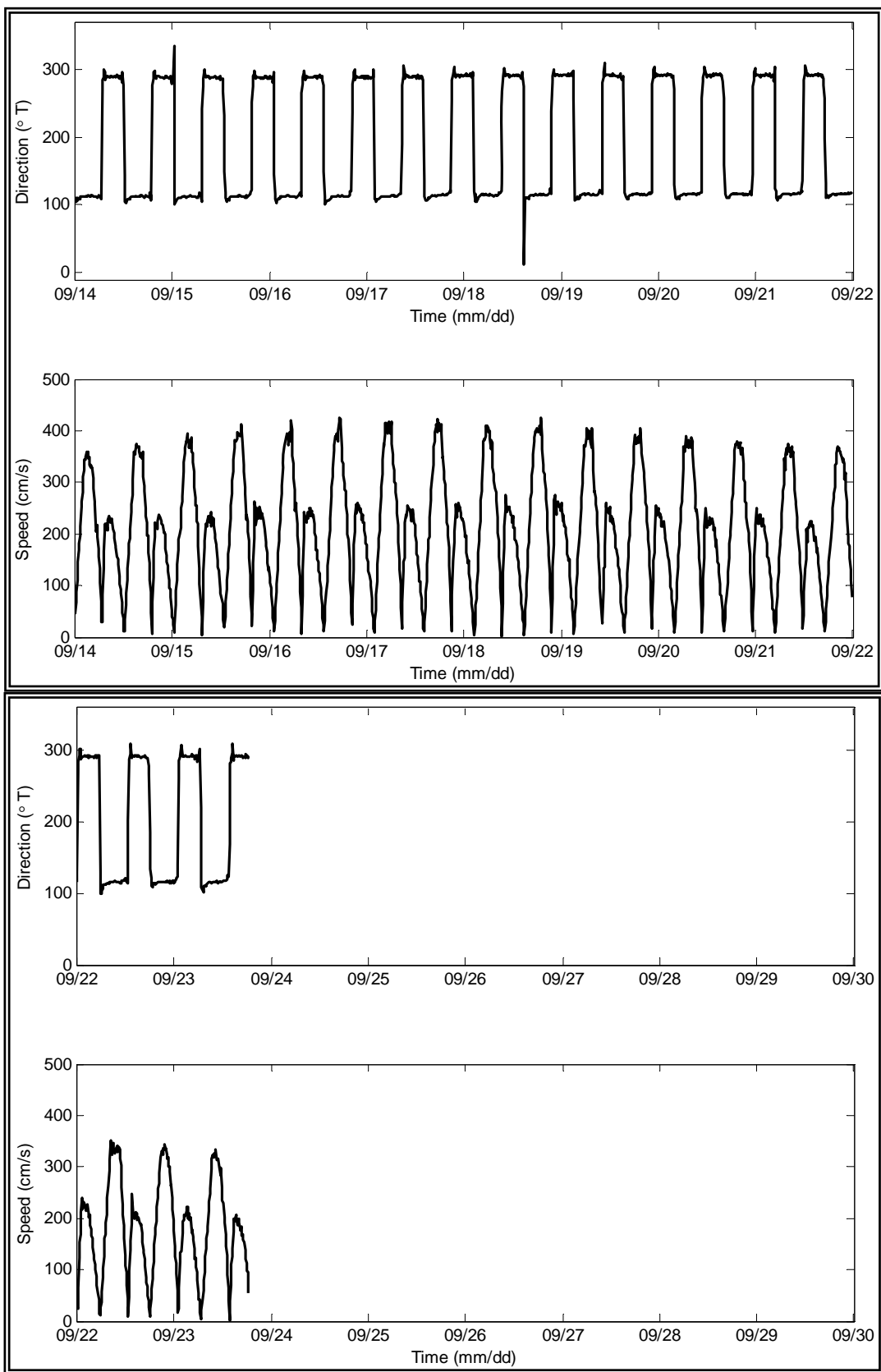




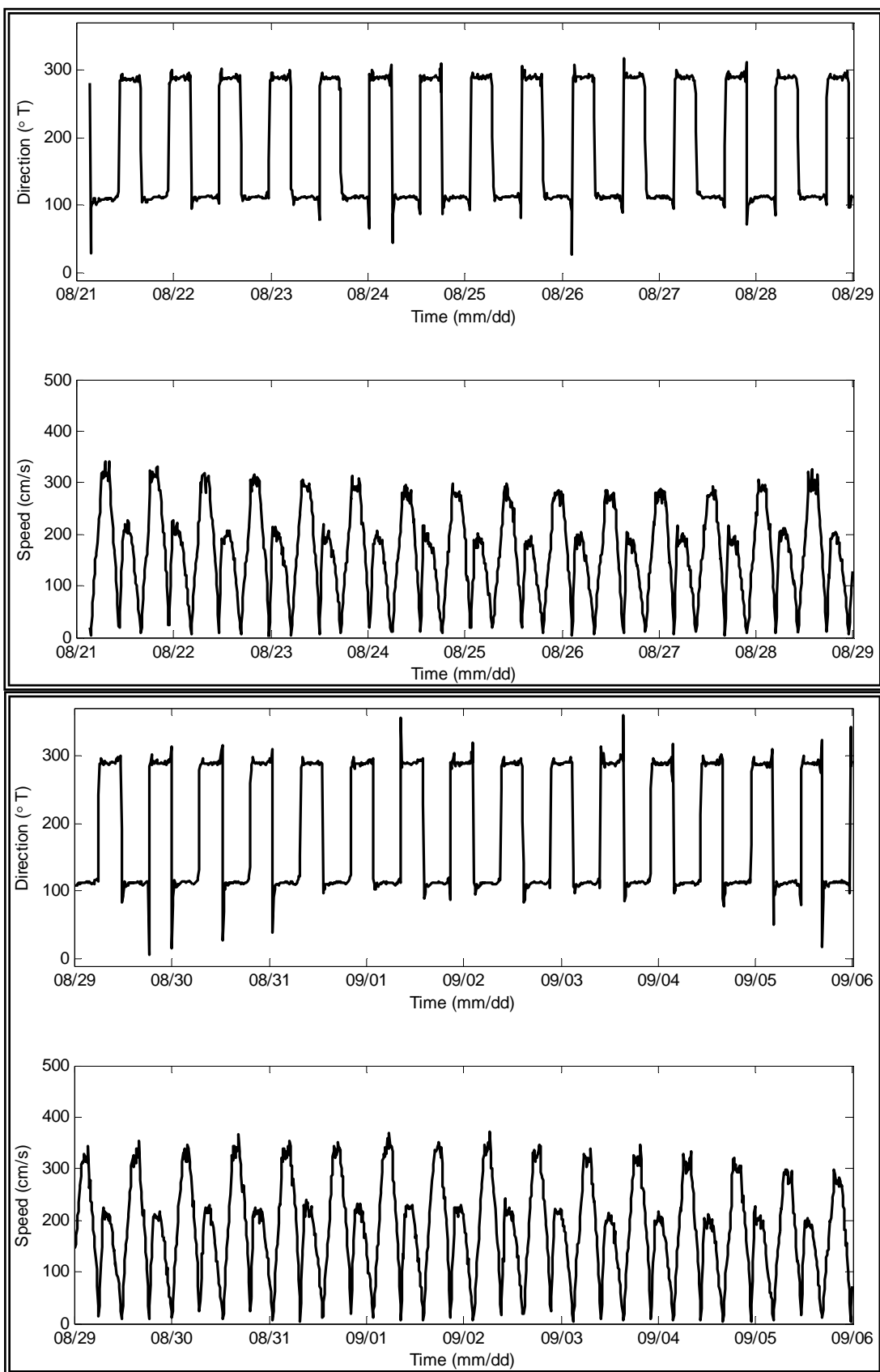
22 m Depth

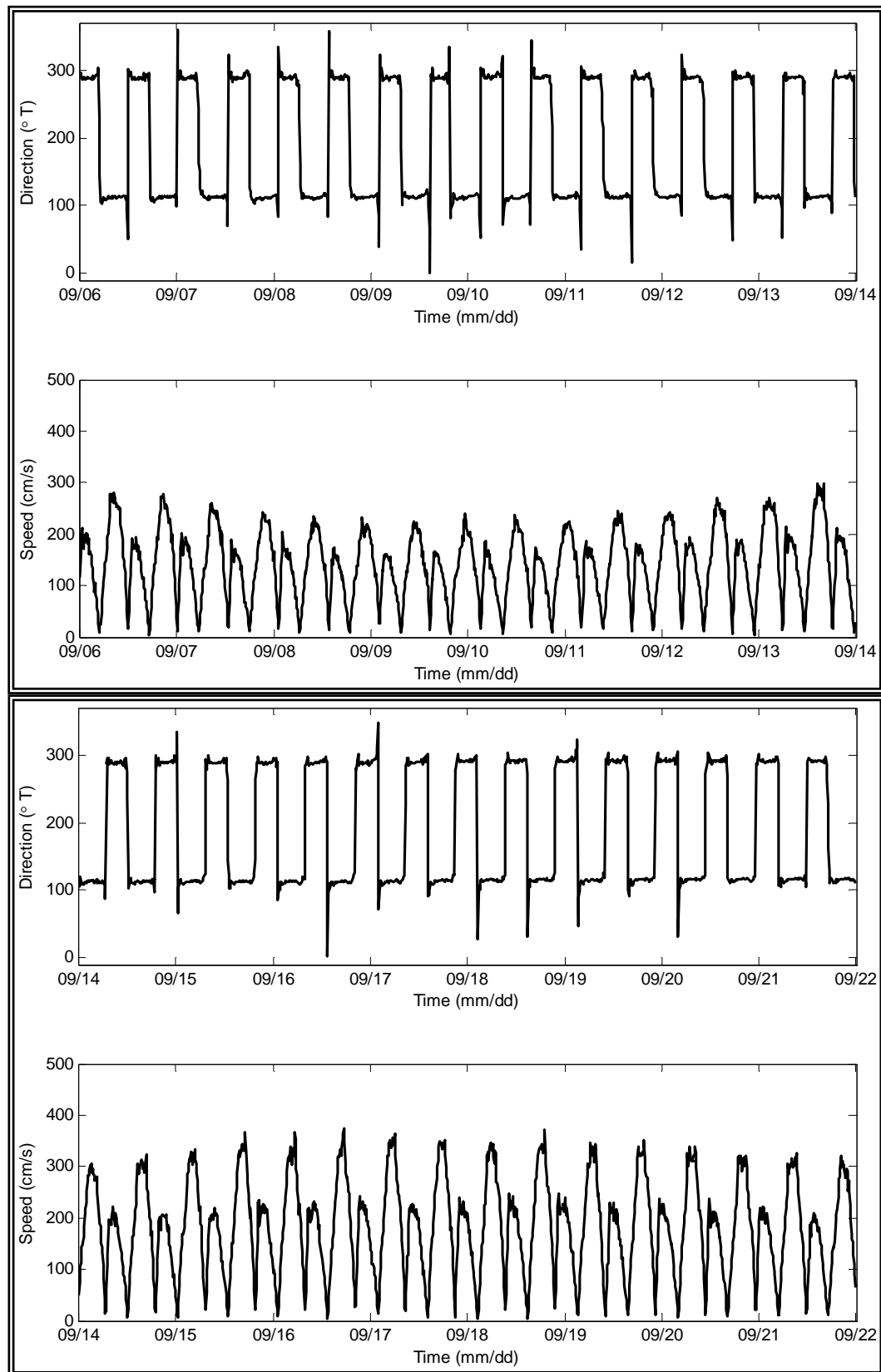


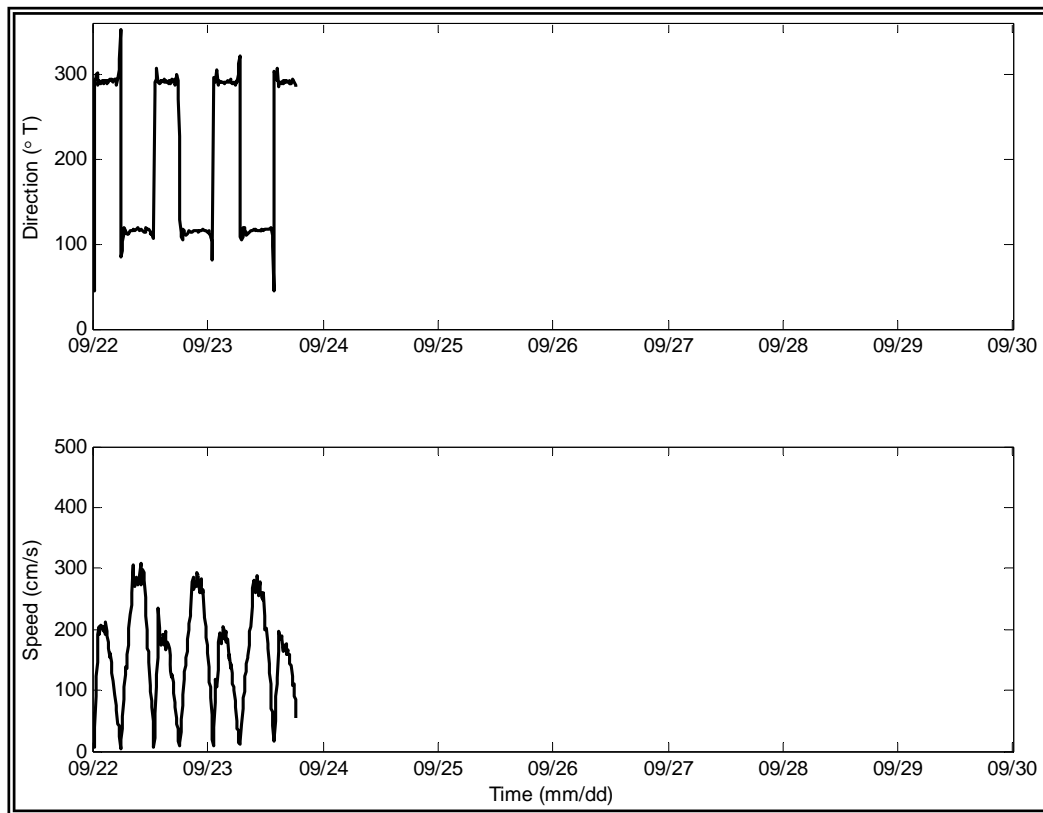




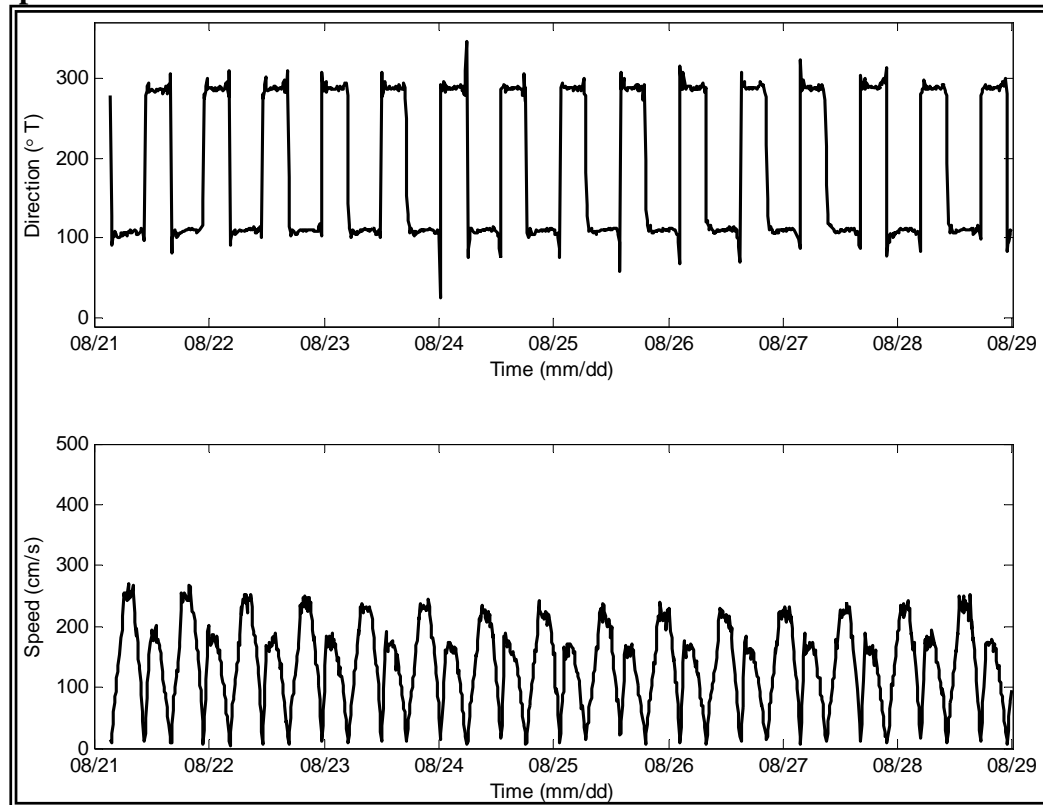
38 m Depth

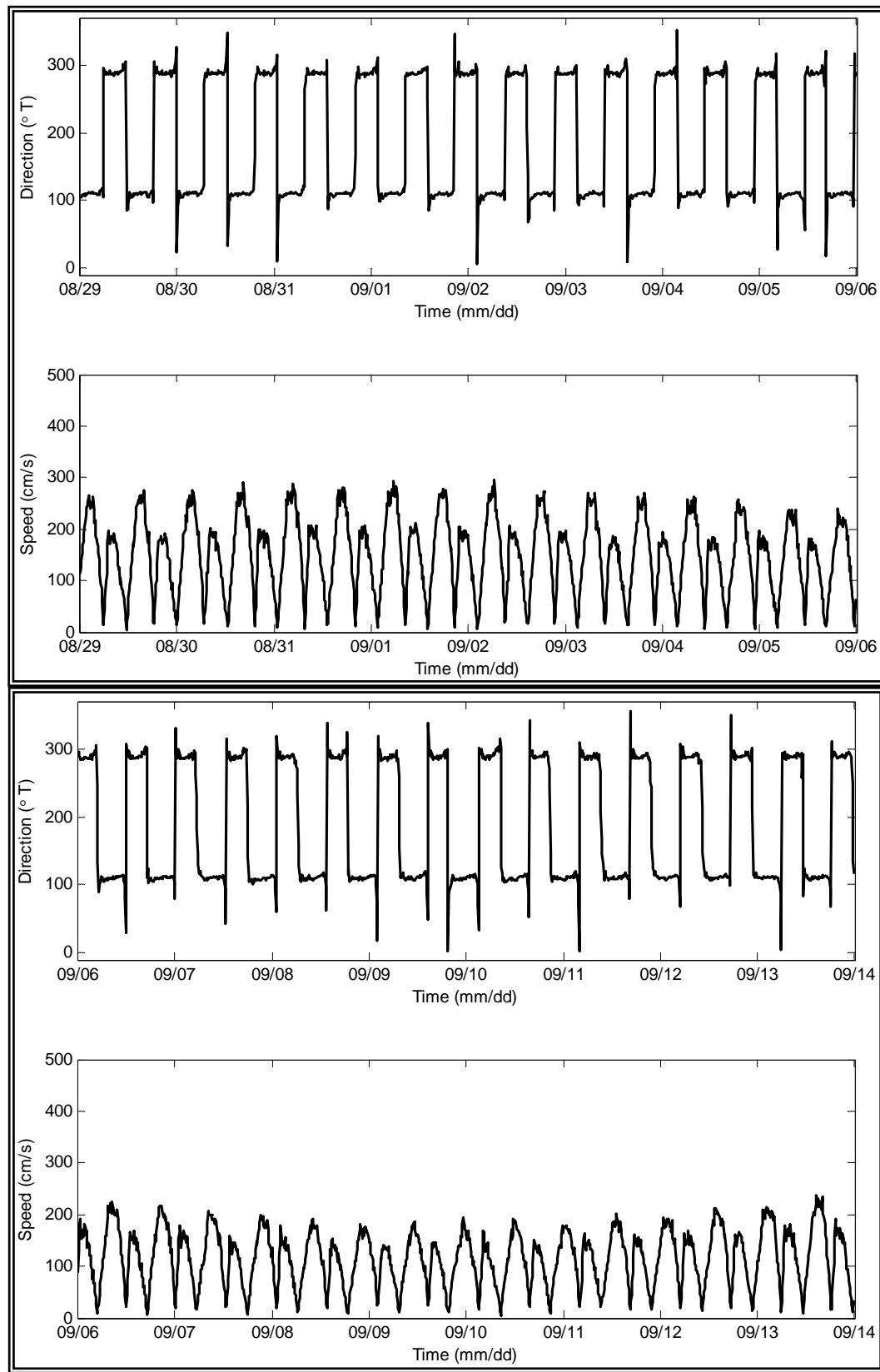


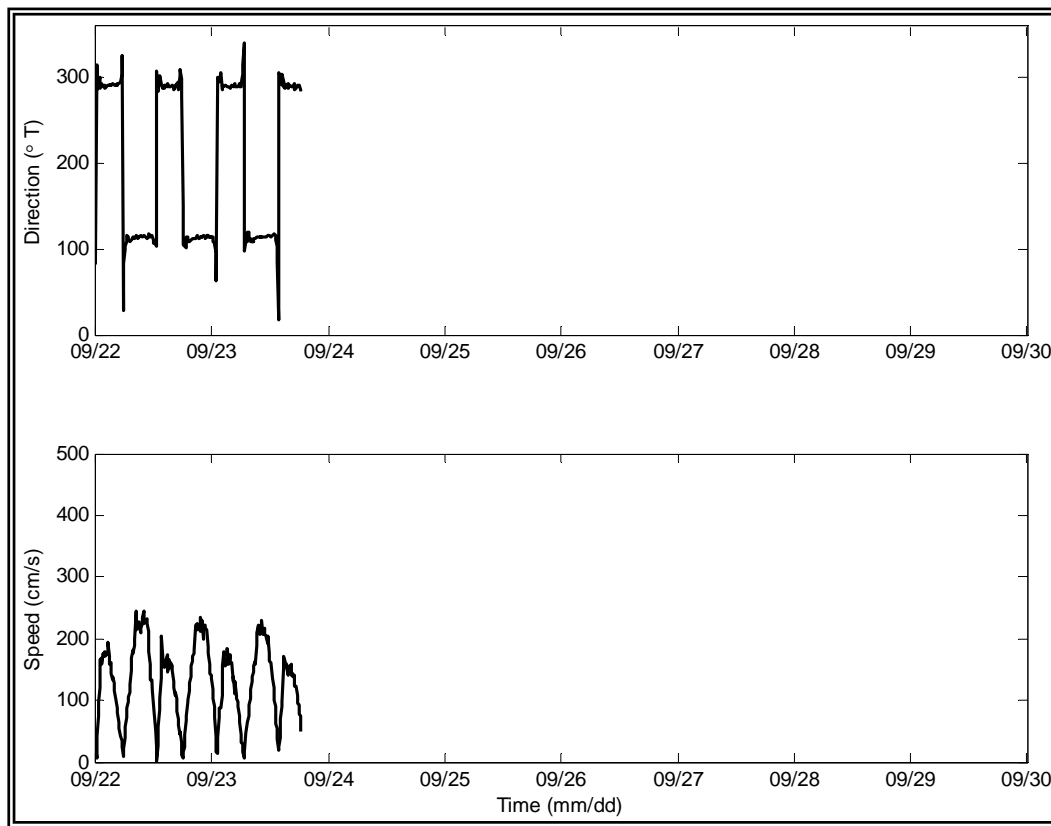
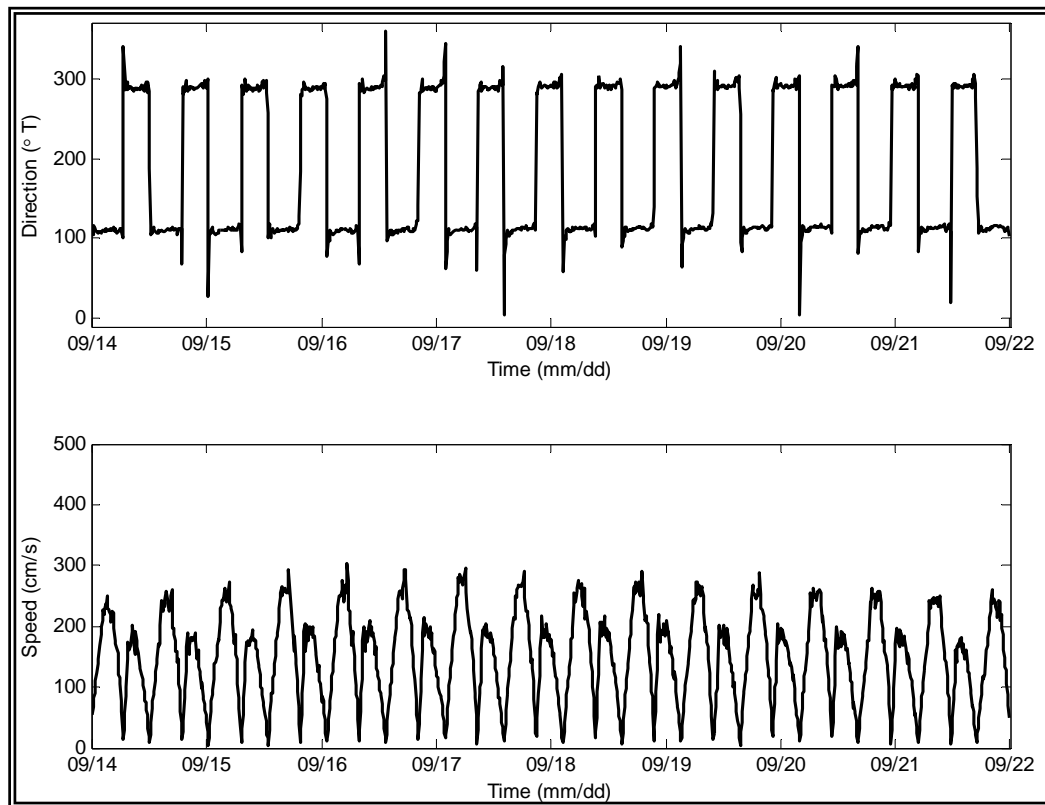




46 m Depth

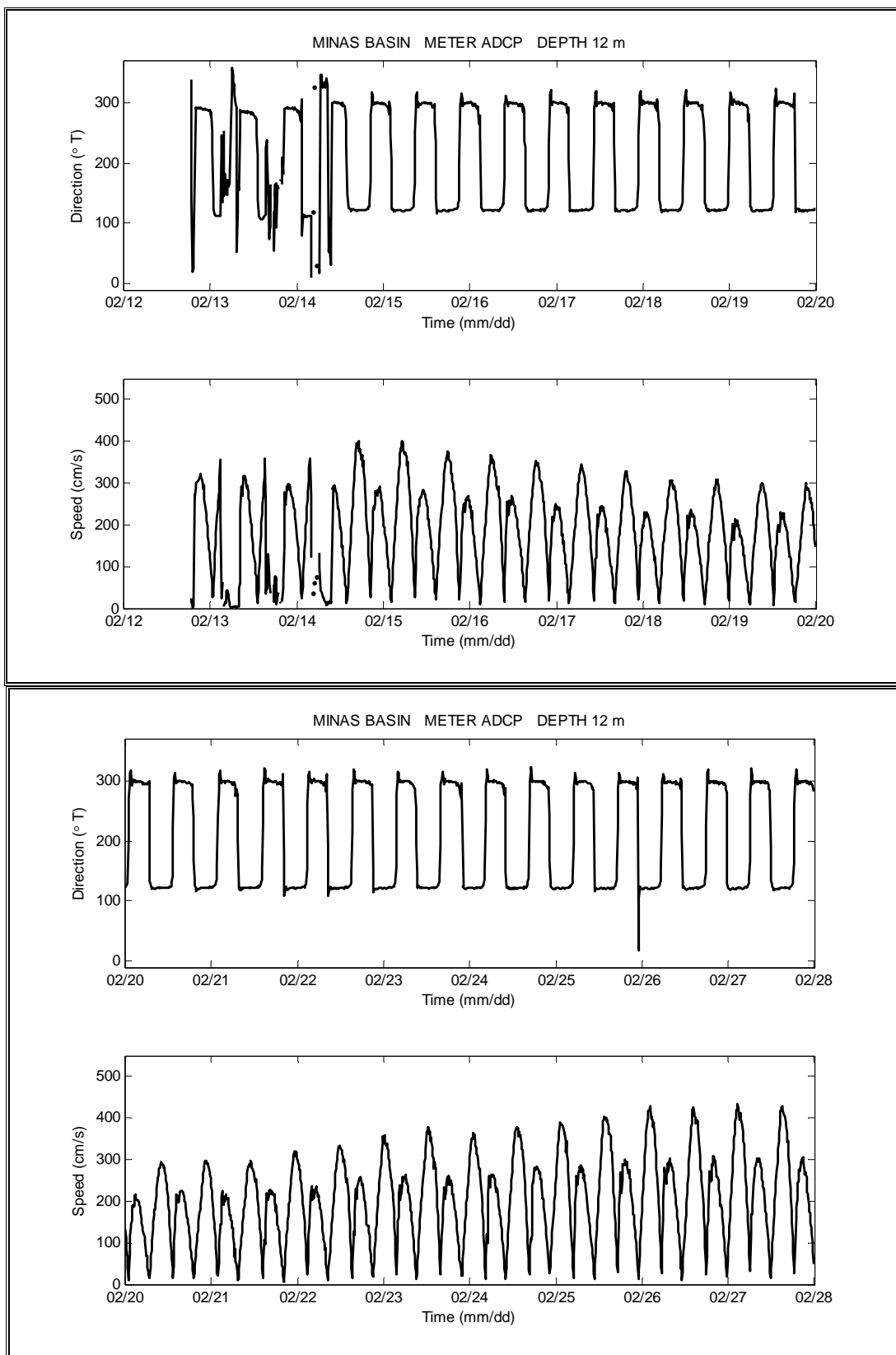


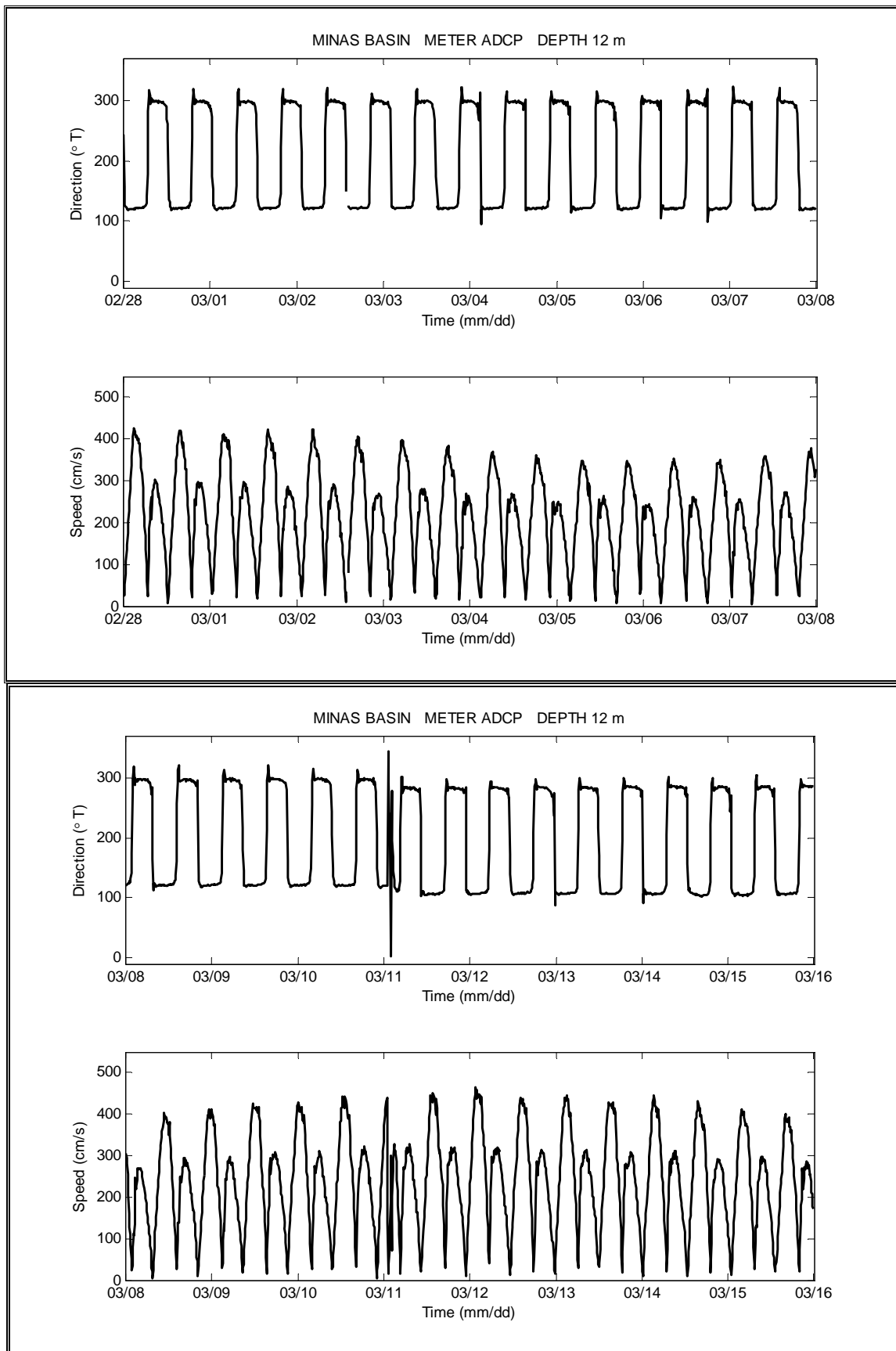


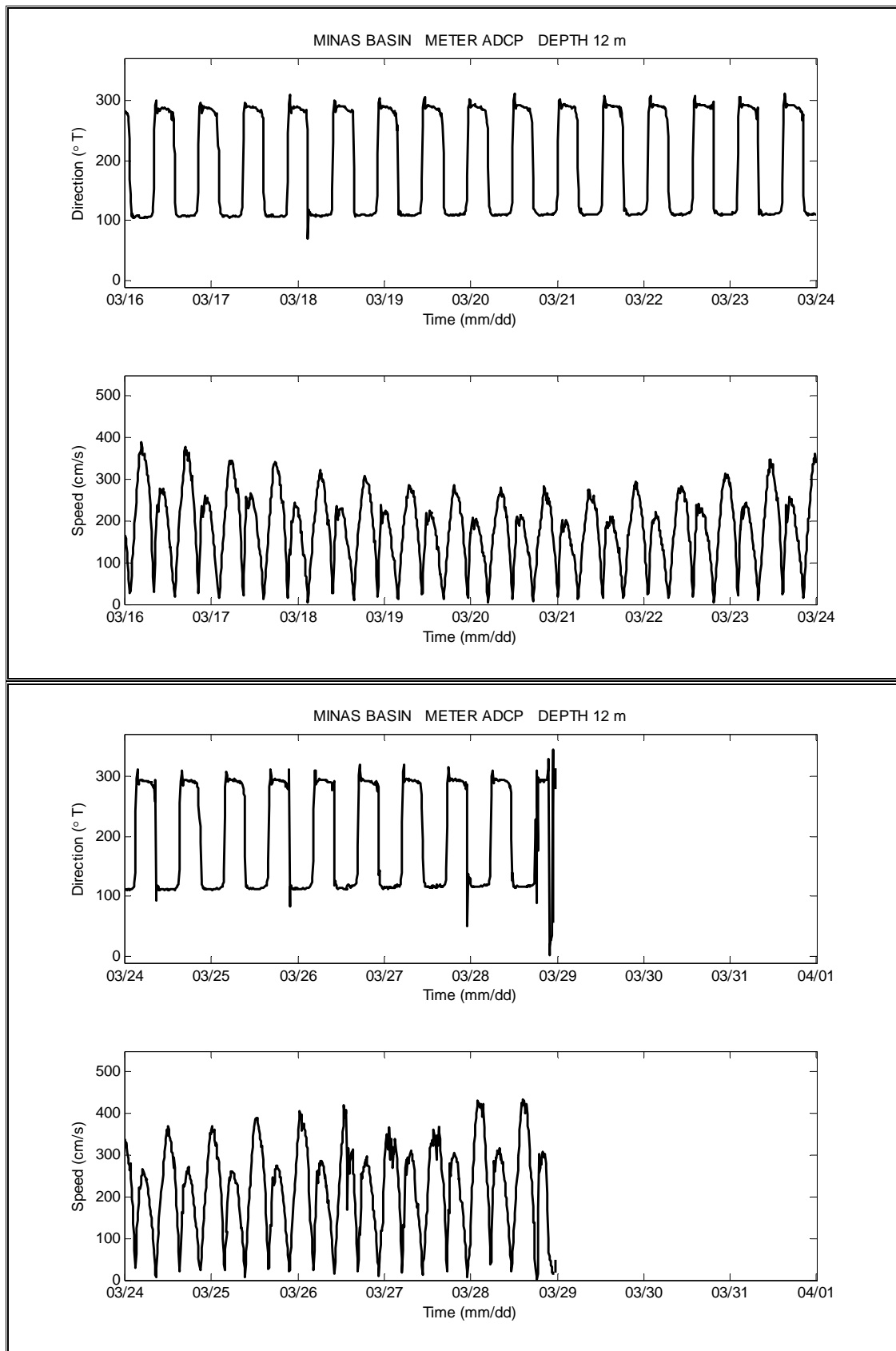


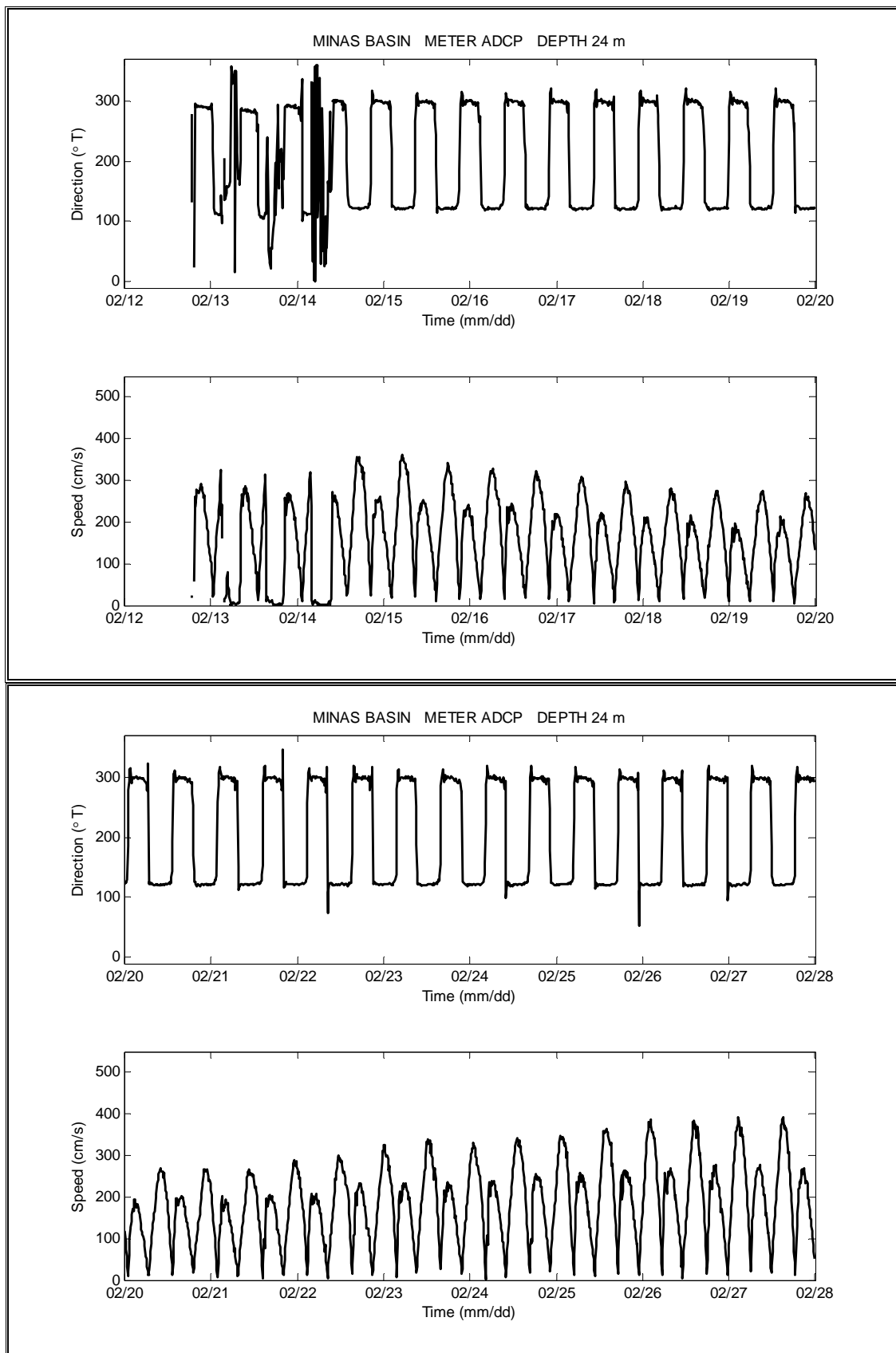
Appendix 5

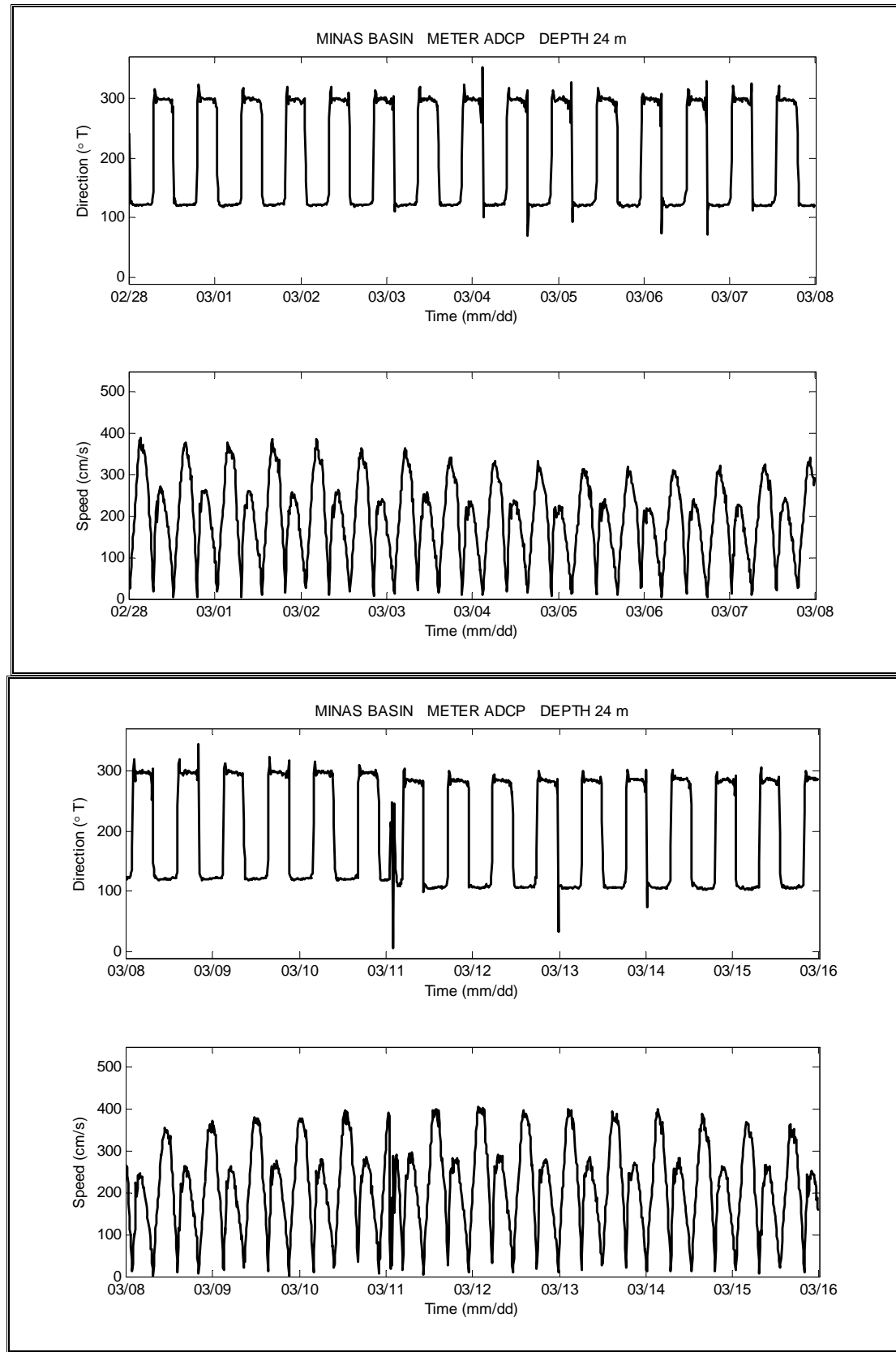
Time Series Plots, ADCP at Site 5

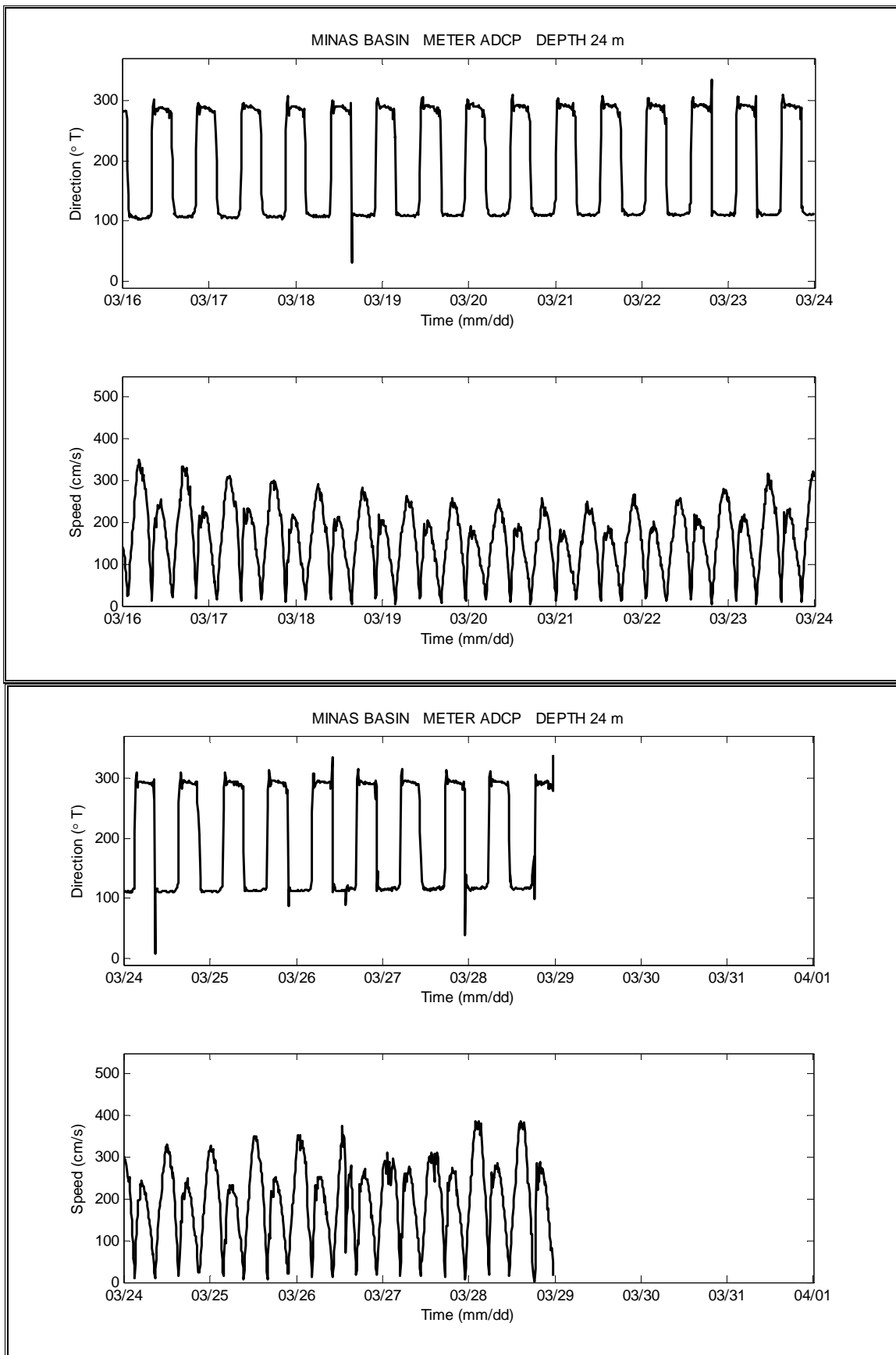
12 m Depth


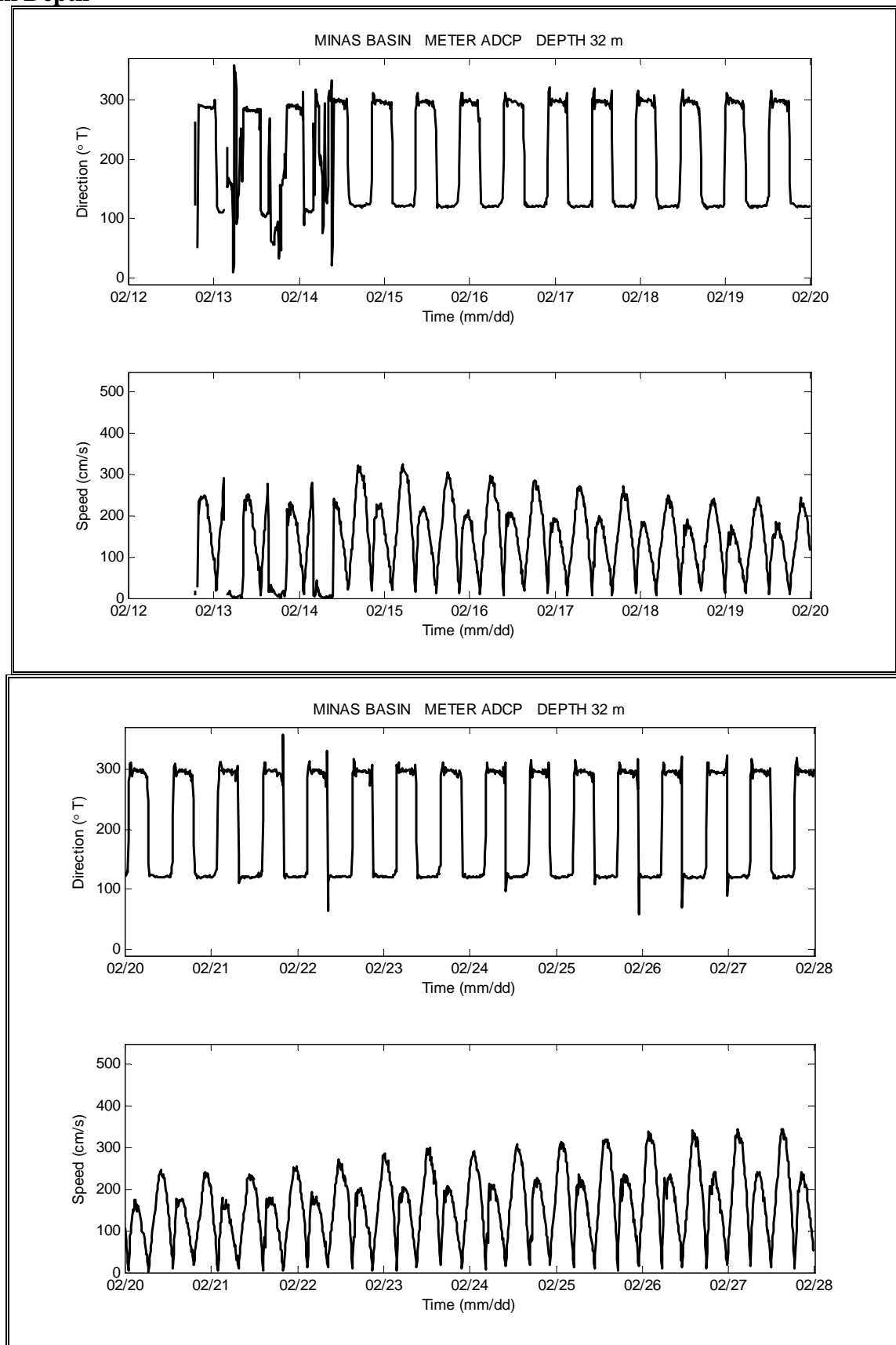


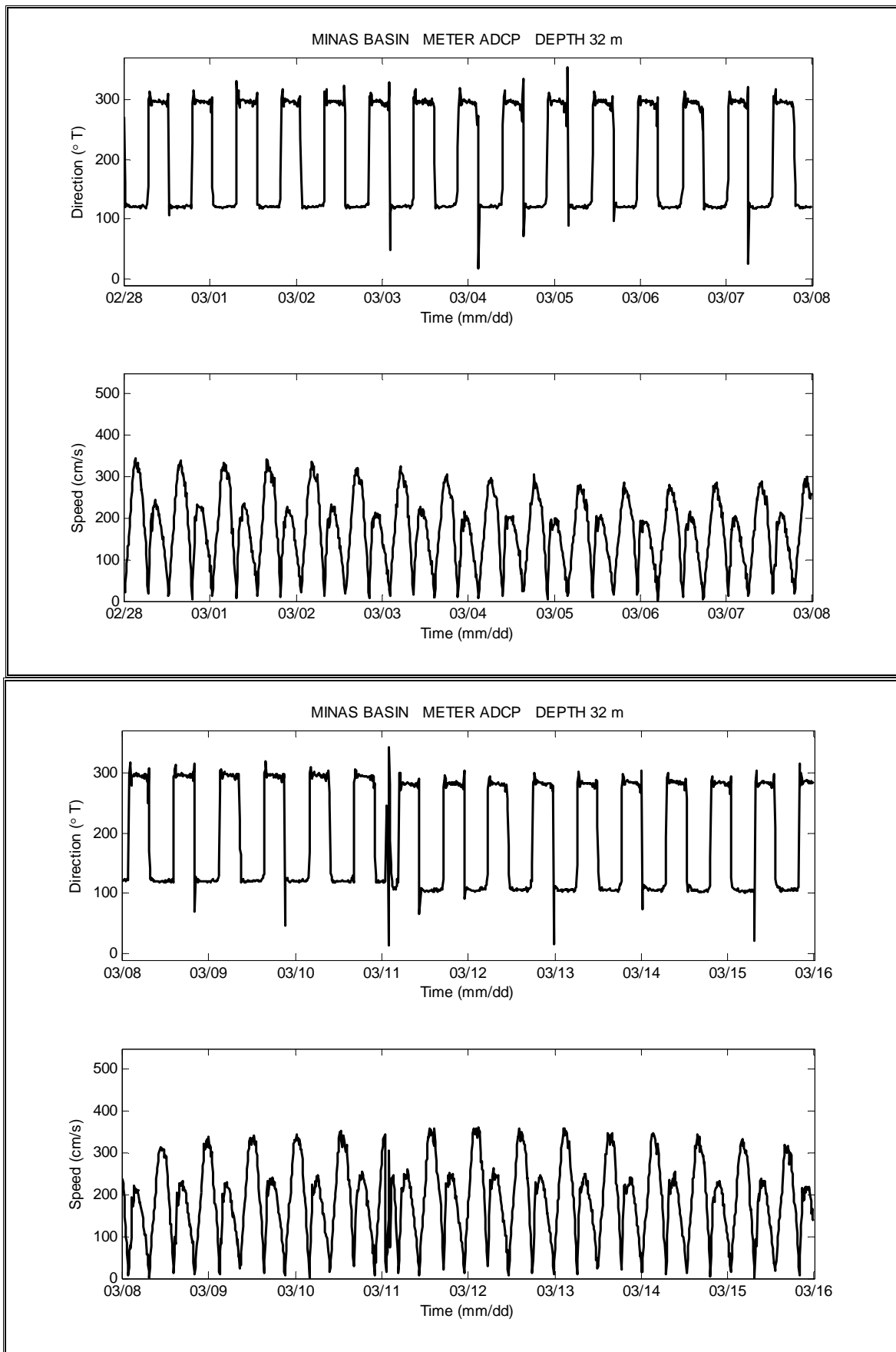


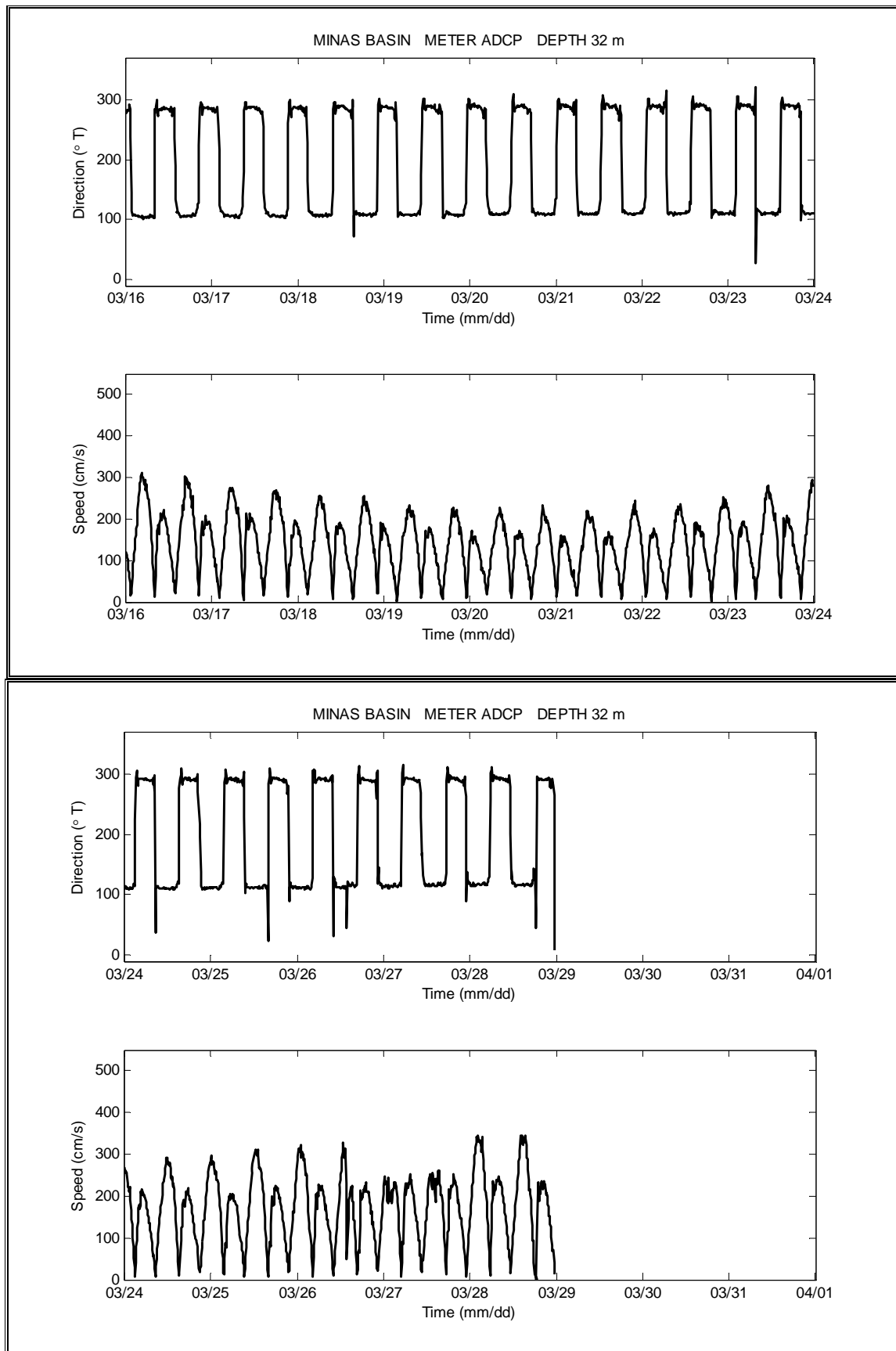
24 m Depth


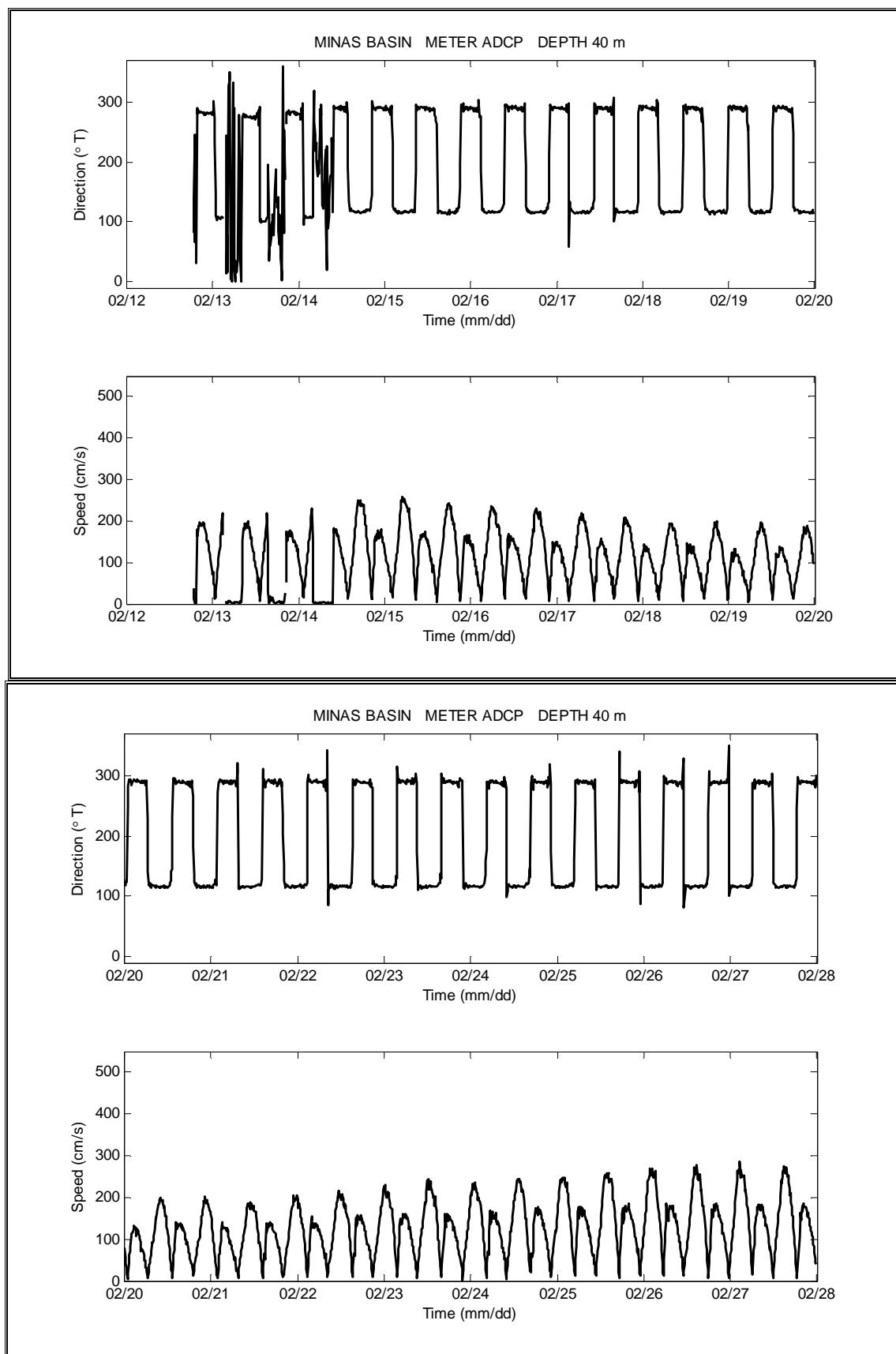


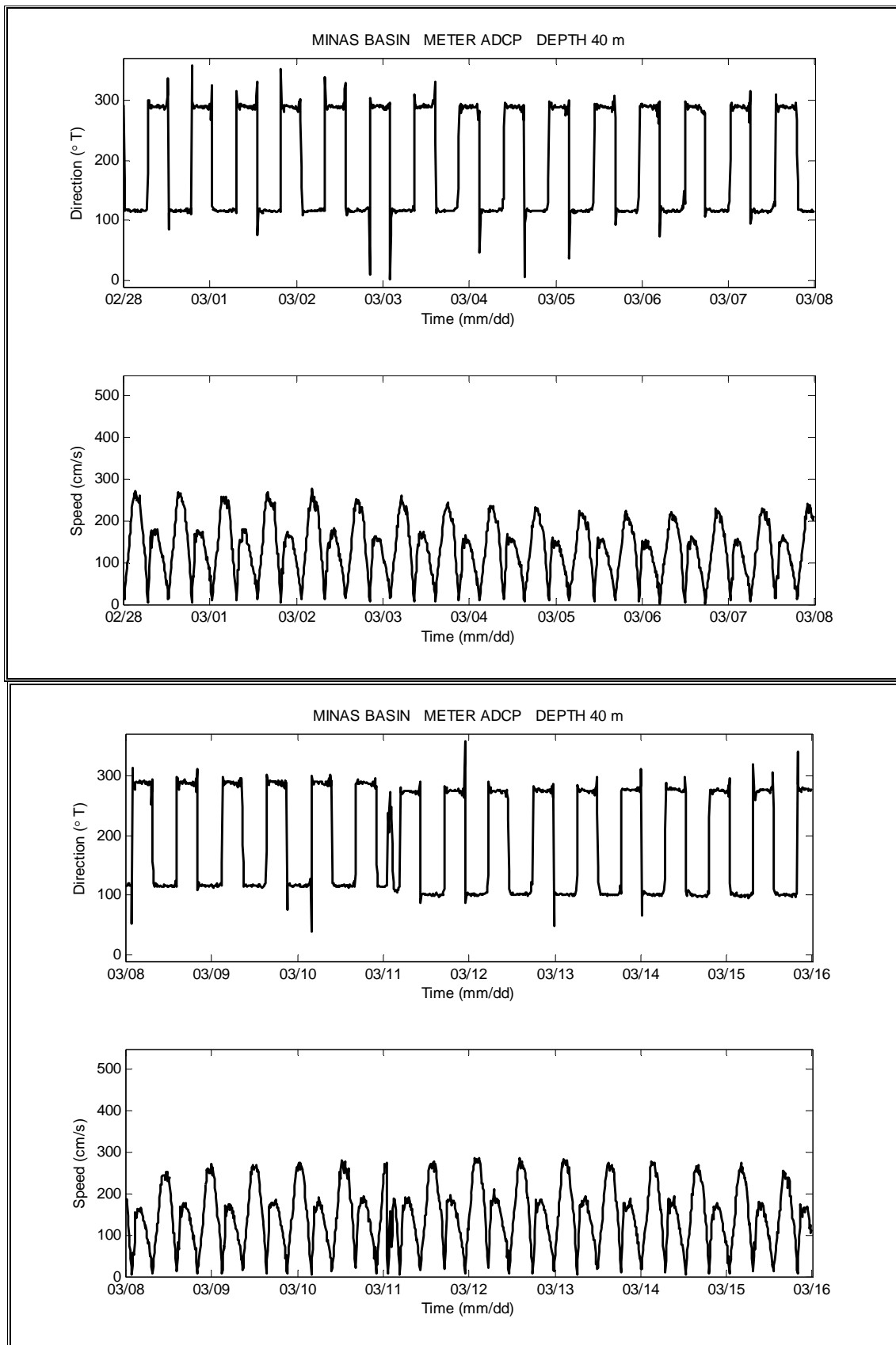


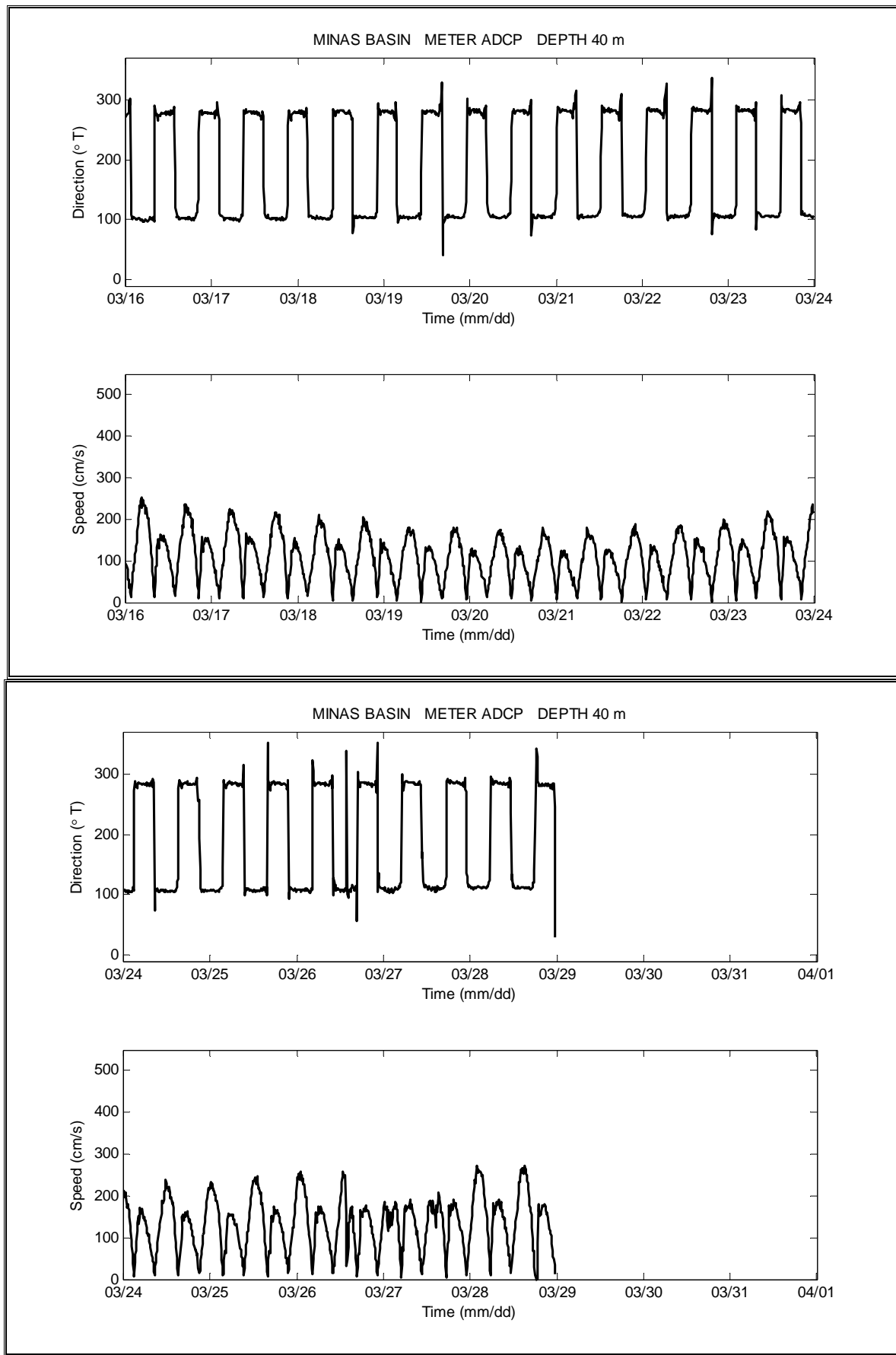
32 m Depth






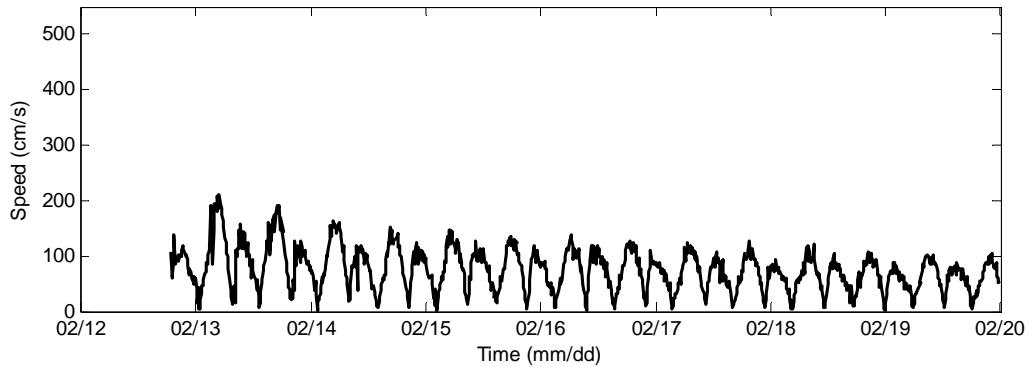
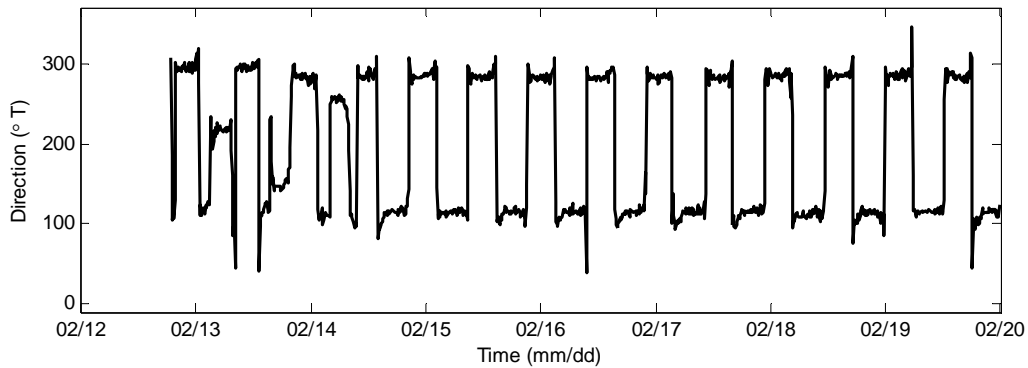
40 m Depth




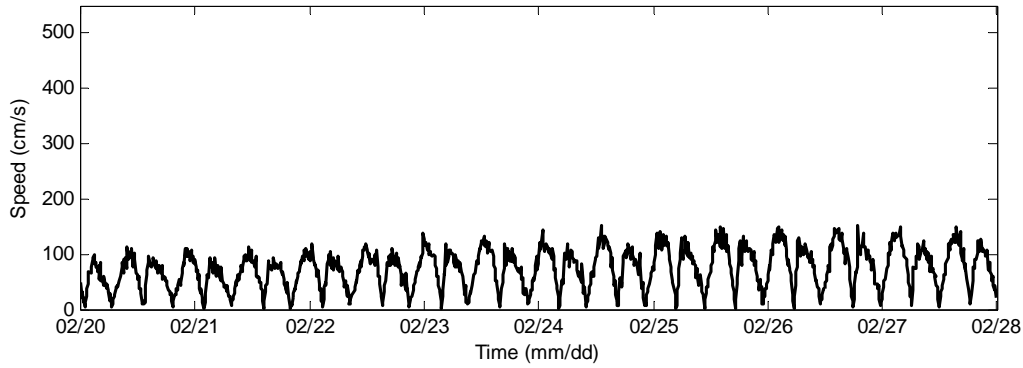
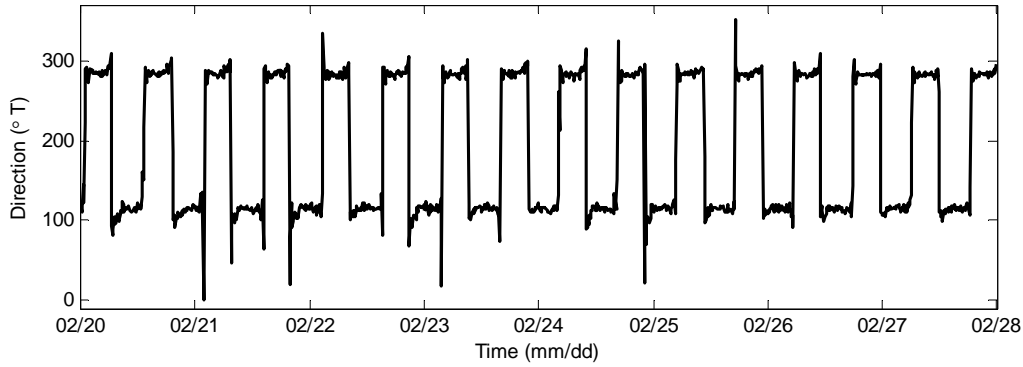


Appendix 6
Time Series Plots, for the InterOceanS4 Current Meter at Site 5

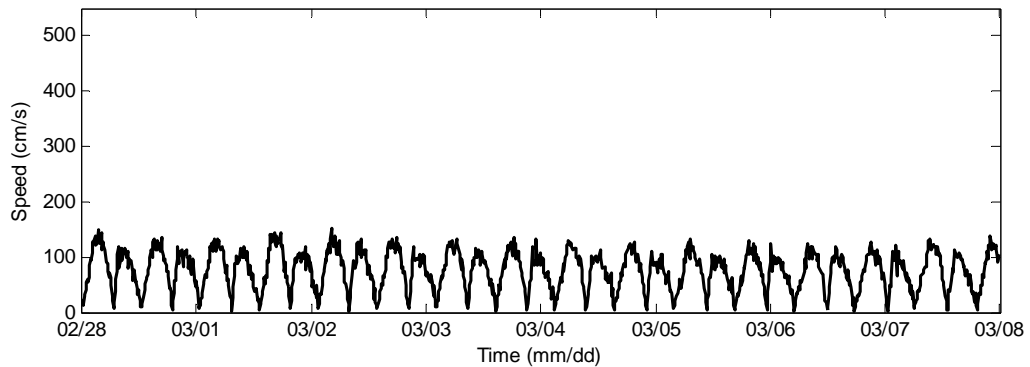
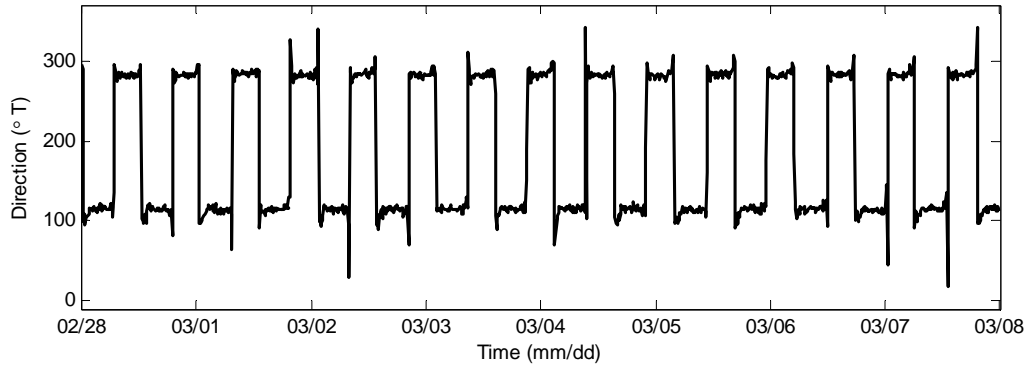
MINAS BASIN METER S4 DEPTH BOTTOM



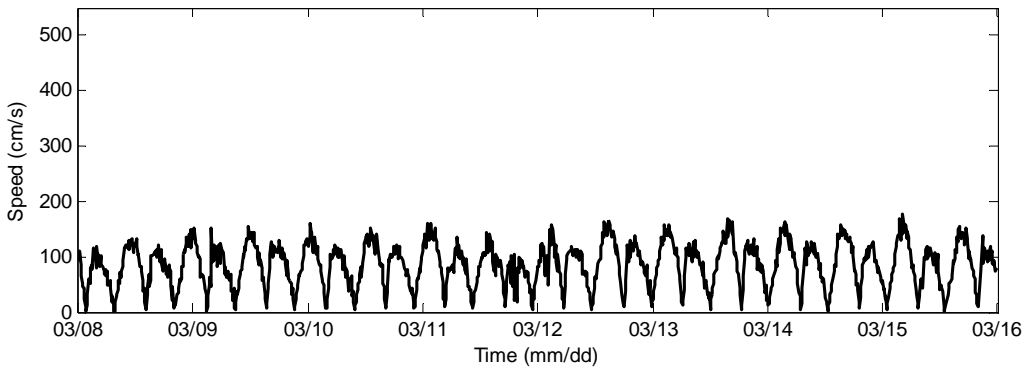
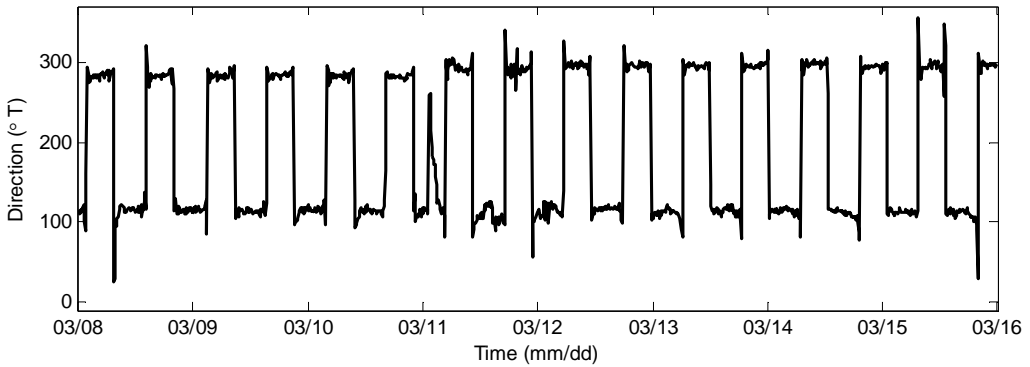
MINAS BASIN METER S4 DEPTH BOTTOM



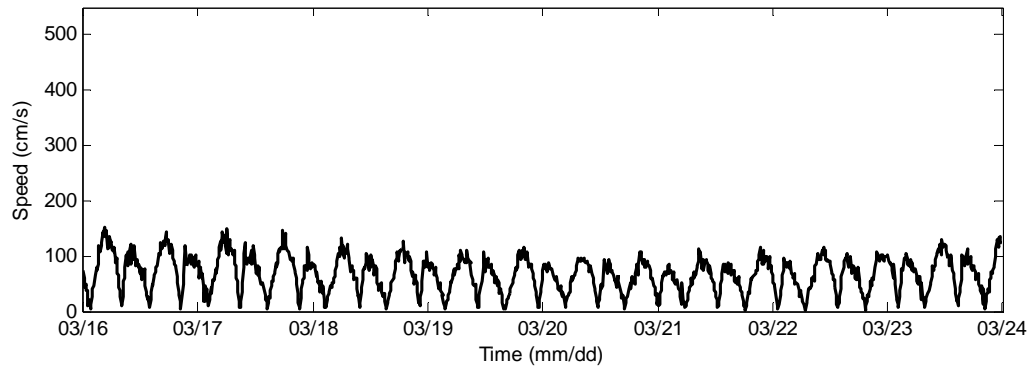
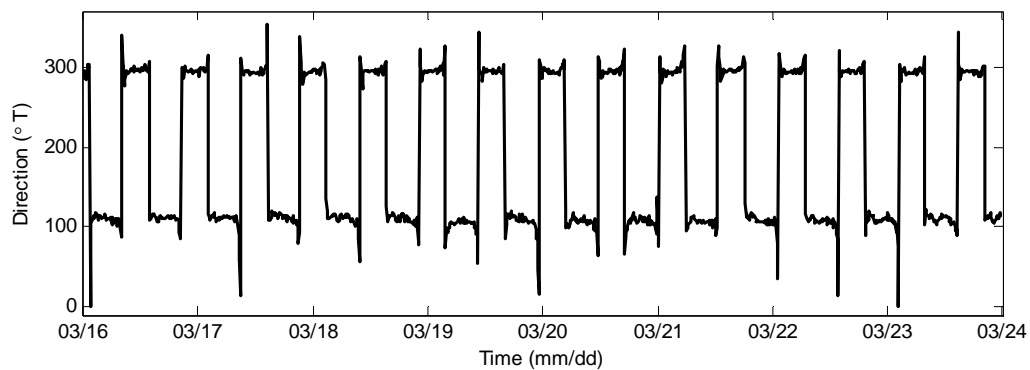
MINAS BASIN METER S4 DEPTH BOTTOM



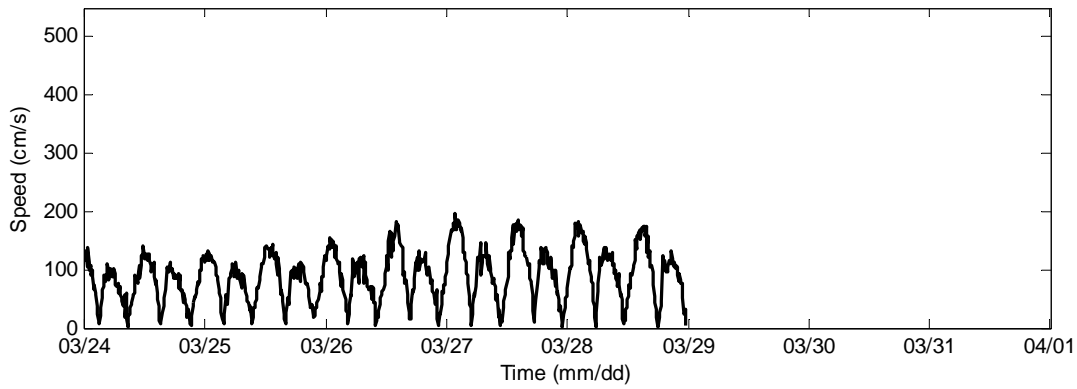
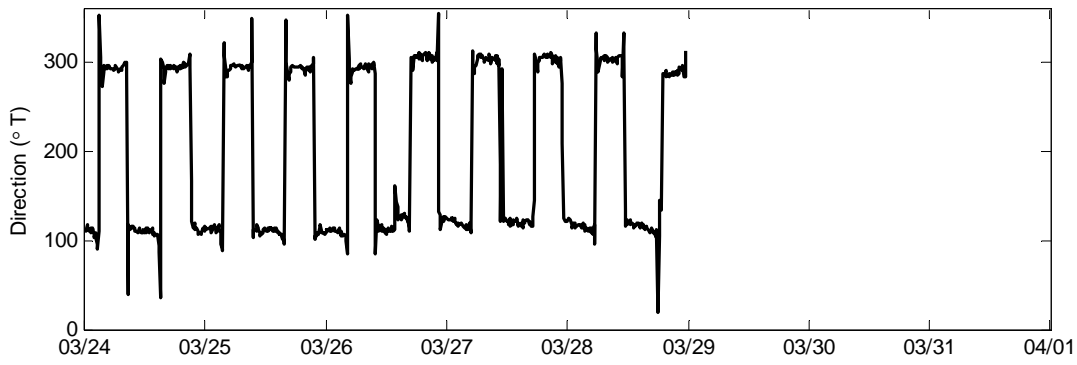
MINAS BASIN METER S4 DEPTH BOTTOM



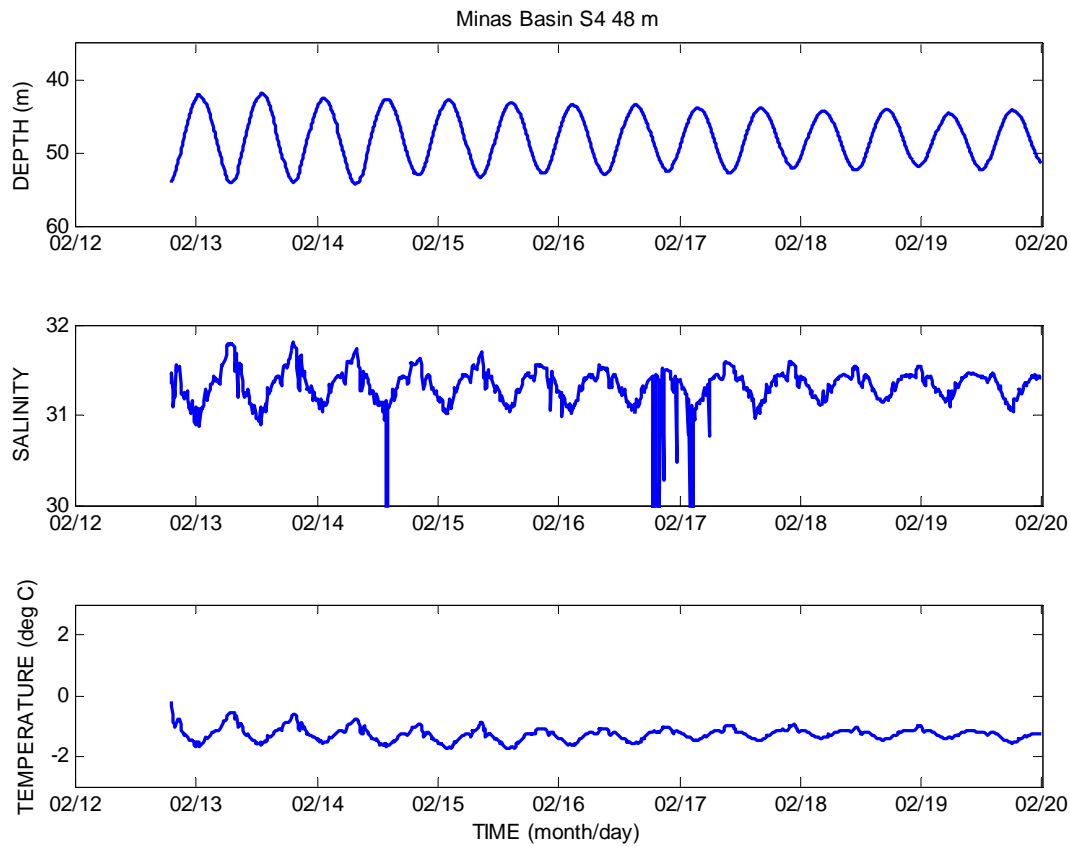
MINAS BASIN METER S4 DEPTH BOTTOM

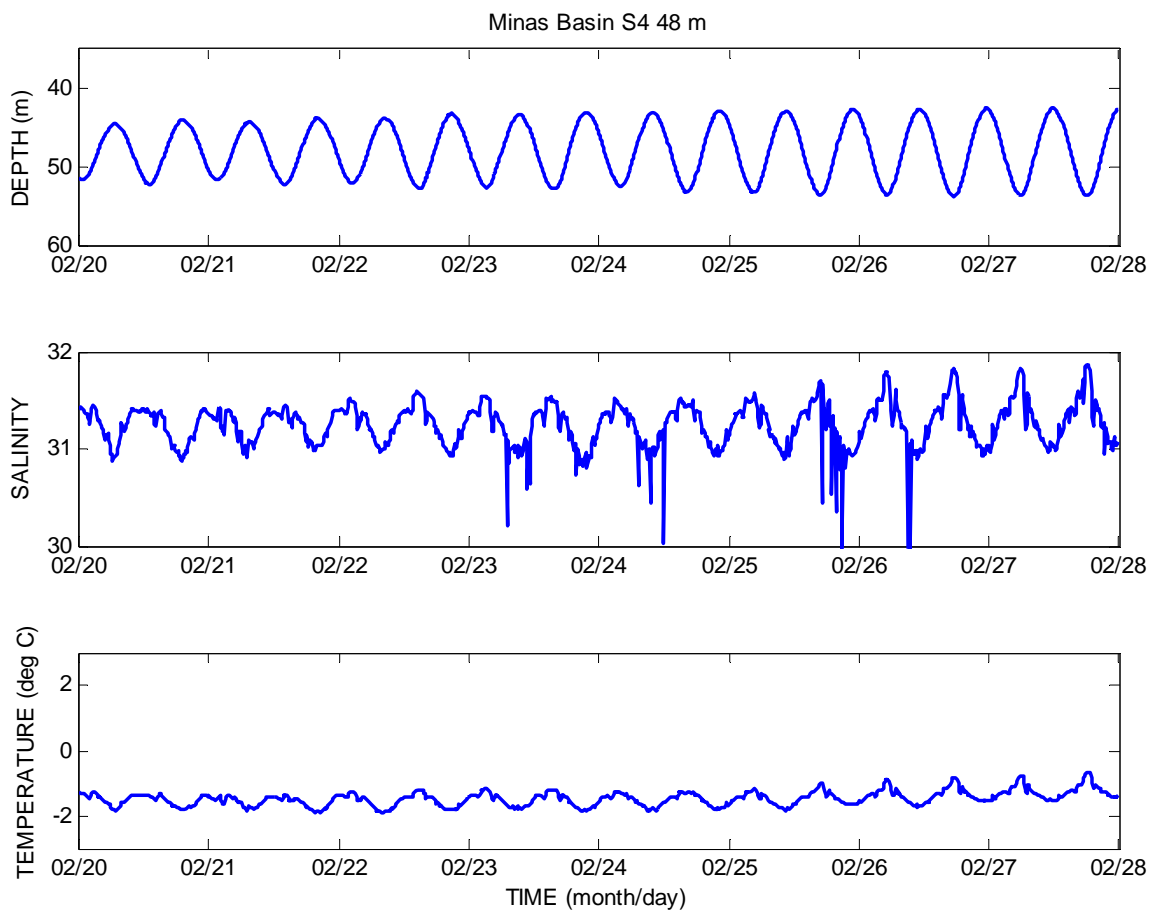


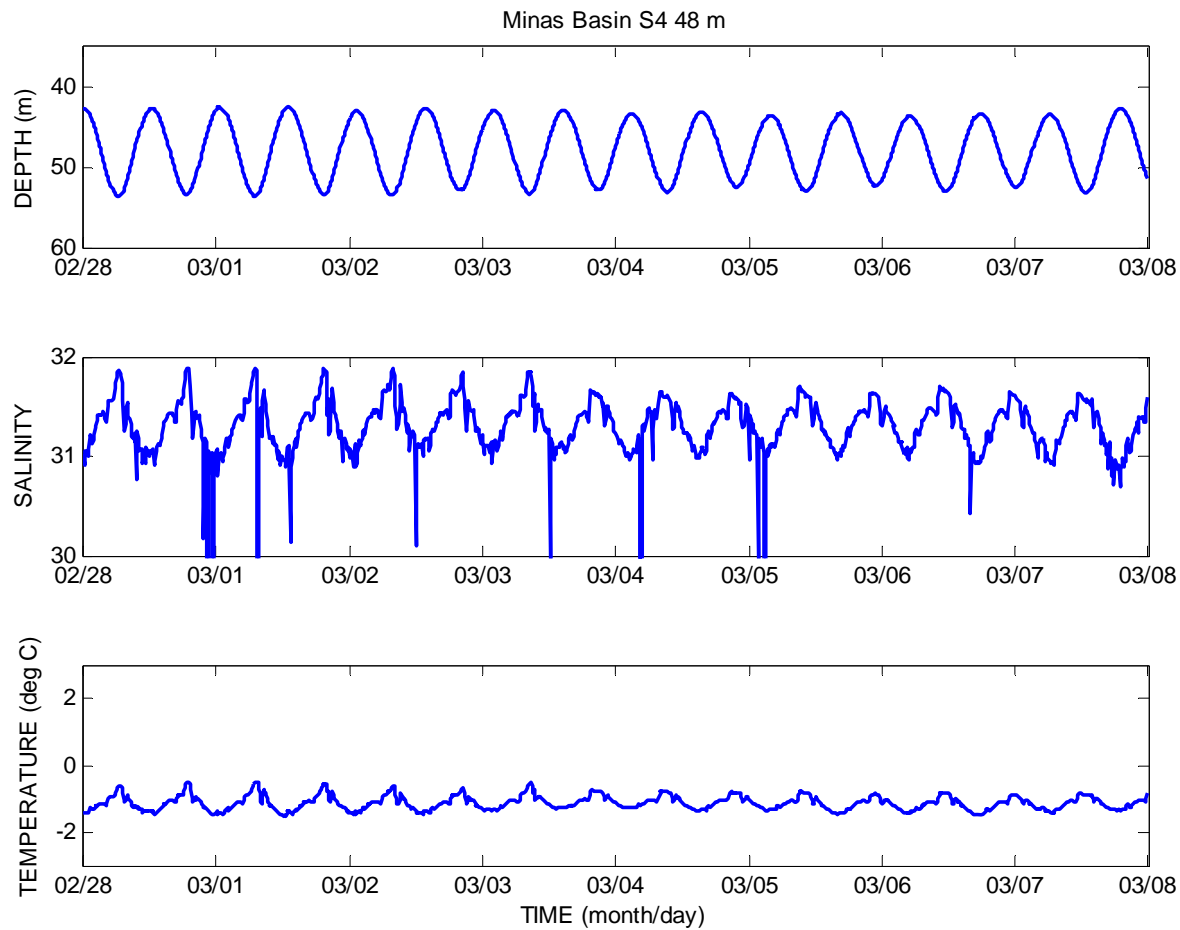
MINAS BASIN METER S4 DEPTH BOTTOM

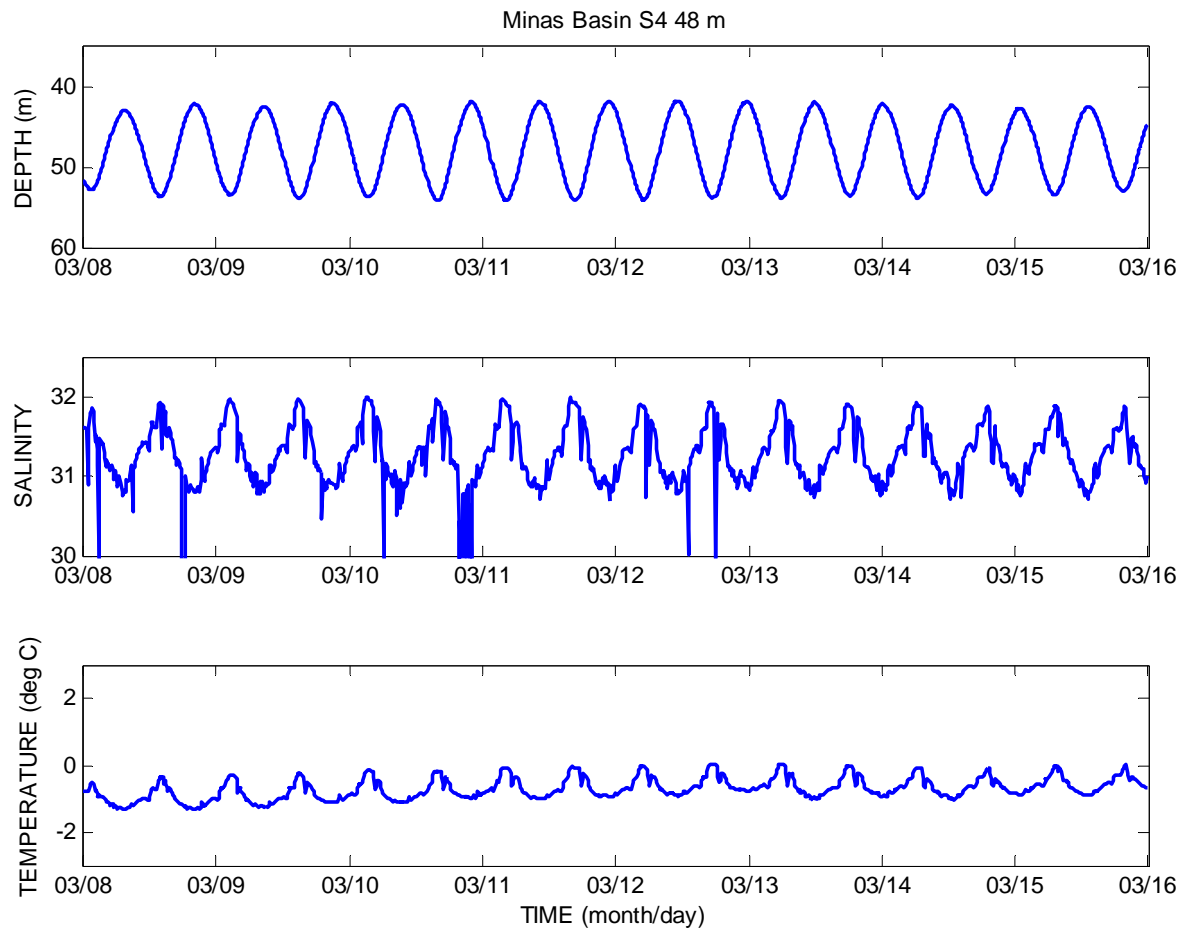


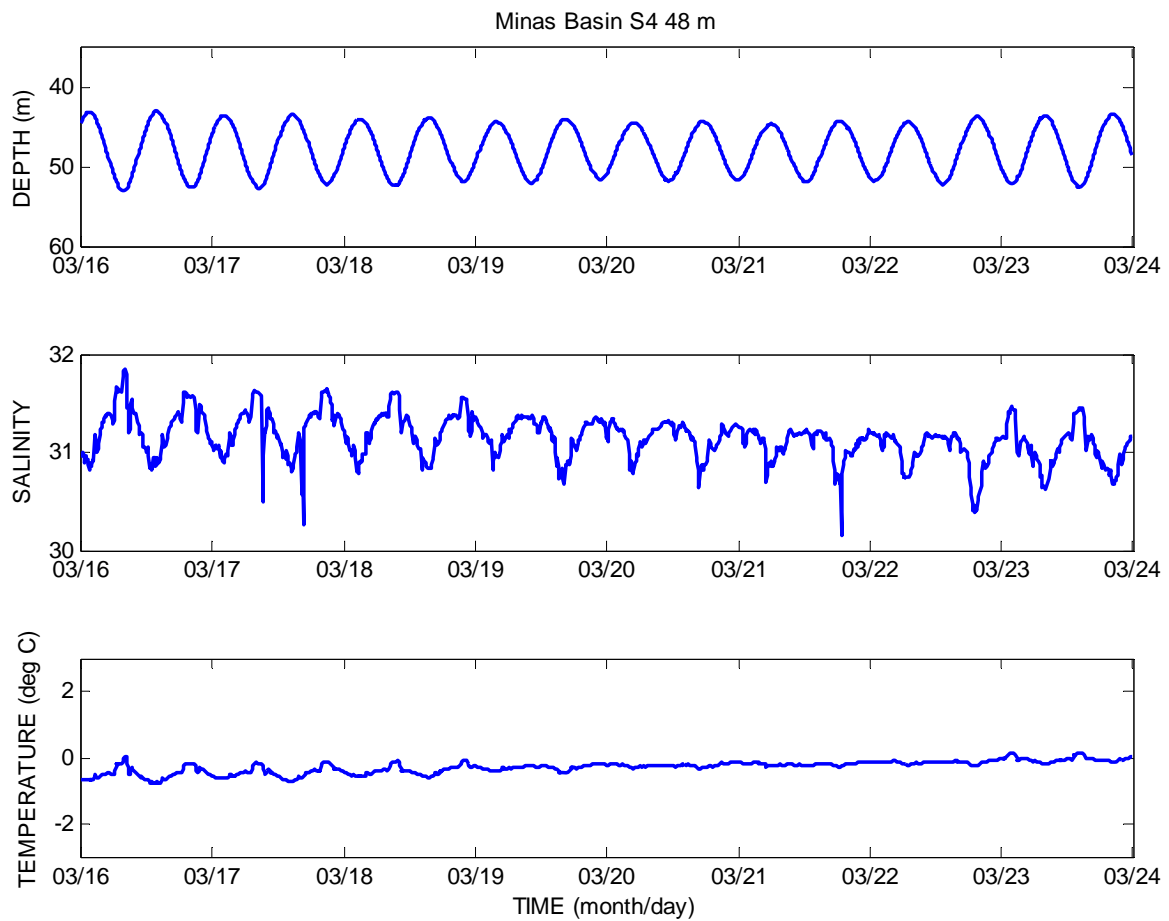
Appendix 7
Time Series of the Pressure, Temperature, and Salinity Data from
the InterOcean S4 Current Meter at Site 5

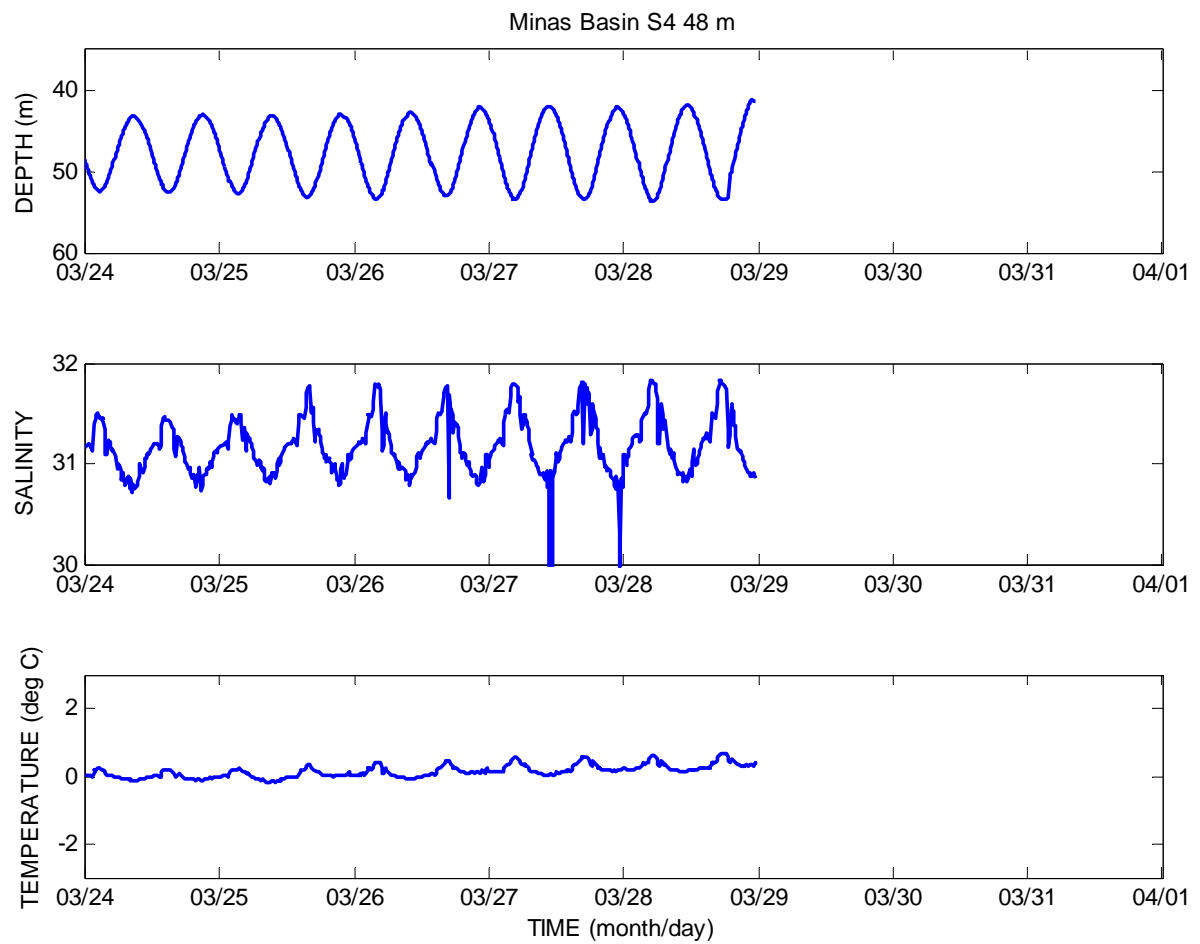






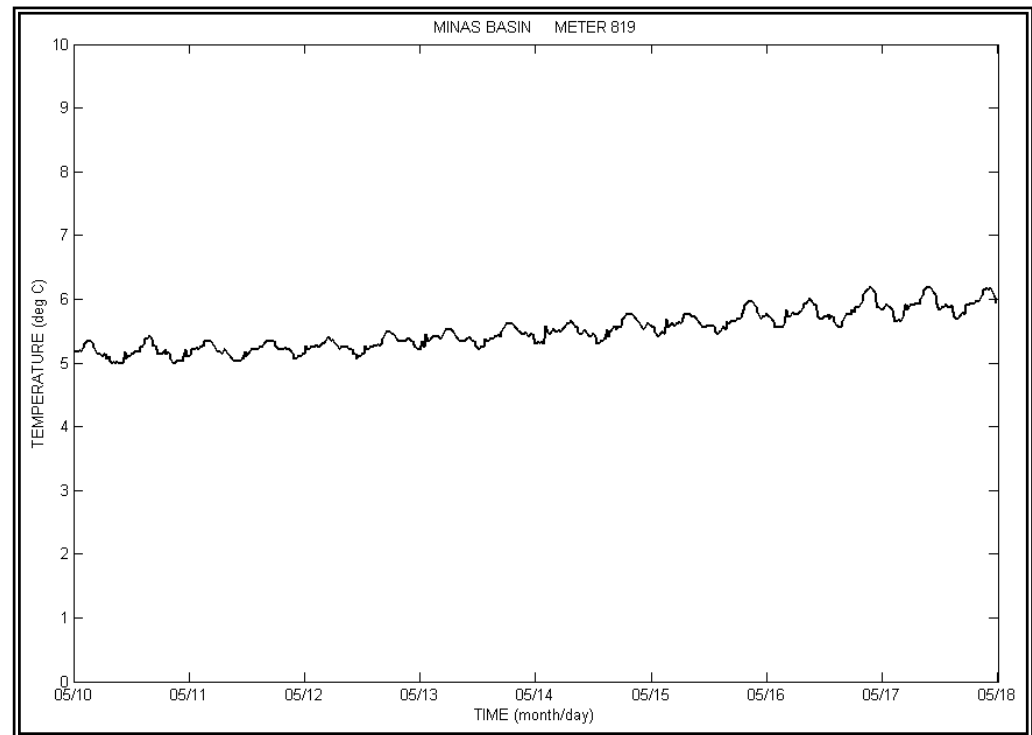
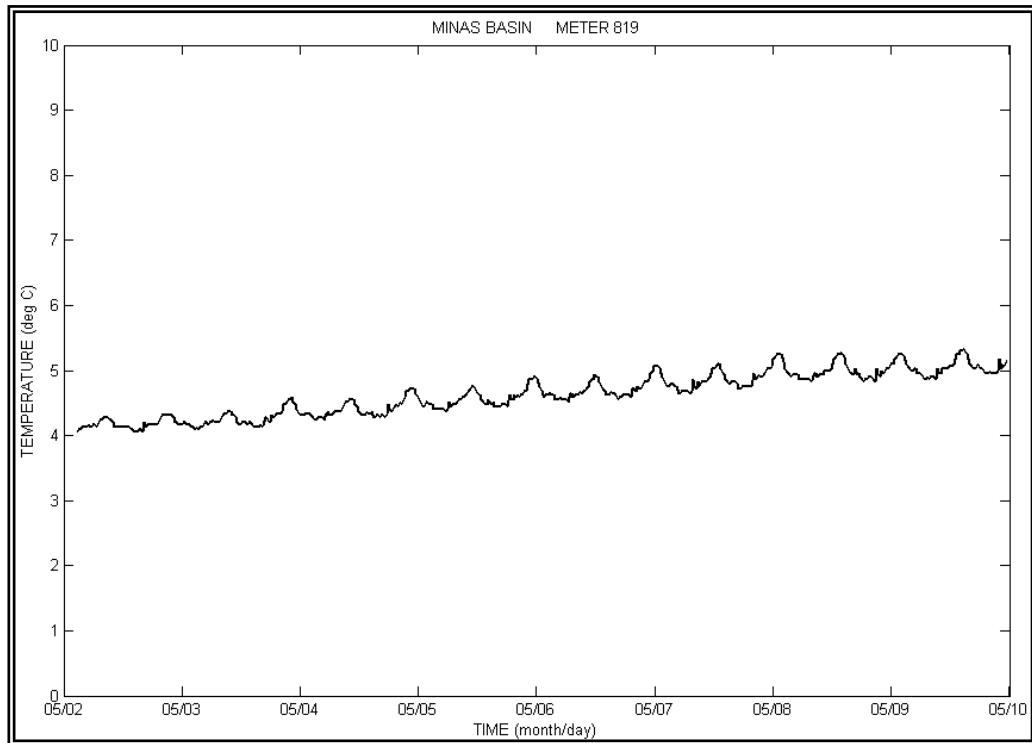


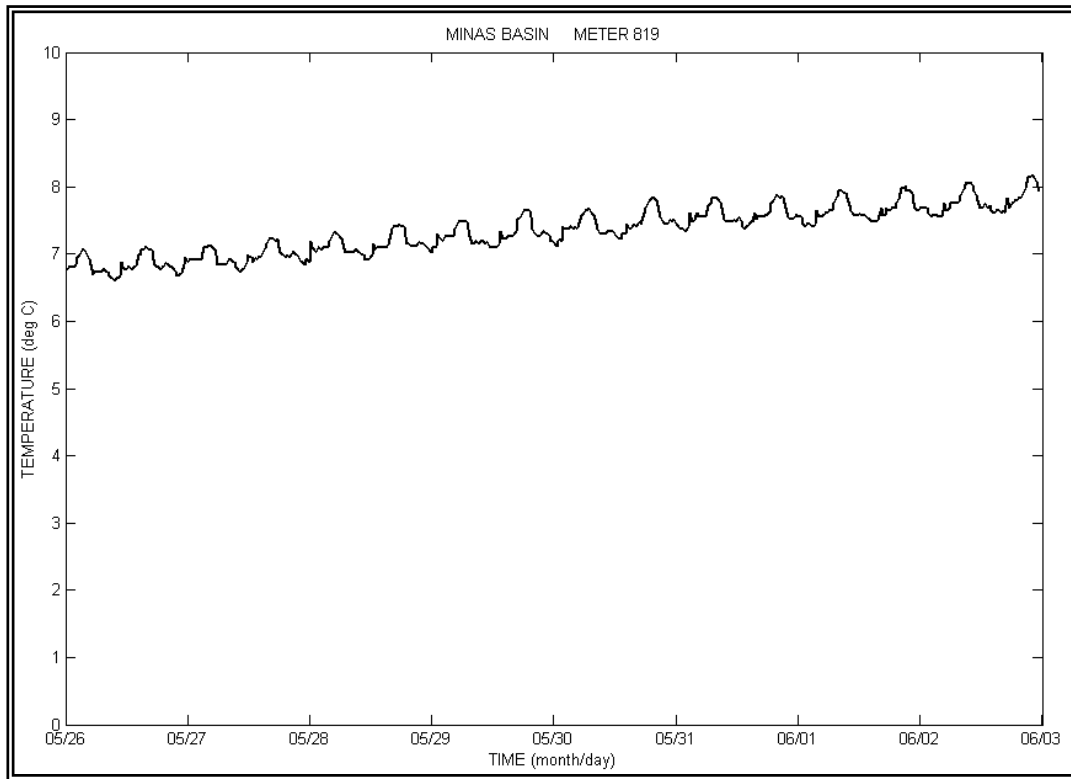
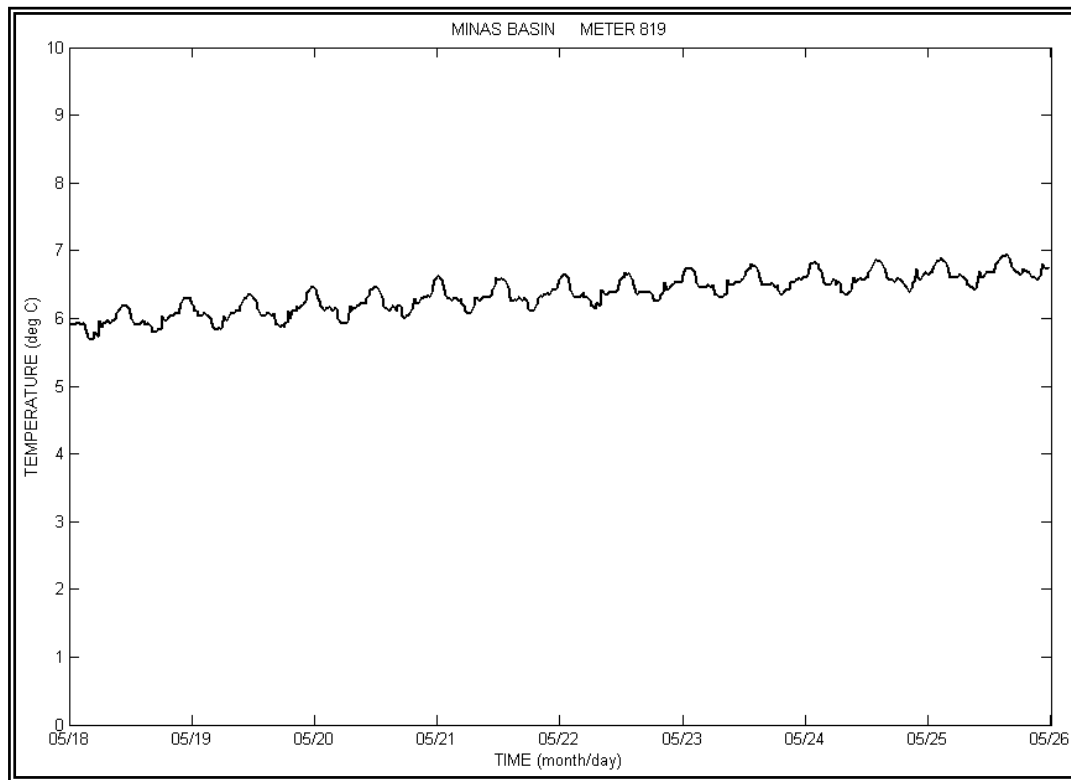


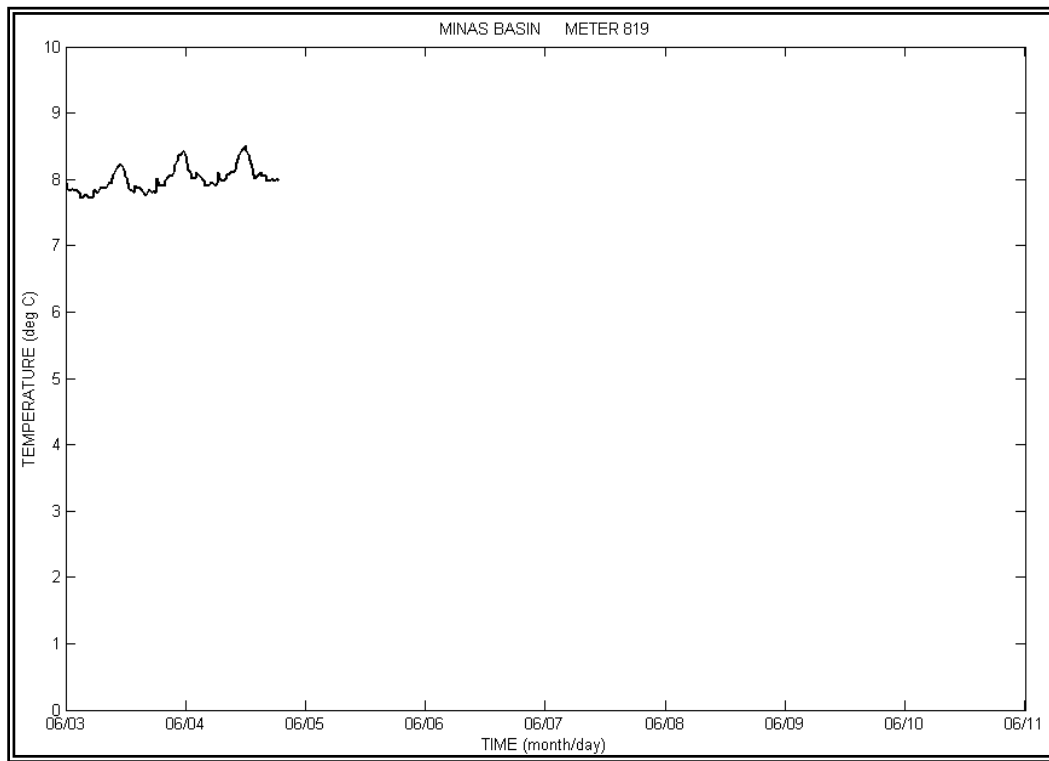


Appendix 8

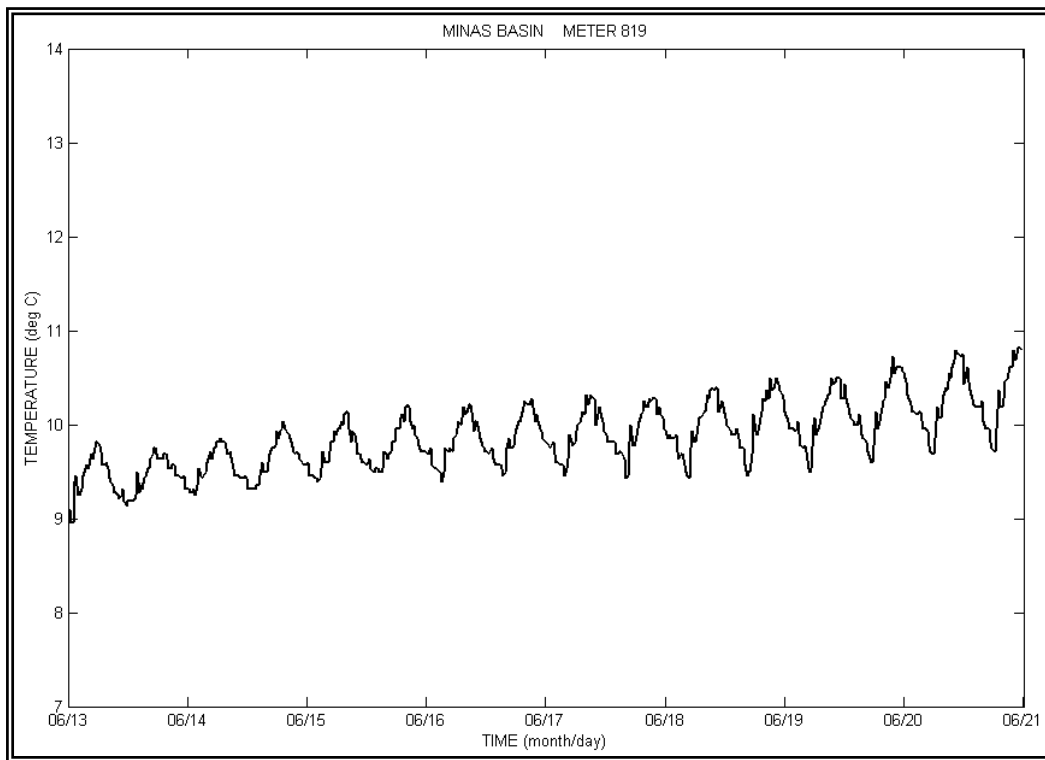
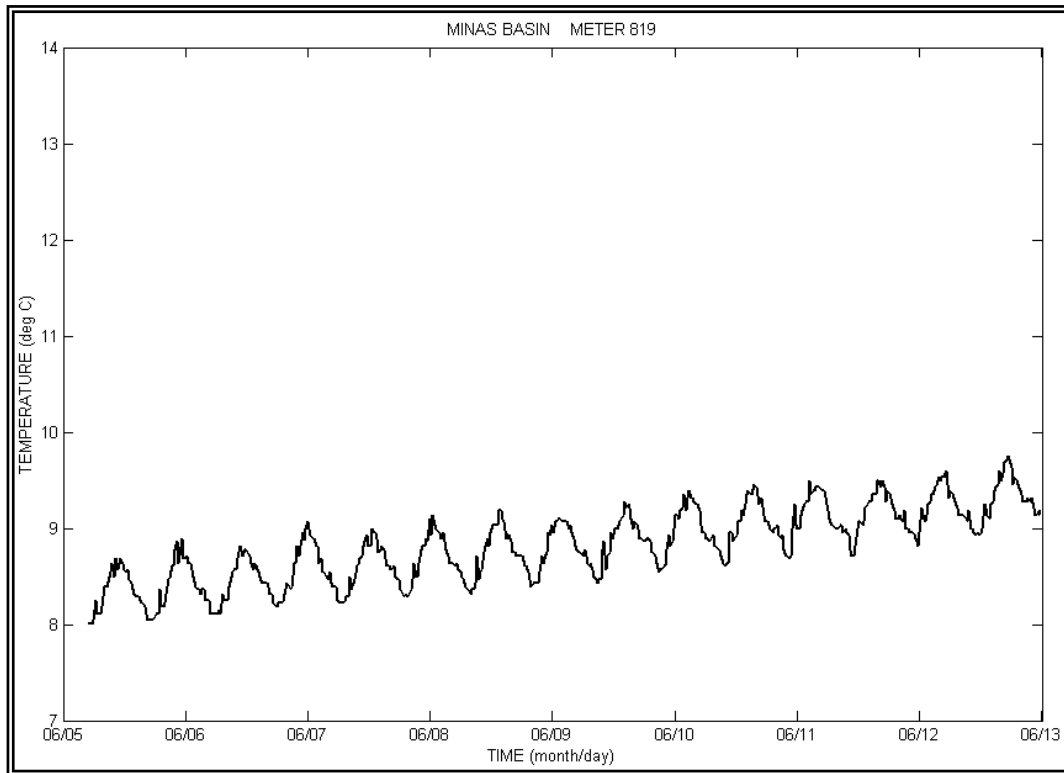
Time Series of Bottom Temperature from the Water Level Recorder at Site 1

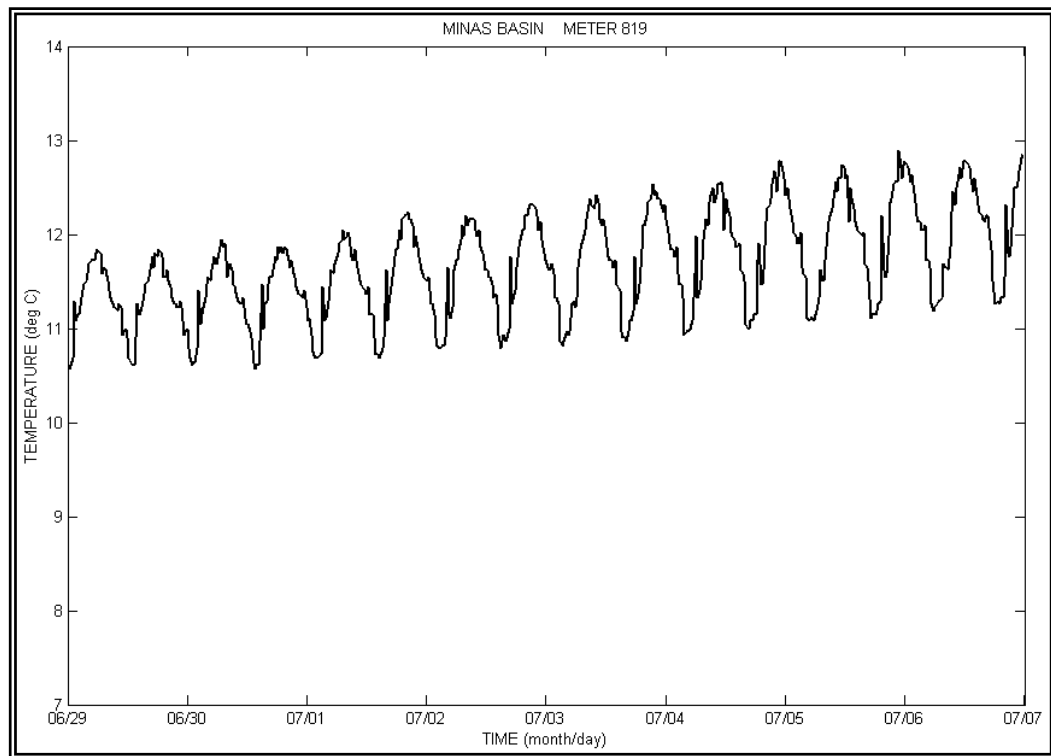
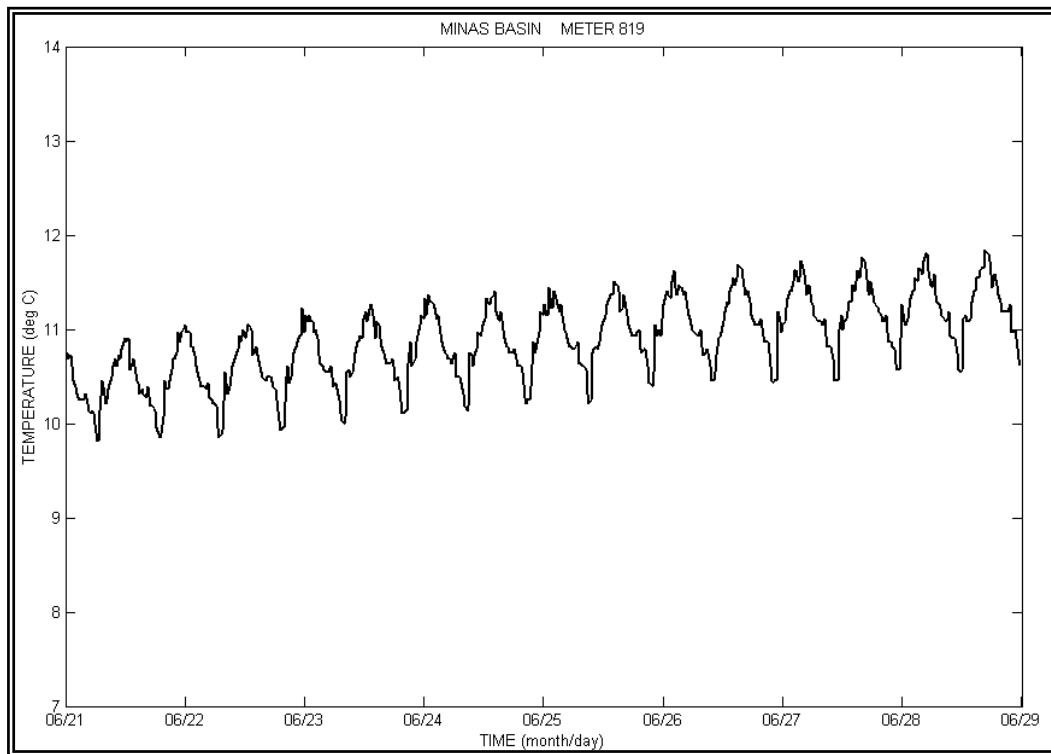


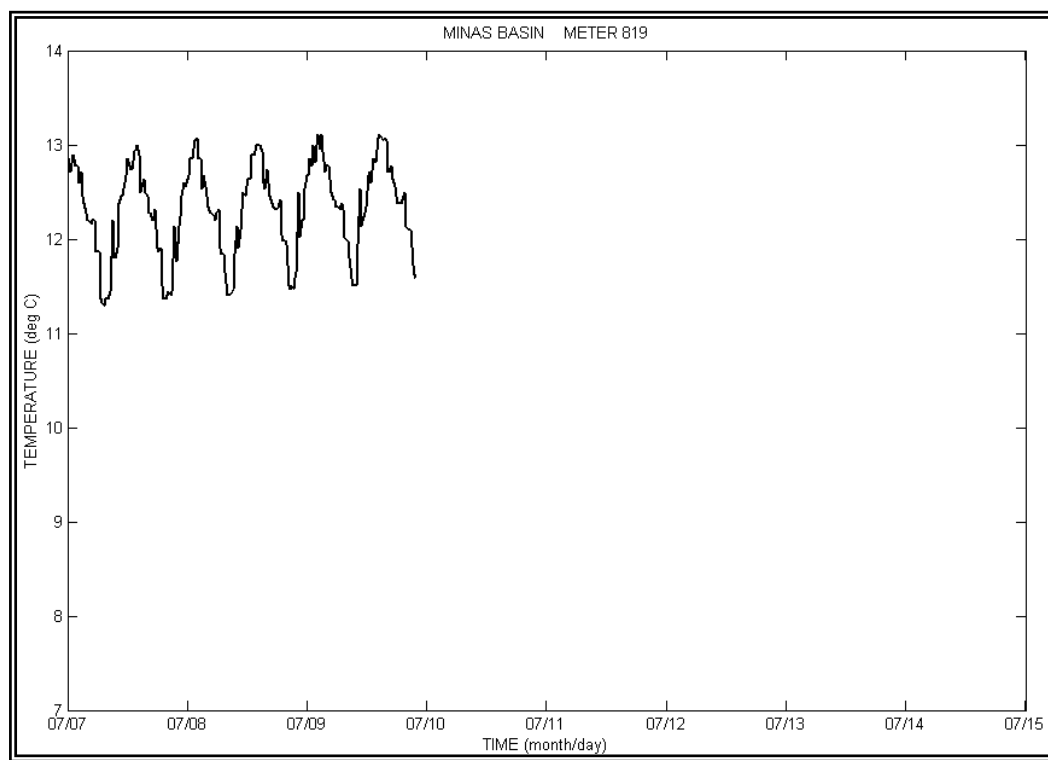




Appendix 9
Time Series of Bottom Temperature from the Water
Level Recorder at Site 3







Wind and Wave Climate Study for the Fundy Tidal Energy Demonstration Facility

Submitted to

AECOM Canada Ltd.
1701 Hollis Street
SH400 (PO Box 576 CRO)
Halifax, NS, Canada

by



Nova Scotia Office:

Suite 202, Purdy's Wharf Tower 2
1969 Upper Water Street
Halifax, Nova Scotia
B3J 3R7
Telephone: 902-492-9222
Facsimile: 902-492-4545

Newfoundland and Labrador Office:

85 LeMarchant Road
St. John's, Newfoundland
A1C 3J3
Telephone: 709-753-5788
Facsimile: 709-753-3301

June 2009

Table of Contents

1.	INTRODUCTION	1
2.	DATA AND ANALYSIS	1
2.1	Winds	1
2.2	Fetch Limits	2
2.3	Wave Modelling.....	3
3.	RESULTS	6
4.	REFERENCES	27

List of Tables

Table 1	Fetch Limits Relative to the Crown Lease Deployment Area	3
Table 2	Monthly Mean and Maximum Winds and Waves	6
Table 3	Number of Hourly Occurrences of Wind Speed by Month	6
Table 4	Number of Hourly Occurrences of Significant Wave Height by Month	7

List of Figures

Figure 1	Study Area and MSC50 Reanalysis Grid Point	2
Figure 1	Key for Wind Rose Speed Categories in Knots	7
Figure 2	January Wind Rose.....	9
Figure 3	February Wind Rose.....	9
Figure 4	March Wind Rose.....	10
Figure 5	April Wind Rose.....	10
Figure 6	May Wind Rose.....	11
Figure 7	June Wind Rose.....	11
Figure 8	July Wind Rose	12
Figure 9	August Wind Rose	12
Figure 10	September Wind Rose	13
Figure 11	October Wind Rose	13
Figure 12	November Wind Rose	14
Figure 13	December Wind Rose.....	14
Figure 14	January Wind Speed Distribution	15
Figure 15	January Wave Height Distribution	15
Figure 16	February Wind Speed Distribution	16
Figure 17	February Wave Height Distribution.....	16
Figure 18	March Wind Speed Distribution	17
Figure 19	March Wave Height Distribution.....	17
Figure 20	April Wind Speed Distribution	18
Figure 21	April Wave Height Distribution.....	18
Figure 22	May Wind Speed Distribution.....	19
Figure 23	May Wave Height Distribution	19
Figure 24	June Wind Speed Distribution.....	20
Figure 25	June Wave Height Distribution	20
Figure 26	July Wind Speed Distribution	21
Figure 27	July Wave Height Distribution.....	21
Figure 28	August Wind Speed Distribution	22
Figure 29	August Wave Height Distribution.....	22
Figure 30	September Wind Speed Distribution.....	23
Figure 31	September Wave Height Distribution	23
Figure 32	October Wind Speed Distribution	24
Figure 33	October Wave Height Distribution	24
Figure 34	November Wind Speed Distribution	25
Figure 35	November Wave Height Distribution	25
Figure 36	December Wind Speed Distribution.....	26
Figure 37	December Wave Height Distribution	26

1. INTRODUCTION

This report presents a wind and wave climatology for the waters of the Crown Lease Deployment Area of the Fundy Tidal Energy Demonstration Facility in the Minas Passage off Nova Scotia. Lying in 30 to 45 metres of water, approximately 2 kilometres southeast of Ram Head, the deployment area is at nearest 1 kilometre from the north shore of the Minas Passage, and about 4 kilometres north of Cape Split.

The report conveys the climatology as monthly wind speed and wave height distribution charts, monthly wind roses, and a table of monthly means and maximums. Section 2 is a brief description of the climate analysis, the study area, and the data sources. The overall results, tables, and charts are in Section 3.

Throughout this report, wind direction refers to the direction from which the wind blows. Wind speeds are in kilometres per hour, and significant wave heights are in metres. The significant wave height is the average of the highest one-third of all of the wave heights, and generally corresponds approximately to the average height of seas observed by a trained mariner.

2. DATA AND ANALYSIS

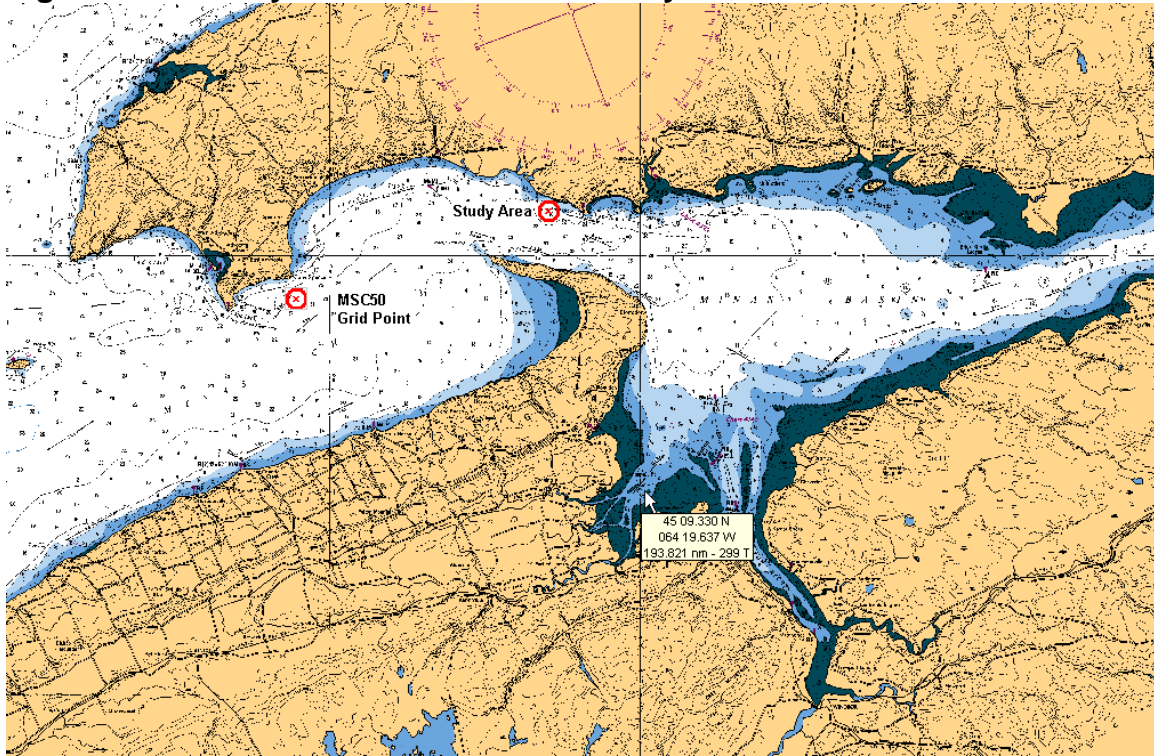
2.1 Winds

The MSC50 wind and wave reanalysis database (Swail et. al., 2006), spanning January 1 1954 to December 31 2005, at hourly intervals, provided a historical time series of winds for the study. The MSC50 reanalysis grid extends only as far north as $45^{\circ} 18'$ north latitude and as far east as $64^{\circ} 30'$ west longitude in the Minas Channel. Although the study site lies 15 to 20 km outside of this boundary to the northeast, reanalysis winds from the grid point at $45^{\circ} 18'$ north latitude and $64^{\circ} 42'$ west longitude were an acceptably accurate simulation of the winds at the study site (see Figure 1).

As this grid point lies over water, at the same proximity to the shoreline as the study site, the influence of water and land on winds at both locations were similar. Furthermore, as

the two locations were only about 20 km apart, any phase difference in wind shift patterns was negligible.

Figure 1 Study Area and MSC50 Reanalysis Grid Point



2.2 Fetch Limits

From the northwest clockwise around to the east, wave development in the study area is fetch limited by approximately 2 to 6 kilometres by north shore of the Minas Passage. From the east to the southeast, the site is open to waves from the Minas Basin with fetches from 25 to 45 kilometres. Cape Split limits the fetch from the southeast to the west-southwest from 4 to 6 kilometres. Long fetch seas from the Minas Channel and the Bay of Fundy propagate to the site along a narrow band to the west-southwest. Beyond this band, the west shore of Greville Bay limits fetch to 10 to 20 kilometres from the west to the northwest. The mean fetch limits for wave growth modelling are in Table 1.

Table 1 Fetch Limits Relative to the Crown Lease Deployment Area

Direction [degrees true]	Mean Fetch Limit [km]
000 - 045	1.0
045 - 055	1.3
055 - 065	1.6
065 - 085	1.8
085 - 095	3.7
095 - 105	45.0
105 - 115	35.0
115 - 125	28.0
125 - 135	24.0
135 - 175	5.5
175 - 205	3.7
205 - 240	5.5
240 - 250	200 ⁽¹⁾
250 - 275	20.0
275 - 285	17.0
285 - 295	13.0
295 - 315	5.5
315 - 325	3.7
325 - 345	1.9
345 - 360	1.3

(1) This direction is open to seas from the Bay of Fundy.

2.3 Wave Modelling

Based on the accepted threshold water depth being greater than one-quarter of a wavelength (WMO, 1998), the following expression determined applicability of deep-water wave equations:

$$T < \sqrt{\frac{8\pi H}{g}}$$

Where H is the wave height in metres, T is the period in seconds, and g is the acceleration of gravity. As the depth at the site varies from about 30 to 45 metres wave periods must exceed 10 to 12 seconds for any noticeable shallow water effects. Such

long period waves are extremely unlikely, given the limited fetch over water relative to the site.

Winds from the MSC50 reanalysis grid point, as discussed above, generated most of the wave time series at the study site, through the Bretschneider empirical deep-water relationships, following the standard procedure outlined in the Shore Protection Manual (1975). For fetch-limited wave growth, the following expression determined wave height:

$$H = 0.238 \frac{U^2}{g} \tanh\left(0.0125 \left(\frac{gf}{U^2}\right)^{0.42}\right) \quad (1)$$

In this expression, U is the wind speed in metres per second from the MSC50 grid point and f is the fetch in metres relative to the study site (see Table 1).

For waves not fully developed before reaching fetch limits, wave growth required solving the following for C_1 and C_2 by linear approximation:

$$F(D) = C_1 D + C_2$$

Where F is a dimensionless fetch parameter, and the dimensionless duration parameter D is:

$$D = \frac{gt \times 10^{-5}}{\bar{U}}$$

The variable \bar{U} is the average wind speed calculated from the MSC50 grid point over the duration t of wind from a particular direction. This gives the equivalent fetch:

$$f_e = \frac{FU}{g}$$

The equivalent fetch f_e replaces f , and \bar{U} replaces U , in equation (1) to solve for the duration limited wave height.

As the MSC50 reanalysis grid covers the Minas Channel west of Cape Spencer, the Bay of Fundy, and beyond, waves from the same MSC50 grid point that generated the winds, simulated the incoming seas from the south to the southwest. As these seas propagate towards the study into the wider waters northeast of Cape Spencer into Greville Bay and the Minas Passage, the waves bend in a curve away from the direction of propagation. This angular spreading disperses energy along each wave front, progressively lowering the wave height with distance from the MSC50 grid point to the study site. The amount this angular spreading diminishes wave height is a function of the ratio of the width across the Minas Channel, from Cape Spencer to Huntington Point d (14 kilometres), to the distance from the MSC50 grid point to the study site d_i (22 kilometres). The angular spreading also depends on the angle θ away from the direction of wave and swell propagation. The wave height at study site H_i , reduced by angular spreading (WMO, 1998), is:

$$H_i = H \sqrt{E(d_i/d)} \cos^2 \theta$$

The variable H is the wave height at the MSC50 grid point, and $E(d_i/d)$ is the angular spreading factor along the vector mean direction of wave and swell propagation, which in this case was 0.38. To reach the study site from the Minas Channel the vector mean direction of waves, simulated at the MSC50 grid point, propagated from 250° southwards to 180° ($\theta = 0^\circ$ to $\theta = 110^\circ$). Combining these seas with the locally generated waves, as a sum of squares, gave the total wave height at the site.

3. RESULTS

Table 2 lists the mean and maximum wind speeds and significant wave heights for each month. The maximum wind and waves are the absolute highest values found for each month over the 52-year record of the study. The number of occurrences in each wind speed range by month over 52 years is in Table 3, while similarly Table 4 lists occurrences for each significant combined wave height range.

Table 2 Monthly Mean and Maximum Winds and Waves

Month	Mean Wind Speed [kph]	Max Wind Speed [kph]	Mean Significant Wave Height [m]	Max Significant Wave Height [m]
January	24	78	0.3	1.7
February	22	74	0.3	1.9
March	21	74	0.3	2.6
April	19	74	0.2	1.5
May	16	60	0.2	1.3
Jun	16	58	0.2	1.1
July	15	82	0.2	2.0
August	15	65	0.2	1.3
September	17	84	0.2	2.3
October	20	107	0.3	3.2
November	22	69	0.3	1.6
December	24	86	0.3	2.2

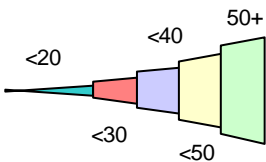
Table 3 Number of Hourly Occurrences of Wind Speed by Month

Mon	00-10 kph	10-20 kph	20-30 kph	30-40 kph	40-50 kph	50-60 kph	60-70 kph	70-80 kph	80-90 kph	90-100 kph	100+ kph
Jan	2982	13351	13422	6562	1946	368	55	2	0	0	0
Feb	3828	13926	11515	4651	1097	186	47	6	0	0	0
Mar	5512	14836	12251	4904	1008	134	39	4	0	0	0
Apr	6613	16661	10213	3295	575	68	13	2	0	0	0
May	9646	19089	8232	1535	177	9	0	0	0	0	0
Jun	9460	19288	7860	799	31	2	0	0	0	0	0
Jul	9850	21184	7096	507	31	8	7	4	1	0	0
Aug	9979	20989	6961	713	21	18	7	0	0	0	0
Sep	7595	18680	9213	1662	195	59	29	4	3	0	0
Oct	4832	17184	12401	3512	574	109	49	20	4	2	1
Nov	3224	14645	12801	5413	1174	166	17	0	0	0	0
Dec	2642	12991	13968	6671	2002	340	59	12	3	0	0

Table 4 Number of Hourly Occurrences of Significant Wave Height by Month

Mon	0.0-0.2 m	0.2-0.4 m	0.4-0.6 m	0.6-0.8 m	0.8-1.0 m	1.0-1.2 m	1.2-1.4 m	1.4-1.6 m	1.6-1.8 m	1.8-2.0 m	2.0+ m
Jan	17803	10681	5101	916	285	70	4	1	0	0	0
Feb	19012	9127	3387	1263	417	112	30	16	5	1	0
Mar	22297	9204	3640	1086	488	144	48	6	11	5	2
Apr	24097	7980	2332	762	336	13	9	2	0	0	0
May	28055	7191	1332	277	36	5	2	0	0	0	0
Jun	26135	7691	1084	129	15	4	0	0	0	0	0
Jul	27123	7973	982	111	10	3	5	3	0	2	0
Aug	27978	7648	1142	166	12	4	1	0	0	0	0
Sep	25080	8623	1809	339	75	24	5	2	4	1	1
Oct	22240	10339	3538	901	266	55	9	6	3	10	7
Nov	18675	10350	4360	1542	482	199	50	24	0	0	0
Dec	16951	11041	5429	2110	867	293	97	34	19	16	3

Figures 2 to 37 present the wind and wave climate for the study area. The first set of figures (2 to 13), depict wind roses of the prevailing winds for each month. Wind roses display both wind speed and direction in a single diagram. The wind rose consists of bars whose length indicates the frequency of winds blowing from a given direction, with wind direction superimposed on a 16-point compass. The bars are also broken into sections, each of which defines a speed range. A longer section indicates that winds blow more frequently at a given speed for that compass direction. Figure 1 below shows the wind speed categories, in knots, for each section of the wind rose bars.

Figure 1 Key for Wind Rose Speed Categories in Knots


Following the wind roses, Figures 14 to 37 are monthly wind speed and wave height distribution charts. For each set of wind speed or wave height ranges depicted along the bottom of the charts, the height of each bar indicates the frequency of the range. These

charts give the expected percentage occurrence of each wind speed or wave height category in the given month.

Figure 2 January Wind Rose

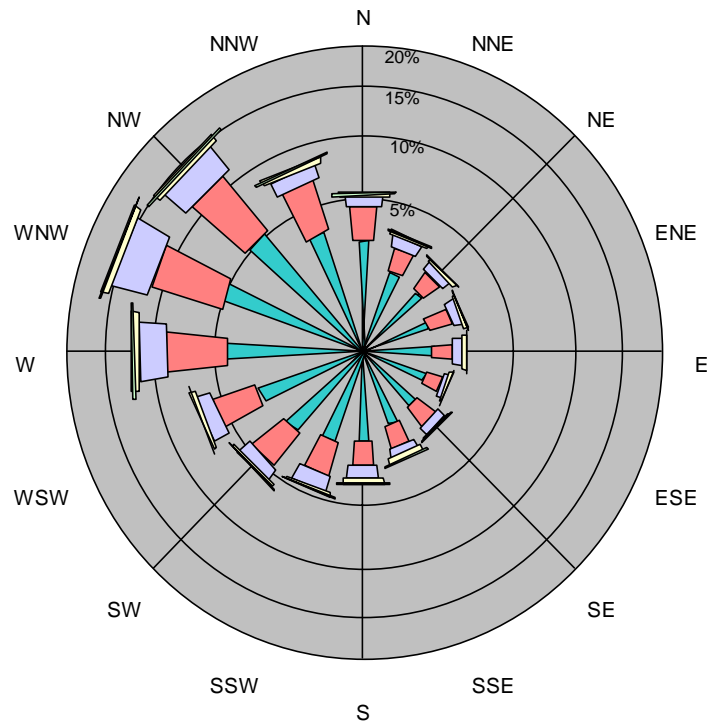


Figure 3 February Wind Rose

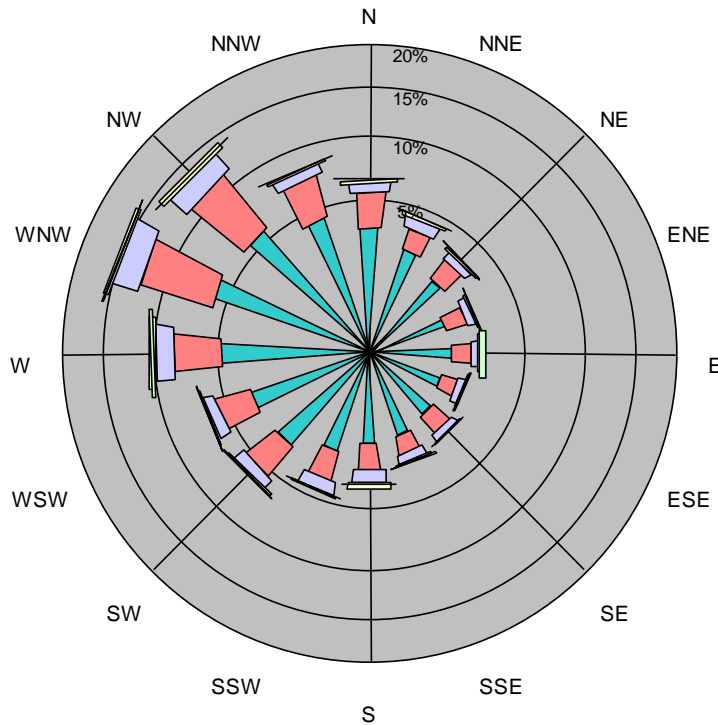


Figure 4 March Wind Rose

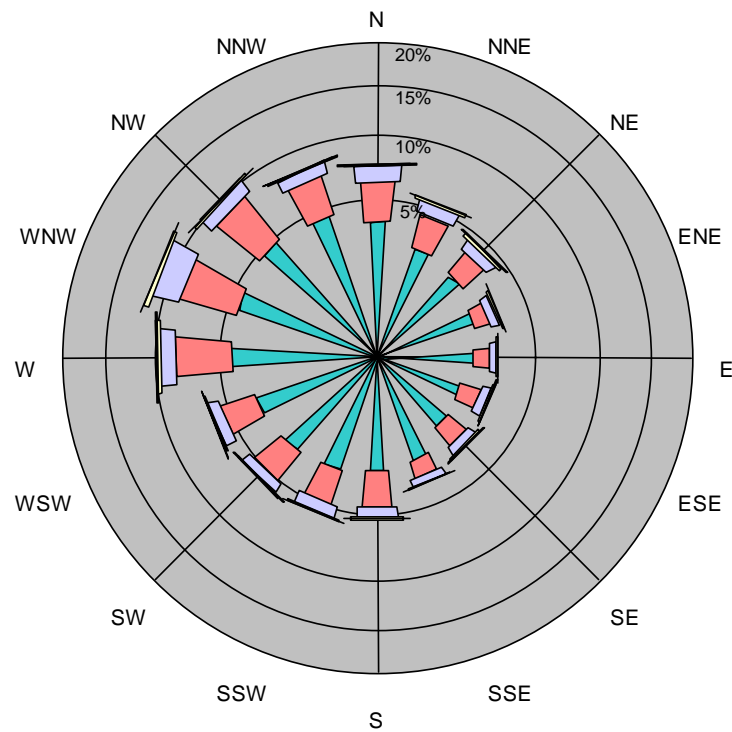


Figure 5 April Wind Rose

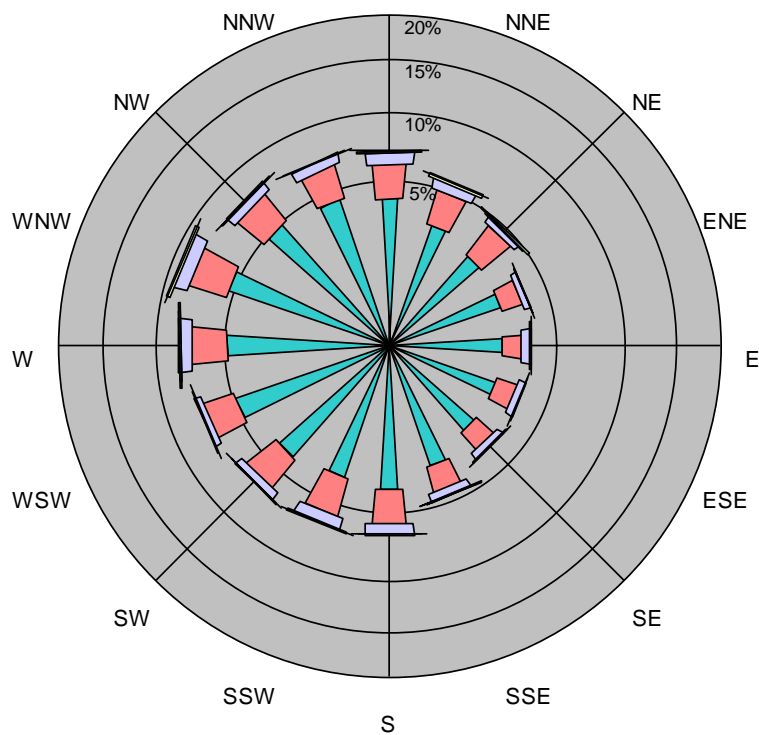


Figure 6 May Wind Rose

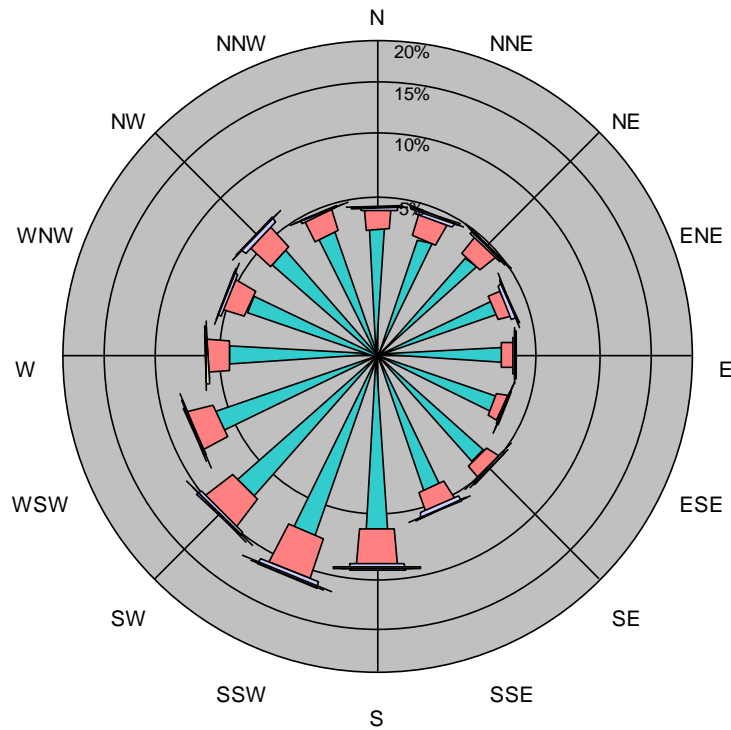


Figure 7 June Wind Rose

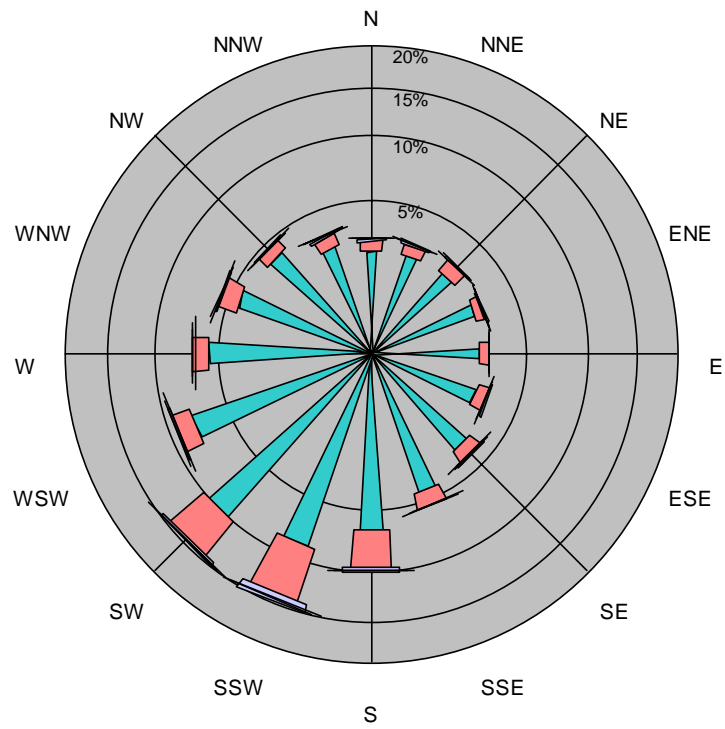


Figure 8 July Wind Rose

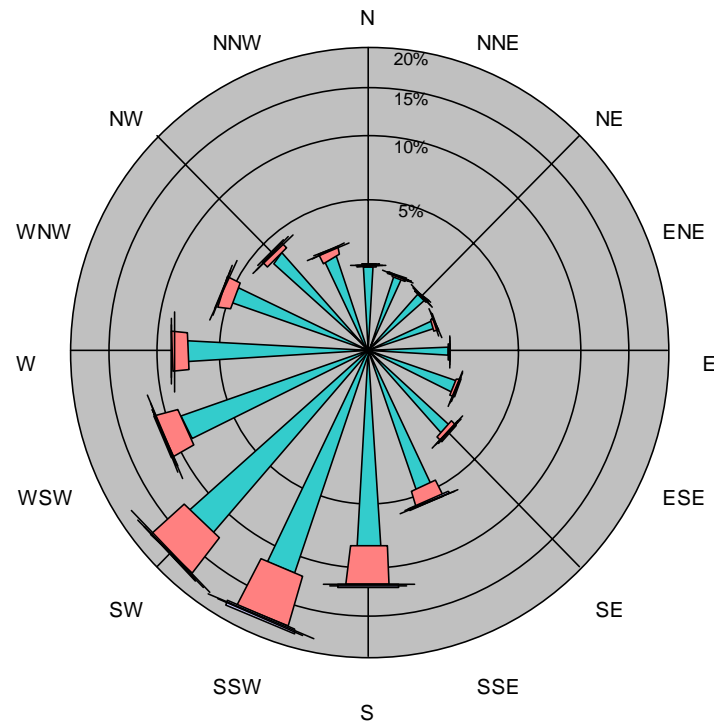


Figure 9 August Wind Rose

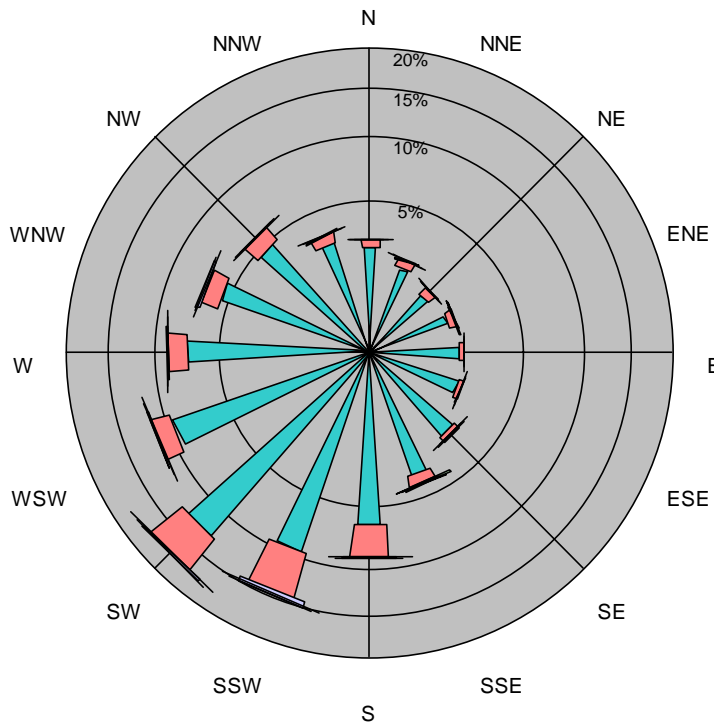


Figure 10 September Wind Rose

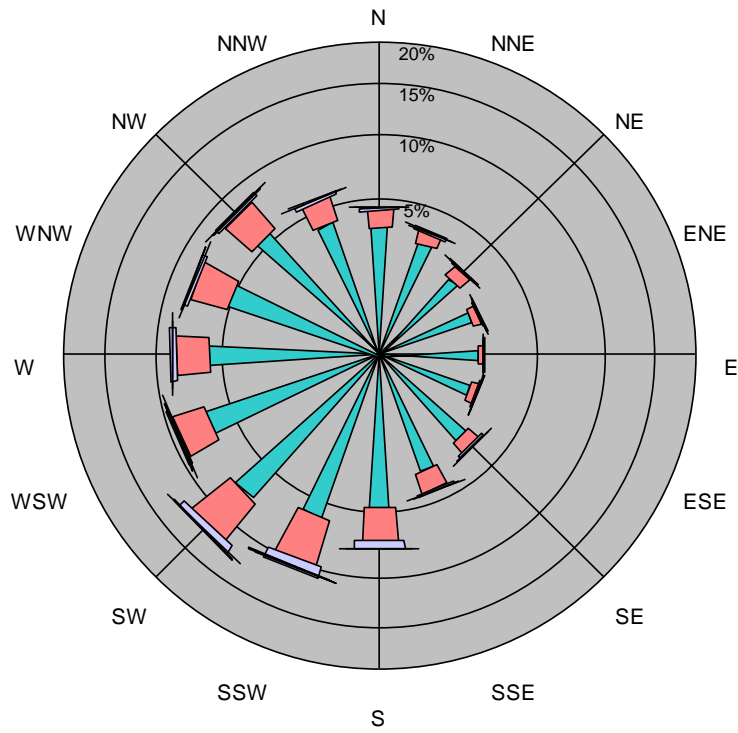


Figure 11 October Wind Rose

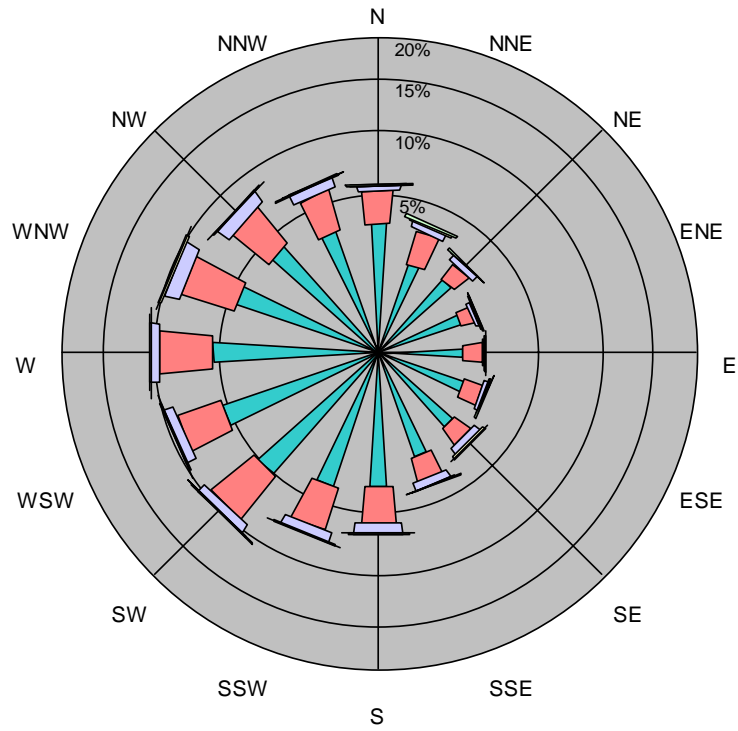


Figure 12 November Wind Rose

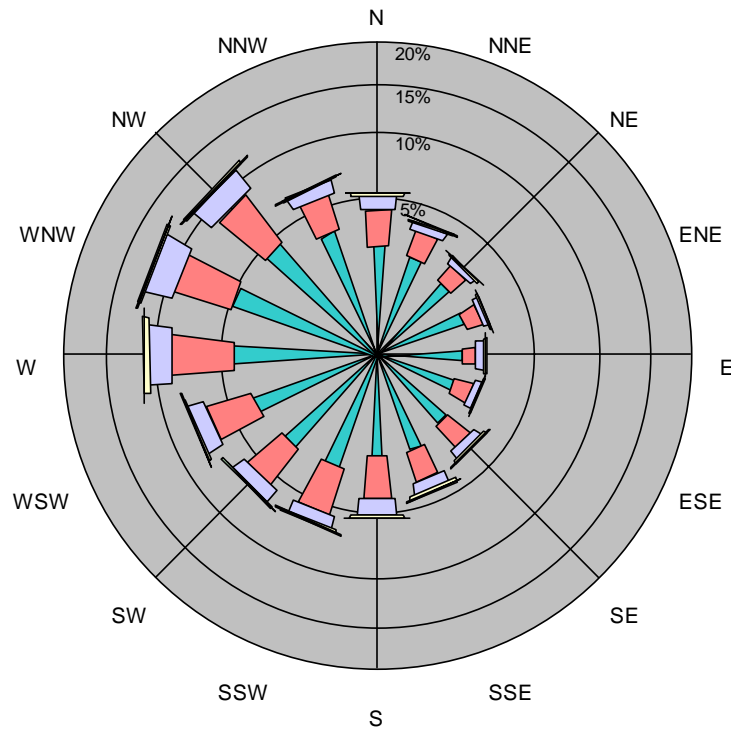


Figure 13 December Wind Rose

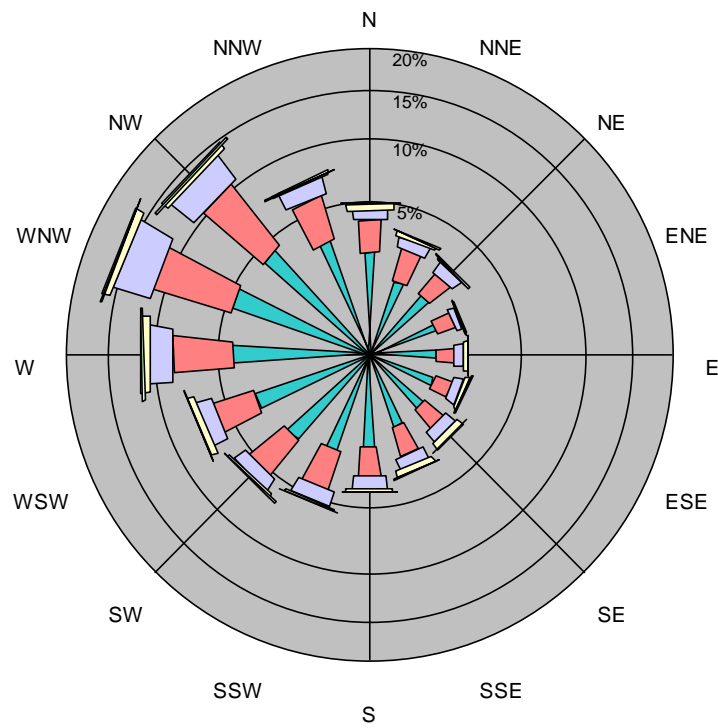


Figure 14 January Wind Speed Distribution

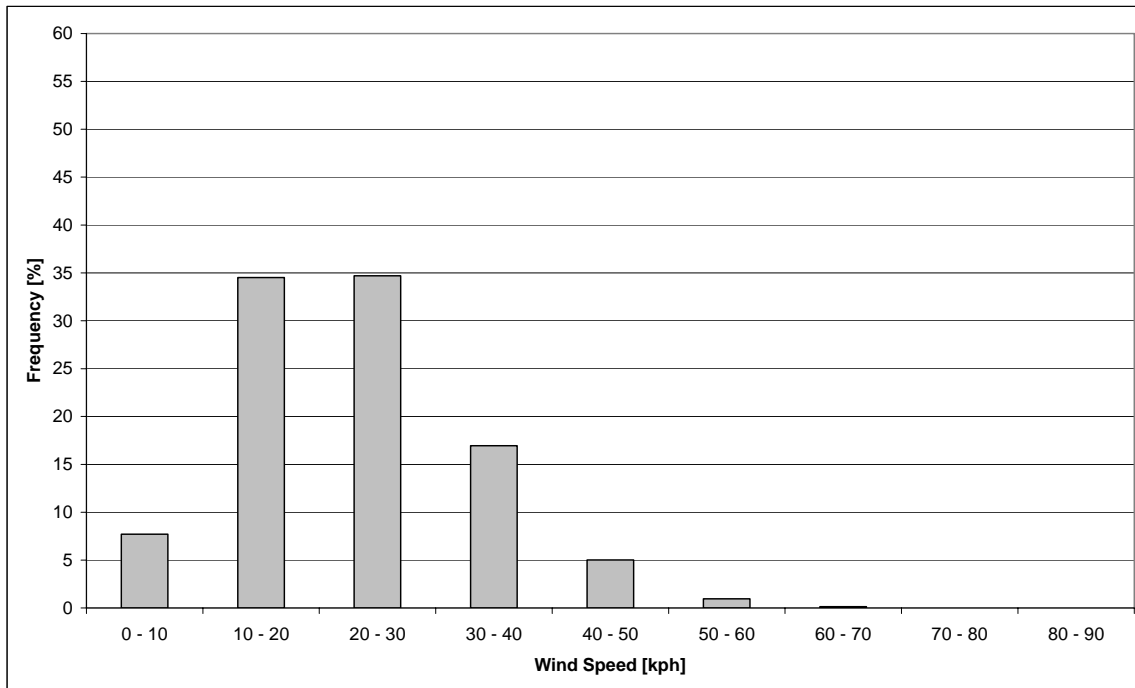


Figure 15 January Wave Height Distribution

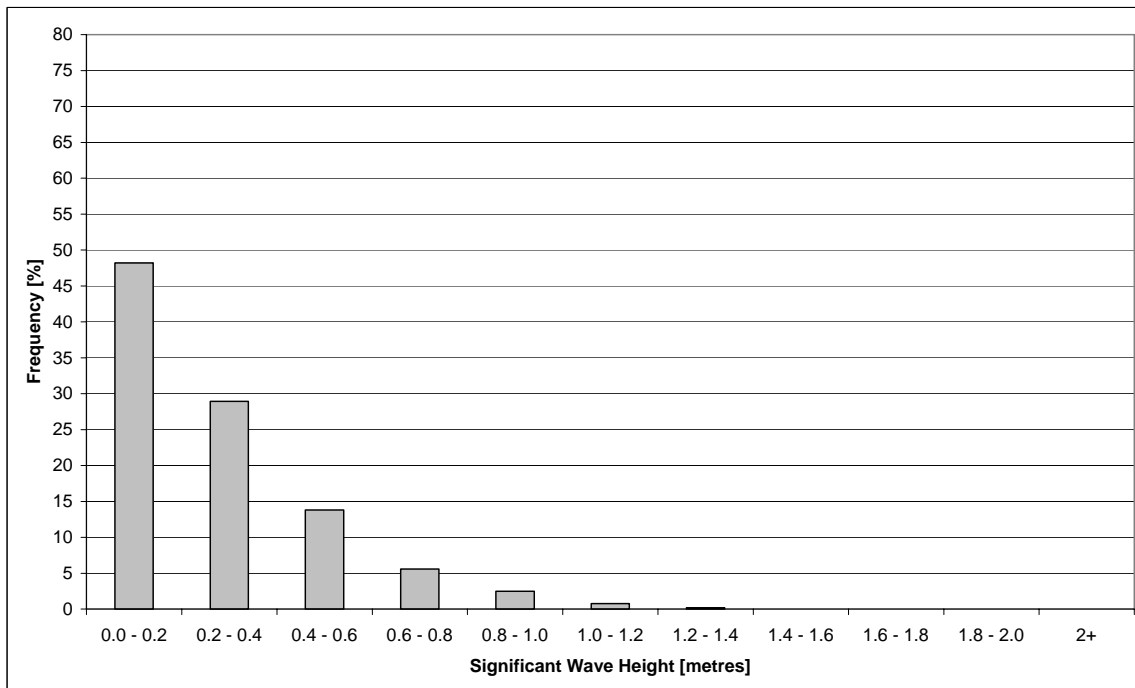


Figure 16 February Wind Speed Distribution

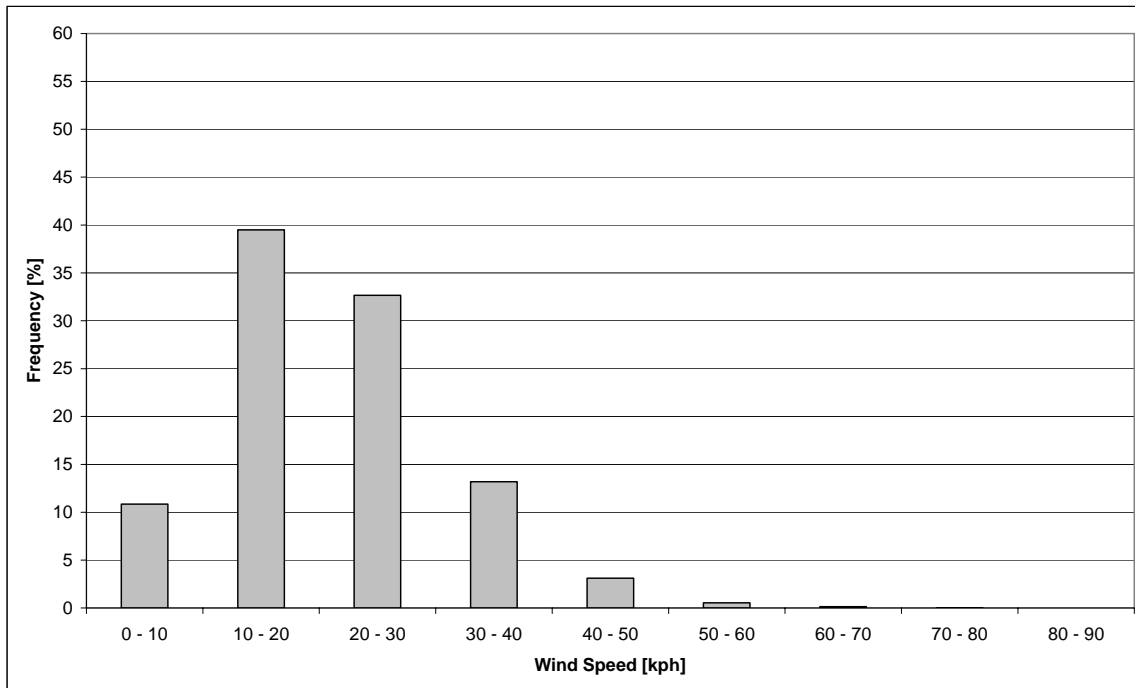


Figure 17 February Wave Height Distribution

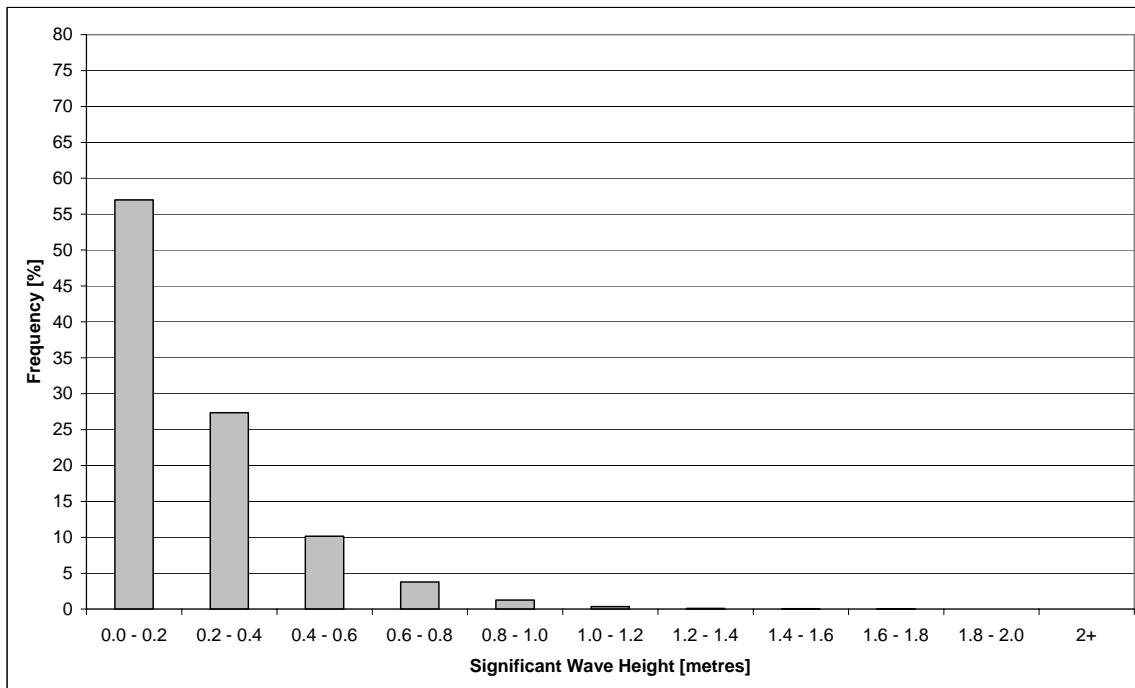


Figure 18 March Wind Speed Distribution

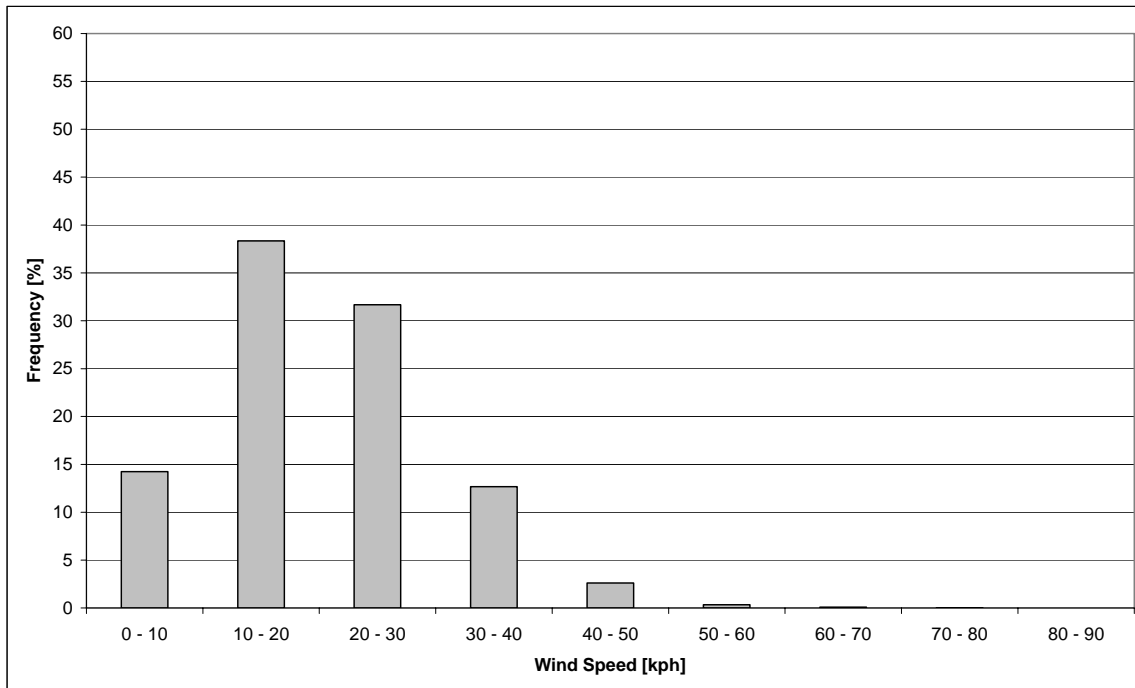


Figure 19 March Wave Height Distribution

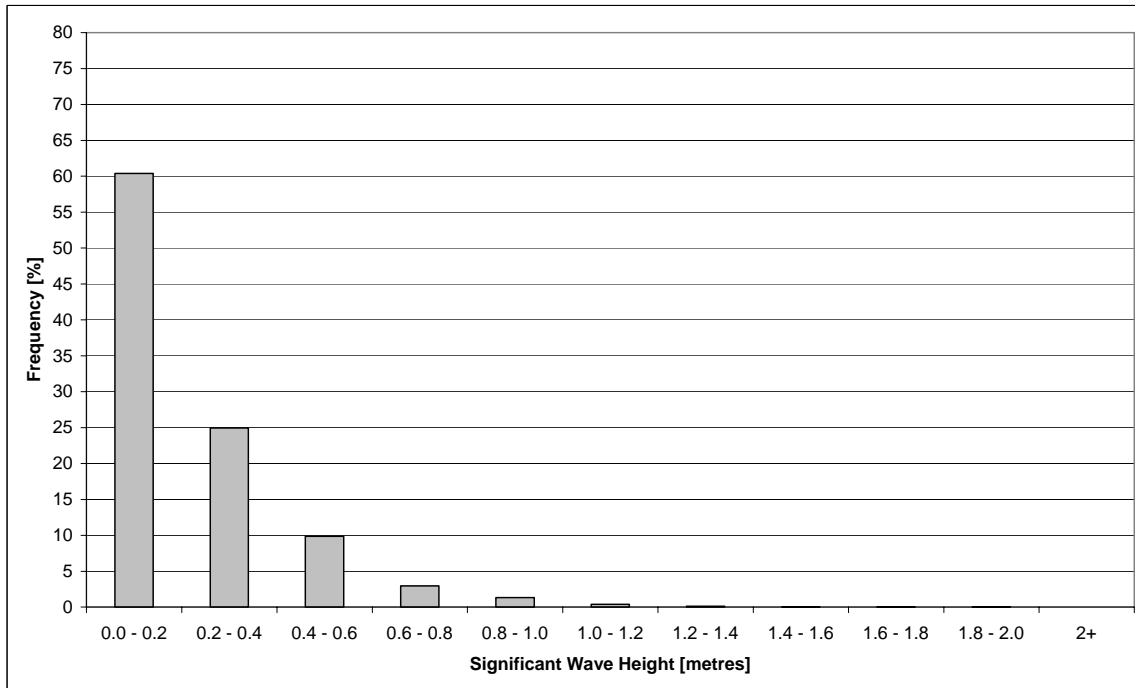


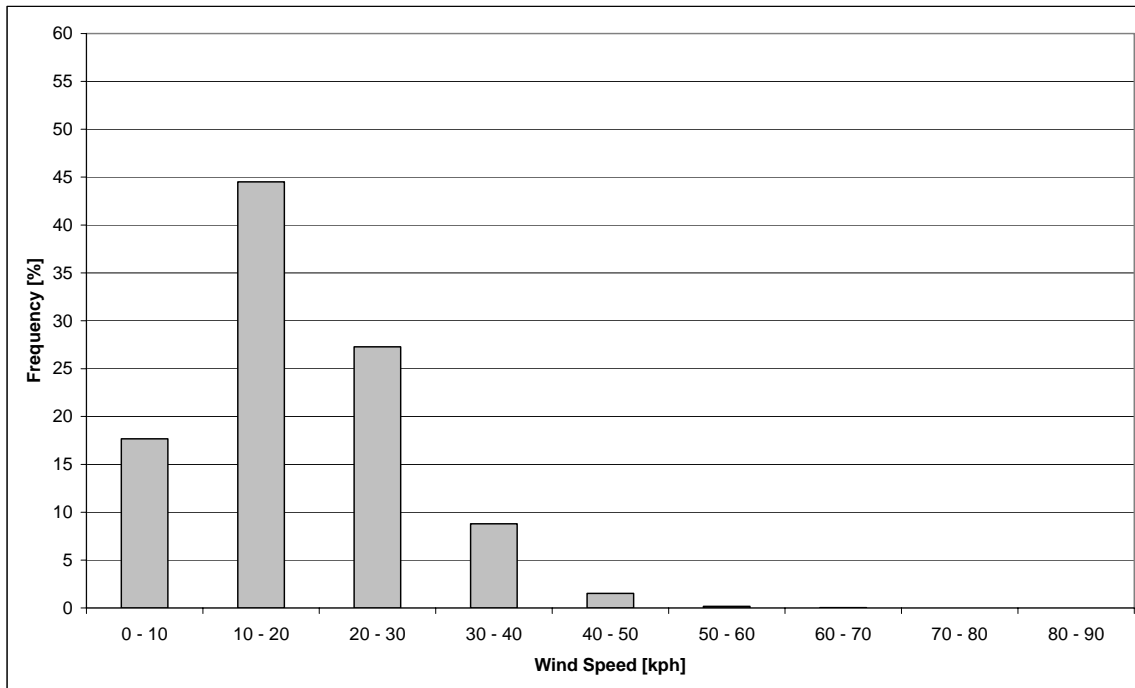
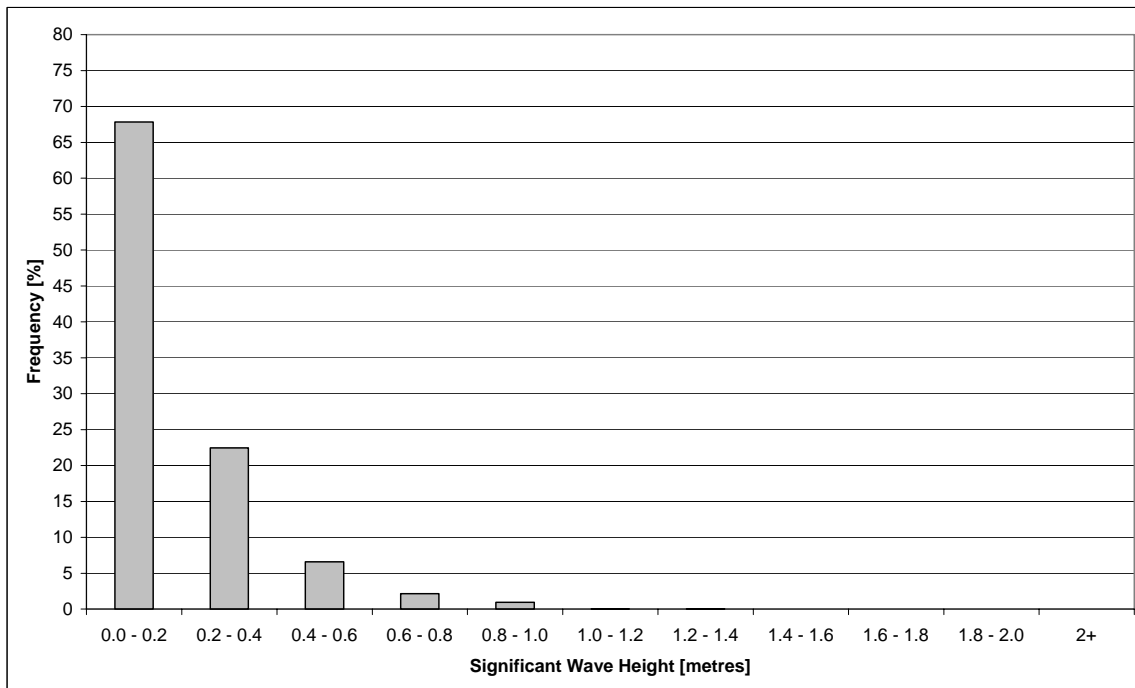
Figure 20 April Wind Speed Distribution

Figure 21 April Wave Height Distribution


Figure 22 May Wind Speed Distribution

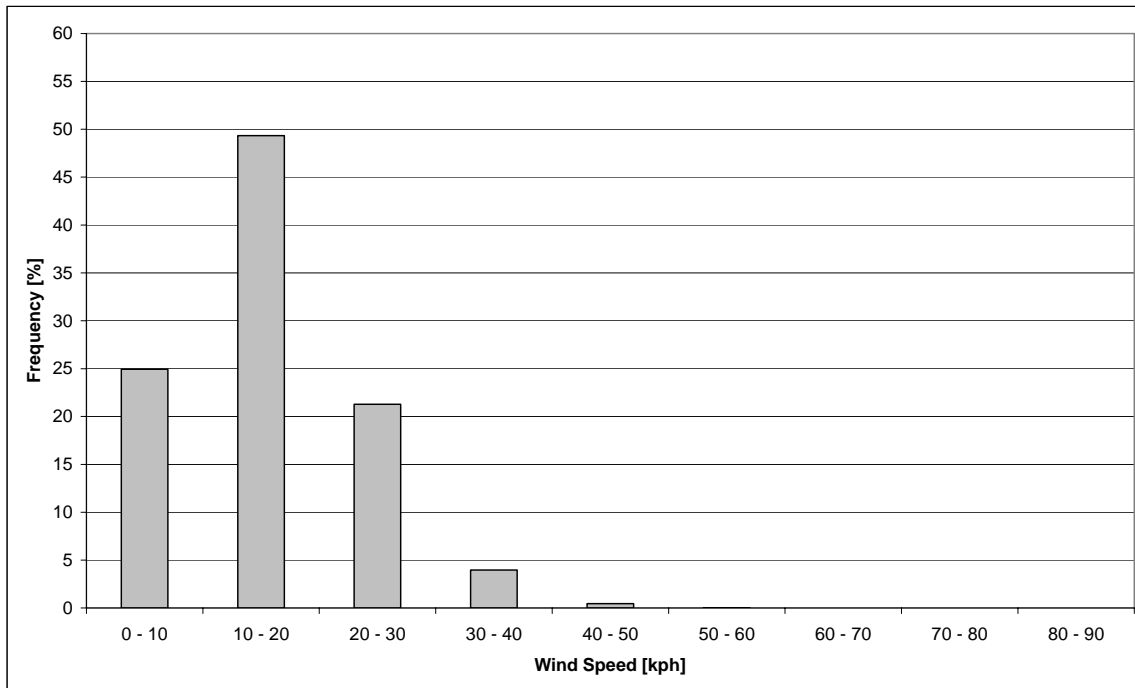


Figure 23 May Wave Height Distribution

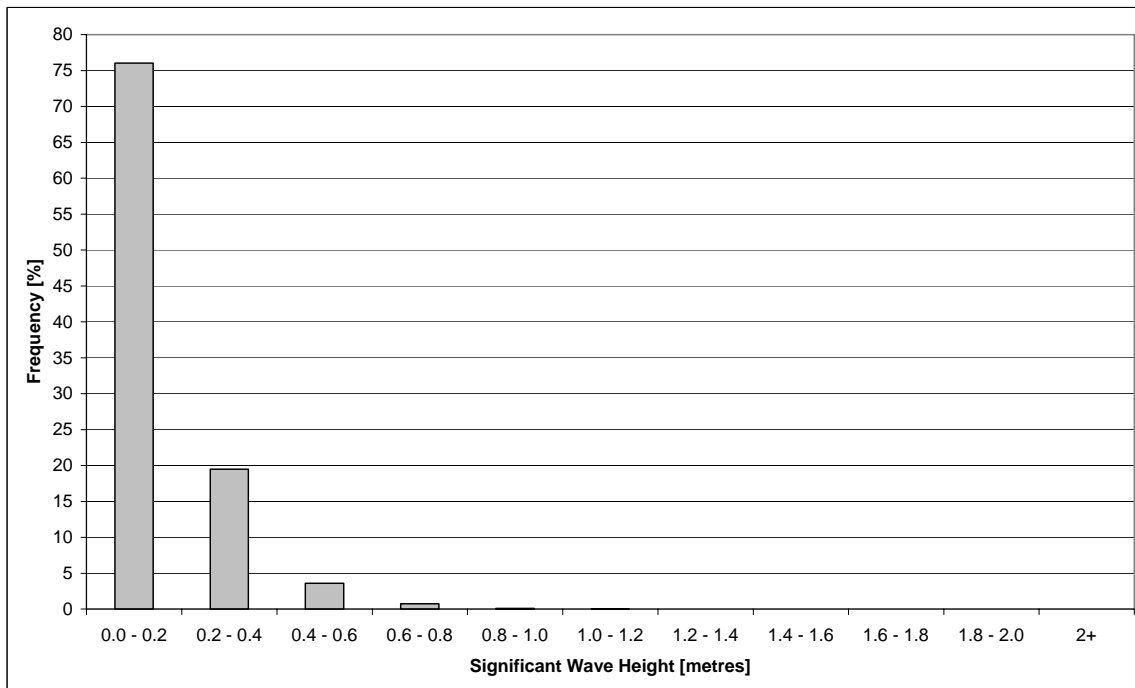


Figure 24 June Wind Speed Distribution

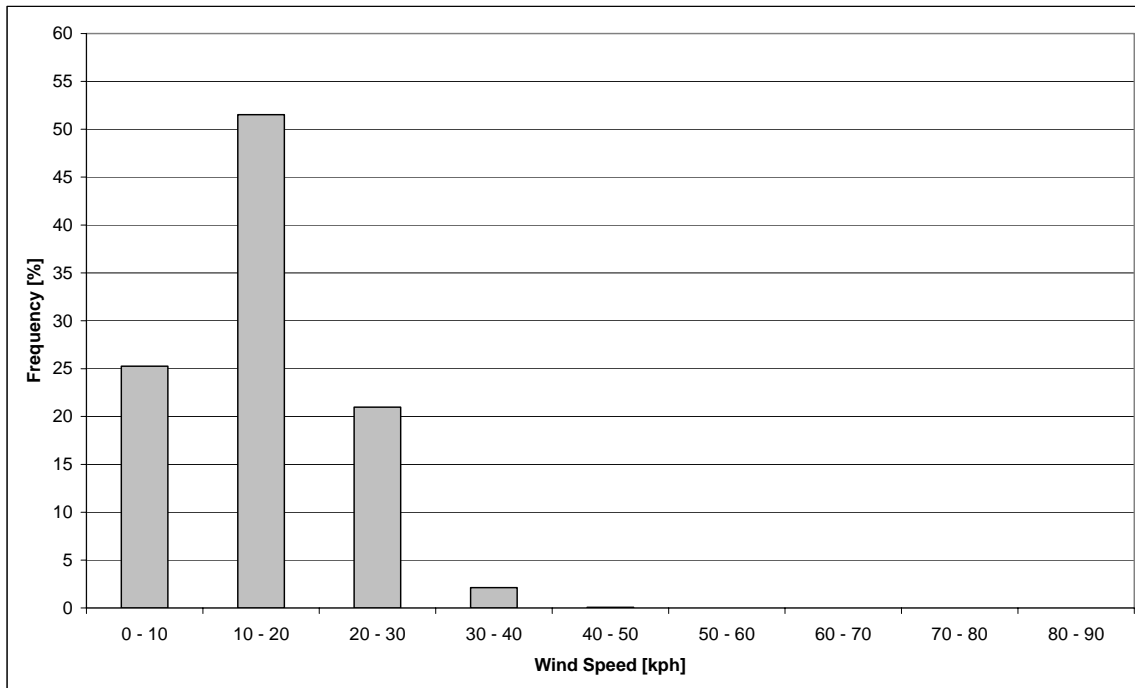


Figure 25 June Wave Height Distribution

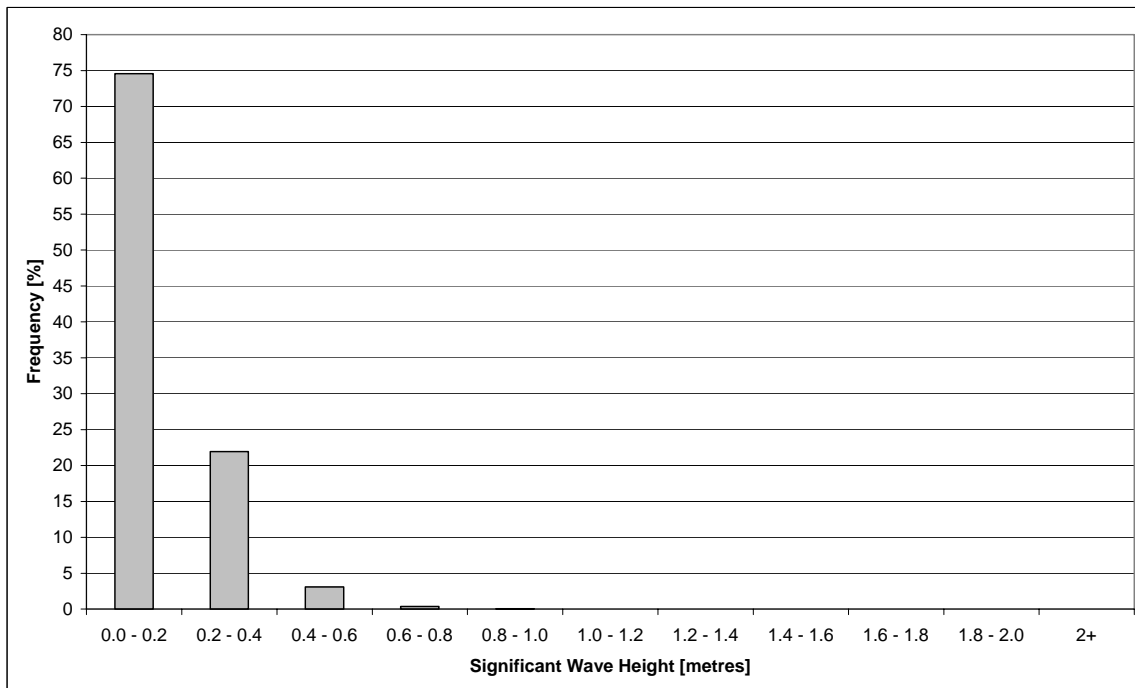


Figure 26 July Wind Speed Distribution

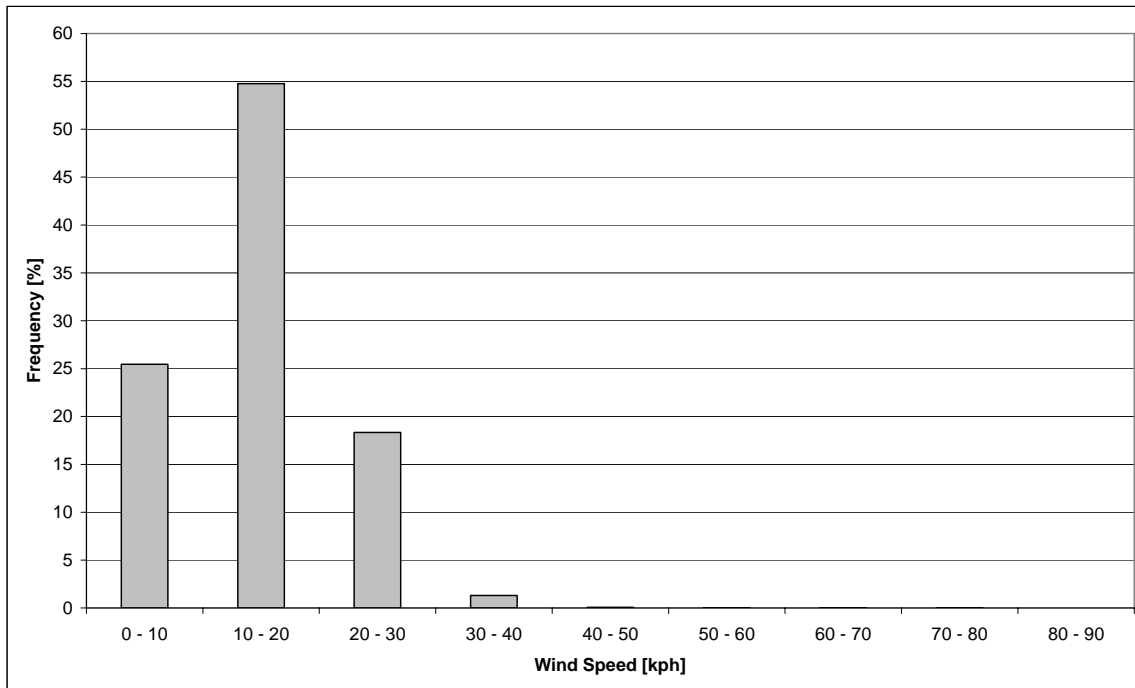


Figure 27 July Wave Height Distribution

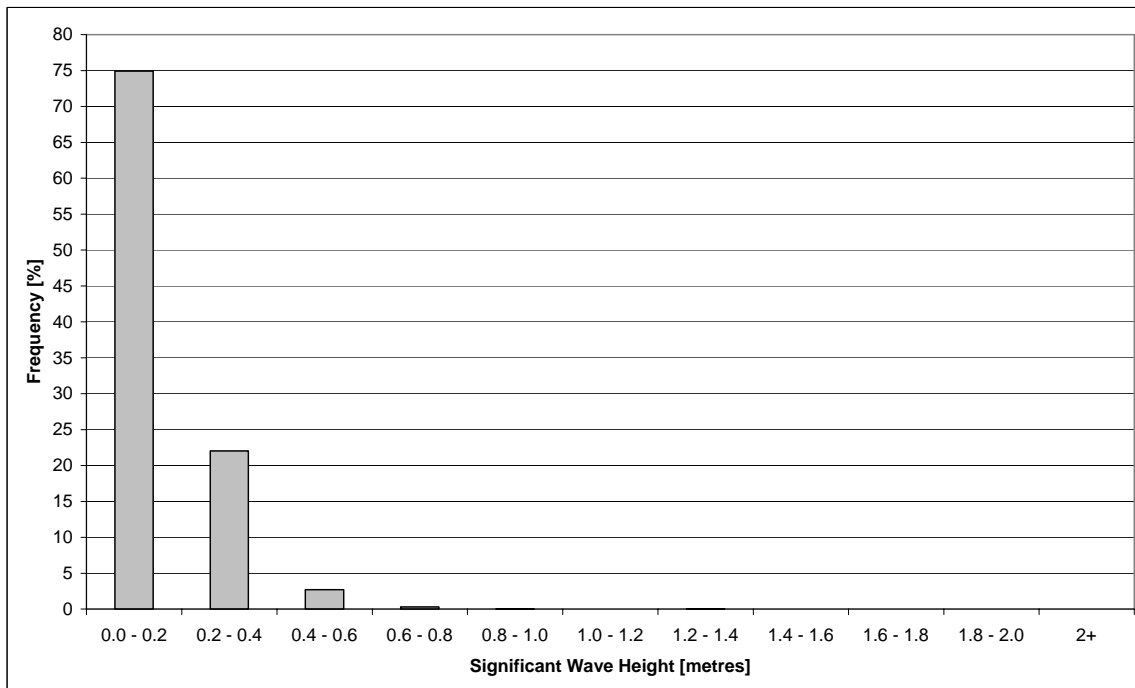


Figure 28 August Wind Speed Distribution

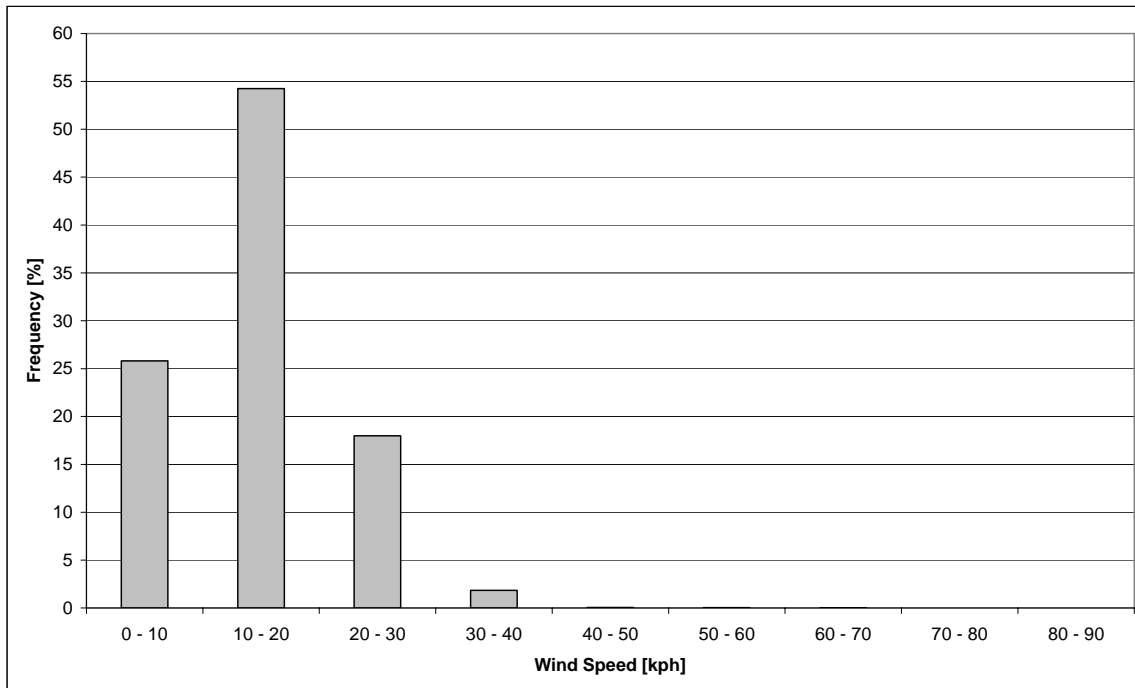


Figure 29 August Wave Height Distribution

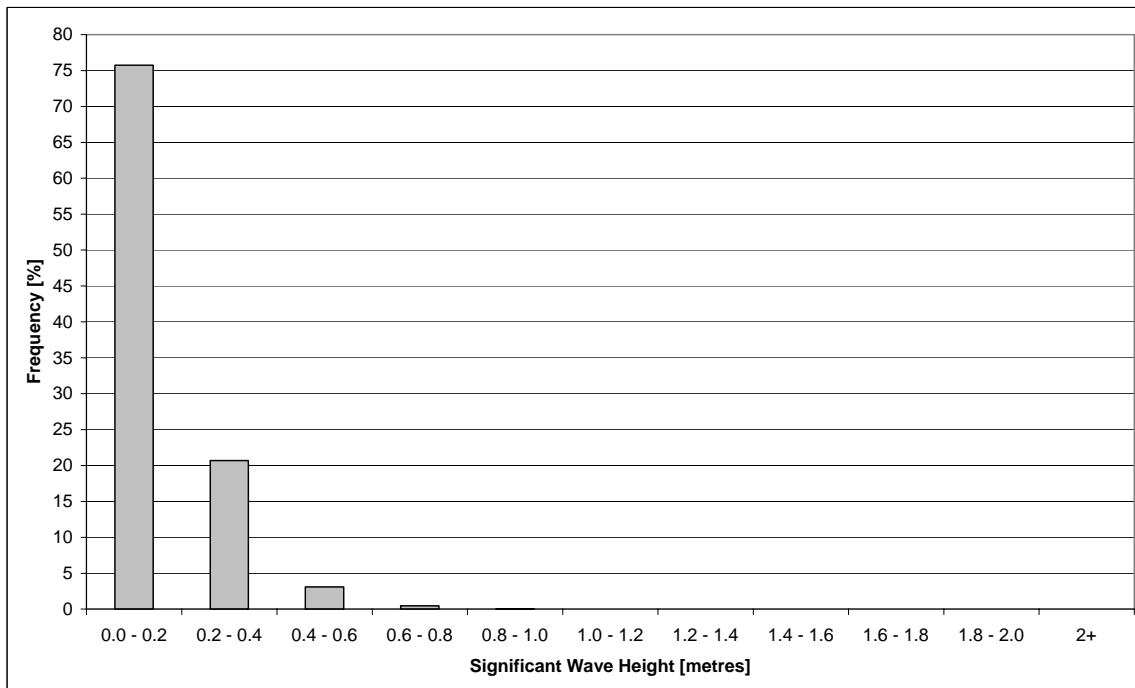


Figure 30 September Wind Speed Distribution

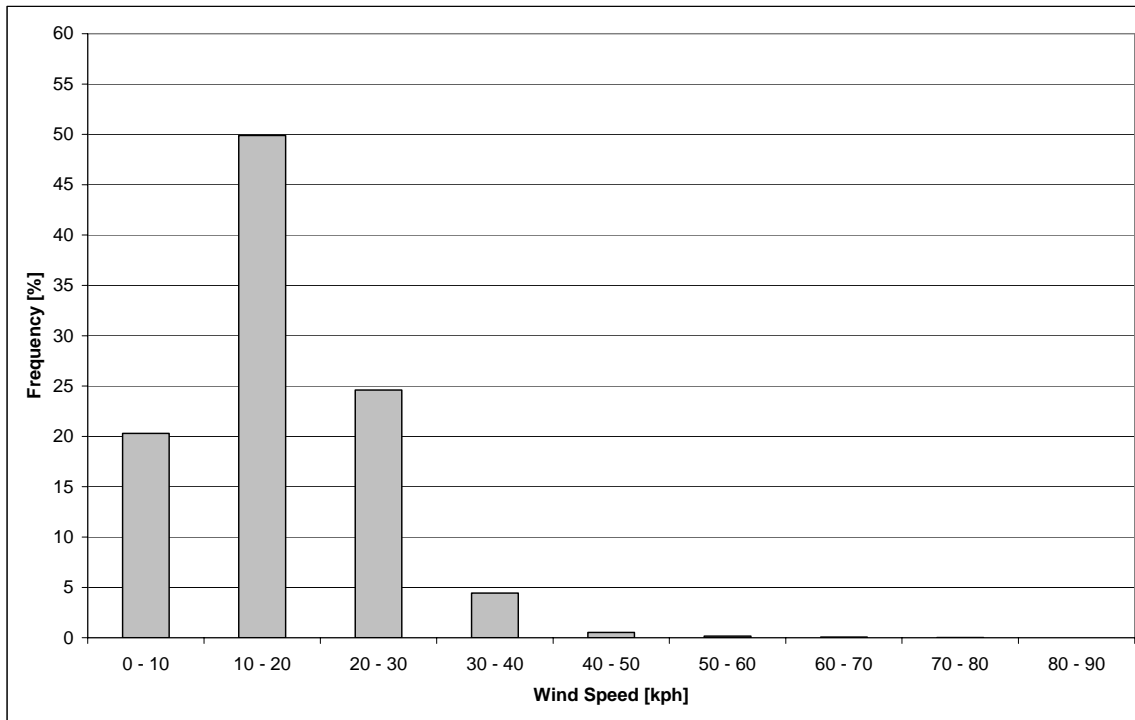


Figure 31 September Wave Height Distribution

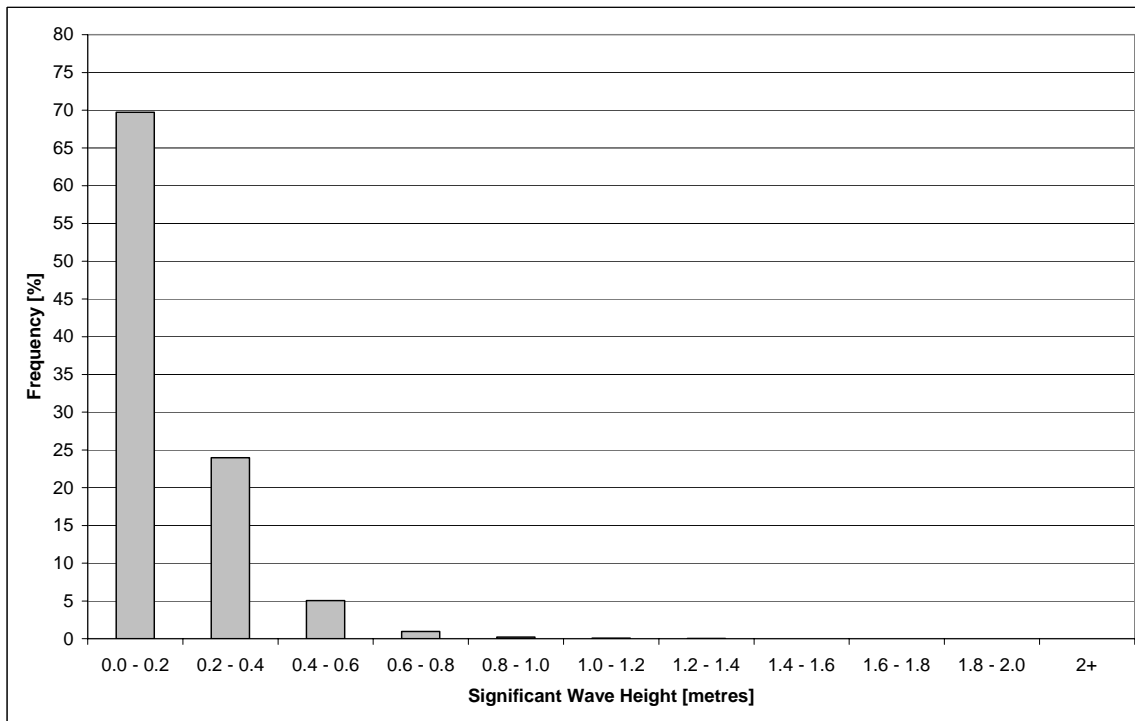


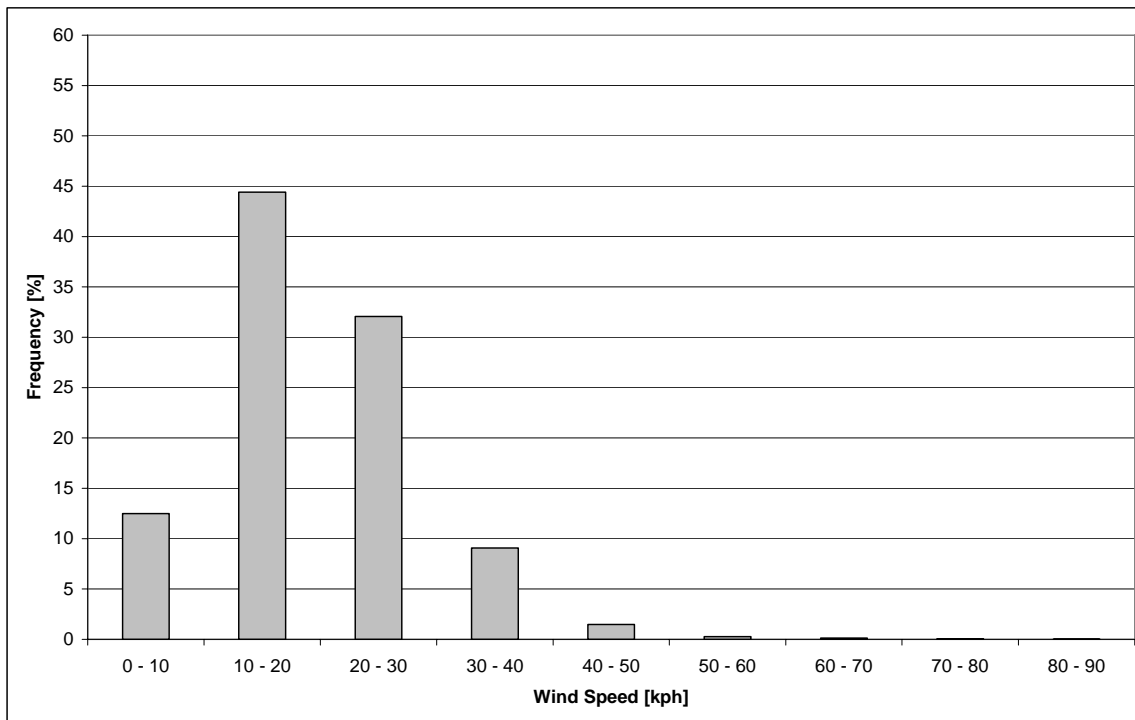
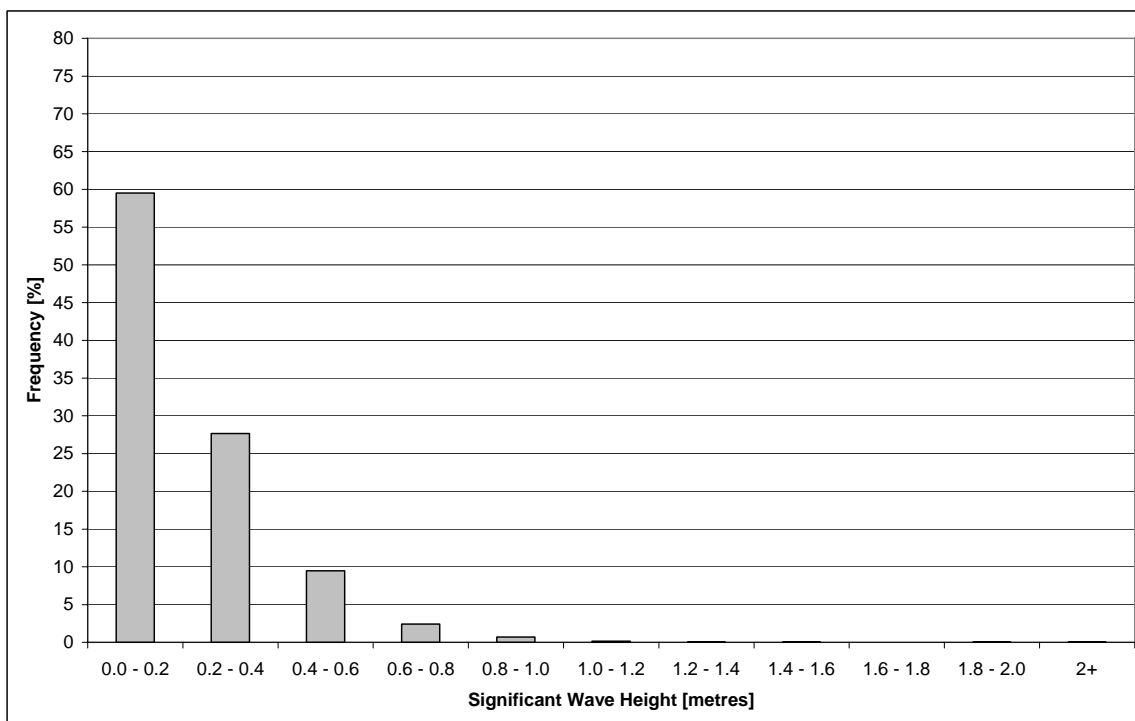
Figure 32 October Wind Speed Distribution

Figure 33 October Wave Height Distribution


Figure 34 November Wind Speed Distribution

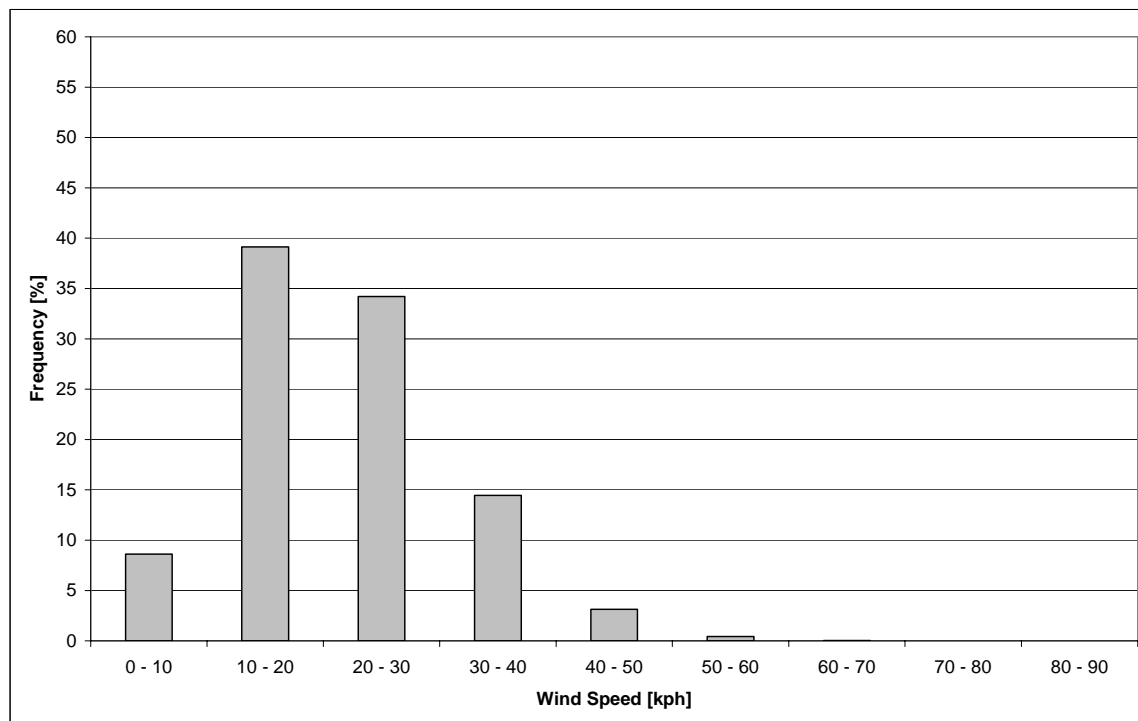


Figure 35 November Wave Height Distribution

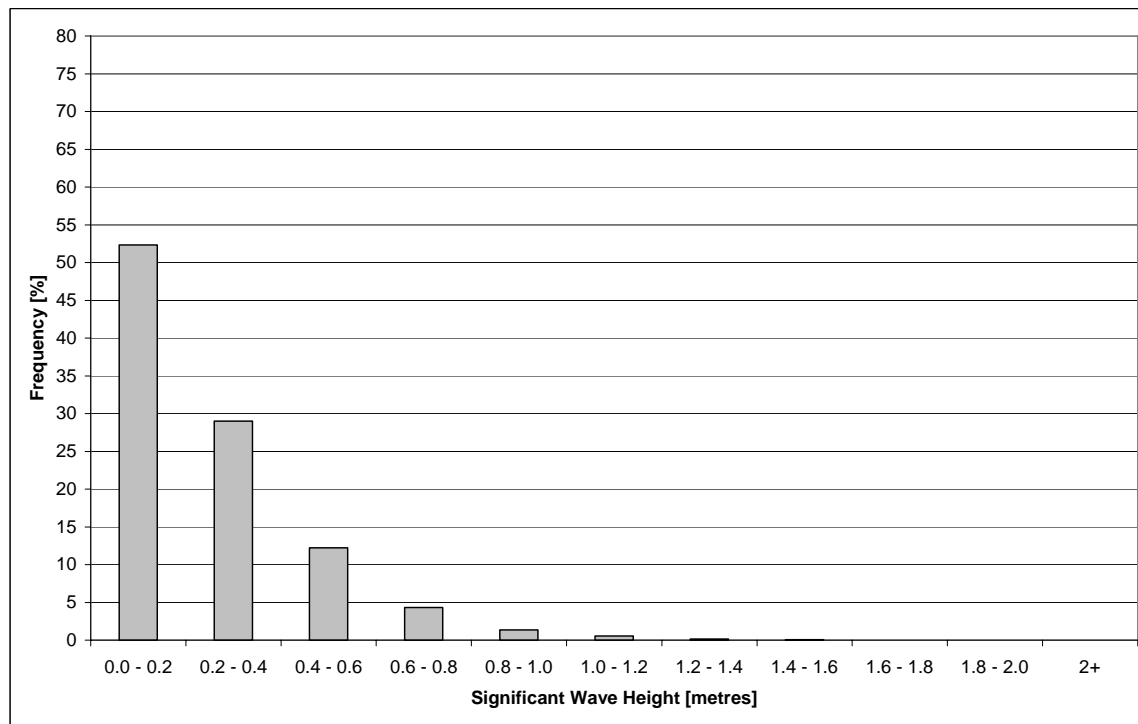


Figure 36 December Wind Speed Distribution

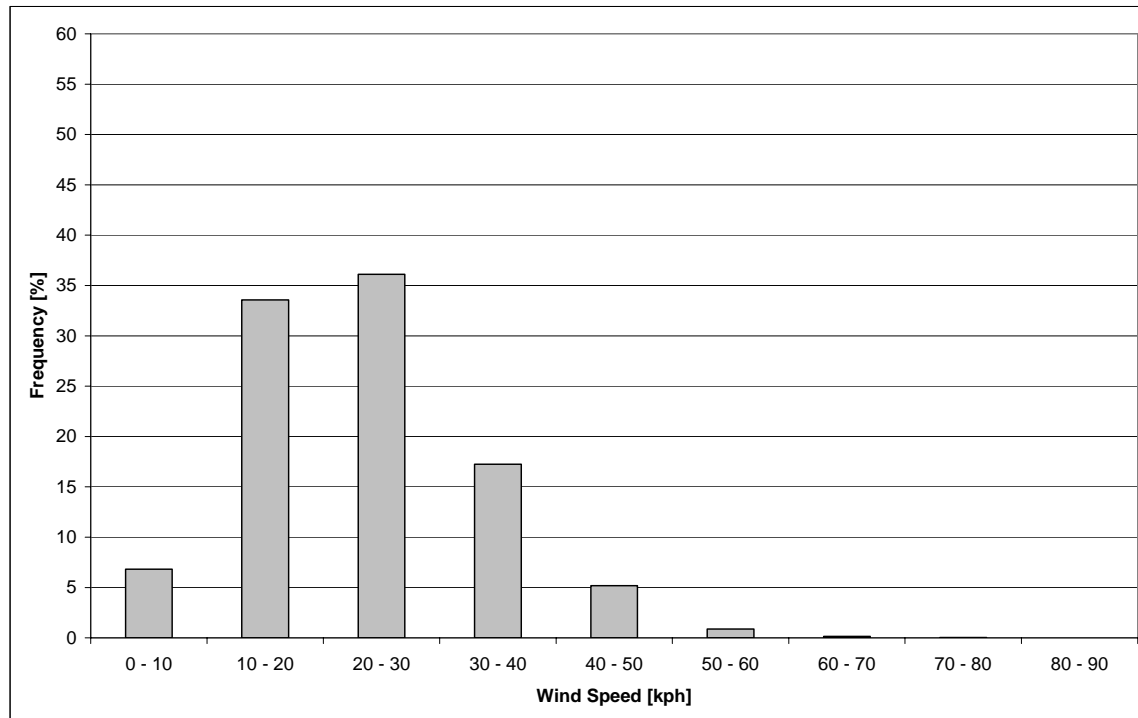
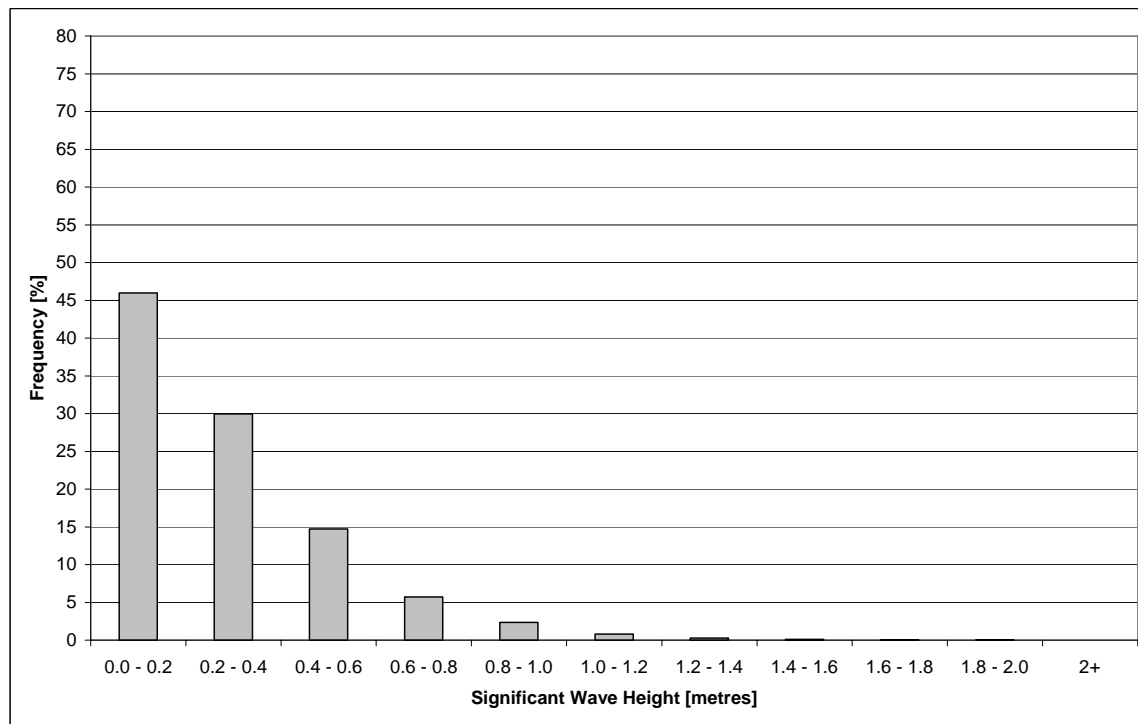


Figure 37 December Wave Height Distribution



4. REFERENCES

- Bretschneider, C. L. 1969. "Wave Forecasting," Chapter 11 in *Handbook of Ocean and Underwater Engineering*. J.J. Myers et al., eds., McGraw-Hill Book Co., New York.
- Secretariat of the World Meteorological Organization. 1998. *Guide to Wave Analysis and Forecasting*. World Meteorological Organization, Geneva.
- Swail, V.R., Cardone, V.J., Ferguson, M., Gummer, D.J., Harris, E.L., Orelup, E.A. and Cox, A.T. 2006. "The MSC50 Wind and Wave Reanalysis", 9th International Workshop On Wave Hindcasting and Forecasting, Victoria, B.C. Canada.
- United States Army 1975. *Shore Protection Manual*, U.S. Army Coastal Engineering Research Center, Fort Belvoir, Virginia.